Multi Internal Nucleophile Ring Expansion Reactions

Dominic Eamon Spurling

MSc by Research

University of York

Department of Chemistry

August 2020

Abstract

This thesis describes a novel method for the cyclisation of linear precursors possessing multiple internal nucleophiles, via multi internal nucleophile ring expansion (multi-INRE) cascade reactions to yield novel heterocyclic-macrocyclic lactones.

Section 2.1 describes the design of proposed novel linear multi-INRE precursor **A** and associated synthetic strategies. Section 2.2 presents the multistep synthesis route to linear multi-INRE precursor **A** which, after considerable optimisation, was achieved on a three-gram scale with an overall yield of 50%. Section 2.3 details the first reported multi-INRE reaction, with the synthesis of heterocyclic-macrocyclic lactone **B**. Section 2.3 also comments on the atroposelectivity of the multi-INRE reaction **A** → **B** with a kinetic model proposed to explain the selectivity. Section 3.3 details the synthesis and subsequent cyclisation of two aliphatic linear precursors (**C**) via multi-INRE reactions. In this section, two novel aliphatic linear precursors possessing two internal amine nucleophiles (**C**) and their respective multi-INRE heterocyclic-macrocyclic lactone products (**D**) are synthesised. Section 3.4 details the screening of multi-INRE reaction **A** → **B**, culminating in the discovery of conditions that enable a yield of 73% for the initial multi-INRE. Finally, chapter four details the design of three other potential linear precursors containing two internal nucleophiles and describes the progress made towards the synthesis of each (**E**, **F** and **G**).

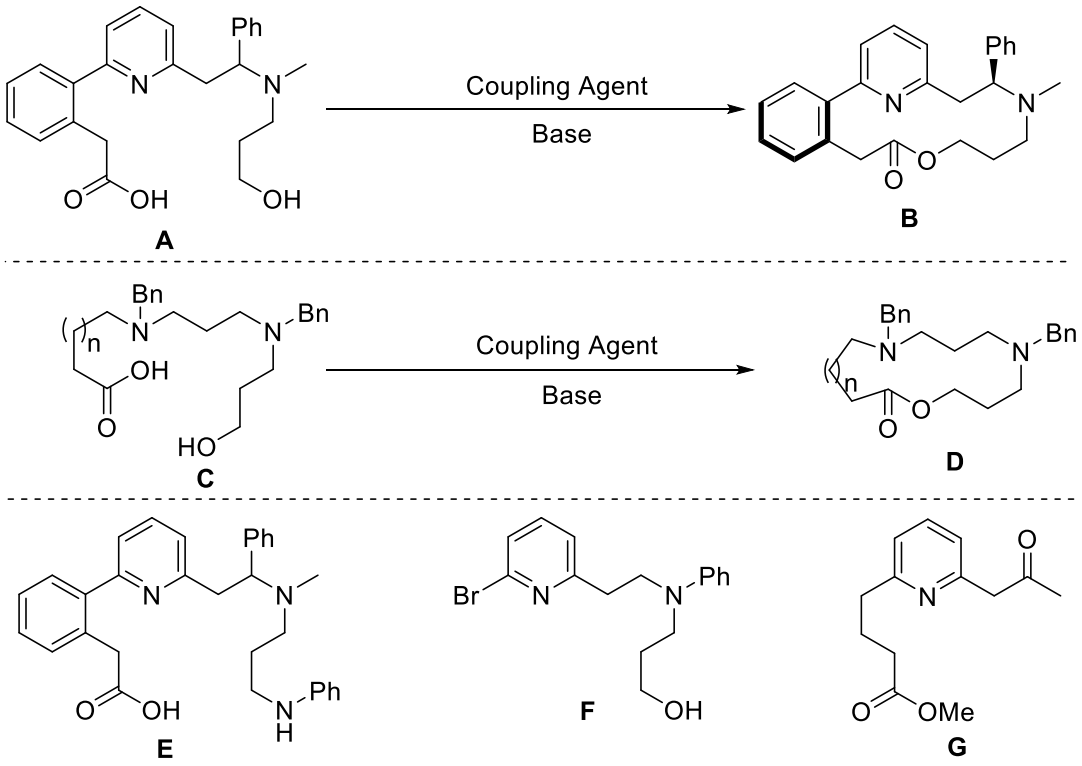

Contents

List of Tables

List of Figures

List of Schemes

Acknowledgements

I would first like to thank Dr William Unsworth for not only being an attentive, enthusiastic, and understanding supervisor but for also giving me the opportunity to grow academically in an amazing group which has allowed me to become a much more competent chemist. As well as Will, I would like to thank Professor Peter O'Brien for not only being my advisory panel member, but for also investing a massive amount of his time and effort into making me a better presenter. I would like to thank everyone from the WPU and POB groups for their welcoming attitudes and keen interest in helping, although I would specifically like to thank Dr Tom Stephens, for his brief, yet intense, introduction into the world of postgraduate chemistry, Dr Aimee Clarke, for her saint-like patience and fantastic supervision in the lab, and Kleo Palate, for having to sit next to me. I would like to also thank all the dedicated technical staff who keep the Department of Chemistry operating around-the-clock. Without the help of these fantastic people the work done in this thesis would not be possible.

Next, I would like to thank my close friends both at and outside the University of York who gave me unconditional love and support during one of the most turbulent and difficult times of my life. Specifically, I would like to thank those who supported me most during this time and by extension who I consider my second family; Phoebe Windham, Aaron Barrett, Elliott Stevens, Dan Aberg, and the other half to my stupidity, Connor Spicer. It is because of these amazing people I had the mental fortitude to persevere and complete my Masters year.

Finally, I would like to thank my mother, Marina Spurling. Without her constant love, compassion, and belief in everything I do, I would not be who I am today. It is hoped that with the work I do, including this thesis, I come close to reflecting the unfathomable amount of effort she put into raising me.

Authors Declaration

I declare that this thesis is a presentation of original work and I am the sole author. This work has not previously been presented for an award at this, or any other, university. All sources are acknowledged as references.

Dominic Eamon Spurling

Introduction

1.1 Medium-sized rings and macrocycles

Medium-sized rings and macrocycles are important in several diverse areas of chemistry and applied science; for example, they are present in many bioactive natural products,[1–4] and medicinal compounds (*e.g.* **1–2**),[5,6] as well as in countless man-made molecules with varied applications, including ligands, sensors (*e.g.* **3**), advanced materials and molecular machines (Figure 1).[7–10] Molecules containing medium-sized rings and macrocycles are therefore in high demand, prompting chemists to develop improved routes to prepare them. However, both macrocycles and medium-sized rings can be challenging synthetic targets.

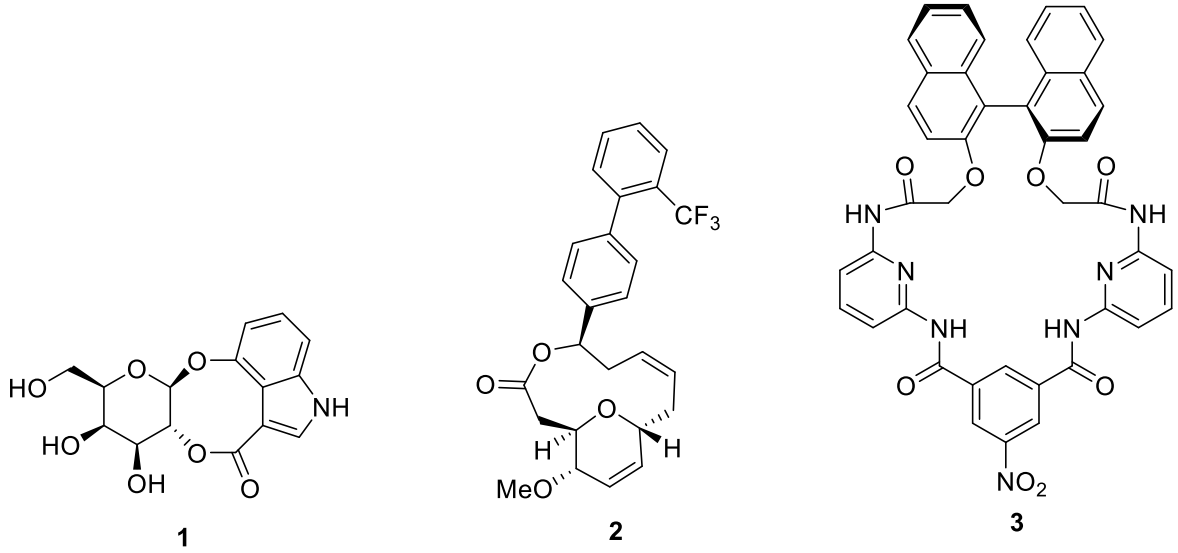

Figure 1: Medium-sized rings and macrocycles in relevant compounds. **1** (-)-ovatolide, **2** PI3Kα inhibitor, **3** NMR chiral shift reagent.

The classical way to make medium sized rings and macrocycles is via the direct end-to-end cyclisation of linear precursors (Figure 2).[11] However, when the target ring size is eight atoms or more, end-to-end cyclisation is often unsuccessful; this is due to several thermodynamic factors, such as the statistical improbability of either end of the linear precursor coming in contact, a net loss of entropy in the cyclisation, and transannular strain present in the target rings (and associated transition states).[12]

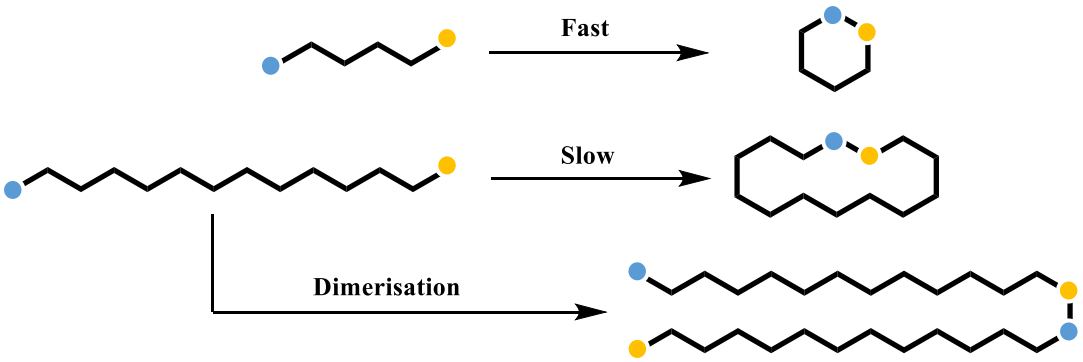

Figure 2: Simple diagram showing the difficulty of end-to-end cyclisation using longer linear precursors.

When cyclisation is relatively inefficient, intermolecular coupling becomes a major competing pathway, resulting in the unwanted formation of dimers and polymers (Figure 2).[13] To minimise these unwanted intermolecular side reactions, different approaches have been adopted over the years, including, but not limited to: high-dilution,[14] pseudo high-dilution,[15] kinetic templation, and thermodynamic templation.[16,17] However, these methods are often impractical and can introduce new problems of their own, for example, the increased financial and environmental cost of running reactions with very high solvent to substrate ratios.[18] One strategy which avoids the dilution problem is the use of ring-expansion reactions.[19] Ring-expansion reactions, in general, take already formed rings and enlarge the ring via a rearrangement reaction. By keeping the size of cyclic transition states lower, this can dramatically reduce the impact of competing intermolecular reactions (providing the rearrangement process is efficient), and as a result such reactions often do not require a specialised set-up or high-dilution.[20]

There is a diverse array of literature on the topic of ring expansion.[8,19,21] This thesis will cover several ring expansion strategies, focusing mainly on sequential/cascade ring expansion, as this subgenre of ring expansion reactions relates most closely to the work done in this thesis. However, selected non-sequential ring expansion reactions have also been included, either to introduce a complex sequential ring expansion strategy, or to exemplify key preliminary work.

1.2 Synthesis of Medium-Sized Rings and Macrocycles via Sequential Ring Expansion Reactions

1.2.1 Transesterification/Transamidation

In general, transesterification/transamidation involves the exchange of acyl subunits of an amide/ester with an amine/alcohol. An instructive example of the use of transamidation in the ring expansion field is a reaction sequence known as the 'zip reaction', a term coined by its pioneer, the late Manfred Hesse,[22] which starts with the *N*-alkylation of a lactam **4** (Scheme 1). In the example below, sodiated lactam **4** was alkylated by undergoing conjugate addition with acrylonitrile and reduced by hydrogenation to form primary amine **5**. The tethered amine of **5** was then alkylated a second time in similar fashion to give **6**. Then, addition of the strong base potassium 3-aminopropylamide (KAPA) promotes intramolecular cyclisation via a kinetically favourable 6-membered cyclic transition state (**6 → 7a)** before fragmentation of the bridging bond (**7a → 7b**), thus forming the 17-membered ring, **7b**. The same type of ring expansion process then takes place a second time, with the primary amine of **7b** attacking into the lactam, again via a 6-membered ring transitions state, to form the 21-membered macrocycle **8**.

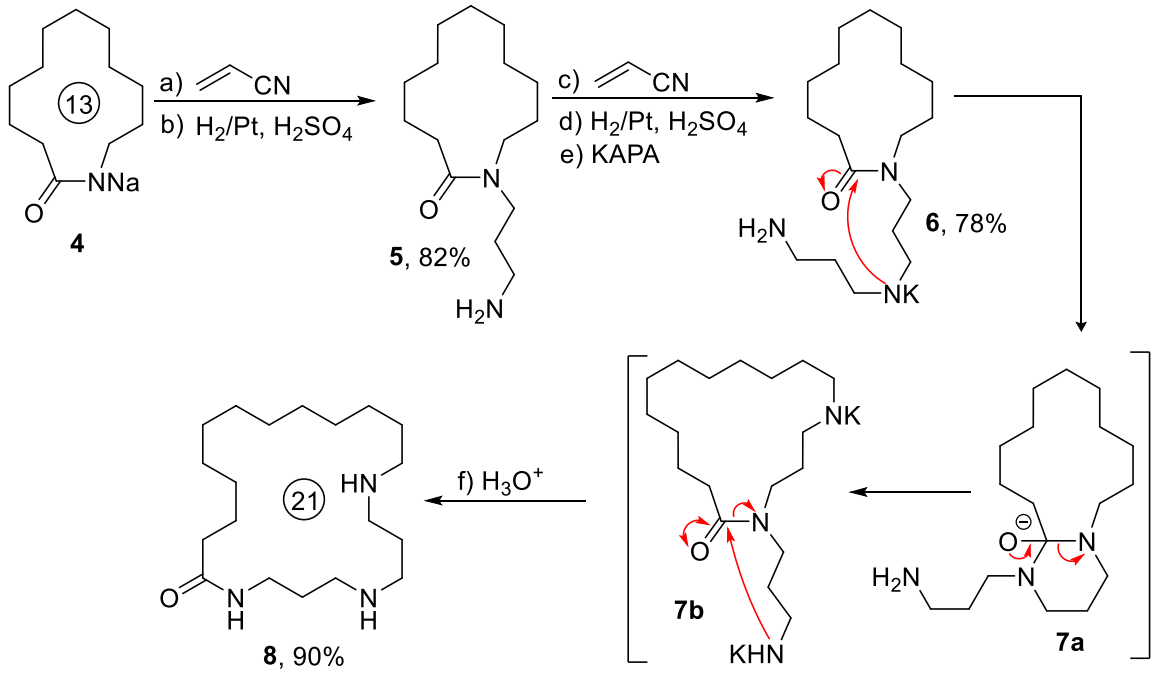

Scheme 1: The first reported incident of a zip reaction using a simple cyclic amide.

The zip reaction has the potential to increase the size of the starting lactam greatly, with the reaction taking its name from an analogy to the ring expansion resembling a zip unfurling. Scheme 2 shows the extent of this method, with the 53-membered macrocycle **10** being

formed from the 13-membered lactam with a long linear alkyl chain containing multiple secondary amines (**9**).[23] It is worth noting that while the yield reported is highly impressive (38%), the resulting 53-membered lactam **10** was characterised only by IR and TLC, and not by NMR spectroscopy or mass spectrometry, so the presence of isomeric impurities in the product cannot be ruled out.

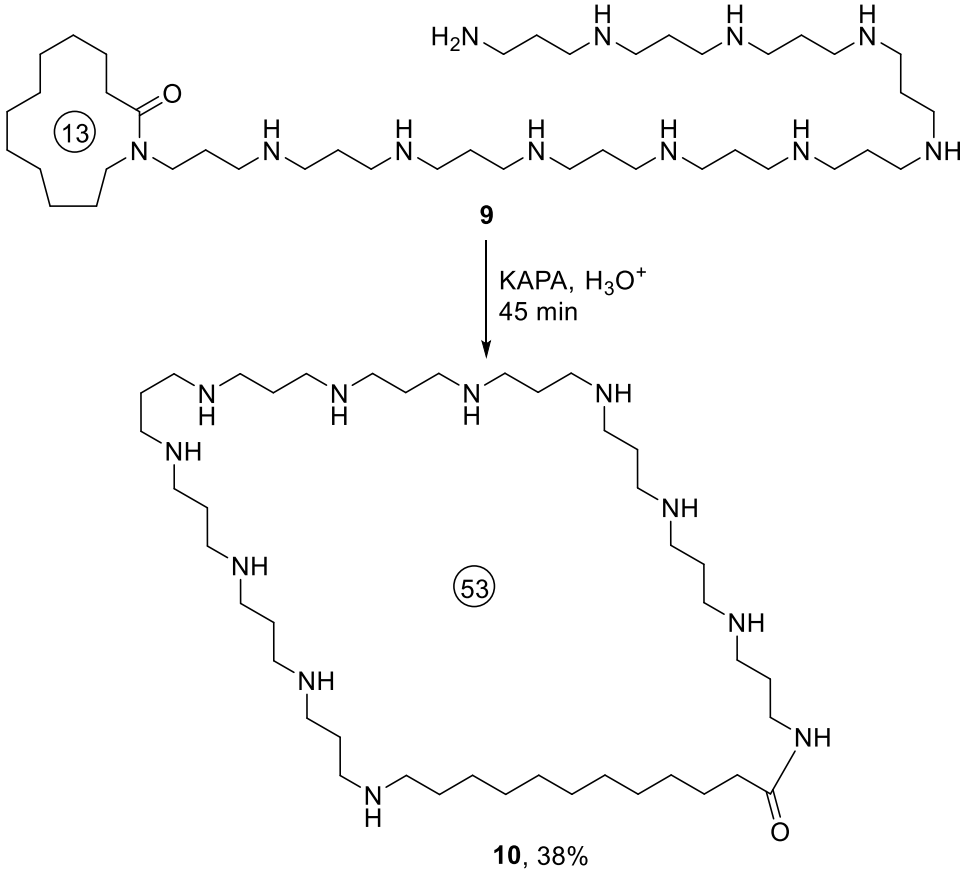

Scheme 2: A zip reaction forming a 53-membered macrocycle.

Transamidation has been frequently used in the total synthesis of macrocyclic lactam natural products (Figure 3).[24–26] A distinct feature of transamidation products is an N–N relationship separated by three to five carbons with functionalised amides, an artefact of the branched linear chain attached to the starting material, and the five to seven membered ring transition states used to make them. This relationship is highlighted in red in total synthesis products (Figure 3).

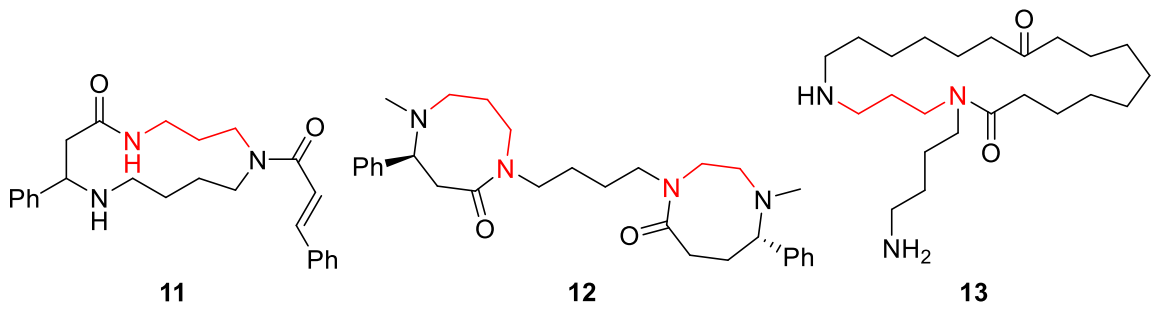

Figure 3: Natural products formed using zip reactions. Celacinnine **11**, homaline **12**, and inandenin-12-one **13.**

There are also examples of related ring expansion transesterification reactions that proceed from esters and thioesters.[27,28] For example, Scheme 3 shows 9-membered lactone **14** undergoing ring expansion via transesterification, to form the ring expanded lactone **15** in excellent 97% yield. The transthioesterification cascade shown in Scheme 4 is an interesting example of macrocyclic peptide synthesis, where the linear peptide with several free thiols, represented in a simplified form by **16**, first forms the thioester **17a** before going on to undergo repeated reversible transthioesterification exchange reactions (*e.g.* **17a** → **17b**), to form the macrocyclic peptide **18**, which is the thermodynamic product in this reaction.

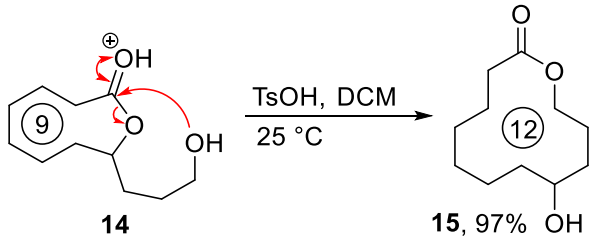

Scheme 3: Corey and Nicolaou – transesterification ring expansion to make a 12-membered ring.

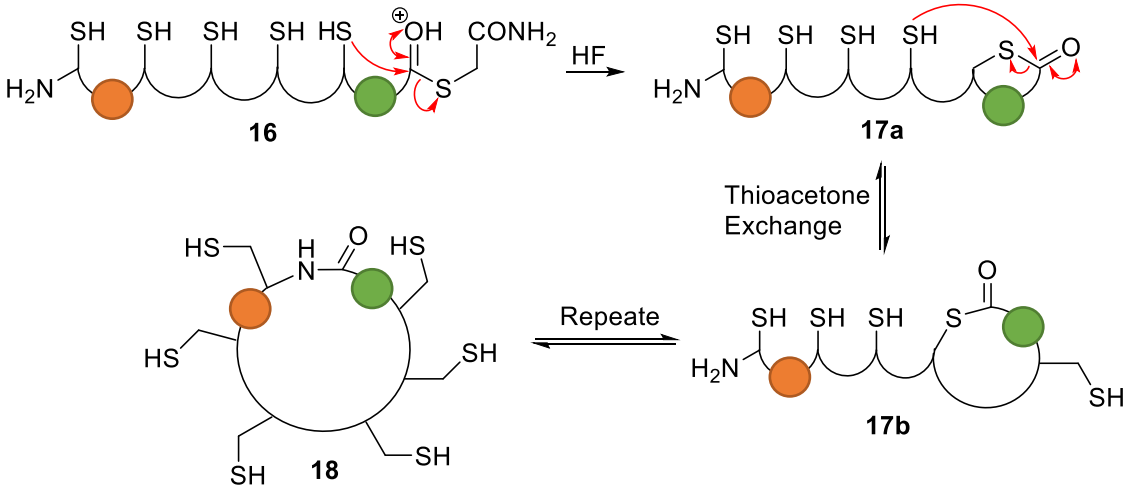

Scheme 4: J. P. Tam *et al.* – the use of transthioesterification to make large peptide macrocycles (*N*-terminal cysteine in orange and C-terminal residues in green).

However, transamidation/transesterification reactions become far less effective when trying to make medium-sized rings which are less than ten atoms in size.[21] This is largely due to the destabilising transannular interactions which are very often present between the functional groups in functionalised medium-sized rings (*e.g.* torsional strain and lone pair repulsion). This problem is especially important in reactions under thermodynamic control (which transamidation reactions usually are), because if the precursors are lower in energy than the ring expanded products, this renders ring expansion unfeasible via this approach.

1.2.2 Radical Cascade Reactions

The formation of medium-sized rings and macrocycles via ring expansion reactions which involve free radical intermediates has been well documented in the literature.[29] Many radical cyclisations involve a single ring expansion step, such as the Dowd–Beckwith reaction, shown in Scheme 5.[30] In this example, pentanone (**19**) was alkylated with dibromomethane to form **20**. The bromine in **20** was abstracted by a tributyltin radical generated using classical azobisisobutyronitrile (AIBN) initiation, to give the free radical intermediate **21a**, which then cyclises to form a cyclopropane unit, giving the bicyclic intermediate **21b**. The bridging bond of the bicyclic intermediate **21b** then fragments, forming cyclohexane structure **21c**, in which the radical is much more stable. Finally, this radial goes on to abstract a hydrogen from tributyltin hydride to give the target molecule **22** in a yield of 73%. This is a simple example of how free radicals can be used in a ring expansion.

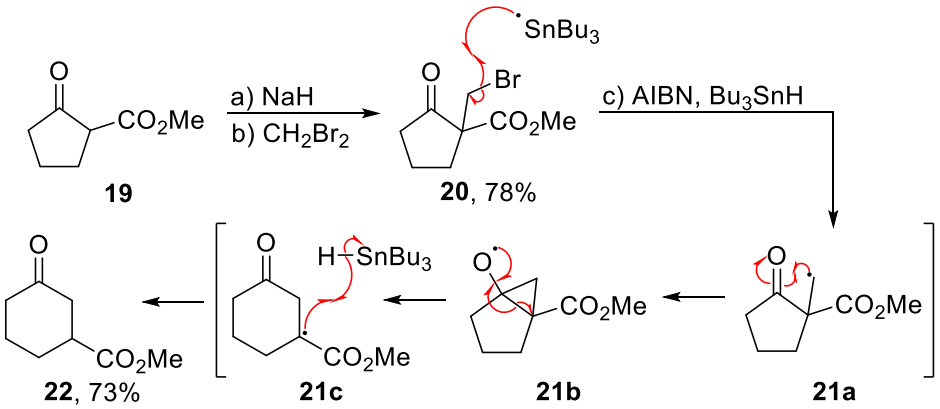

Scheme 5: Free radical ring expansion of 5-membered ring **18** into 6-membered ring **21**.

Free radical ring expansion can also be paired with other ring expansion reactions as part of sequential ring expansion strategies. Dowd and Zhang introduced sequential ring expansions mediated by free radical generation,[31] allowing for the generation of much larger cyclic

ketones (Scheme 6). Thus, silyl enolate **23** underwent a [2+2] cycloaddition with a ketene formed *in situ* from acid chloride **24**, thus forming cyclobutane **25**. Next, free radical **26a** was created from the abstraction of bromine from **25** using tributyltin hydride and AIBN. The free radical **26a** went on to cyclise and then fragment, which is presumably driven by relief of ring strain in the cyclobutene unit, affording **26b**. Hydrogen was abstracted from tributyltin hydride to give **27** before radical de-chlorination furnished the bicyclic ketone **29**. Reduction, mesylation and deprotection gave **30**, which underwent a final Grob-type fragmentation to form the final 11-membered macrocycle **31** in an overall yield of 20%.

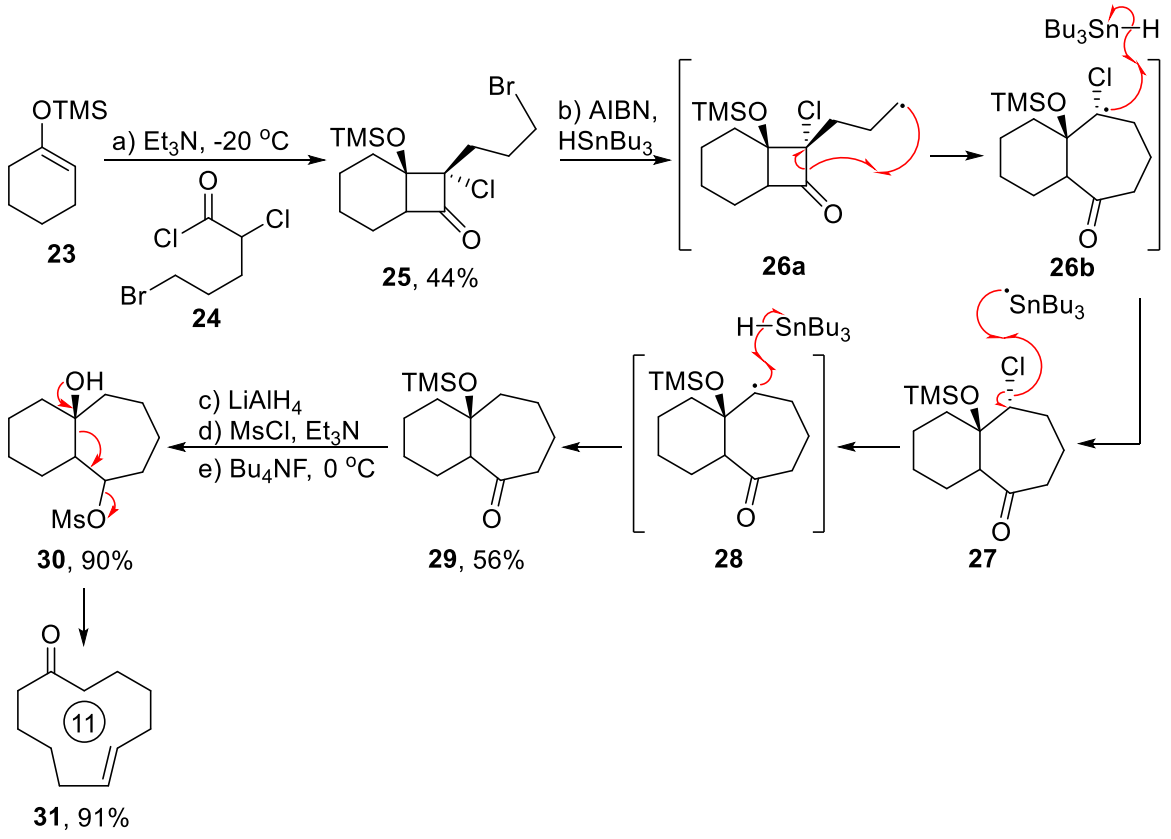

Scheme 6: Cascade radical ring expansion followed by Grob fragmentation.

Pattenden and Schulz also reported a radical-based cascade ring-expansion reaction method, that showcases the ability to use free radicals in two discrete sequential ring expansions (Scheme 7).[32] The initial vinyl radical, **33a**, was made from the alkyne **32** using $HSi(SiMe_3)_3$ and AIBN. Then, free radical **33a** readily cyclised to form the bicycle intermediate **33b**. Fragmentation of the bridged bond of bicyclic molecule **33b** led to the formation of 8-membered intermediate **33c**, which then recyclised to form the more stabilised α-silyl radical **33d**. Free radical **33d** then reacted with the oxime group to form an unstable cyclopropane unit **33e**, which ring expanded to form 6-membered ring **33f** before a silane radical was

ejected, thus propagating the chain, and forming the ring expanded oxime **34**, in a good yield of 70%.

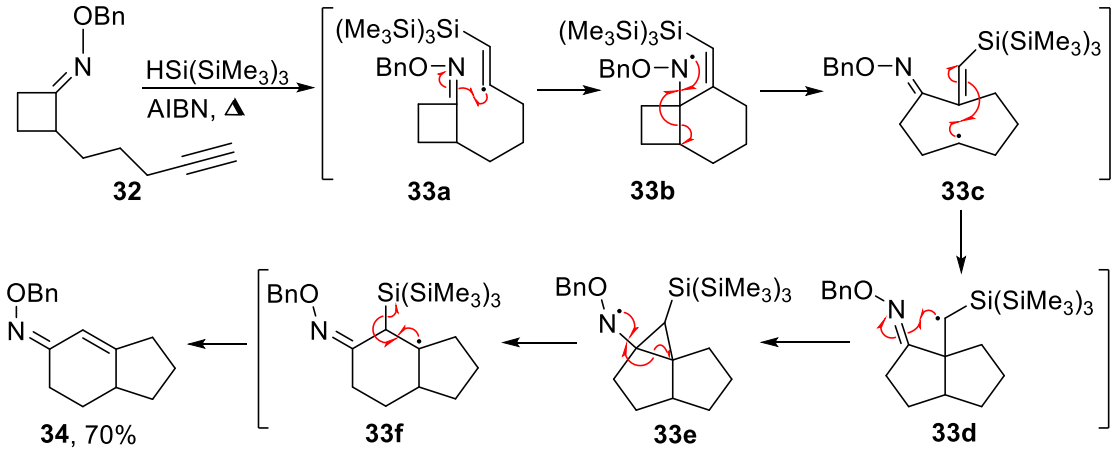

Scheme 7: Radical cascade for the conversion of four membered ring oxime **31** into 6 and 5 membered bicyclic oxime **34**.

1.2.3 Fragmentation Reactions

A classic method for forming macrocycles from polycyclic precursors is through sigma-bond fragmentation of bicyclic precursors. This is arguably best demonstrated through Grob/Wharton/Eschenmoser-type fragmentations,[33] which are all reactions in which a bridging bond in a bicyclic starting material fragments, forming a single, larger ring. Work done by Thommen *et al.*, shows an impressive example of a reaction sequence featuring sequential Grob fragmentation reactions, in which 15-membered ketone **41** was made from the tricyclic ketone **35** (Scheme 8).[34] Reduction of ketone **35** gave the tricyclic triol **36**, which was tosylated to give **37**. Diol **37** underwent Grob fragmentation promoted by *tert*-butoxide, thus ejecting the tosylate group, resulting in the ring expansion of **37** into **38** in a yield of 59%. The Grob fragmentation process was then repeated, with reduction of ketone **38** using lithium aluminium hydride to give diol **39**, tosylation to form **40** then a second Grob fragmentation to furnish the 15-membered ketone **41**, with defined *Z*,*Z* stereochemistry, in excellent yield of 90%.

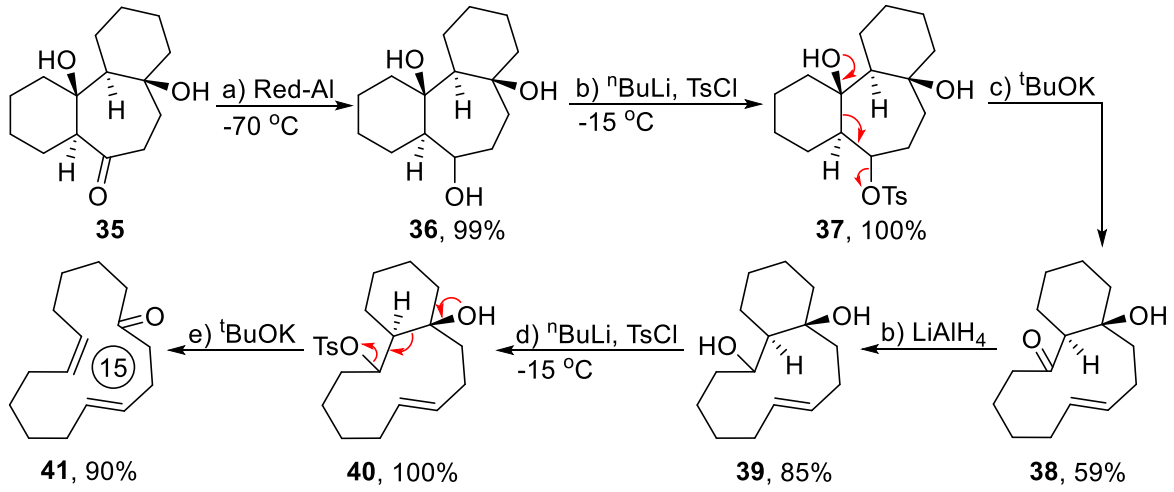

Scheme 8: Double ring expansion *via* Grob fragmentation.

As detailed before (Scheme 6), Grob fragmentation can be used in conjunction with other ring expansion reactions. This is demonstrated by Ikeda *et al* [35] in the synthesis of the natural product (±)-phoracantholide M (Scheme 9). In this example, an initial Grob-type fragmentation (**44** → **46**) preceded an oxidative ring expansion fragmentation of bicyclic molecule **46**, to form the 12-membered lactone **47**. Initial cyclisation of tethered alkene **42** was achieved through a [2+2] photocycloaddition, forming the strained tricyclic structure of **43**. Mesylation of the alcohol **43** gave **44**, which underwent Grob fragmentation giving **45**, which tautomerised to form the bicyclic ether **46**. Oxidation of the more nucleophilic alkene of diene **46** to epoxide **47** with *m*-CPBA and subsequent ring expansion of **47** furnished the 12-membered lactone **48** in a yield of 58%.

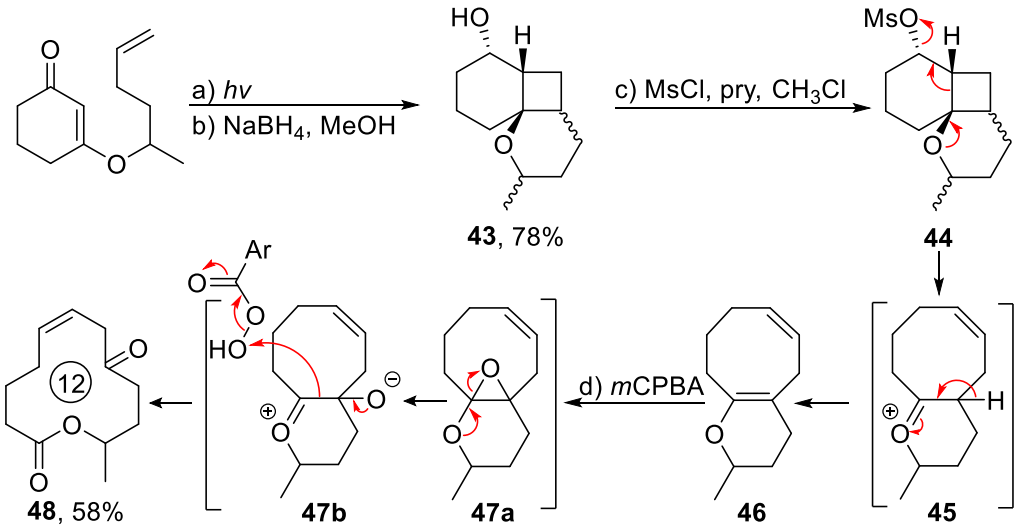

Scheme 9: Grob fragmentation followed by oxidative expansion leading to a cascade ring expansion.

Work from Maio *et al.*[36] shows an interesting oxidative fragmentation reaction preceding transesterification to give sequential ring expansions, thus forming the 11-membered lactone

54 (Scheme 10). Nucleophilic attack of α-silyl cycloalkanone enolate **49** into oxetane **50** gave the bicyclic hemiketal **51**. Oxidative fragmentation of hemiketal **51** with ceric ammonium nitrate (CAN) then formed the 8-membered lactone **52**. Lactone **52** was reduced by hydrogen on palladium before undergoing acid catalysed transesterification (**53** → **54**), forming the 11-membered lactone **54**, in yield of 47%.

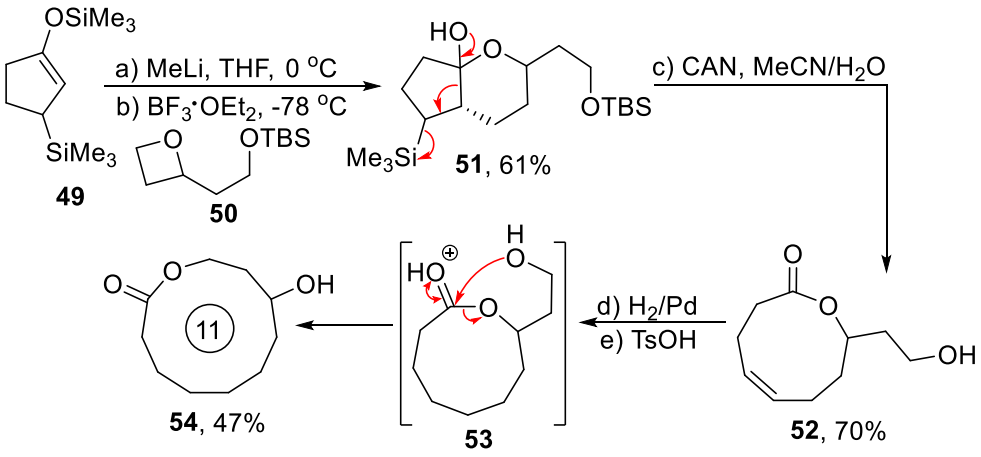

Scheme 10: Oxidative fragmentation followed by a transesterification.

With numerous routes to build multicyclic rings and the ability to combine fragmentation with other classes of ring expansion, fragmentation reactions have great scope and versatility when forming medium-sized rings and macrocycles through sequential ring expansions.

1.2.4 Pericyclic Reactions

A pericyclic reaction is the process by which bonds are made or broken via a concerted, cyclic transition state.[37] They have been used to make medium-sized rings and macrocycles in cascade ring expansion sequences, examples of which are summarised in this section. The examples shown focus on the use of hetero-conjugated species with sigmatropic rearrangements mediated by nitrogen and sulfur.

Taking advantage of the diverse reactivity of sulfur ylides, a reaction conceived by Vedejs *et al.*,[38] (Scheme 11) is a good example of consecutive sigmatropic rearrangements. Acid catalysed addition of diazo **56** to cyclic sulfide **55** formed sulfide salt **57**, which was subsequently deprotonated to form sulfur ylide **58**. The first of two [2,3]-sigmatropic rearrangements then gave the expanded 8-membered ring **59**. Next, sulfide **59** was converted into **60** via a Wittig olefination, before the alkylation process was then repeated with the

addition of diazo **61** to form the ylide **62**, followed by a sigmatropic rearrangement to form the 11-membered sulfide ring **63**, with Z,Z stereochemistry.

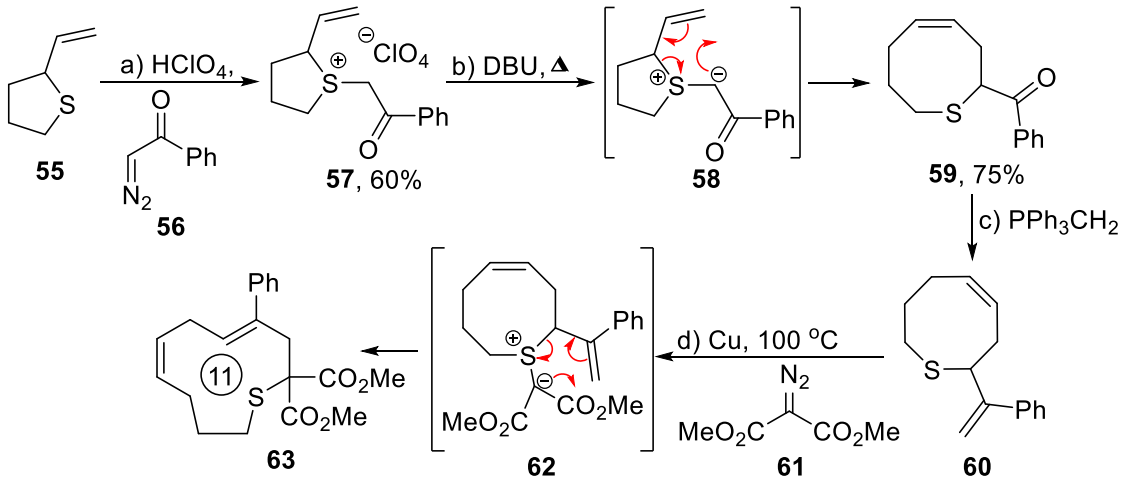

Scheme 11: Successive sigmatropic rearrangement using sulfur ylides to form an 11-membered ring.

This strategy of consecutive ring expansion via sigmatropic rearrangements of cyclic sulfides was simplified and expanded by Schmid *et al.*[39] who built upon the procedure presented by Vedejs through simple alkylation of cyclic sulfides using alkyl halides and TFA as part of a two-step addition/expansion. This is illustrated in Scheme 12; alkylation of sulfide **55** with allyl bromide which gave sulfide salt **64**, and subsequent deprotonation with potassium hydroxide gave sulfur ylide **65**. Ylide **65** then rearranged to give the ring expanded sulfide **66**. This is the key point where Schmid's sigmatropic rearrangement approach differs to that of Vedejs is that **66** now is ready for alkylation without further modification, making cascade ring expansions much easier in fewer steps. Thus, Scheme 12 also shows a second iteration of alkylation/expansion forming the 11-membered ring **69** with overall yield of 49%.

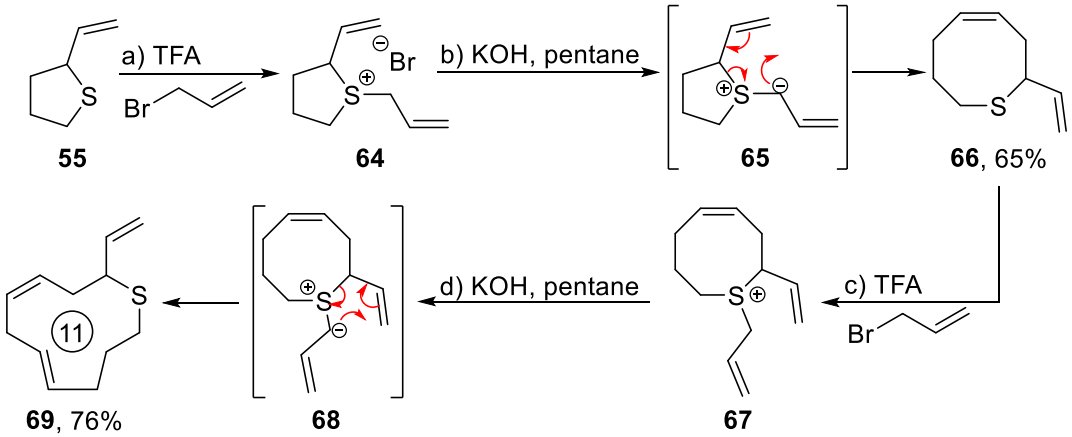

Scheme 12: Ring expansion *via* alkylation and sigmatropic rearrangement.

However, a drawback to the simplified alkylation rearrangement method (Scheme 12) was highlighted by Vedejs *et al.*,[40] who isolated a side-product in equal quantities to the ring expanded product **66**, thus revealing an unwanted side reaction. As is shown in Scheme 13, deprotonation of the proton α- to sulfur on the ring in sulfide **70**, rather than the exocyclic proton, forms ylide **71** and this led to a rearrangement to form undesired side product **72**. Sulfide **72** can go on to become alkylated and disrupt the reaction further. This problem is caused by the lack of regioselectivity from the DBU in the deprotonation step (**70** → **71**); as both environments appear to be relatively similar, and hence would be expected to have a similar pK_a value, arguably this side reaction is not surprising.

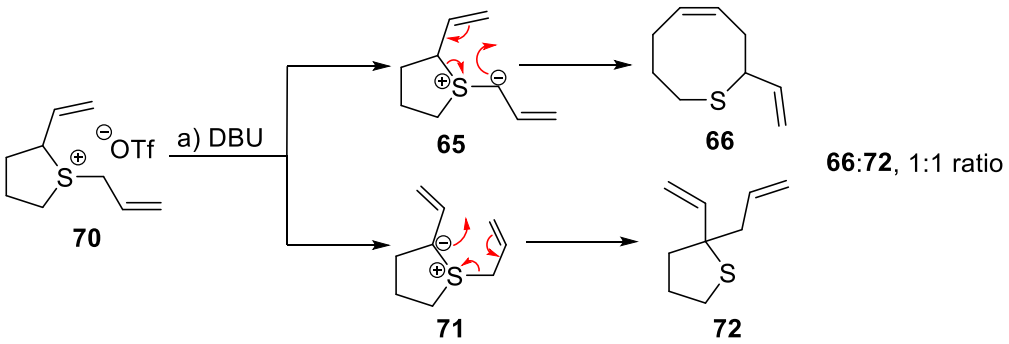

Scheme 13: Undesired side product formation in sulfur ylide sigmatropic rearrangement.

Sequential ring-expanding sigmatropic rearrangements of molecules containing nitrogen are less common than those containing sulfur, but there are notable exceptions. Work done by Back *et al.*[41] (Scheme 14) shows two [3,3]-sigmatropic rearrangements of a pyrrolidine to form the 14-membered *N*-heterocycle **80**. Electrophilic addition of the acetylenic sulfone to heterocycle **73** gave ammonium zwitterion **74** which underwent aza-Cope sigmatropic rearrangement, expanding **74** to the neutral 10-membered enamine **75**. Enamine **75** was selectively hydrogenated in the presence of palladium on carbon to give enamine **76**. Alkylation of enamine **76** with a Grignard reagent and removal of the tosyl group furnished the saturated heterocycle **78**, which underwent electrophilic addition with acetylenic sulfone to give ammonium zwitterion **79**. The unstable ammonium zwitterion **79** once more underwent a sigmatropic rearrangement forming the expanded 14-membered ring **80** in a good yield of 89%.

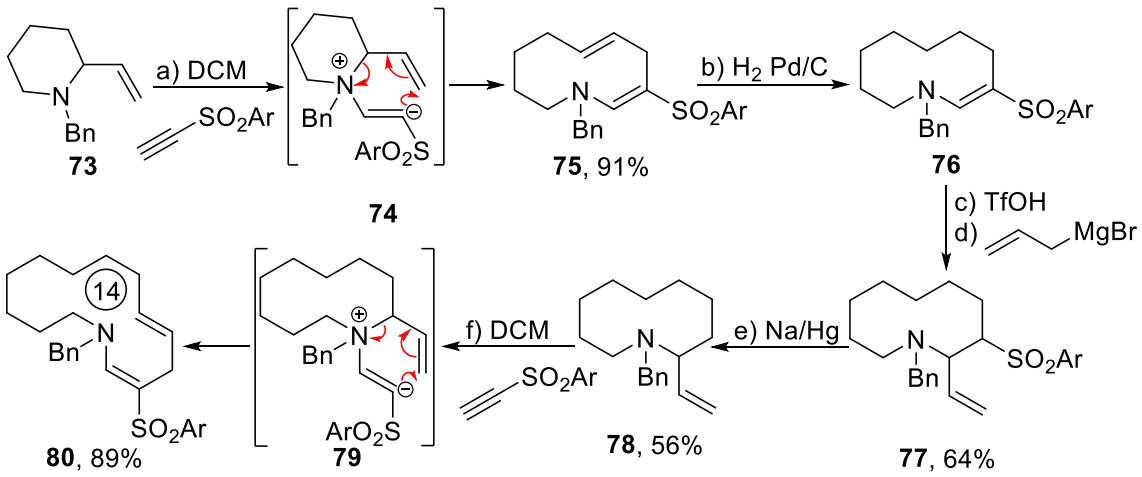

Scheme 14: Consecutive aza-Cope sigmatropic rearrangement.

Scheme 15 shows a tertiary amine mediated sigmatropic rearrangement by Suh *et al.*,[42] who demonstrated the use of aza-Claisen rearrangements in consecutive ring expansions in their total syntheses of fluvirucinines. Enolisation of the cyclic amide **81** to enolate **82** gave the conjugation needed for the aza-Claisen rearrangement. This rearrangement proceeded via the breaking of the cyclic N-C bond and formation of the cyclic C-C σ-bond and thermodynamically favoured *E*-isomer π-bond in turn expanding the ring into the medium-sized lactam (**83**). After several steps (**83** → **84**, not shown) the same process was repeated to convert **85** into **87**. Cyclic secondary amine **85** was then acylated before undergoing enolization and sigmatropic rearrangement to give lactam **87** in good yield of 74%.

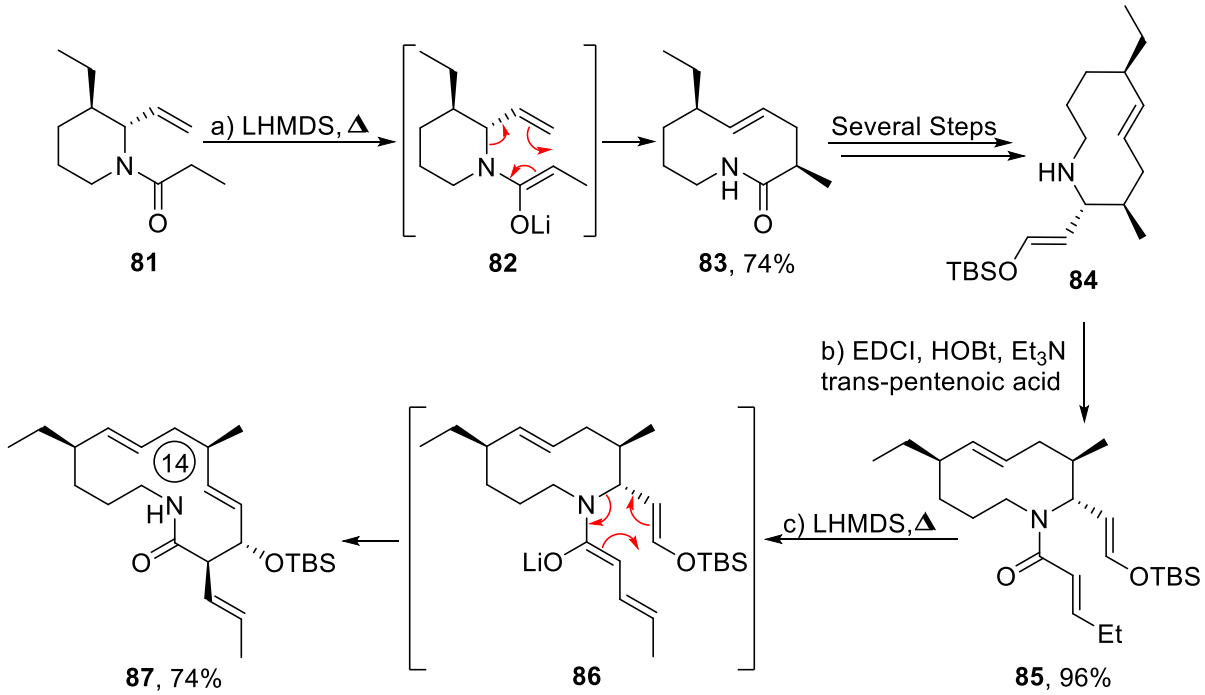

Scheme 15: aza-Claisen rearrangements giving ring expanded macrocycles.

A creative method of expanding a ring in an iterative fashion is presented by Seyden-Penne *et al.* [43] who reported a way to expand saturated lactones by one carbon at a time. This is done through the generation of chlorocarbenes and their subsequent cycloaddition with silyl enolates to form cyclopropane units which collapse into rings one atom larger than the precursor (Scheme 16). Starting with enolization of lactone **88**, silyl enolate **89** was reacted with a chlorocarbene (formed *in situ*) to form the strained bicyclic system **90** which readily collapsed into the much less strained lactone **91**. After hydrogenation (**91** → **92**), the same process can be repeated until the desired sized lactone is formed, in this case a 10-membered lactone was formed (**93**) through two more iterations.

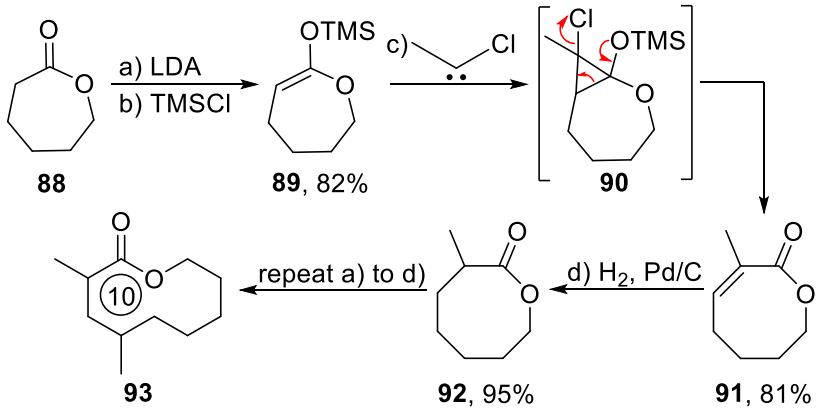

Scheme 16: Formation of macrocycles through iterative carbene cyclopropanation and expansion.

This single atom ring expansion strategy could theoretically be performed any number of times to make any ring size desired; however, the overall yield of **88** → **92** is 63%, and this restricts the utility of the reaction somewhat, as after only three iterations, the ring is expanded by three atoms with an overall yield of 25%. Compared to other methods which allow for ring expansion of similar magnitudes with higher yields, single atom ring expansion is therefore less favourable, at least when larger changes in ring size are required.

1.2.5 Ring Expansion Metathesis Polymerisation

Olefin metathesis is a reaction popular in synthesis that involves the exchange of substituents between a pair of alkenes to generate a new pair of different alkenes.[44] This reaction has been expanded on greatly since its inception, and has been used in many areas of synthetic chemistry, including macrocycle formation. However, many methods to make macrocycles through metathesis do so through ring-closing metathesis (RCM),[45] using a long, linear precursor, which can encounter the same problems with competing intermolecular reaction

discussed earlier.[13] In order to avoid this, metathesis can be used to expand the size of an olefin containing cyclic compounds.

Scheme 17 is an example of ring expansion metathesis polymerisation (REMP), first showcased by Grubbs *et al.* [46,47] Cyclopentene **95**, Grubbs catalyst II (**94**) and acyclic diene **96** were heated at reflux for 12 hours in DCM to yield the ring expanded product **100** in 43% yield, in going from a 5-membered ring to an 18-membered ring. Mechanistically, this proceeded through the ring opening metathesis of **95** to form **97b**, which underwent cross metathesis with diene **96** to award the long linear diene **98**. Diene **98** then underwent ring closing metathesis (RCM) using the same catalyst **94** to yield the final macrocycle **100** in yield of 43%. Scheme 16 shows the formation of an 18-membered ring using the bis-vinyl ketone **96** which reacts selectively with terminal olefins in excellent yields, minimising by-products and driving the reaction forward. The largest ring size reported in this manuscript using REMP was 26, however, it is worth noting that once ring opening metathesis of pentene (**95**) occurs, the molecule becomes linear. For this reason, it could be argued that with the ring opening of pentene (**97a** → **97b**) diminishes the advantages that ring expansion has over end-to-end cyclisation.

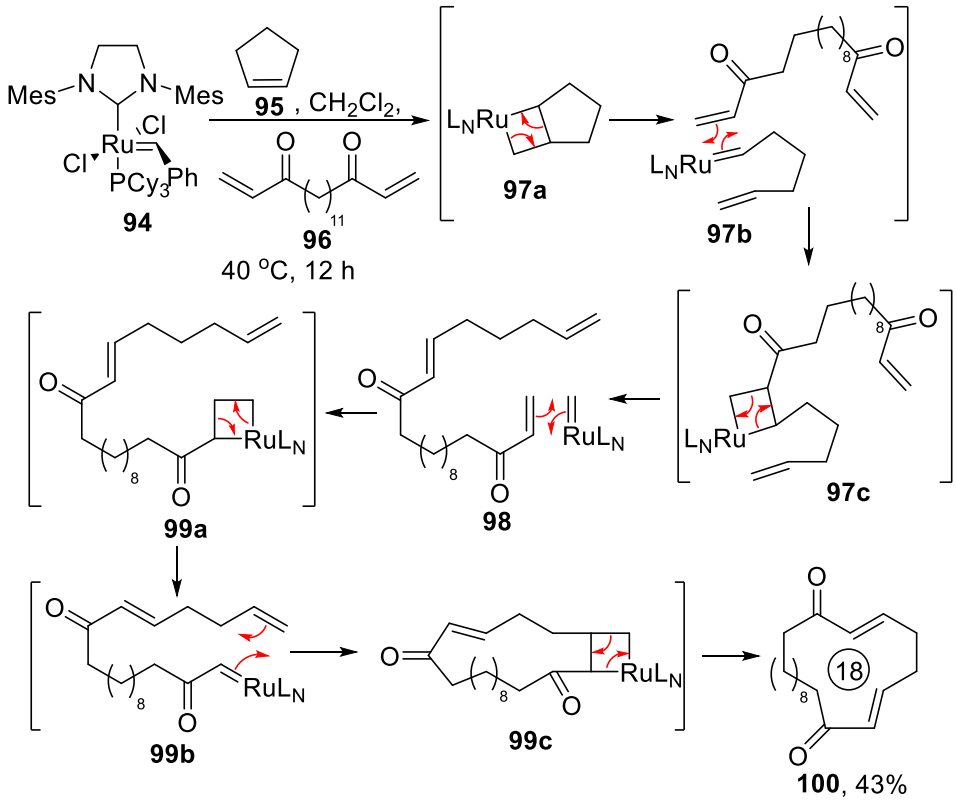

Scheme 17: Formation of 18-membered macrocycle **100** through REMP.

This idea was developed further by Veige *et al.*,[48] who reported a tungsten catalyst (**101**) able to cyclise norbornene monomers into a single large cyclic polymer using successive REMP in a catalytic cycle. A generic example is shown in Scheme 18, in which an *n* number of norbornene units are cyclised to form a ring which is 5*n* carbons in size.

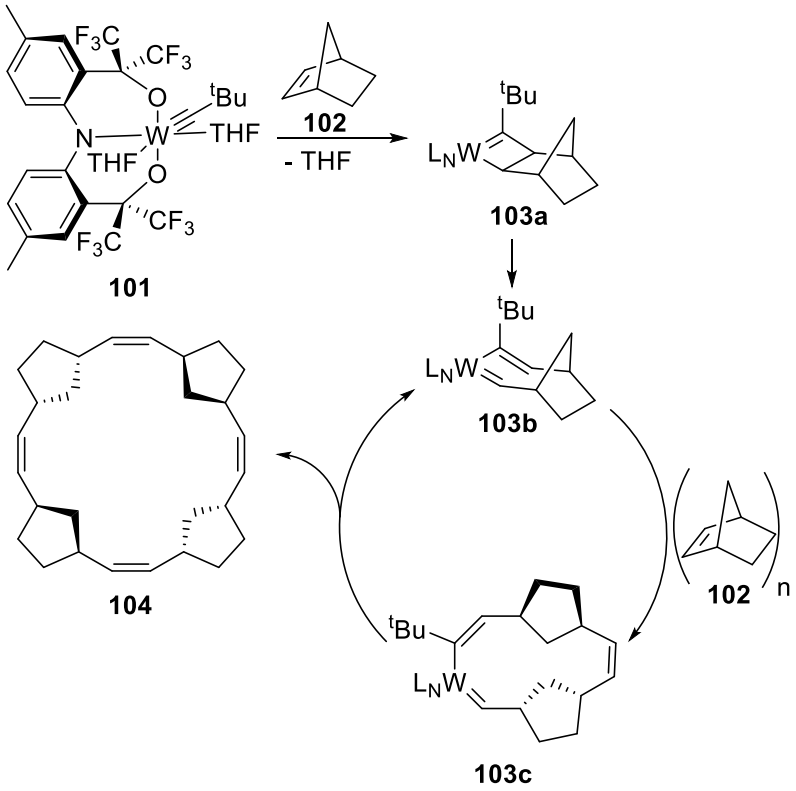

Scheme 18: Catalytic cycle of successive REMP through polymerisation of norbornene units.

Tungsten catalyst **101** is activated by a norbornene through the [2+2] cycloaddition between the alkene group of the norbornene and the catalyst to form complex **103a**. Intermediate **103a** then underwent a [2+2] cycloaddition to give the less strained active catalyst **103b**, possessing a reactive alkene which underwent metathesis with another norbornene, expanding the intermediate ring, to give **103c**. This process is repeated until the intermediate undergoes a final RCM step, to yield a macrocycle with 5*n* carbons in size, where *n* is the number of norbornene units. Once the macrocycle product is detached (**103c** → **104**) the active catalyst **103b** can go on to react further to generate more macrocyclic polymers. A noteworthy point is the ring expanded macrocycle contains only *cis* alkene isomers, and is highly syndiotactic, demonstrating the stereoselectivity of the catalyst.

Although REMP allows for the construction of large macrocycles and cyclic polymers alike, there are few examples of using pre-functionalised rings and reagents, most likely due to the difficulty of finding suitable reaction conditions that avoid competing cross metathesis and

linear polymerisation.[47] This somewhat limits the scope of this reaction for the synthesis of bioactive molecules and natural products, and at present, there are no examples of this method being used in total synthesis.

1.2.6 Rhodium-Catalysed Ring Expansion

Over the past decade there has been keen interest in the use of rhodium complexes to expand strained cyclopropane/cyclopropene rings into larger medium sized rings via the generation of rhodacyclopentanones.[49] Expansion of a ring through the insertion of a rhodium complex was first reported in 2010 by Wang *et al.*,[50] who expanded a strained cyclopropene unit into a 5,6-bicyclic molecule in a Rh(I)-catalysed carbonylative carbocyclisation reaction (Scheme 19).

The catalytic cycle is summarised in Scheme 19, for the formation of bicyclic amine **108** from propene **105** using $[Rh(CO)_2Cl]_2$ (5% mol) in DCE at 80 ^oC for 12 h. The rhodium catalyst undergoes an oxidative addition reaction via insertion into the cyclopropene **105** to form intermediate 4-membered rhodium complex **106a**, partially relieving the strain of the previous cyclopropene unit. Insertion of carbon monoxide into the ring then increases the size of the rhodium-containing ring from a 4- to a 5-membered ring, affording the rhodacyclopentenone complex **106b** which then undergoes a [3+1+2] cycloaddition with the tethered alkyne, to give rhodium intermediate **106c**. Reductive elimination of intermediate **106c** then takes place to regenerate the active catalyst and yield the target 5,6-bicyclic compound **107**, which tautomerises to form the aromatic compound **108** in yield of 83%.

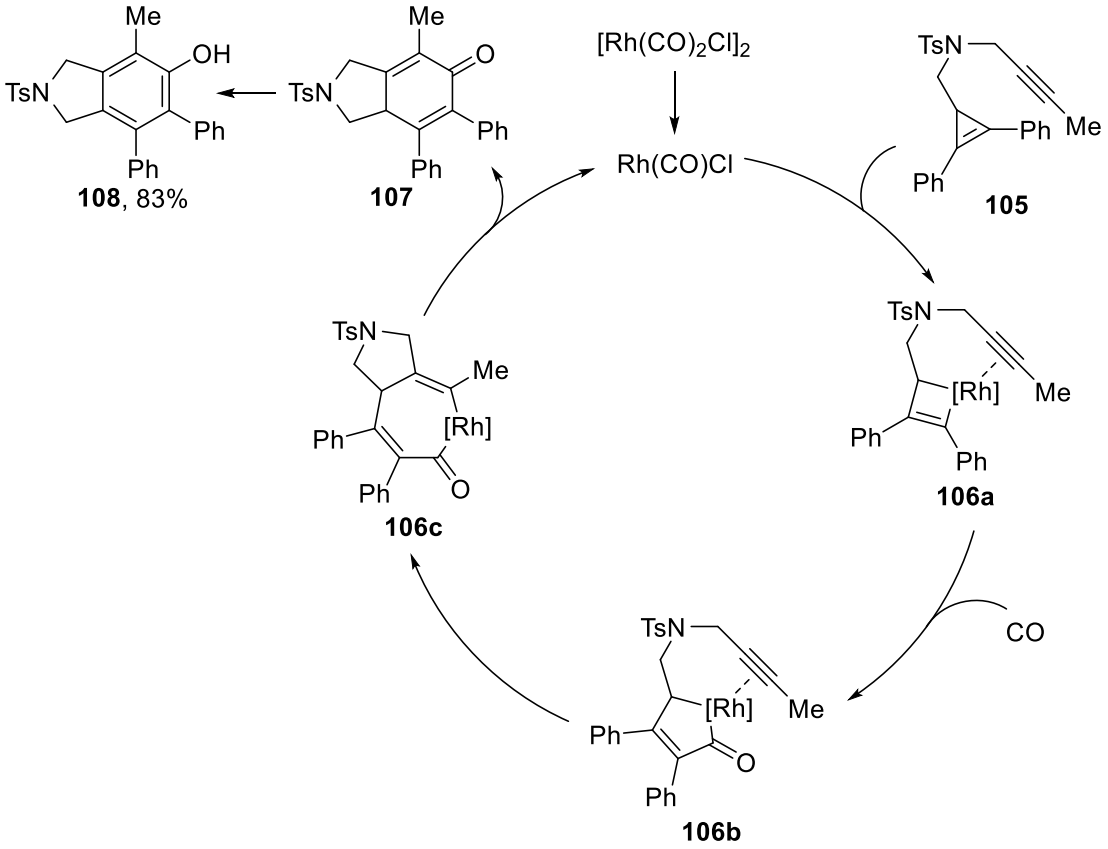

Scheme 19: Proposed catalytic cycle for Rh(I)-catalysed carbonylative carbocyclisation of cyclopropene.

This work has since been expanded on, by increasing the ring size of the target molecule and by the introduction of heteroatoms into the ring. Bower *et al.* showcase both of these features in their work summarised in Scheme 20, with the directed ring expansion of an aminocyclopropane into an 8-membered *N*-hetrocycle.[51] The rhodium catalyst inserts into cyclopropane unit of indole **109** to give the 4-membered rhodium ring **110a**. Next, chelation to the amide carbonyl group directs the insertion of CO, forming rhodacyclopentenone **110b**. The nucleophilic C3-position of the indole unit on **110b** can coordinate to the rhodium metal centre, a process termed "capture", to form **110c**, and the tricyclic structure **110c** then "collapses" by undergoing reductive elimination, in turn gaining a proton and forming the 8-membered target N-heterocycle **111**, in a good yield of 77%.

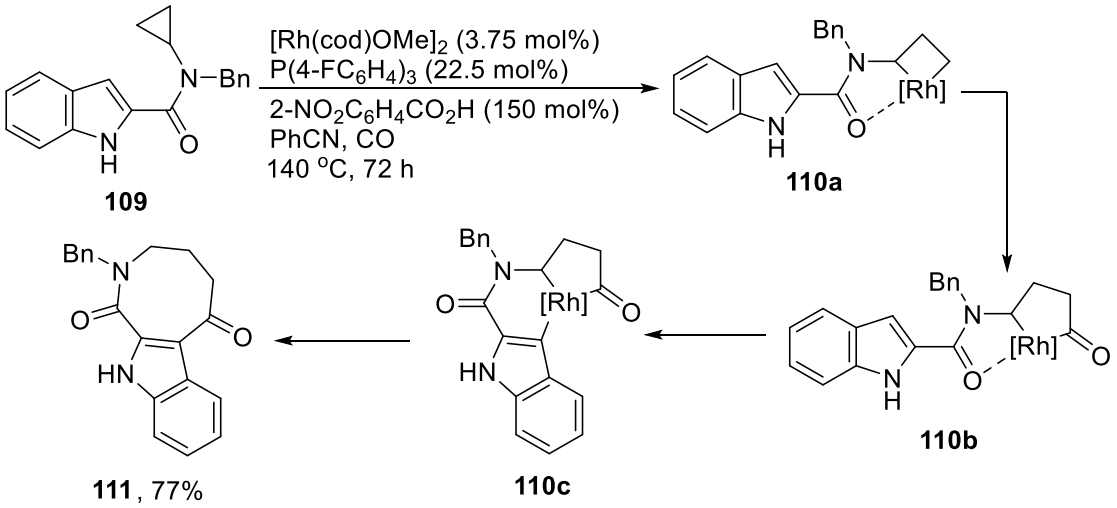

Scheme 20: "Capture-collapse" directed carbonylative C-C ring expansion of aminocyclopropane.

It is also possible for rhodium to insert into cyclobutane units. Ito *et al.*[52] showcased the ability of rhodacyclopentanone complexes to form lactones from cyclobutene units via the ring expansion of cyclobutanone **112** (Scheme 21). In this study, the rhodium complex inserts into the cyclobutanone unit of **112** to generate rhodacyclopentanone complex **113a**. Thus, the rhodium atom first coordinated to the phenolic hydroxy group of **112**, bringing the rhodium into close proximity to the α C-C bond, allowing for insertion and formation of **113b**, and finally, β-hydride elimination yields the target 7-membered lactone **114** in 86% yield. It is worth noting that although the reaction was carried out under a CO atmosphere, CO is not directly involved in the reaction mechanism unlike previous rhodium-catalysed ring expansion reactions (See Scheme 19).

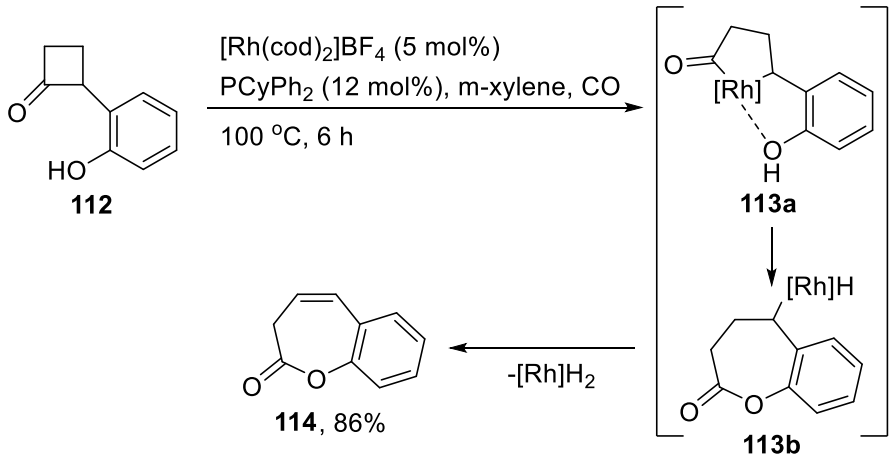

Scheme 21: Lactone formation by rhodium-catalyzed C−C bond cleavage of cyclobutanone.

1.2.7 Successive Ring Expansion

Successive ring expansion (SuRE) is a method pioneered in York by Unsworth *et al.*,[53] and is based on the iterative insertion of hydroxy acids/amino acid derivatives into cyclic β-ketoesters to form lactones/lactams. The iterative nature of the method enables ring expansion to be performed several times to form a range of different sized rings via a relatively short reaction sequence. An early example is summarised in Scheme 22. In this reaction, 12-membered β-ketoester **115** was reacted with acid chloride **116** in the presence of magnesium chloride and pyridine to promote acylation of the β-ketoester. Following acylation, the Fmoc protecting group on the tethered amine of **117** was cleaved using piperidine, exposing primary amine **118a** which then underwent rapid cyclisation to form **118b**, via a 6-membered ring transition, and fragmented to form the ring expanded macrocyclic lactam **119**, in an impressive overall yield of 80%. As the product **119** also contains a cyclic β-ketoester motif, the same sequence of reactions can then be repeated; thus, the process was repeated using the same conditions, to yield the 20-membered macrocycle **120**, and then again to form the large 24-membered macrocycle **121**.

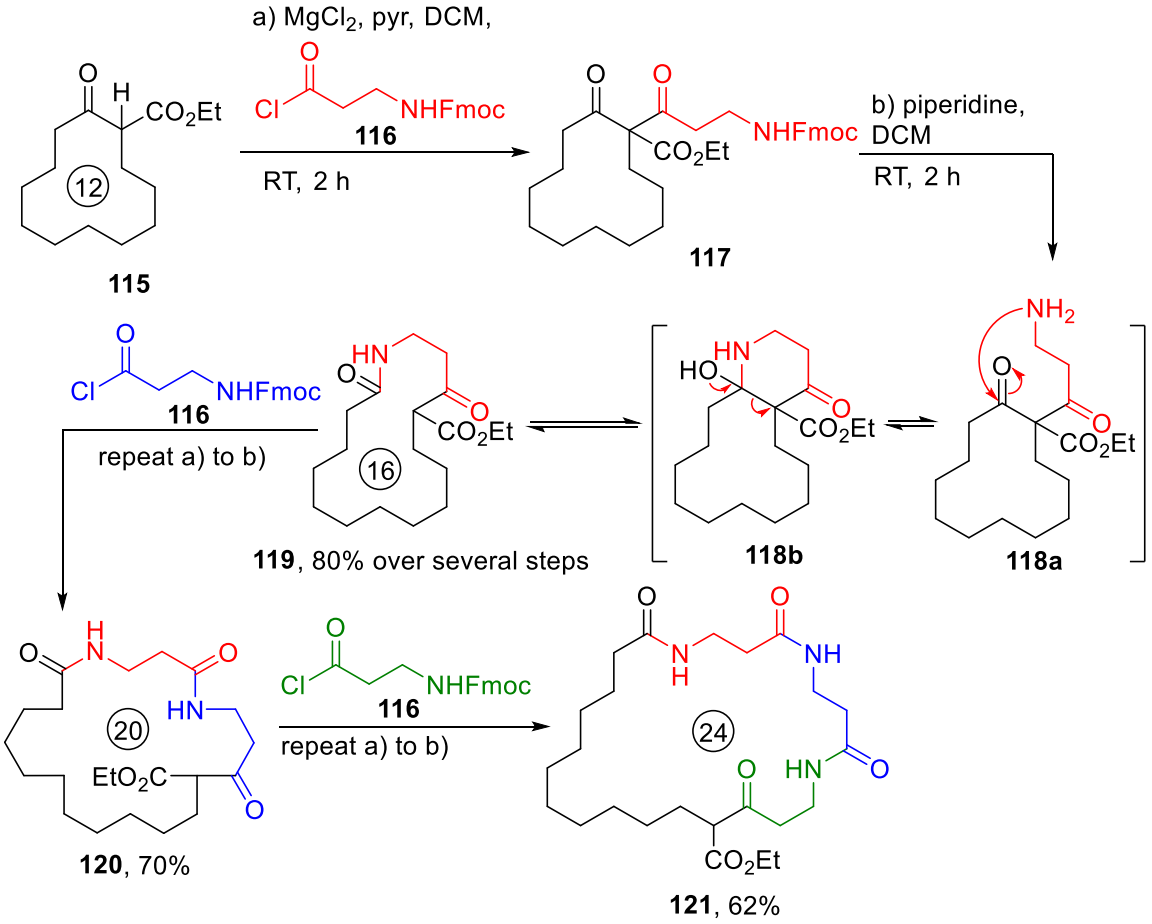

Scheme 22: Successive ring expansion reactions with β-amino acid fragments.

Successive ring expansion allows for the acylation of rings with amino acid fragments varying from three or four atoms long, and the high yielding nature of successive ring expansion allows for up to three iterations, before inefficient acylation prevents further expansion. This makes it an appealing and practical route for macrocycle synthesis. The linear fragments can be pre-functionalised with a variety of useful handles before ring expansion, make SuRE an attractive way to construct diverse functional macrocycles and medium sized rings, and to exemplify this, the group used the method to create a of library medium-sized ring scaffolds for inclusion in a high-throughput-screening library. [54]

Successive ring expansion can also be used for the expansion of lactam starting materials (Scheme 23).[55] For example, 12-membered lactam **122** can be acylated with acid chloride **123** at reflux in DCM with 4-dimethylaminopyridine (DMAP) and pyridine. In this work, tethered amine **125a** was revealed through Fmoc cleavage of **124,** this time using DBU as base, and this amine underwent *in situ* cyclisation to **125b** and fragmentation, forming the ring expanded lactam **126** in an excellent overall yield of 91%. Lactam **126** can be acylated and expanded again in the same way, and thus, using this procedure the expansion (steps a and b) was repeated three times to form the 24-membered lactam **128**. After three iterations of the SuRE method, the lactam **122** had near doubled in size with an overall yield of 58%.

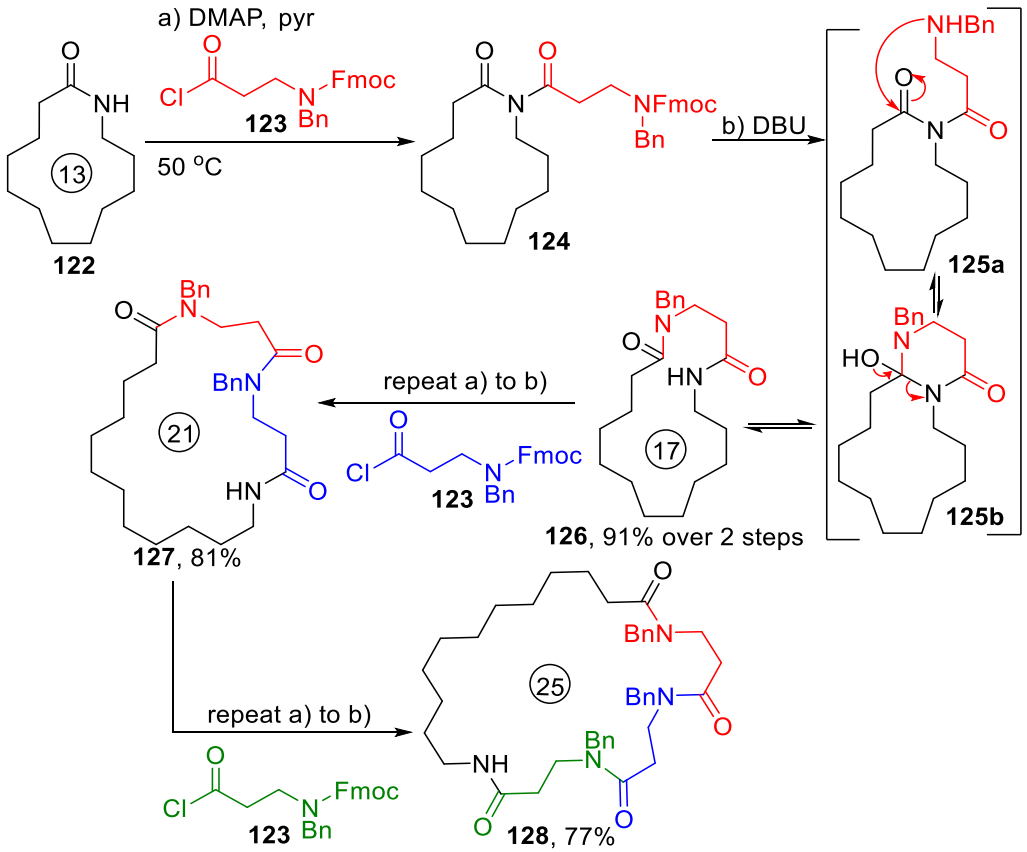

Scheme 23: Successive ring expansion using simple lactams and β-amino acid fragments.

The insertion of hydroxy acid fragments is also possible using lactam starting materials, allowing for the synthesis of macrocyclic lactones.[56] The chemistry outlined in Scheme 24 is conceptually similar to the amino acid variant shown in Scheme 23, with the same acylation conditions used to convert lactam **129** into **131**, but in this case acylation was done with a benzyl protected hydroxy acid derivative **130**. Now, the deprotection step was performed via hydrogenolysis to cleave the benzyl group and reveal the tethered alcohol (**131**→**132a**) and following addition of triethylamine as a weak base, lactam **132a** underwent smooth ring expansion to form lactone **133** in high yield of 94%. Expanded lactam **133** could then be acylated and ring expanded twice more in the same way, to form first 17-membered macrocycle **134**, and then the 21-membered macrocycle **135** in 84% yield.

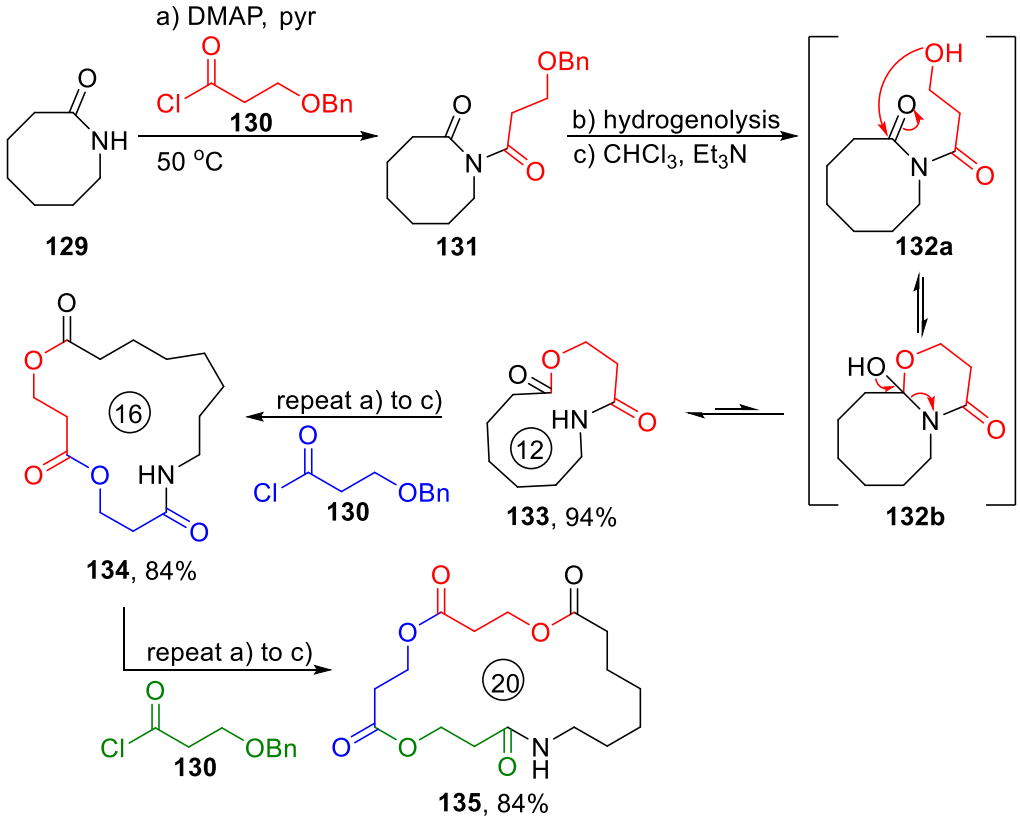

Scheme 24: Successive ring expansion using simple lactams and β-hydroxy acid fragments.

Hydroxy and amino acid fragments (both α and β) can be used interchangeably in successive ring-expansion reactions. This is illustrated by the successive ring expansion product **138**, where the starting material, 13-membered lactam **123**, was acylated and expanded using β-hydroxy acid fragment **130** (red) before being acylated and expanded by α-amino acid fragment **137** (blue), to furnish the 20-membered macrocycle **138** in overall yield of 77%, with several similar mixed examples also having been reported.

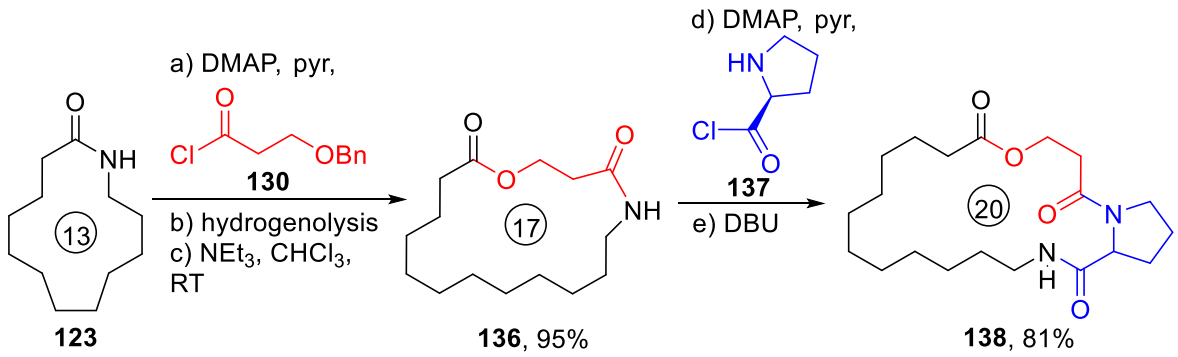

Scheme 25: Successive ring expansion with both hydroxy and amino acids.

1.2.8 Internal Nucleophile Ring Expansion

Internal nucleophile ring expansion (INRE) is a methodology discovered and reported recently (2019) by the Unsworth group.,[57] and is a method by which medium-sized rings can be made directly from linear precursors via a cyclisation/ring expansion cascade. A central design feature of this approach is to ensure that all cyclisation reactions involved in the overall process proceed via thermodynamically favourable transition states in terms of ring size (specifically 5–7-membered ring cyclic transition states). In contrast, medium-sized ring transition states, which are typically destabilised by transannular interactions and strain, are completely avoided. This is done by installing an internal nucleophilic into the linear starting material, to promote a cyclisation/ring expansion cascade (Figure 4). By ensuring that the reaction proceeds through "normal" sized cyclic transition states, this is proposed to result in a more kinetically favourable reaction profile. This more favourable reaction profile will be followed, as illustrated in the stylised reaction coordinate for cyclisation of linear precursors which do (blue line) and do not (red line) contain an internal nucleophile, depicted in Figure 5. In turn, this lower energy pathway reduces likelihood that intermolecular side reactions compete with the desired process, even at normal dilution, which contrasts to classical end-to-end cyclisations of medium sized rings, in which high dilution is often required to minimise side reactions. This concept is summarised as a generic scheme in Figure 4.

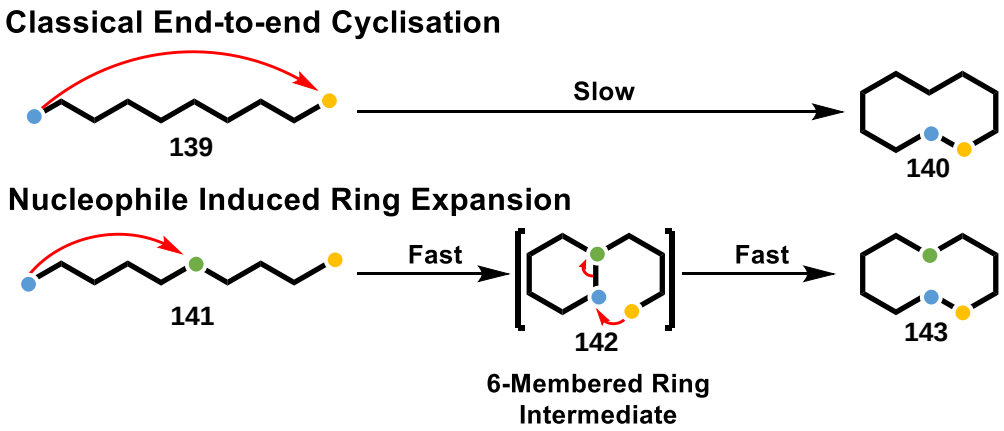

Figure 4: Model demonstrating function of the internal nucleophilic catalyst (green) in an internal nucleophile ring expansion reaction.

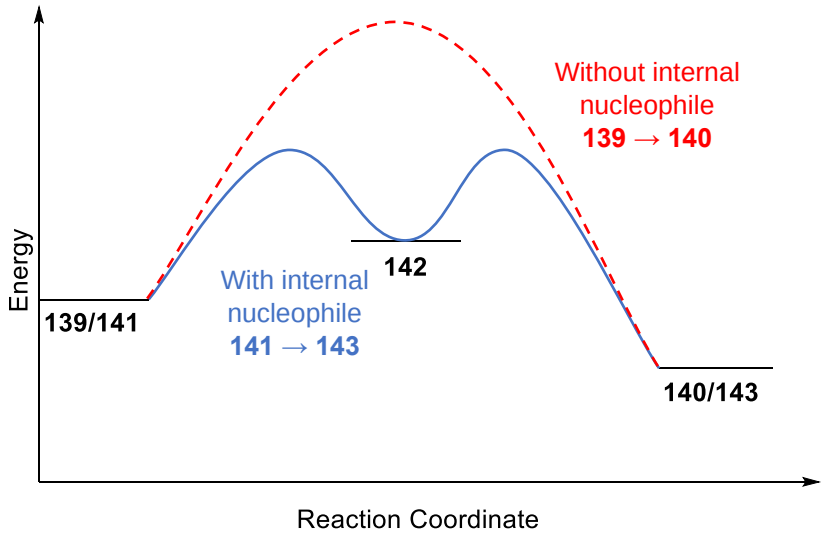

Figure 5: Hypothetical reaction coordinate of a generic INRE reaction.

An illustrative example is shown in Scheme 26, for the lactonisation of linear biaryl acid **144**. First, carboxylic acid **144** is activated by the coupling reagent propanephosphonic acid anhydride (T3P) to form the activated acid **145**. It is then proposed that the pyridine motif present in **145** attacks the activate acid intramolecularly to form the positively charged 6-membered ring acyl ammonium intermediate **146a**. The tethered alcohol of **146a** can then attack the same carbonyl, forming bicyclic intermediate **146b**, before fragmenting to form the medium sized lactone **147**, in an excellent yield of 90%. Crucially, if the same conditions are used on an analogous starting reagent lacking an internal nucleophile pyridine (**148**), the only product isolated is dimer **150**, with none of lactone **149** formed, clearly highlighting the importance of the internal N-nucleophile (Scheme 27).

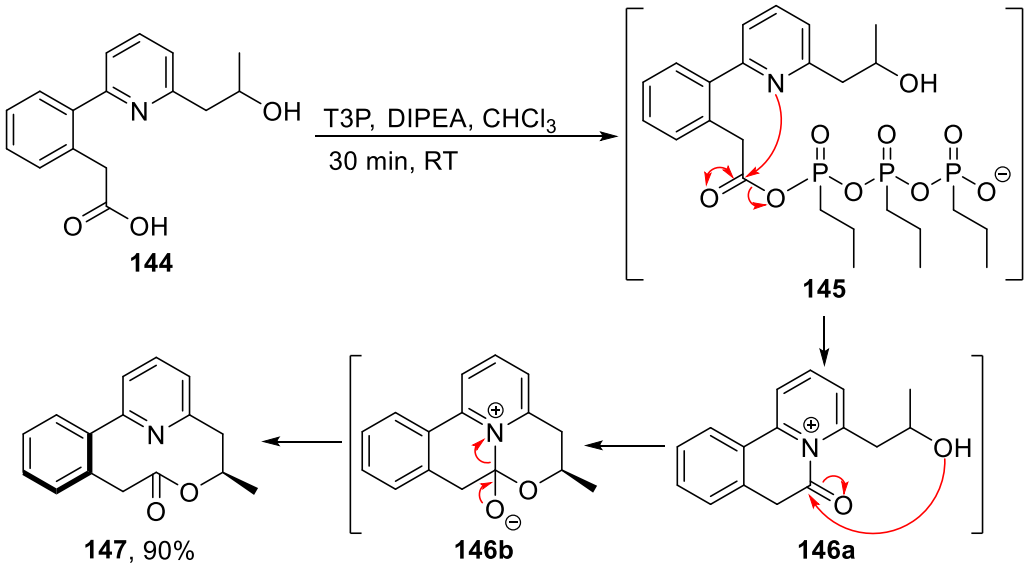

Scheme 26: INRE with a biaryl linear precursor.

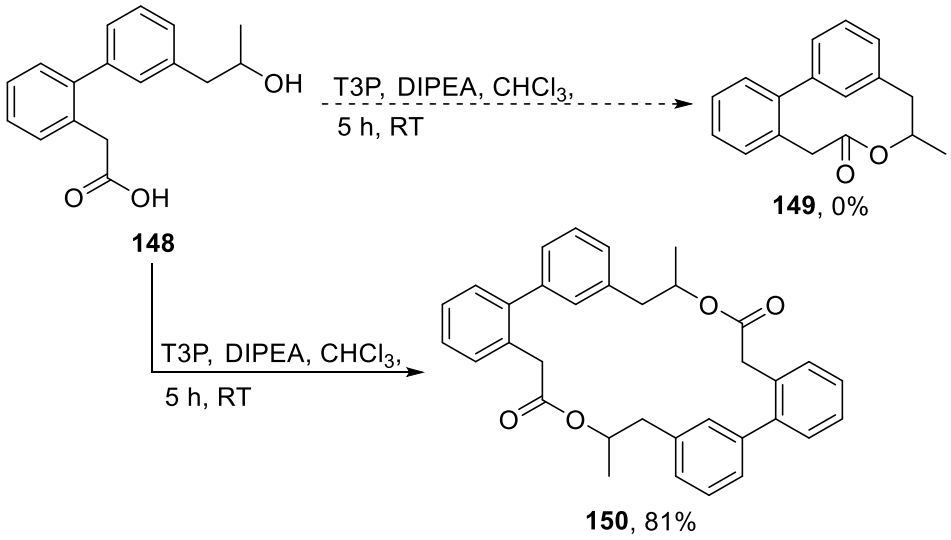

Scheme 27: Dimerization of N-free precursor **148**.

An interesting feature of INRE is its atroposelectivity. Atropisomerism can play a vital role in drug discovery and development, given the key role shape and conformation play in any ligand-target interaction in biology.[58] Due to the biaryl nature of the compound there is a lack of free rotation around the C-C bond connecting the two aryl groups in the products (supported by DFT studies). As a result of this, it is possible to form and isolate single atropisomers of medium-sized ring products using this chemistry. For example, in biaryl systems containing secondary alcohols as the terminal nucleophile, two atropisomers are possible, but only one atropisomer is formed exclusively. Scheme 28 shows a kinetic model for why it is thought that only one atropisomer is observed, based on a sterically preferred Si face attack to form the acyl ammonium intermediate.

It is proposed that the 6-membered transition state **146a** is similar to that of a chair/boat-like conformation. The observed stereochemical outcome **147(i)** arises from the facial selectivity of the alcohol attacking the prochiral intermediate *N*-acylammonium ion, and when attacking via the Si face, this places the methyl group of the secondary alcohol in a pseudo-equatorial orientation (**146a** → **146b(i)**). However, when the alcohol attacks the Re face (**146a** → **146b(ii)**), this would force the methyl group to be in a pseudo-axial orientation, presumably resulting in increased steric repulsion, and leading to the transition state being higher in energy.

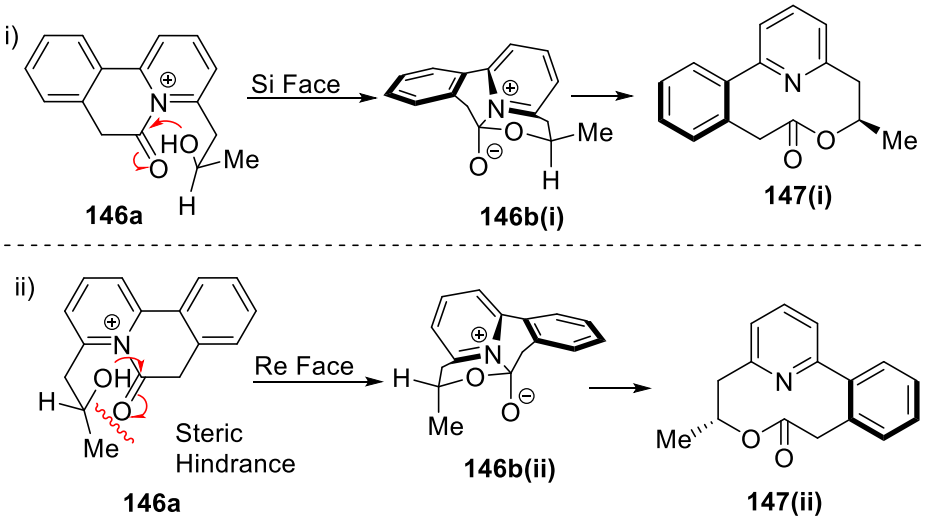

Scheme 28: A kinetic model based on diastereoselective attack into prochiral N-acyliminiumion

It is also possible to use INRE with precursors which use free amines instead of alcohols as the terminal nucleophile to form lactams, such as **155** → **156** (Scheme 29). Equally, aliphatic tertiary amines can be used as the internal nucleophilic catalyst (**151** → **152**), and the length of the linear precursor can also be varied, with ring sizes from 8 (lactone **154**) to 11 atoms (lactone **152**) all being made via INRE.

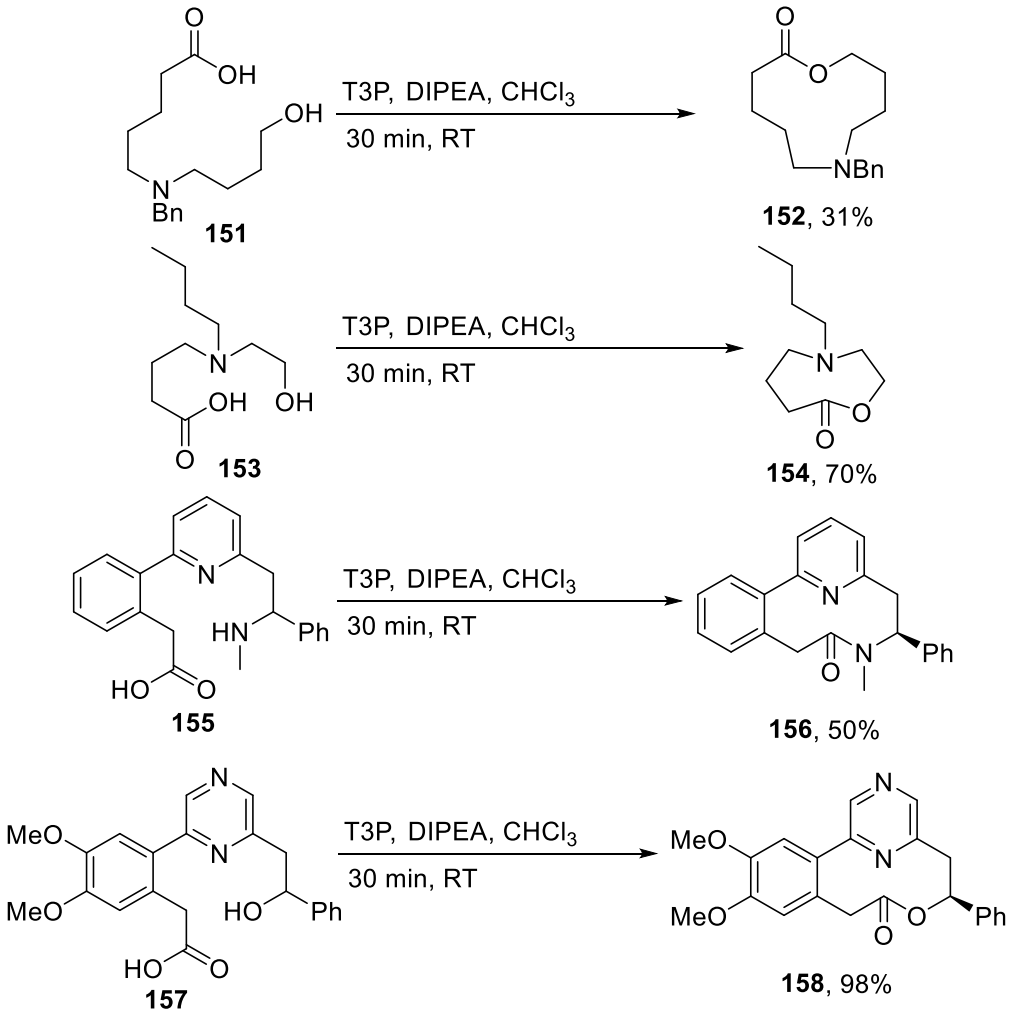

Scheme 29: Diverse selection of INRE reactions.

1.3 Project Aims

Heterocyclic medium-sized rings and macrocycles are interesting compounds in medicinal chemistry, and developing improved ways to make complex systems of this type is important.[59] Therefore, in this project, we wanted to further develop the INRE strategy, with specific focus on the development of more elaborate cascade sequences to form larger, more complex ring systems more quickly. Thus, a new strategy was conceived, whereby longer linear precursors would be designed, that contain more than one internal nucleophile. In theory, this would allow for multiple cyclisation/expansion processes in a single cascade sequence, thus enabling the formation of larger macrocycles from a linear precursor in one pot, in a multi internal nucleophile induced ring expansion (multi-INRE).

A generic representation of this concept is shown is Scheme 30, where "X" and "Y" represent internal nucleophiles and "ZH" signifies a terminal nucleophile. Thus, a linear

precursor **159** would be activated by a coupling reagent before cyclising to form the intermediate **160a**. The carbonyl of this intermediate could then be attacked by the internal nucleophile 'Y' of **160a** to form the 10-membered intermediate **160b**, before finally being attacked by the tethered nucleophile 'ZH' and expanded again, to form the ring expanded 14-membered macrocycle product **161**. As with single internal nucleophile ring expansion, the system in question is expected to follow a more kinetically favourable reaction profile when compared with the analogous direct end-to-end cyclisation. Figure 6 illustrates a hypothetical reaction coordinate for cyclisation of a generic linear precursor which constitutes two internal nucleophiles. Intriguingly, there is also no obvious reason why the linear starting material could not be extended even further to include more internal nucleophiles.

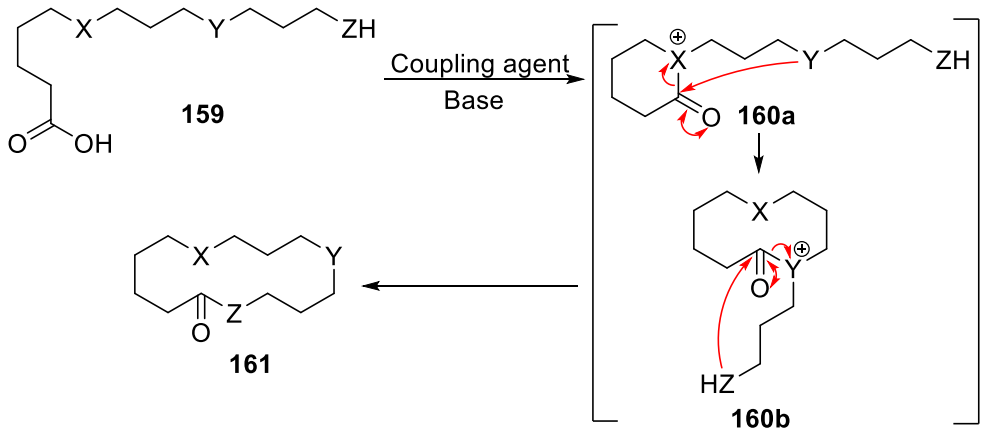

Scheme 30: Example of an internal nucleophile ring expansion reaction with two internal nucleophiles.

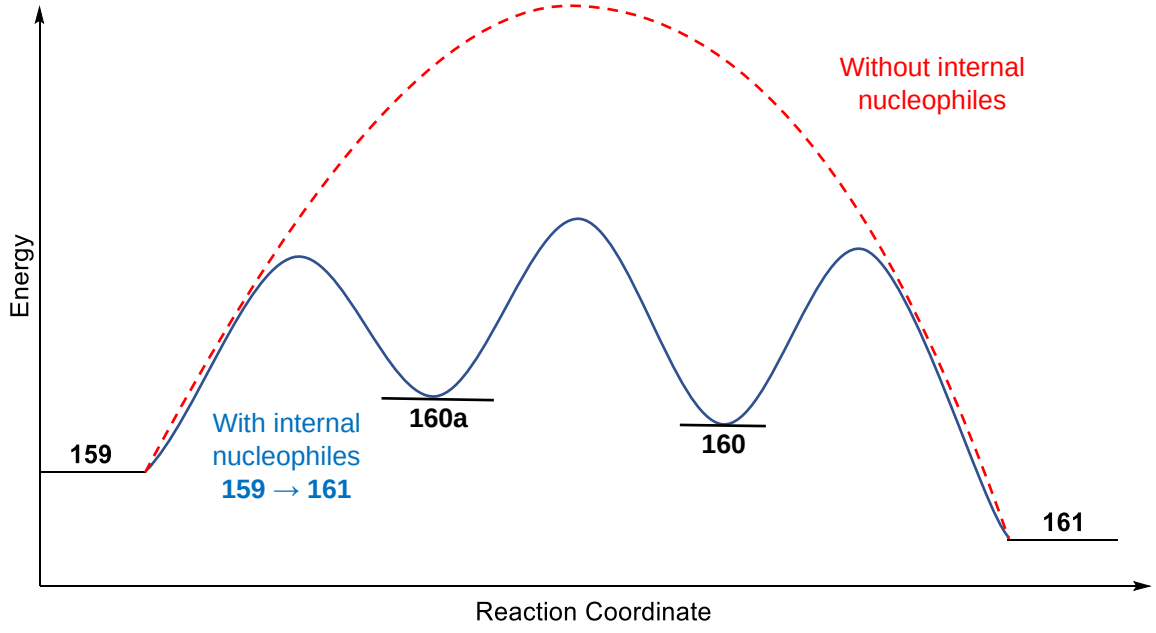

Figure 6: Hypothetical reaction coordinate of a general multi-INRE reaction.

The overriding aim of this project was to establish the multi-INRE concept as an important new method for macrocycle synthesis. To facilitate this, the following objectives were devised:

- To explore the viability of the multi-INRE strategy using a simple model system.
- To optimise the multi-INRE reaction by screening against an array of different reaction conditions.
- To explore the scope and limitations of the multi-INRE strategy by building and testing an assortment of linear precursors.
- To gain insight into the diastereoselectivity of multi-INRE when used on longer precursors.
- To gain further insight into the mechanistic pathway by which INRE proceeds.

Initial Multi-Internal Nucleophile Ring Expansion Precursor Design and Synthesis

2.1 Designing an Initial Precursor

To explore the viability of a multi-INRE system with more than one internal nucleophile, we first designed a linear starting material that contains two internal nucleophiles which were previously shown to be successful in single-INRE reactions in the Unsworth group.[57] It was hoped that by incorporating an additional nucleophile into a system already known to undergo single-INRE with one internal nucleophile, it would allow two successive ring expansions to occur in a cascade process. It was also hoped that the toolbox of synthetic procedures already in place for making single-INRE precursors would facilitate the preparation of novel multi-INRE precursors.

The first precursor conceived, and the proposed multi-INRE mechanistic pathway, is shown in Scheme 31. The precursor **162** is based on the use of two tertiary amine groups as the internal nucleophiles, the first a pyridine, which was the most successful internal nucleophile in the previous Unsworth group work, and the second a simple aliphatic tertiary amine. The idea was that the carboxylic acid in **162** would be activated by a suitable coupling agent before undergoing nucleophilic attack with the pyridine internal nucleophile to give the first intermediate **163a,** a 6-membered pyridinium ring. The hope then was that the carbonyl generated would then be electrophilic enough to be attacked by the second internal nucleophile, the tertiary amine, to give the 10-membered ammonium ring **163b**. Then, the 10-membered intermediate **163b** would be primed to undergo another ring expansion as the terminal alcohol attacks the electrophilic carbonyl moiety to open the ring and form macrocyclic lactone **164**.

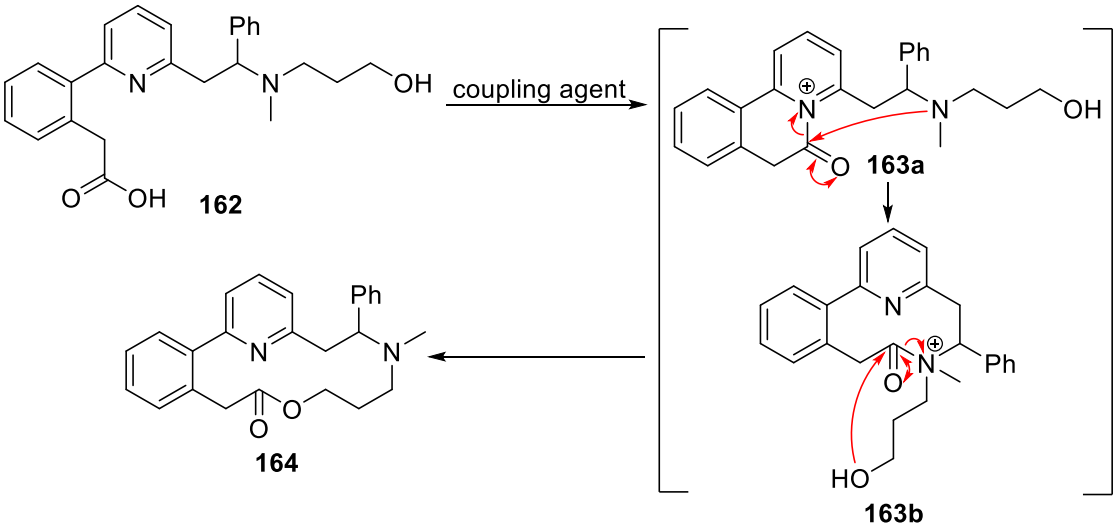

Scheme 31: Mechanistic pathway of ring expansion using precursor **162**.

Scheme 32 shows our planned retrosynthetic route to precursor **151**. It was envisaged that the initial precursor **151** would be constructed from the pyridine **160** containing two synthetic handles; an *ortho*-halide for cross-coupling and an *ortho*-methyl group suitable for lithium ion-trapping.

Protection of the carboxylic acid when building the precursor was thought to be prudent to avoid unwanted side reactions, and this could be done via esterification. The key retrosynthetic disconnection would be the C-C biaryl bond, which splits the precursor into two synthetic targets, aryl halide **167** and borylated aryl ester **166**, which would be connected through a cross-coupling reaction. Borylated aryl ester **166** would be accessed through a Miyaura cross-coupling between haloaryl ester **168** and B_2Pin_2. The tertiary amine internal nucleophile present in pyridine **167**, would be prepared via an S_N2 reaction between secondary amine **169** and alcohol **170**. Finally, secondary amine **169** would be synthesised via lithiation-trapping of the 2-methyl present in pyridine **171** with electrophilic imine **172**. With a synthetic strategy in place, the synthesis of a haloaryl of the form **169** was attempted.

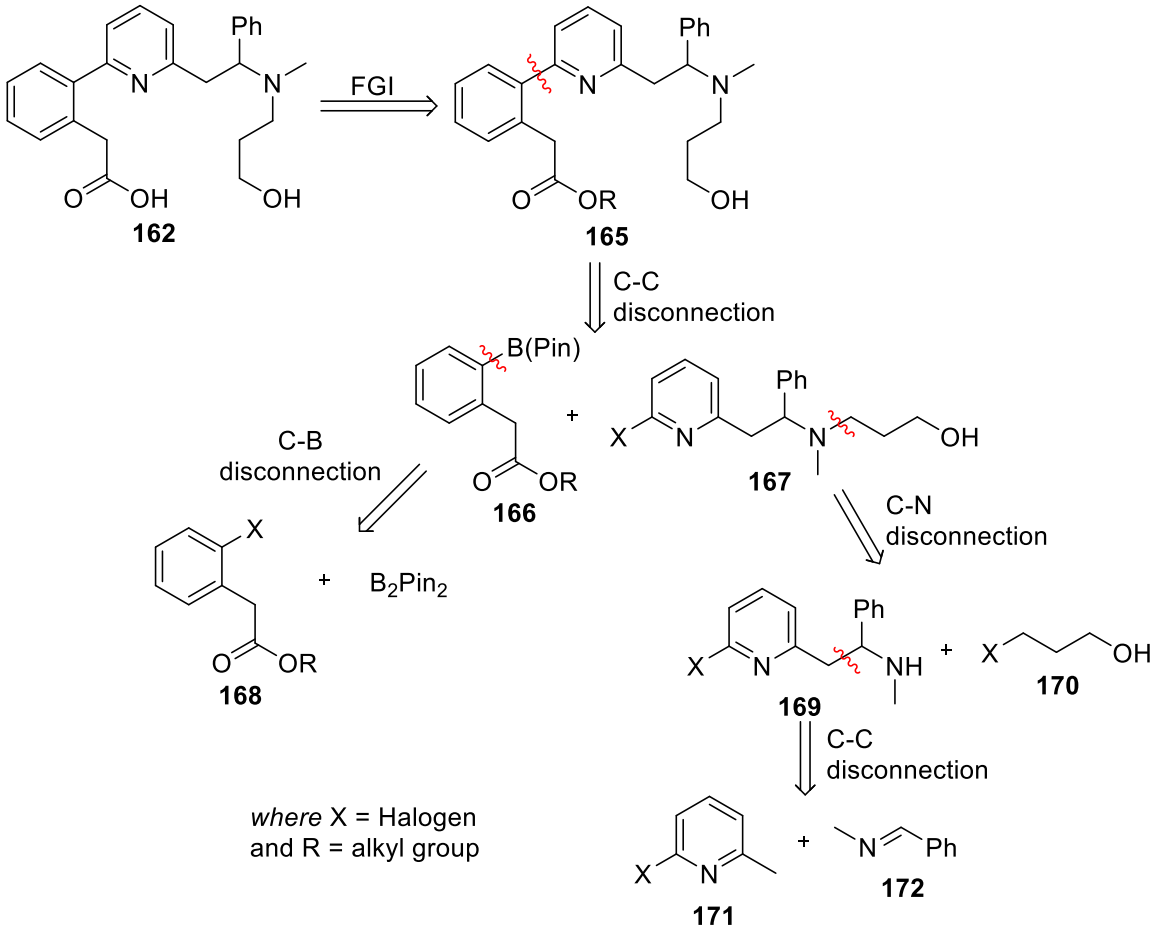

Scheme 32: Retrosynthetic route towards the initial multi-INRE precursor **162**.

2.2 Building Initial Multi-INRE Precursor 162

We started by seeking to establish conditions for the lithiation-trapping of bromopyridine **173** with imine **172**. Several lithiation-trapping reactions were performed using conditions previously identified for similar reactions.[57] Table 1 shows all the different conditions tested, each with their respective yield. Thus, when using two equivalents of both imine **172** and LDA (Entry 1) a moderate yield of 70% was obtained for amine **174**. However, both TLC and ^{1}H NMR spectroscopy analysis of the unpurified reaction mixture showed pyridine **173** was still present. In an attempt to convert all starting material **173** into product, the reaction time was increased from 30 minutes to two hours (Entry 2), which led to an increase in yield to 81%. Next, we questioned whether the use of two equivalents of LDA was necessary, given that only one deprotonation was required; thus, the reaction was trialled using reduced equivalents of LDA (1.2 equiv.) but this led to a significant drop in yield from 81% to 60% (Entry 3). Furthermore, a number of uncharacterisable side-products were also observed by TLC and ^{1}H NMR spectroscopy under these conditions, most likely caused by the

polymerisation of **173** via S_NAr. Simultaneously, a lithiation-trapping reaction with both reduced equivalents of imine **172** and LDA was trialled in the same hope of generating a more efficient lithiation-trapping reaction (Entry 4). Using only 1.5 equivalents of imine **172** and LDA gave the best result, furnishing amine **174** in 80% yield; this result was particularly pleasing as the amount of imine **172** could be reduced, allowing for a more efficient synthesis.

Table 1: Lithiation trapping optimisation for amine **174** synthesis

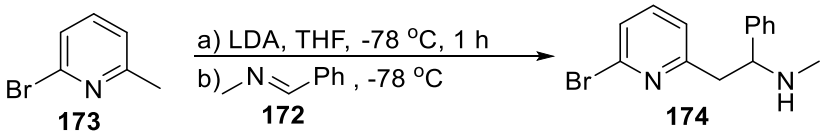

Entry	LDA (Equiv.)	Imine **172** (Equiv.)	Reaction Time (b) / h	Yield / %
1	2.0	2.0	0.5	70
2	2.0	2.0	2	81
3	1.2	2.0	2	60
4	1.2	1.5	2	80

The next step in the synthesis towards precursor **162** was the alkylation of secondary amine **174**. It was envisioned that an S_N2 reaction between amine **174** and a halogenated propanol should be an efficient and high yielding way to install the terminal alcohol group. However, this reaction transpired to be the most challenging to optimise, with the conditions of the S_N2 reaction requiring five revisions until the yield was brought up to an acceptable level.

Scheme 33 shows the different reaction conditions tested for the synthesis of alcohol **176**. Scheme 33 (i) shows the first attempted S_N2 reaction, in which amine **174** was heated at reflux in acetonitrile for three hours with 2.0 equivalents of potassium carbonate and 1.5 equivalents of chloropropanol **175**. Surprisingly, TLC and ^{1}H NMR spectrum analysis of the unpurified reaction mixture showed no evidence of product **176** being formed, despite believing that secondary amine **174** would be reactive enough to undergo the desired S_N2 reaction. This lack of reactivity is thought to be caused by amine **174** being a worse nucleophile than initially thought.

In an attempt to improve the reactivity, bromopropanol **177** was used instead of chloropropanol **175** in the hope that this switch to a superior leaving group would help promote the S_N2 reaction (Scheme 33 (ii)). The S_N2 reaction was heated overnight to give the best chance of success. This change did have a positive effect, with product **176** isolated successfully, but the yield was poor (24%). TLC and ^{1}H NMR spectrum analysis of the

unpurified reaction mixture again showed starting material **174** was still present, indicating that the reaction did not go to completion. Scheme 33 (iii) shows the next modification: leaving the reaction over the weekend to allow all starting material **174** to be consumed. Pleasingly, the yield increased to 53%, however, starting material **174** was again identified in the unpurified reaction mixture. This prolonged reaction time was also impractical, as a three-day reaction would likely create a bottleneck in the synthesis of precursor **162**.

More forcing conditions were therefore used in an attempt to convert all starting material **174** into product. Scheme 33 (iv) shows an increase in bromopropanol **177** equivalents to 2.5 afforded product **176** in a yield of 65%. However, starting material was still present in the reaction mixture, suggesting that the yield of **176** could be increased further. Scheme 33 (v) showcases a final attempt to increase the yield, using a better electrophile, iodopropanol **178**, at a higher concentration (0.5 M) to drive conversion of starting material **174** into product **176**. The reaction furnished alcohol **176** in a good yield of 75% which signifies a major improvement upon the initial reactions. However, a small amount of starting material **174** was still identified from the unpurified reaction mixture in both TLC and ^{1}H NMR spectroscopy, albeit in much smaller quantities, suggesting that further optimisation could still be possible in future studies. Use of a stronger base, such as sodium hydride, was avoided as it was suspected that a stronger base would lead to the E2 elimination of the haloalkane.

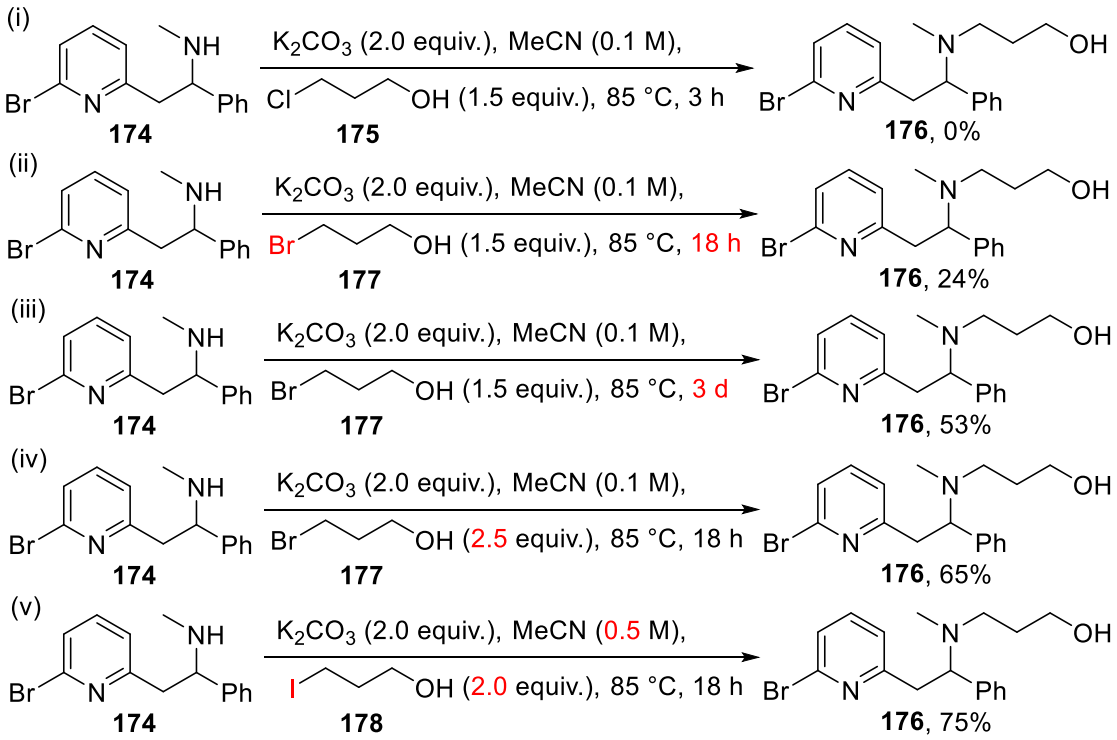

Scheme 33: S_N2 reactions for precursor **164** synthesis.

The next step was to start making the other half of the precursor (**166**) needed to cross-couple with bromopyridine **176**. As previously shown in Scheme 32, the target molecule **166** should possess a boron synthetic handle, which could be made from an aryl halide ester (**168**). However, no such aryl halide ester was commercially available, so a commercially available acid analogue, bromoaryl acid **179**, was used instead and converted into an ester, via the simple procedure shown in Scheme 34; thus, esterification of acid **179** using sulfuric acid in methanol at reflux for 90 mins afforded methyl ester **180** in an excellent yield of 99%.

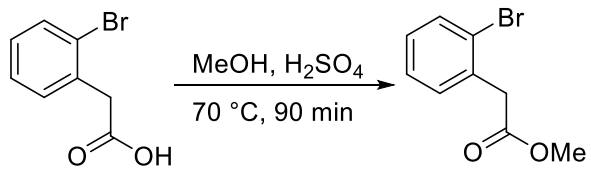

179 **180**, 99%

Scheme 34: Fischer esterification of aryl halide.

With the carboxylic acid group protected as a methyl ester, the bromide could now be converted into the desired pinacol borate **181** using a Miyaura cross-coupling. Using conditions based on previous literature,[57] aryl bromide **180** was stirred in dioxane at 80 °C overnight under argon with [1,1′-bis(diphenylphosphino)ferrocene]dichloropalladium(II), potassium acetate, and bis(pinacolato)diboron to give aryl borate **181** in an isolated yield of 56% after purification (Scheme 35). While successful, this reaction was a bottleneck in the construction of precursor **162** for several reasons. First, for the subsequent cross-coupling reaction (**166 + 167 →165**) aryl borate **181** was used in excess of 2.0 equivalents, which meant that a large quantity of **181** needed to be produced. This in turn required a relatively large quantity of reagents, including a large amount of the expensive catalyst $Pd(dppf)Cl_2$. Second, the chromatographic purification of boronic ester pinacol **181** was extremely difficult, especially on scales of 2 g and above. Analysis using 2D TLC revealed that boronic ester pinacol **181** slowly decomposes on silica. This instability, coupled with the presence of an undesired side-product in the crude reaction mixture, which had a similar R_f to the boronic ester pinacol **170** in all tested solvent systems, made the isolation of **181** from chromatographic purification very challenging. Third, to make purification easier, a proportionally large column was required for the purification, which was costly in terms of solvent, silica requirements, and in time. This limited the amount of product **181** which could be successfully purified in a single column to 2 g, this required the purification of boronic ester pinacol **181** to be performed in batches.

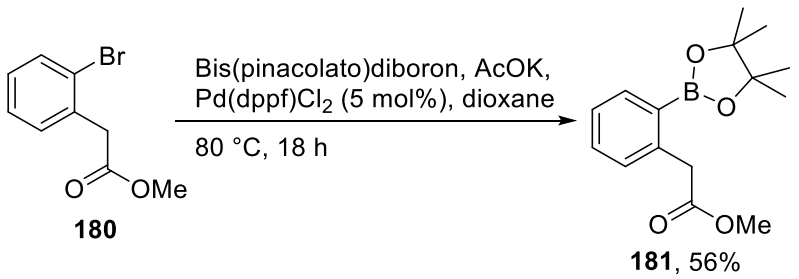

Scheme 35: Miyaura cross-coupling of aryl bromide **170** with bis(pinacolato)diboron.

Having successfully synthesised both halves of the target precursor **162**, the next stage of the synthesis was to couple the two molecules **176** and **181**. Scheme 36 shows the Suzuki-Miyaura cross-coupling reaction, which was adapted from conditions reported in the literature.[57] Aryl bromide **176** and boronic ester pinacol **181** were stirred overnight at 80 °C under argon with potassium phosphate and Pd(dppf)Cl_2 in a THF/H_2O mixture to make the biaryl **182** in a pleasingly high yield of 87%. As the Suzuki-Miyaura cross-coupling reaction was high yielding, no further optimisation was required, and every repeated synthesis of **182** used the conditions shown in Scheme 36.

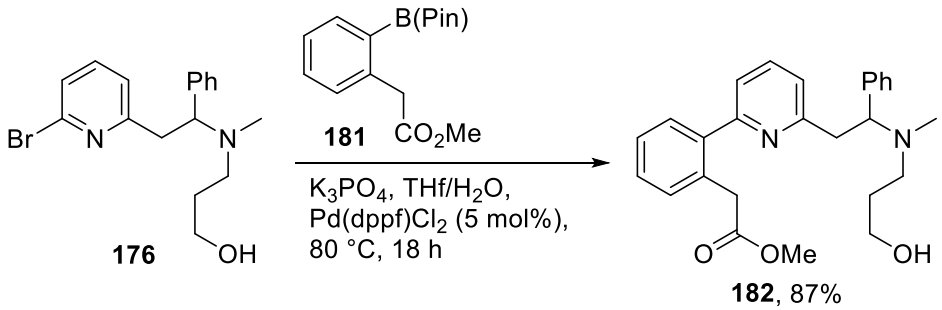

Scheme 36: Suzuki-Miyaura cross-coupling of boronic ester pinacol **181** and bromopyridine **176**.

The final step in the synthesis of precursor 1**62** is the hydrolysis of the methyl ester **182** (Scheme 37). Typical ester hydrolysis conditions were used; ester **182** was stirred overnight in a lithium hydroxide/THF solution at room temperature to yield the desired precursor **162**. Although it was thought that the hydrolysis cleanly converted all starting material **182** into product **162**, based on ^{1}H NMR spectrum analysis, the product was still purified via column chromatography to remove any trace impurities carried through from previous reactions. After purification, precursor **162** was isolated in an excellent yield of 96%. The purified product was isolated as a powder. We believe that hydroxy acid **162** takes the form of zwitterion **162a** based on typical acid and amine pK_a values, however, the ^{1}H NMR peaks of environments near the protonated quaternary amine do not show a significant change in chemical shift when compared to the ^{1}H NMR of methyl ester **182**, which would be expected after protonating the tertiary amine.

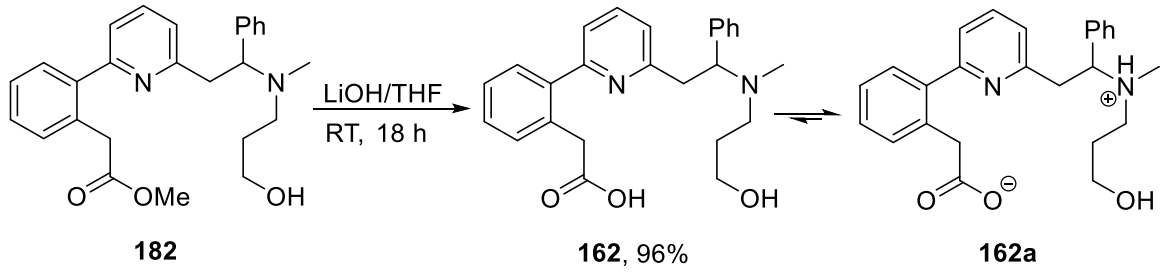

Scheme 37: Hydrolysis of methyl ester **182**.

With the initial precursor synthesised and each step having good yield, we focused on making a relatively large quantity of precursor **162** in order to screen the initial internal nucleophile ring expansion reaction (**162 → 164**) against a large array of conditions. Scheme 38 shows all the reactions involved in the synthesis of the linear precursor **162** from bromomethyl pyridine **173** in an overall yield of 50%. Considering the number of steps in the synthesis, with each one requiring chromatographic purification in highly polar solvent systems, the overall yield is pleasing. With an optimised synthetic route in hand, 3 g of bromomethyl pyridine **173** was used to furnish 3.5 g of hydroxy acid **162**, which was ample for initial screening to commence.

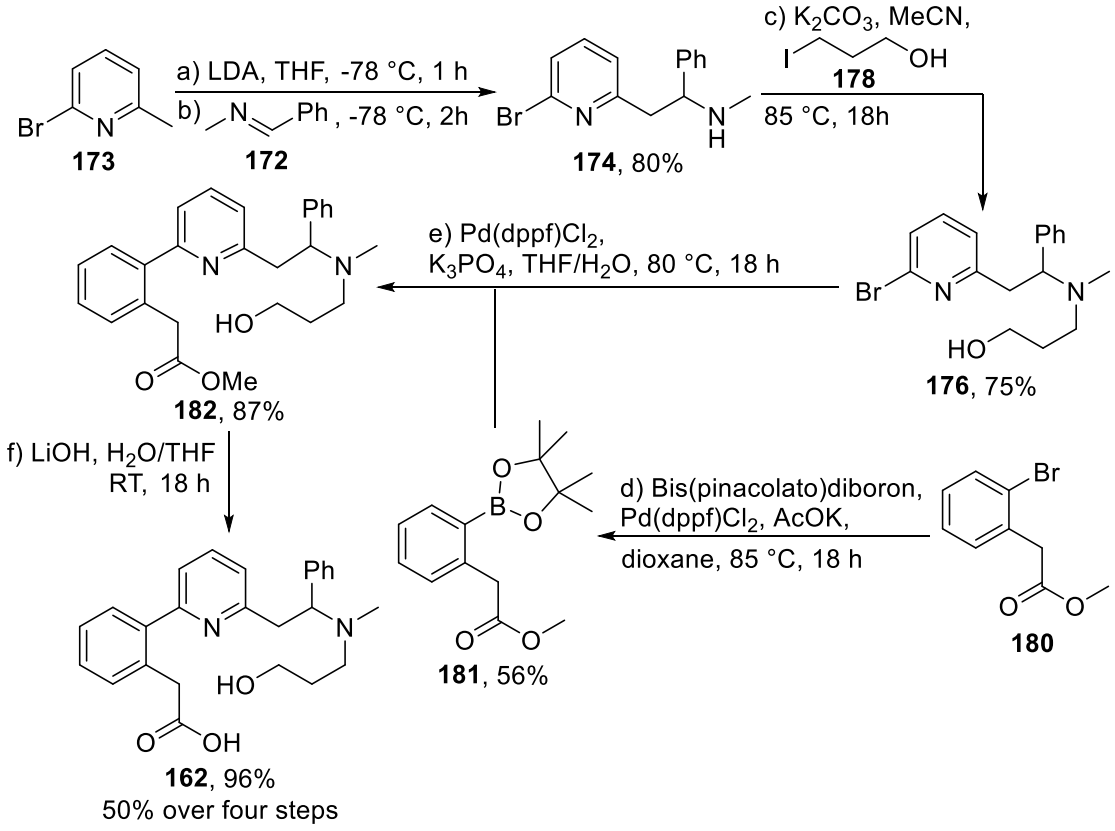

Scheme 38: Synthesis route to linear precursor **162**.

2.3 Initial Multi-INRE Reaction

With access to a sufficient quantity of precursor **162**, we could now attempt a multi-INRE reaction. The INRE reaction was performed on precursor **162** by adapting conditions previously reported for ring expansion by the Unsworth group. It was assumed that more energy would be required to promote this multi-INRE reaction as two successive intramolecular nucleophilic substitutions needed to take place, compared to single-INRE reactions which used precursors containing one internal nucleophile. With this considered, the initial multi-INRE reaction using precursor **162** was heated overnight at reflux (60 °C) to allow for the best chance of success (Scheme 39). Thus, hydroxy acid **162** was refluxed in chloroform with the coupling agent T3P and DIPEA which afforded lactone **164** in an isolated yield of 17%. Notably, biaryl lactone **164** was isolated as a single atropisomer, with the reasoning behind this stereoselectivity explained below.

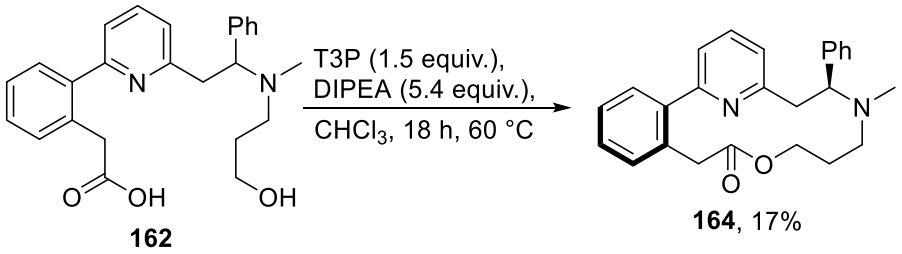

Scheme 39: First trialled multi-INRE using hydroxy acid **162**.

Cyclisation of hydroxy acid **162** to form macrocyclic lactone **164** was confirmed by HRMS, and IR, ^{1}H NMR and ^{13}C NMR spectroscopic analysis. Figure 7 shows the ^{1}H NMR spectrum of macrocyclic lactone **164** with all non-aromatic peaks assigned to their respective environments. In lactone **164**, free rotation is expected to be restricted relative to the linear precursor; indeed, this is seen in the ^{1}H NMR spectra, with the aliphatic protons that were previously equivalent in precursor **162** distinguishable in the ^{1}H NMR spectrum of macrocyclic lactone **164**. This is clearly seen with the CH_2 protons adjacent to the carbonyl in lactone **164** (H_j and H_k in Figure 7). In the linear precursor **162**, the two protons are indistinguishable by ^{1}H NMR, however, due to the presumably more rigid confirmation, they can be differentiated via ^{1}H NMR spectroscopy, with H_j and H_k presenting a distinct doublet at δ_H 4.46 and δ_H 4.00, respectively. Thus, with evidence obtained from the all spectroscopic methods described, including the ^{1}H NMR spectrum (Figure 7), we could confidently confirm the synthesis of novel macrocyclic lactone **164** via a multi-INRE reaction, the first of its kind.

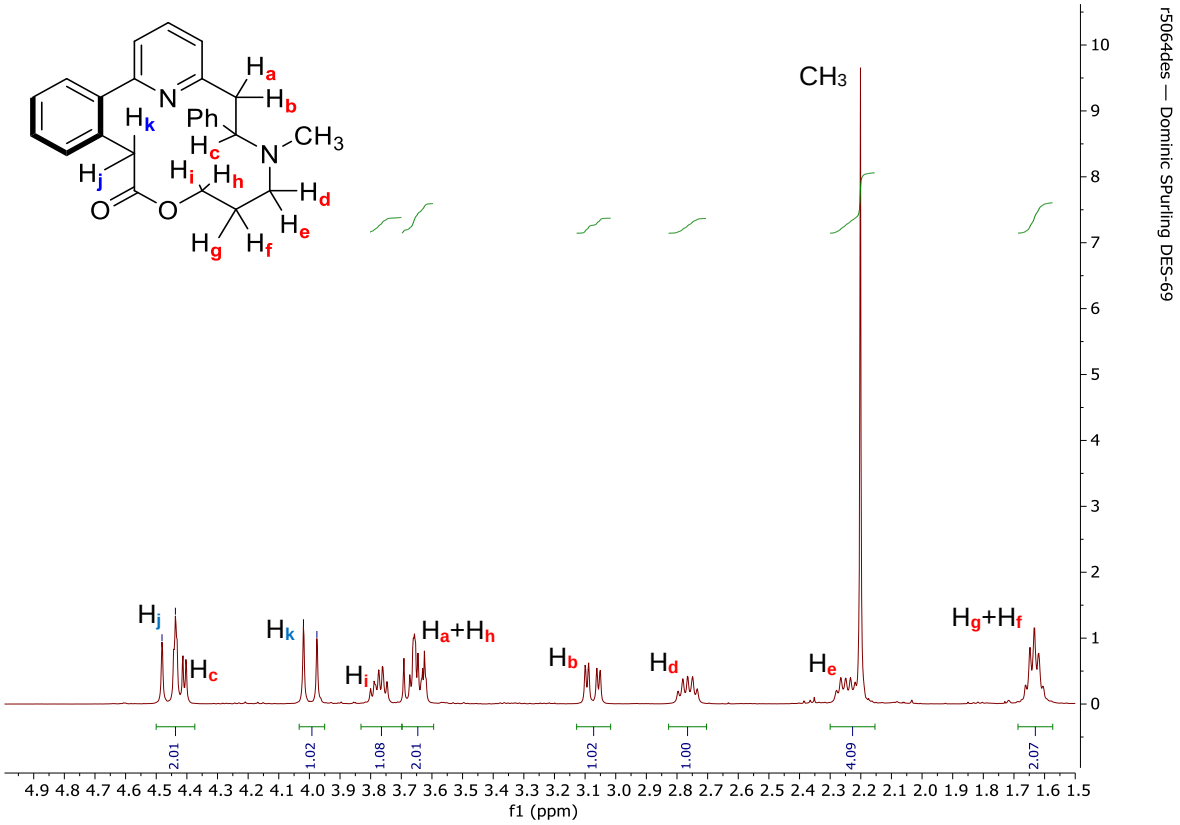

Figure 7: ^{1}H NMR Spectrum of multi-INRE product lactone **164**.

The isolation and characterisation of macrocyclic lactone **164** demonstrates that INRE can be achieved using linear precursors containing more than one internal nucleophile. This gratifying discovery underpinned the direction taken for the rest of the project; focus was turned towards increasing the yield and exploring the limitations of multi-INRE reactions using linear precursors containing multiple internal nucleophiles.

Interestingly, analysis of the ^{1}H and ^{13}C NMR spectra of lactone **164** also gave additional insight into the stereoselectivity of multi-INRE systems which use precursors containing multiple internal nucleophiles. Both ^{1}H and ^{13}C NMR spectra provided evidence suggesting that the multi-INRE reaction **162** → **164** produced only one diastereoisomer. Figure 9 shows the ^{13}C NMR spectrum of the isolated lactone **164**, with all appropriate peaks assigned to their respective carbon environment. The ^{13}C NMR spectrum of lactone **164** shows a notable absence of peaks corresponding to a chemically different diastereomer, suggesting that only one diastereoisomer is formed in the multi-INRE reaction. It could be argued that such a diastereoisomer could have been removed during chromatographic purification of the unpurified reaction mixture containing lactone **164**. However, only one macrocyclic compound could be identified from ^{1}H NMR spectroscopy of the unpurified reaction mixture.

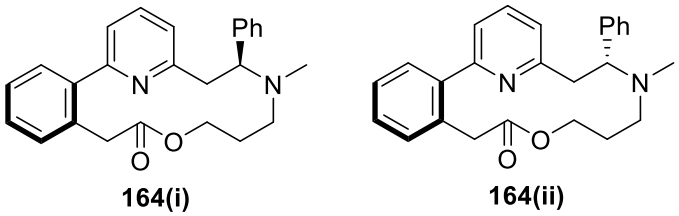

Figure 8: Possible diastereoisomers which could yield from the multi-INRE reaction.

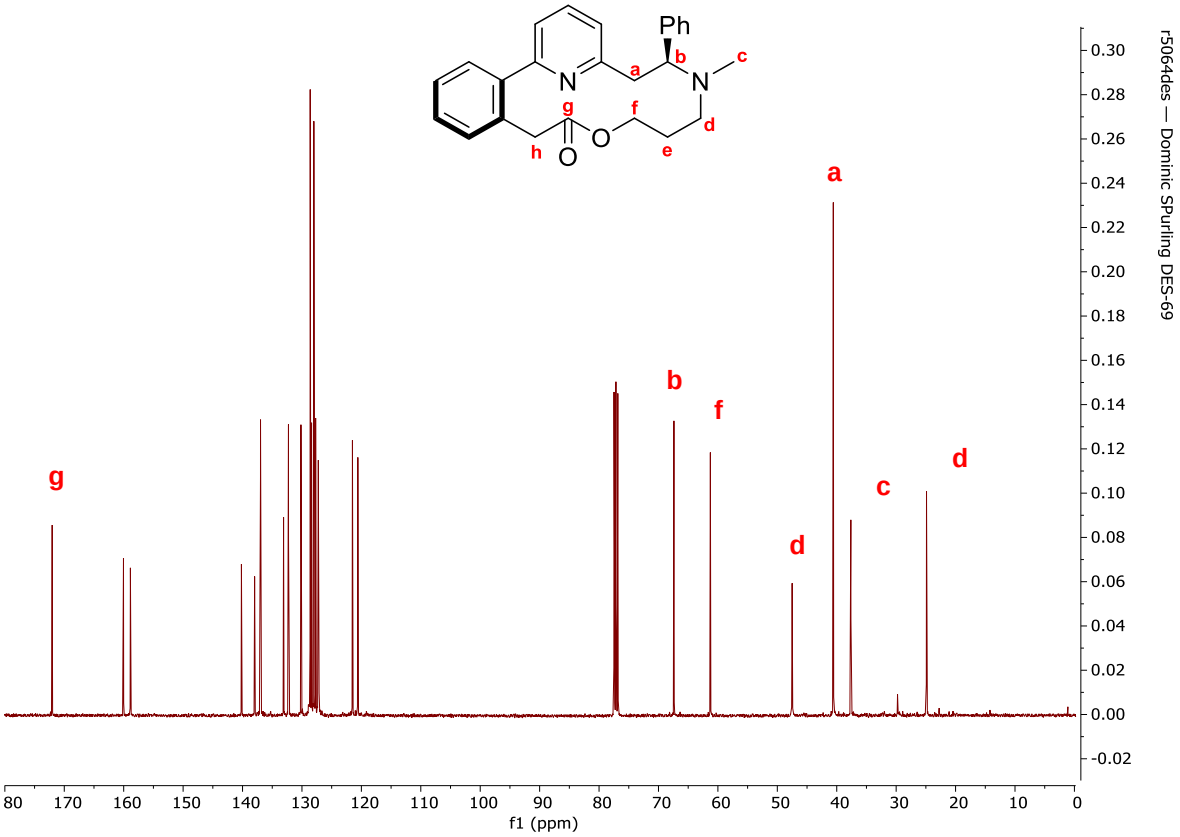

Figure 9: ^{13}C NMR spectrum of macrocyclic lactone **164**.

To assign the relative stereochemistry of **164**, we turned to X-ray crystallography. Thus, a crystal was grown (from **164**) and the result is shown in Figure 10. The structure of the crystal grown revealed it to be atropisomer **164(i)**, which possessed the same sense of stereochemistry as that seen in the previously reported single-INRE biaryl lactone **147**.[57]

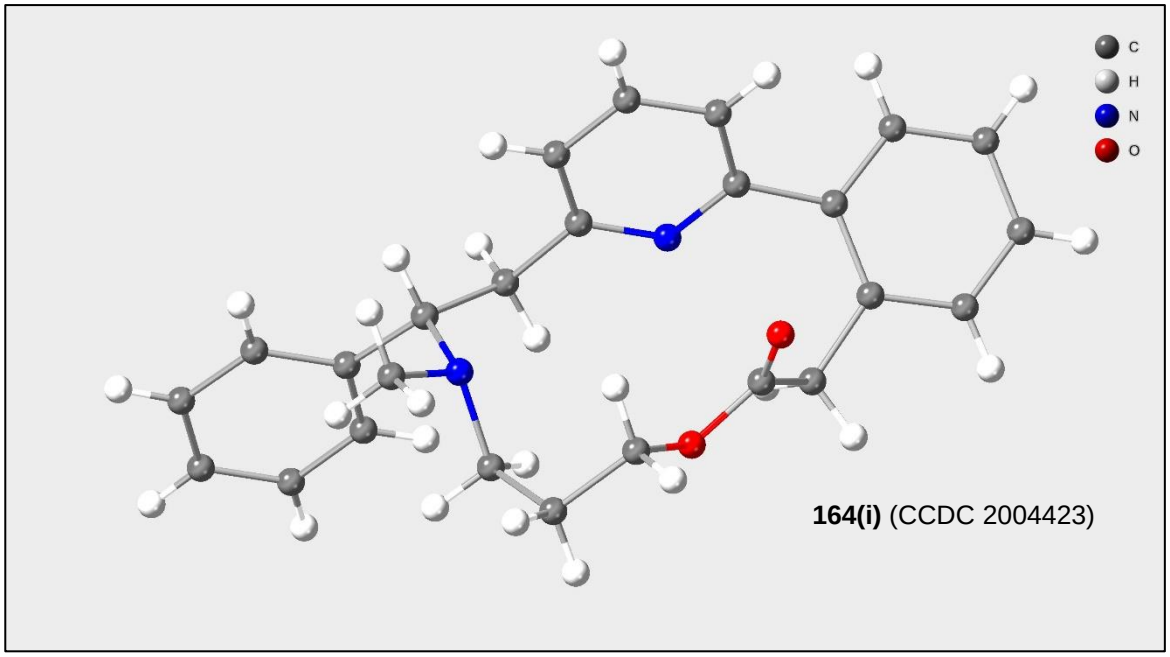

Figure 10: Single crystal XRD structure of macrocyclic lactone **164(i)**.

This atroposelectivity is presumed to have the same origin as in the previous work, resulting from facial selectivity of the attacking internal nucleophile. Similar to previous single-INRE reactions, this system allows for point-to-axial chirality transfer.[58] The atroposelectivity in both single- and multi-INRE reactions can be explained using the same kinetic argument (Scheme 40). It is presumed that the observed stereochemical outcome (formation of **164(i)**) arises from the facial selectivity of the tertiary amine attacking into the prochiral intermediate *N*-acylammonium ion, and when attacking via the Si face, it places the phenyl group in a pseudo-equatorial orientation (**163a → 163b(i)**). However, when the tertiary amine attacks the Re face (**163a → 163b(ii)**), this would force the phenyl group to be placed in a pseudo-axial orientation, presumably causing steric hinderance, and leading to the transition state being higher in energy, in turn preventing the formation of atropisomer **164(ii)**. It was pleasing to see that the diastereoselectivity of INRE reactions was transferred when synthesising larger macrocycles from linear precursors containing two internal nucleophiles.

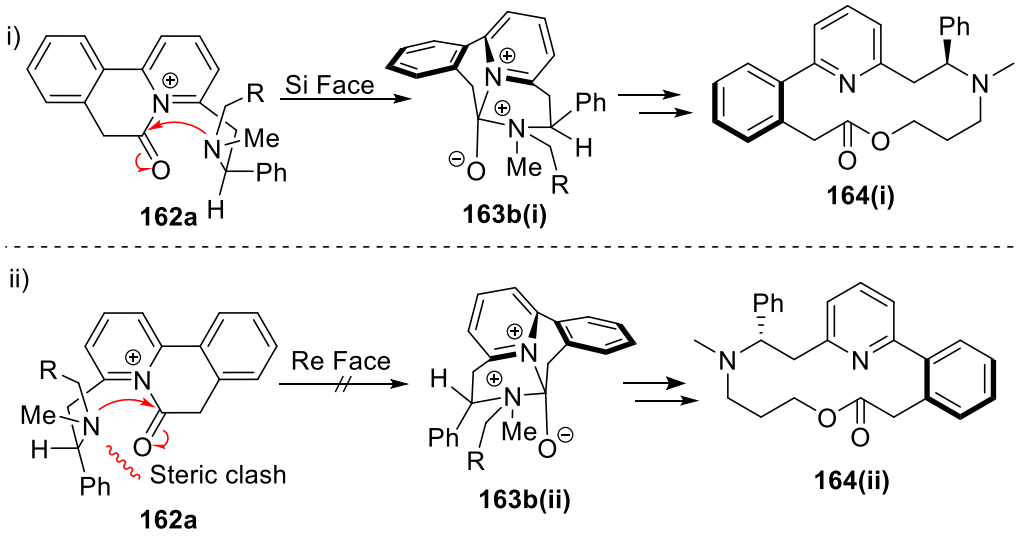

Scheme 40: A kinetic model based on diastereoselective attack into prochiral *N*-acyliminium ion.

2.4 Summary

The first cyclisation of a linear precursor containing two internal nucleophiles via a multi-INRE reaction has been reported. The design and subsequent synthesis of the novel biaryl linear precursor **162** was achieved in 50% overall yield over four steps. The synthetic route to access novel precursor **162** was optimised to ensure all reaction steps gave their respective product in good yield, allowing for the efficient generation of precursor **162** for subsequent screening.

The initial cyclisation of precursor **162** affording novel heterocyclic-macrocycle **164** via multi-INRE was successfully achieved in 17% yield, using modified conditions previously identified for single-INRE reactions. This result demonstrates that INRE reactions are possible with precursors containing two internal nucleophiles.

A single diastereoisomer of heterocyclic-macrocyclic lactone **164** was isolated and characterised via ^{1}H and ^{13}C NMR spectroscopy and single crystal XRD. This data suggested that the multi-INRE reaction was atroposelective; allowing for point-to-axial chirality transfer. A kinetic argument based on single-INRE atroposelectivity was also developed.

Multi-INRE Screening and Aliphatic Precursor Synthesis

3.1 Initial Screening of multi-INRE reaction 162 → 164

Having established that a multi-INRE reaction using a precursor containing two internal nucleophiles is possible, the next step was to increase the yield of product **164** through optimisation of reaction **162 → 164**. This was done by testing a range of reaction conditions for the INRE of precursor **162**. Screening was carried out on 100 mg scale unless stated and the variables changed during the initial screening process of reaction **162 → 164** were solvent, temperature, reaction time, concentration, and coupling agent. Table 2 shows the reaction conditions tested and the respective yield from each reaction.

Table 2: Initial screening conditions for reaction **162 → 164** and their respective isolated yields. [a] Performed on 300 mg scale.

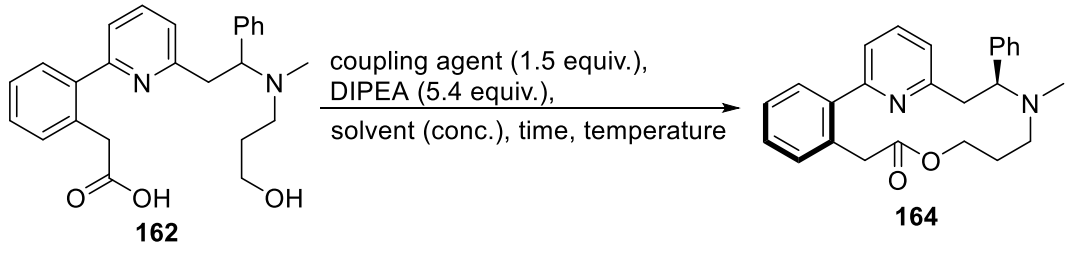

162 **164**

Entry	Coupling Agent	Solvent	Concentration / M	Time	Temperature / °C	Yield / %
1	T3P	$CHCl_3$	0.1	18 h	60	17[a]
2	T3P	$CHCl_3$	0.001	18 h	60	7
3	T3P	DCE	0.1	18 h	85	9
4	T3P	$CHCl_3$	0.1	18 h	25	6
5	T3P	$CHCl_3$	0.1	1 w	60	8
6	**T3P**	**DMF**	**0.1**	**18 h**	**60**	**33**
7	T3P	DMA	0.1	18 h	60	19
8	CDI	DMF	0.1	18 h	60	11
9	HATU	DMF	0.1	18 h	60	19

First, the concentration of hydroxy acid **162** in solution was changed from 0.1 M to 0.001 M (Table 2, Entry 2). It was assumed that a higher dilution would lower the probability of hydroxy acid **162** reacting with other hydroxy acid molecules, and although ideally we did not want to resort to high dilution in INRE reactions, we still considered that testing at lower concentrations would allow for greater insight into multi-INRE systems. If a higher yield of product **164** was observed using high dilution, it could be inferred that intermolecular reactions and the formation of polymers are the underlying reason for the poor yield of **164** at standard concentrations of 0.1 M. However, the yield of the diluted reaction was lower,

7%, suggesting that competing intermolecular reactions were not the main cause of the poor yield of product **164**.

Next, the reaction solvent was switched from chloroform to a chlorinated solvent with a higher boiling point, 1,2-dichloroethane (DCE) (Entry 3), allowing the reaction temperature to be raised to 85 °C. It was hoped that increasing the reaction temperature would supply intermediates **163a** and **163b** with enough energy to overcome any possible kinetic barriers that may have been preventing formation of the product **164**. However, the decreased yield of 9% contradicted the proposed hypothesis. Next, the opposite was tested, with the hope that lowering the reaction temperature and in turn reducing the energy supplied to the INRE system we would reduce the prevalence of competing side-reactions that could be consuming starting material **162** and in turn reduce the number of undesired side-products (Entry 4). However, a lower yield of 6% was observed which once again contradicted this assumption.

In an attempt to allow complete conversion of starting material **162** into product **164**, the reaction time was increased to one week (Entry 5), however this also led to a lower yield of 8%. Next, a change to the more polar solvent DMF was explored, based on a notion that a more polar would help stabilise any charged intermediates formed during the reaction (**163a** and **163b**). We hoped this would in turn lower the energy required to form intermediates **163a** and **163b**, thereby increasing the rate of product **164** formation (Entry 6). Pleasingly, this led to a relatively large increase in yield to 33%, nearly double the yield of the initial multi-INRE reaction (Entry 1). Dimethylacetamide (DMA), another polar solvent, was also screened in the reaction (Entry 7) but a lower yield of 19% was obtained.

As DMF gave the best results for multi-INRE reactions at this stage, it was then used as a standard when screening other variables, such as the coupling agent. Both 1,1'-carbonyldiimidazole (CDI) (Entry 8) and hexafluorophosphate azabenzotriazole tetramethyl uronium (HATU) (Entry 9) were used as alternative coupling agents to T3P in the hope of finding a more suitable coupling agent, however, both reagents led to a decrease in the yield of lactone **164** to 11% and 19% respectively.

With moderate screening of reaction **162** → **164** we achieved a significant increase in yield (17% to 33%). Although there is substantial room for improvement, the noteworthy increase in yield arising from a small number of screening experiments suggests that with more intensive screening of the multi-INRE reaction **162** → **164** and further optimisation, a considerable increase in the yield of lactone **164** is possible. Interestingly, throughout the

initial screening process, none of starting material **162** could be identified in the unpurified reaction mixture by TLC or ^{1}H NMR spectroscopy, suggesting that all starting material had been consumed. Due to the low yields of lactone **164**, it was assumed that hydroxy acid **162** was instead being converted to an undesired side-product in greater quantities than the desired lactone **164**. At this point, optimisation of this reaction was paused, to examine alternative substrates (section 3.3) and the reaction mechanism (section 3.2). However, additional optimisation of this system (leading to much improved yields) is described later in the thesis (section 3.4).

3.2 Theorised INRE Reaction Intermediate

When performing the INRE reaction, the addition of T3P to the hydroxy acid **162** causes the reaction solution to instantaneously undergo a colour change, from colourless to deep red. This suggested that a highly conjugated intermediate could be formed in the reaction **162** → **164**, given that strong colours in organic molecules are often associated with extended conjugation. Scheme 41 shows the proposed formation of a highly conjugated, aromatic species (**183**) which could be formed from intermediate **163a**. Thus, deprotonation α to the carbonyl of charged intermediate **163a** would give conjugated heterocycle **183**, which would be both aromatic and neutral, hence this putative intermediate **183** might be expected to be more thermodynamically stable than intermediate **163a**. It was therefore speculated that intermediates **163a** and **183** are in equilibrium, and in order for ring expansion to procced, heterocycle **183** would first need to revert to intermediate **163a**, thus introducing an energy barrier that slows the rate of formation of product **164**. A hypothetical reaction coordinate for this scenario (which assumes that **183** is lower in energy than **163a**) is depicted in Figure 11.

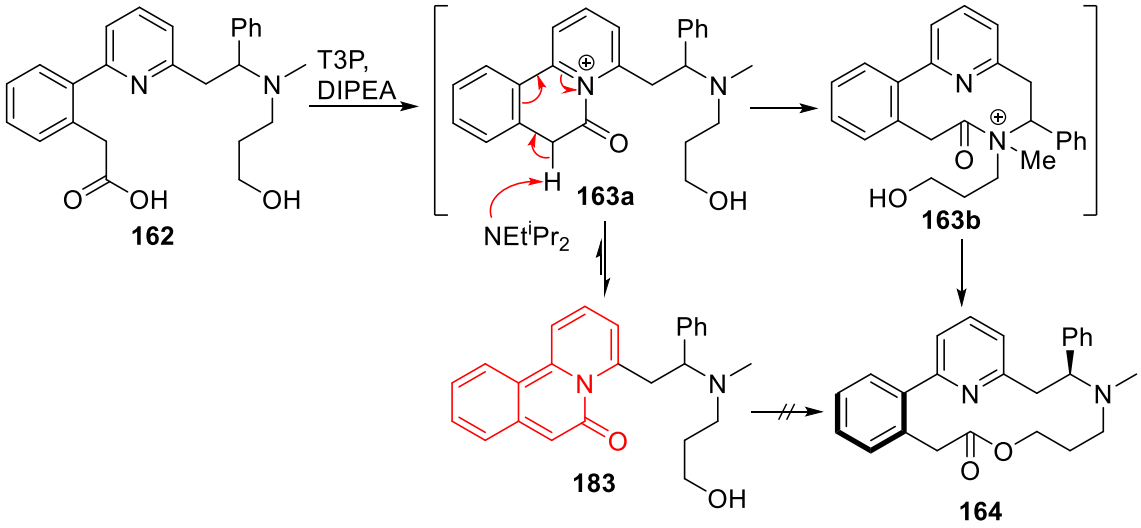

Scheme 41: Mechanism for the formation of the theorised undesired by-product **183**.

It was believed that if the reaction pathway **162** → **164** proceeded without formation of by-product **183** (blue), the reaction would proceed to form product **164**, as the two intermediates **163a** and **163b** possess favoured energy minimums. However, if the reaction pathway proceeded via the formation of by-product **183** (red), then the energy minimum would hypothetically be much lower than the energy minimum possessed by charged intermediate **163a**, in turn creating a steep energy barrier which slows the rate of formation of intermediate **163b** and in turn product **164**.

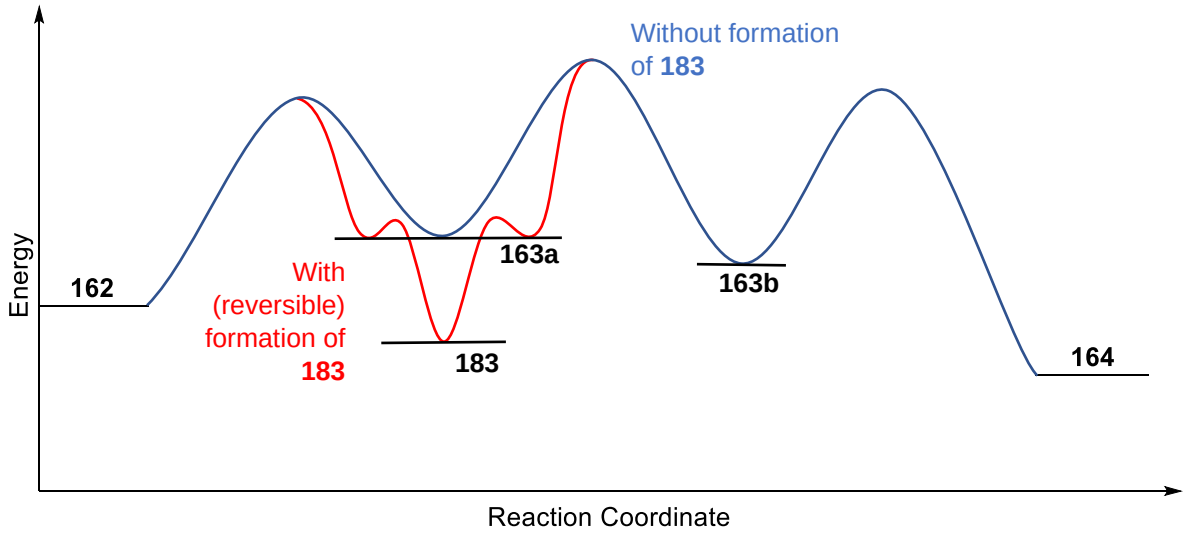

Figure 11: Hypothetical reaction coordinate illustrating energy minimums with and without formation of by-product **183**.

All attempts to isolate intermediate **183** from the reaction mixture were unsuccessful. This is presumed to be due to its decomposition either during chromatographic purification or upon work up of the reaction mixture with water. Nevertheless, there is evidence suggesting

that products of similar type to **183**, are formed in related work conducted in the Unsworth group, which led to the isolation of a similar aromatic heterocycle (**189**). Scheme 42 shows the formation of aromatic heterocycle **189** using standard single-INRE conditions. In this example, there is a key difference with the precursor compared with typical starting materials; the terminal nucleophile of the INRE precursor **187** is protected with a TBS group, making INRE unfeasable.[60]

When unprotected hydroxy acid **184** was reacted with T3P and DIPEA using typical single-INRE conditions, lactone **186** was formed in excellent yield of 90%. However, when the alcohol was protected by TBS (**187**) and reacted using the same conditions, the now protected alcohol of intermediate **188** cannot promote ring expansion, which instead allows deprotonation and subsequent aromatisation of intermediate **188** to occur to form the aromatic heterocycle **189** in over 99% yield. Heterocycle **189** can be isolated whilst side-product **183** cannot. It is assumed that the toluene group present on heterocycle **189** provides further conjugation into the aromatic moiety, in turn increasing the stability of heterocycle **189** and making the conjugated molecule less prone to decomposition, thus allowing aromatic **189** to be isolated and characterised.

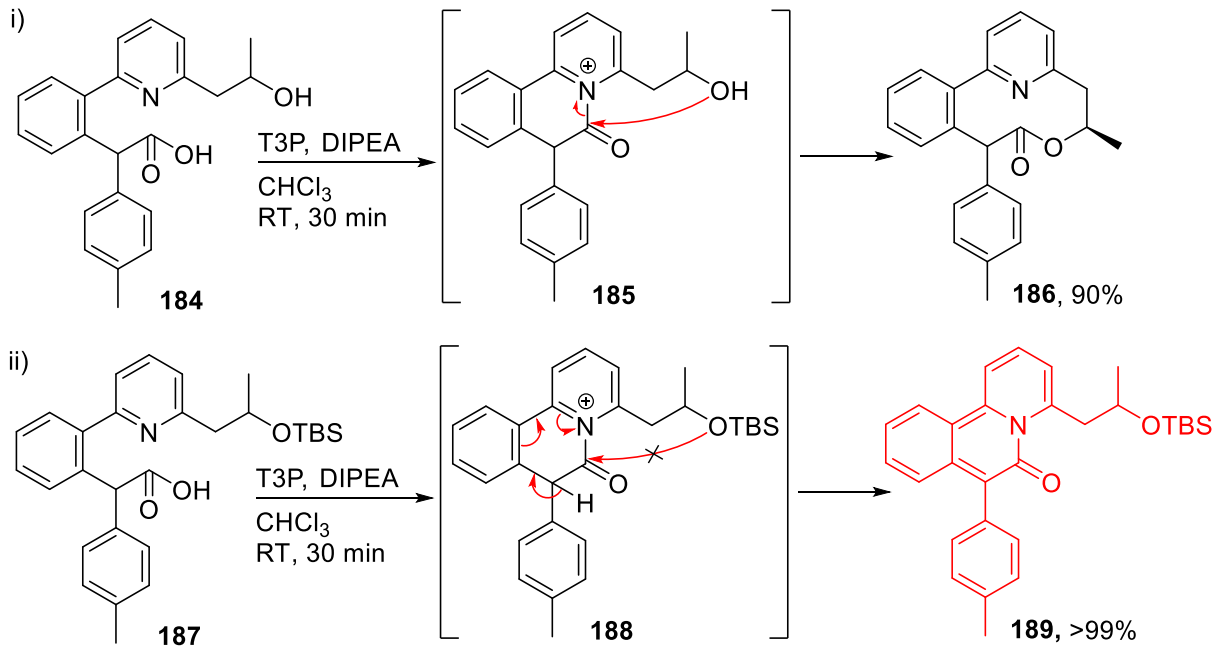

Scheme 42: Attempted INRE of a precursor that does (**187**) and does not (**184**) have a protected alcohol.

3.3 Exploration of Aliphatic Precursors

In an attempt to circumvent the formation of side-product **183**, we decided to design an aliphatic linear precursor which could undergo a multi-INRE reaction without the possibility of a highly conjugated stable intermediate forming. This proposed precursor (**190**) contains two tertiary benzylic amines functioning as internal nucleophiles as well as a primary alcohol group functioning as the terminal nucleophile. Scheme 43 shows the designed aliphatic precursor **190** and the proposed multi-INRE mechanistic pathway. Thus, the carboxylic acid of **190** would undergo activation by the coupling agent T3P, in turn activating acid **190**, allowing for the first internal nucleophile (benzylic amine) to attack into the carbonyl to form cyclic intermediate **191a**. The second internal nucleophile (benzylic amine) would then attack into the same carbonyl, displacing the first internal nucleophile to form the 9-membered intermediate **191b**. Finally, the terminal nucleophile (primary alcohol) would attack into the carbonyl, displacing the second internal nucleophile before stabilising the charge via deprotonation to form the saturated ring expanded lactone **192**. It was hoped that the lack of aryl groups in the main carbon backbone would remove the possibility of aromatisation during the reaction, and hopefully in turn would reduce the formation of any competing conjugated side-products.

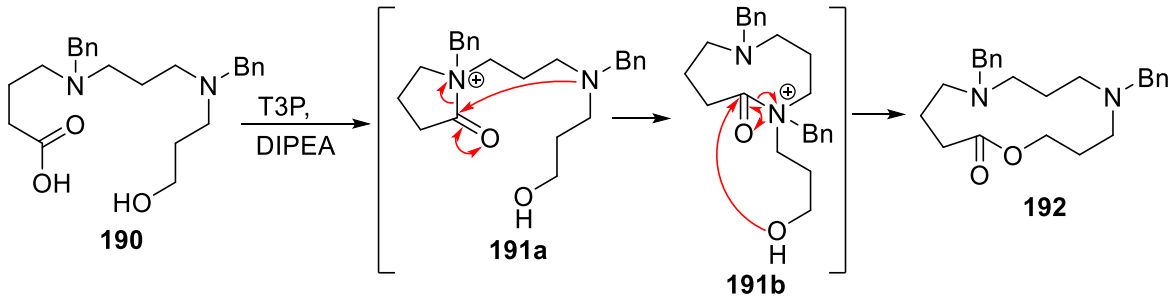

Scheme 43: Proposed multi-INRE mechanism of aliphatic precursor **190** to form aliphatic lactone **192**.

We envisaged the synthesis of precursor **192** to procced via repeated S_N2 reactions between alkyl bromides (**193**) with secondary amines (**194**) to afford longer alkyl chains containing primary alcohols (**195**) which could be converted into alkyl bromides (**196**) in order to repeat the sequence. Scheme 44 outlines the general synthetic strategy used. If successful, this strategy would allow for the synthesis of multiple alkyl precursors of differing lengths from a single synthetic strategy. It was also hoped that by altering the alkyl chain length between functional groups and in turn altering the ring size of individual intermediates, greater insight into the optimum intermediate ring size for multi-INRE reactions would be obtained.

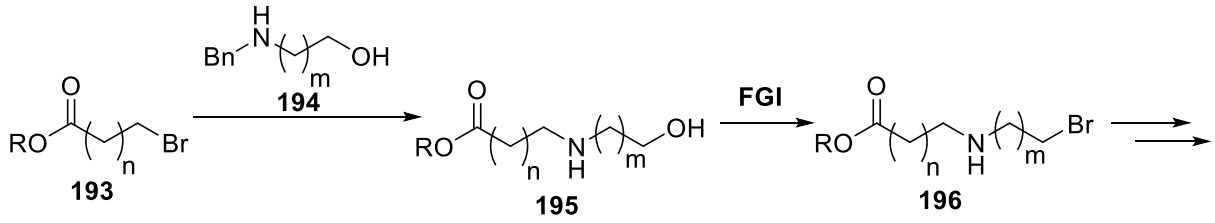

Scheme 44: General synthetic strategy for the synthesis of aliphatic multi-INRE precursors.

For the synthesis of precursor **190**, we started with methyl-4-bromobutyrate (**197**) (Scheme 45). Alkyl bromide **197** underwent nucleophilic attack from benzylic amine **198** in an S_N2 reaction to afford hydroxy ester **199** in a yield of 39%. As with similar S_N2 reactions previously conducted with an alkyl bromide electrophile, the yield of product **199** was not ideal, however, we could not readily access the iodoester analogue of bromoester **197** and in turn could not easily test previously optimised S_N2 conditions for the synthesis of precursor 1**90**. For future optimisation, a catalytic amount of sodium iodide could be added to the S_N2 reaction to form an alkyl iodide *in situ*, which in turn could lead to an increased in yield of **199**.

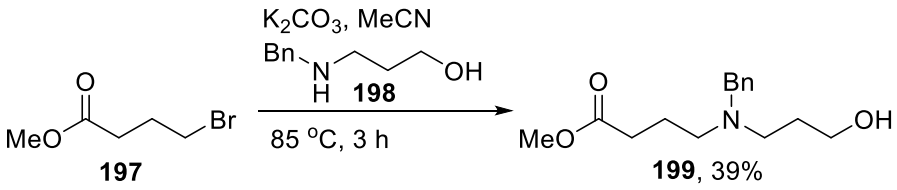

Scheme 45: S_N2 of bromobutyrate **197** to yield hydroxy ester **199**.

With the hydroxy ester **199** in hand, we then looked to install the second benzylic amine and terminal alcohol. To prepare hydroxy ester **199** for a another S_N2 reaction using benzylic amine **198**, the nucleophilic alcohol would first need to be swapped for an electrophile. This was achieved using an Appel reaction, in which the terminal alcohol was converted into a bromide (Scheme 46); thus, hydroxy ester **199** was stirred in DCM with carbon tetrabromide and triphenylphosphine at 0 °C for one hour to give alkyl bromide **200** in good yield of 72%.

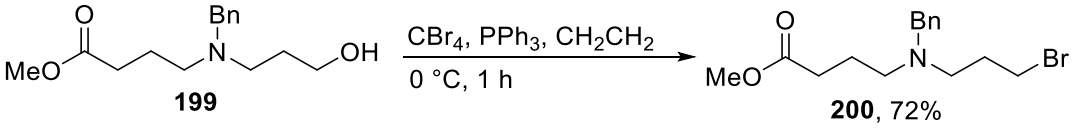

Scheme 46: Appel reaction of hydroxy ester **199** to alkyl bromide **200**.

The next step in the synthesis of aliphatic precursor **190** was an S_N2 reaction between benzylic amine **198** and alkyl bromide **200** (Scheme 47). The conditions for the S_N2 reaction were identical to the conditions used in the previous S_N2 reaction **197** → **199**. The alkyl

bromide **200** was reacted with 3-(benzylamino)propan-1-ol (**198**) and potassium carbonate in acetonitrile at 85 °C for 3 h to afford hydroxy ester **201** in yield of 45%. The yield for this reaction was not ideal, and could potentially be improved with further optimisation (see future work); nevertheless, sufficient quantities of hydroxy ester **201** was synthesised to allow the synthesis of precursor **190** to continue.

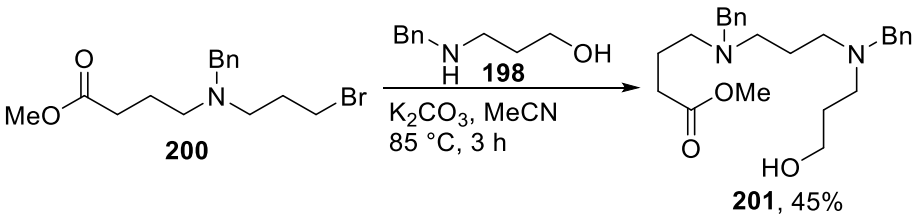

Scheme 47: Alkylation of alkyl bromide **200** to yield hydroxy ester **201**.

The final step of the synthetic route was hydrolysis of ester **201** to reveal the hydroxy acid precursor (**190**) that would undergo the aliphatic multi-INRE reaction. Scheme 48 shows the hydrolysis of ester **201** using previously identified conditions (**182** → **162**). Accordingly, hydroxy ester **201** was vigorously stirred in a solution of water and THF with lithium hydroxide for 18 h at room temperature to afford hydroxy acid **190** in yield of 40%. As we would expect the hydrolysis of methyl ester **201** into acid **190** to proceed to completion under the conditions used, the 40% yield obtained was disappointing. It is assumed that the poor yield was caused by two key factors. First, impurities carried forward from previous reactions were removed in a more polar chromatographic purification solvent system (ethyl acetate and methanol), reducing the isolated mass retrieved. Second, the impurities carried forward were eluting at similar R_fs to product **190**, making separation of product **190** from side-products via column chromatography more challenging. It is hoped that revising the synthesis of hydroxy acid **190**, the quantity of impurities could be severely reduced.

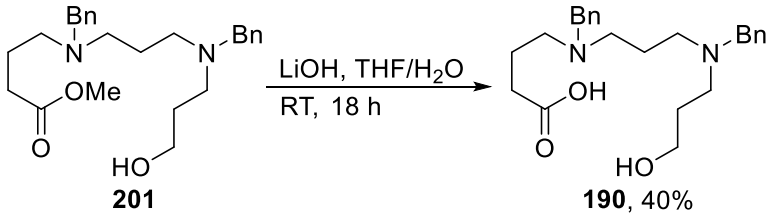

Scheme 48: Hydrolysis of ester **201** to yield INRE precursor **190**.

With the synthesis of linear precursor **190** complete, we now had a synthetic route (albeit unoptimised) to access both the aliphatic precursor at hand, that could also be applied to make other aliphatic linear precursors of differing lengths. Scheme 50 shows the synthetic route for hydroxy acid **190**, which has an overall yield of 5% over four steps. As previously

mentioned, we are confident that the synthetic route could be improved if needed in future work, with specific focus on improving the S_N2 reaction conditions. Nevertheless, a sufficient quantity of aliphatic hydroxy acid **190** was synthesised and could now be used to perform the first multi-INRE reaction with an aliphatic linear precursor.

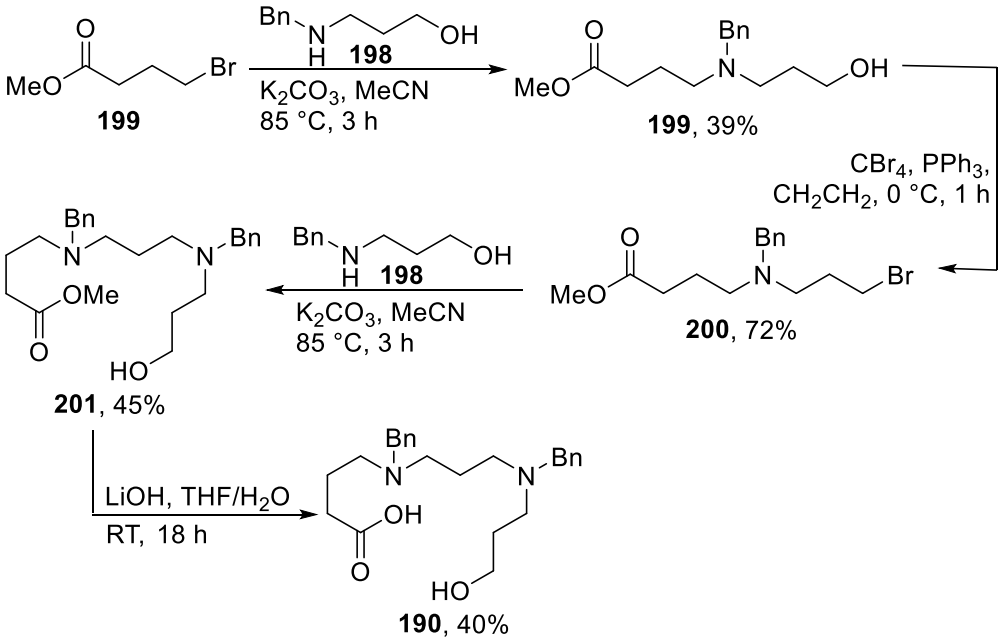

Scheme 49: Synthetic route for the aliphatic precursor **190**.

As well as having precursor **190** available for INRE testing, a 15-membered analogue (**202**) was inherited from a previous member of the Unsworth group (T. Stephens), which was synthesised using a similar synthetic strategy.[61] With both aliphatic linear precursors **190** and **202** in hand, it was time to conduct multi-INRE tests on both (Scheme 51). Precursors **190** and **202** were stirred with T3P and DIPEA at 60 °C overnight to yield lactones **192** and **203** in yields of 29% and 15%, respectively. Surprisingly, the shorter precursor **190** gave a higher yield than the standard 6-membered precursor **202**, despite the formation of a more strained 5-membered ring intermediate. This is speculated to be due to the shorter distance between the activated acid and the first internal nucleophile, in turn providing a higher chance of contact between the two groups.

Nevertheless, the yield of neither product **192** nor **203** is greater than the yield of lactone **164** from the multi-INRE of biaryl precursor **162**. As aromatisation of the aliphatic intermediate **191a** is impossible, the formation of unwanted side-products of the form **183** cannot be reason for low yields, in these systems at least. However, the aliphatic precursors lack any conformational bias imparted by aromatic rings and possess more flexibility from unrestricted C-C rotation, leading to higher degrees of freedom when compared to aromatic

precursor **162**, leading to a higher entropic penalty when cyclising, which could explain the decreased in yields.

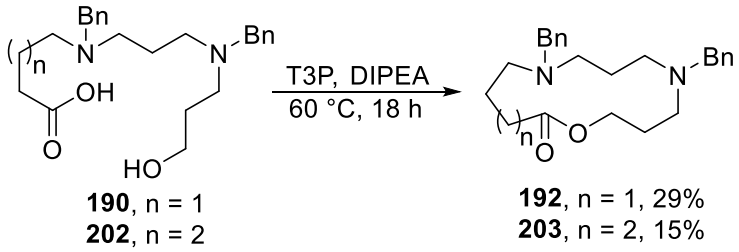

190, n = 1
202, n = 2

192, n = 1, 29%
203, n = 2, 15%

Scheme 50: INRE reactions yielding 13- and 14-membered lactones (**192**/**203**).

In spite of this unsatisfying result, the isolation of macrocyclic lactones **192** and **203** confirmed that multi-INRE reactions are possible with aliphatic linear precursors containing two internal nucleophiles to make both 13- and 14-membered heterocyclic lactones. Lactones **192** and **203** were characterised by HRMS, IR, and both ^{1}H and ^{13}C NMR spectroscopy. The key evidence for cyclisation of both linear hydroxy acids **192** and **203** is the change in chemical shift of the ^{13}C NMR peak representing the carbonyl environment (a in Figure 12). Figure 12 shows the stacked ^{13}C NMR spectra of biaryl lactone **164** (top), 13-membered aliphatic lactone **192** (middle) and 14-membered aliphatic lactone **203** (bottom). It can be seen that the carbonyl peak of the 13- and 14-membered aliphatic lactones are at δ_C 174.3 ppm and δ_C 174.0 ppm respectively, and the carbonyl peak of biaryl lactone **164** is seen at δ_C 172.1. ppm. The chemical shift of the key carbonyl peak of the 13- and 14-membered aliphatic lactones **192** and **203** is near identical to the carbonyl peak of the biaryl lactone **164**, strongly suggesting that the carboxylic acid's **190** and **202** have been converted into their respective lactones via INRE. The chemical shift of the carbonyls in ^{13}C NMR, along with other means of characterisation, strongly support the successful multi-INRE of linear hydroxy acids **190** and **202** to form the novel aliphatic macrocyclic lactone **192** and **203**. As anticipated, there was no proton peak splitting in the ^{1}H NMR which indicated restricted rotation of C-C bonds in the formed aliphatic macrocycles.

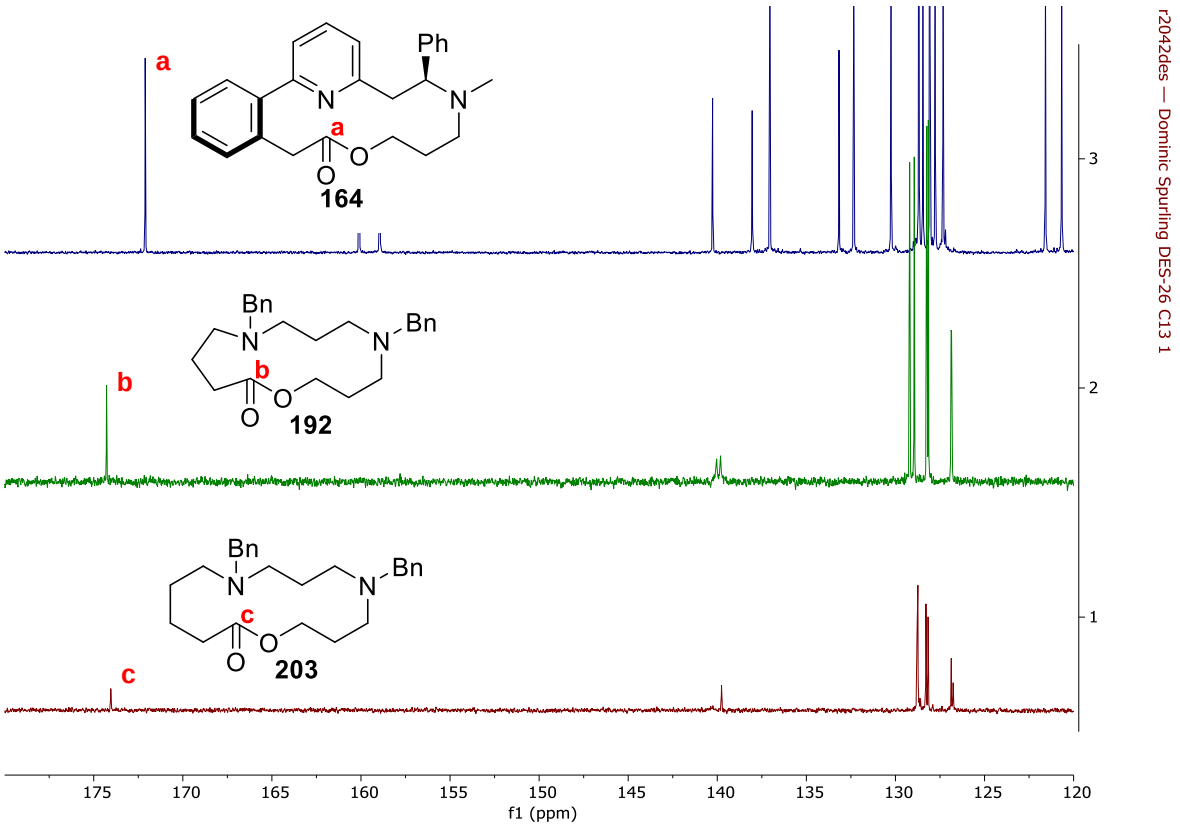

Figure 12: ^{13}C NMR spectra of biaryl lactone **164** (top), 13-membered aliphatic lactone **192** (middle), and 14-membered aliphatic lactone **203** (bottom).

3.4 Screening of Multi-INRE Reaction 162 → 164 With Internal Standard

With the multi-INRE reactions of aliphatic precursors constantly presenting low yields, attention was directed back to the biaryl multi-INRE precursor **162** with the intention to further screen conditions for the reaction of **162** → **164** in order to find higher yielding reaction conditions which could be used for the cyclisation of all linear multi-INRE precursors. As the purification and isolation of product **164** from several reactions performed simultaneously would be time consuming, a more efficient screening method employing an internal standard was used to avoid purification of the crude reaction mixtures. Thus, a known amount of internal standard was added to the crude reaction mixture before performing an aqueous workup to remove water soluble impurities, such as the T3P by-product tripropyl-diphosphonic acid. With the use of ^{1}H NMR spectroscopy, the unpurified reaction mixture is then analysed, where a ratio of the quantifiable internal standard and product **164** can be calculated. From this, the yield of product **164** present in the crude

reaction mixture could be determined. Figure 12 shows an example of a ^{1}H NMR spectrum of the unpurified reaction mixture from a multi-INRE reaction containing the internal standard. 1,3,5-Trimethoxybenzene (TMB) was chosen as the internal standard, as its aromatic protons give a distinct singlet at δ_H 6.08 ppm in a clear region of the ^{1}H NMR spectrum of the reaction mixture **164** (Figure 13). Screening of **162** → **164** was performed on a 0.1 mmol scale, therefore addition of 100 µL of a 0.1 M solution of internal standard, added 0.01 mmol of internal standard into each reaction. Thus, for every 1.0 equivalent of starting material **162** there was 0.1 equivalents of TMB. To account for this, the internal standard singlet at 6.08 ppm (which correlates to three identical proton environments) is integrated and set to 0.3 so that the yield of product **164** is proportional to the integration of its environments. An example of this is shown in the following spectra (Figure 13); the area integrated at 4.51 ppm correlates to two overlapping peaks produced by two protons (H_a+H_{b*}) belonging to product **164**, thus the yield of product **164** is equal to half of the multiplet's integration (at 100% yield the multiplet H_a+H_{b*} would integrate for 2.00). In Figure 13 the H_a+H_{b*} peak integrates to 0.57, thus the yield of product **164** is 29%. Like with all INRE reactions conducted, there is no evidence of starting material **162** present, so complete starting material consumption is assumed.

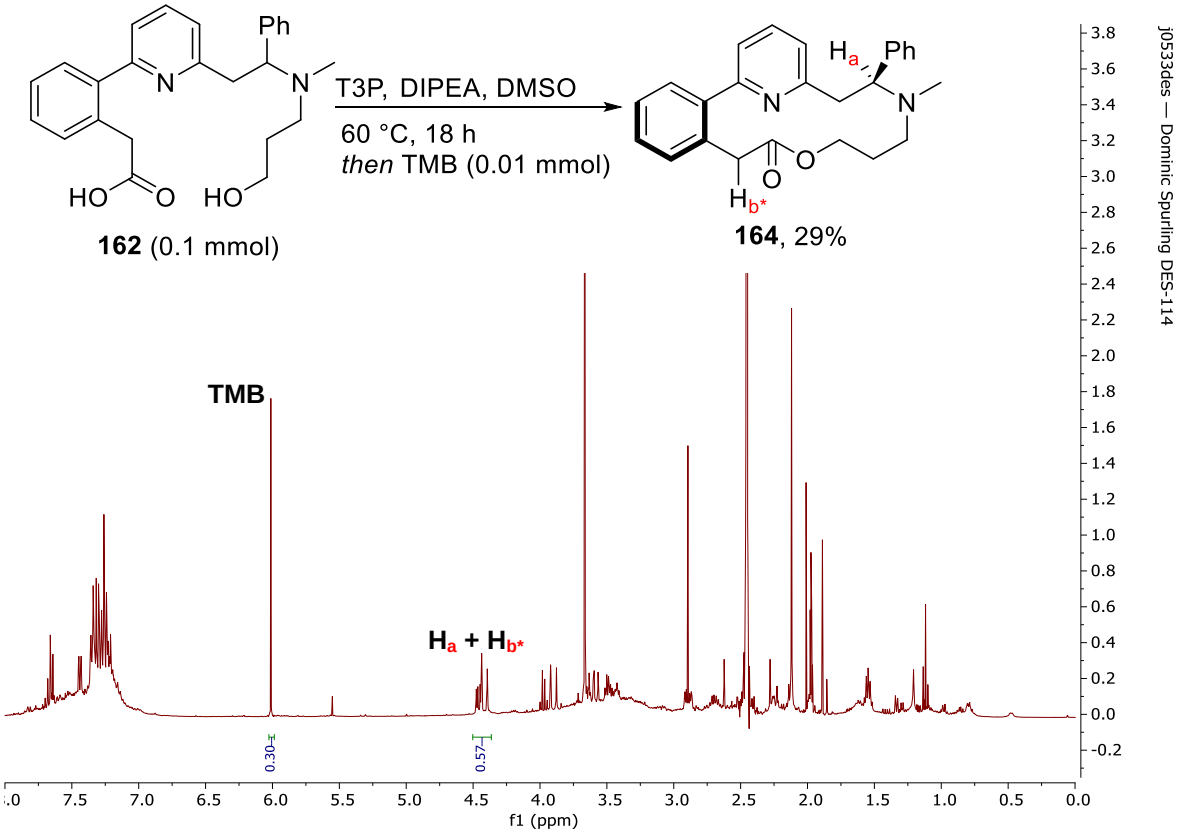

Figure 13: ^{1}H NMR spectrum of crude reaction mixture and internal standard 1,3,5-trimethoxybenzene.

By using this method of high throughput screening, eight reactions could be set up simultaneously, and analysed relatively quickly, increasing our screening capabilities considerably. In total, 21 INRE reactions were conducted using this method, as seen in Table 3, with modifications to the temperature, coupling agent and solvent.

Table 3: Screening conditions using internal standard and their respective yield. [b] Solvent dried out.

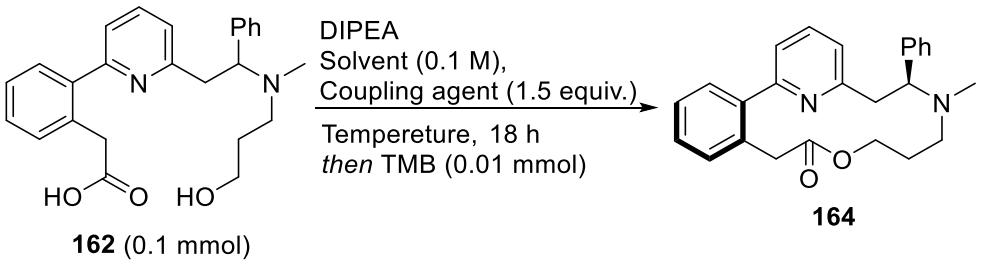

162 (0.1 mmol) **164**

Entry	Coupling Agent	Solvent	Temperature / °C	Yield / %
1	T3P	DMF	60	30
2	EDC	DMF	60	15
3	2-Chloro-1-methylpyridinium iodide	DMF	60	0
4	T3P	DMSO	25	29
5	T3P	PhMe	25	16
6	T3P	THF	25	22
7	T3P	MeCN	25	31
8	T3P	$CHCl_3$	25	10
9	T3P	DMSO	60	29
10	T3P	PhMe	60	5
11	T3P	THF	60	20
12	T3P	$CHCl_3$	60	15
13	T3P	DMSO	190	0 [b]
14	T3P	PhMe	110	7
15	T3P	THF	66	trace
16	T3P	MeCN	82	trace
17	EDC + HOBt	DMF	25	72
18	EDC + HOBt	DMSO	25	40
19	EDC + HOBt	PhMe	25	69
20	EDC +HOBt	THF	25	66
21	**EDC + HOBt**	**MeCN**	**25**	**70**

The first modification came from replacing T3P for other coupling agents commonly used in peptide coupling reactions in an attempt to find a better suited coupling agent. The coupling agents tested were 1-ethyl-3-(3-dimethylaminopropyl)carbodiimide (EDC) (Entry 1) and 2-chloro-1-methylpyridinium iodide (Entry 2). Disappointingly, when using these coupling agents the yield of **164** was dramatically reduced, which led us to focus our attention on changing other variables, such as solvents. Five solvents, DMSO, toluene, THF, acetonitrile, and chloroform were screened at room temperature, 60 °C, and reflux (Entry 4–

16). It was hoped that using a diverse selection of solvents with varying polarities and boiling points would give further insight into how the reaction proceeded, and in turn would lead to further optimisation. However, after screening each solvent at the aforementioned temperatures, none of these solvents proved to be particularly effective, however, multi-INRE reactions conducted in DMSO and acetonitrile gave yields similar to the multi-INRE reactions carried out in DMF. The ~30% yield obtained in different polar solvents further supports the idea that a charged intermediate, such as pyridinium **163a** and ammonium **163b** are formed during the reaction. Also, the yield of lactone **164** was reduced when solvents were heated to reflux (Entry 13–16), indicating that temperatures above 60 °C are unfavourable for multi-INRE reactions.

EDC was then used once again, but now with the addition of a hydroxybenzotriazole (HOBt) additive using DMF as the solvent. Pleasingly, this gave a significant increase in yield of product **164**, with an increase in yield from 30% to 72% (Entry 17). The HOBt additive was tested in combination with other solvents in hope of finding a less toxic alternative which was more volatile. Pleasingly, a solvent swap to acetonitrile was found to be similarly successful, and due to easier removal (in view of its volatility) and lower toxicity compared with DMF, it was retained for future studies.

Scheme 51 shows the optimised conditions; EDC and HOBt (1.5 equivalents), and DIPEA in acetonitrile (0.1 M) at room temperature for 18 h, as well as the mechanism for carboxylic acid activation using EDC. The electrophilic carbodiimide **204** was attacked by the deprotonated carboxylic acid of precursor **162** to give the intermediate **205a**. The now more electrophilic carbonyl of intermediate **205a** was then attacked again by the hydroxylamine of HOBt (**206**), ejecting a urea by-product and forming the activated acid **205b**. The carbonyl of the activated acid **205b** was then attacked by the pyridine internal nucleophile, starting the multi-INRE cascade which subsequently yields product **164**. Pleasingly, we found the isolated yield (following column chromatography) using these conditions to be 73%, slightly higher than what was seen using internal standard.

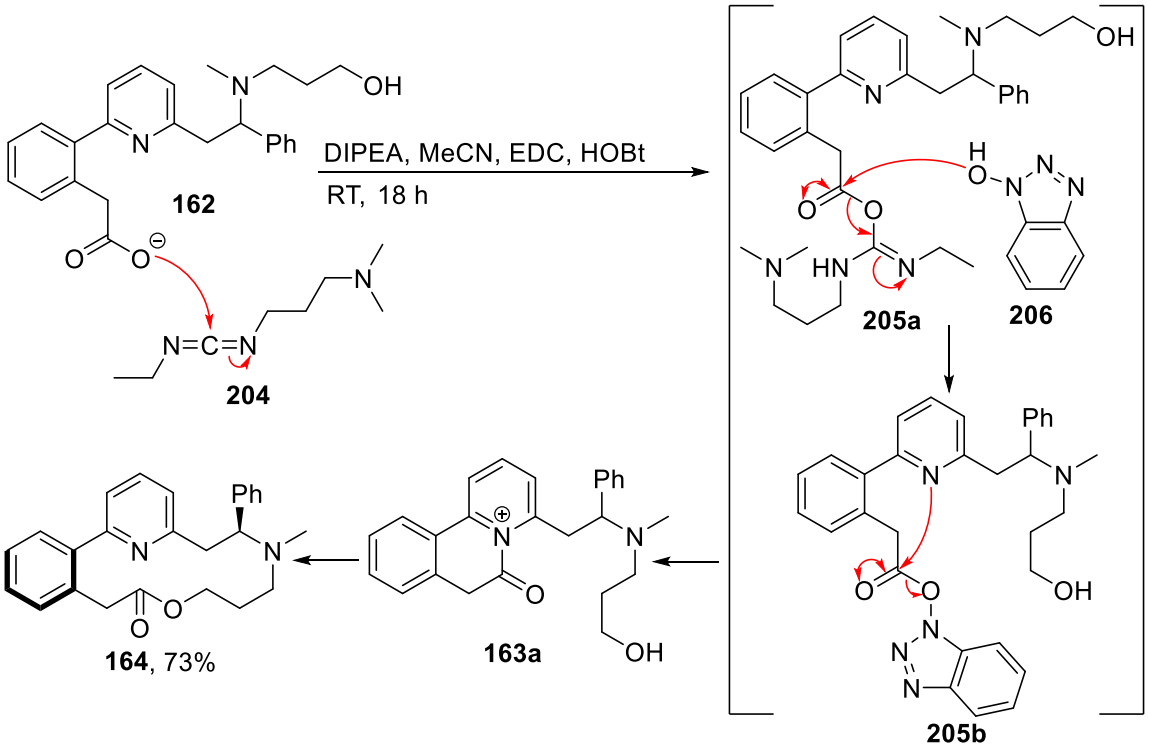

Scheme 51: Mechanism of activation of precursor **162** using finalised multi-INRE reaction conditions.

The aliphatic multi-INRE precursors **190** and **202** were then cyclised using the improved HOBt and EDC conditions. Pleasingly, both saw a significant increase in yield of their respective product (Scheme 52) compared to previously tested conditions, however, the yield of neither product was higher than 50%, suggesting that the biaryl INRE precursor **162** is more susceptible to cyclisation in the presence of HOBt and EDC when compared to aliphatic precursors **190** and **202**. However, as previously mentioned, precursors **190** and **202** may be less prone to cyclisation due to a larger loss of entropy during cyclisation when compared to cyclisation of precursor **162**.

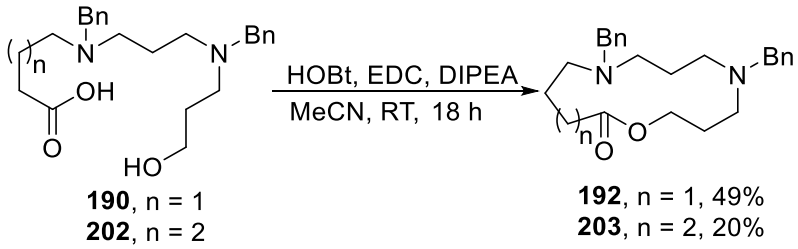

Scheme 52: Multi-INRE of aliphatic precursors **190** and **202** using finalised conditions (EDC, HOBt and MeCN).

3.4 Summary

The yield for the cyclisation of linear precursor **162** into heterocyclic-macrocycle **164** via a multi-INRE reaction has been raised from the initial 17% to a much more satisfying 73%. The increase in yield was achieved through the high throughput screening of the INRE reaction with use of an internal standard. EDC was found to be the optimal coupling reagent along with an HOBt additive and acetonitrile was the optimal solvent.

A novel aliphatic linear multi-INRE precursor (**190**) was prepared in a four-step synthesis. Using aliphatic precursors **190** and **202**, novel aliphatic heterocyclic-macrocycles **192** and **203** were synthesised via a multi-INRE in yields of 49% and 20% respectively. Thus, multi-INRE reactions have proven to be successful when synthesising both 13- and 14-membered aliphatic heterocyclic-macrocycles.

The possible formation of a conjugated side-product (**183**) from the multi-INRE of biaryl precursors has been explored, although no firm conclusions have been made and its role in the mechanistic pathway is still unclear.

Further Exploration of Scope

4.1 Synthetic Targets

With the conditions for multi-INRE reactions finalised, we moved towards exploring what macrocycles could and could not be made via multi-INRE, giving insight into the limitations of the multi-INRE reaction. Several precursors and their respective products were designed in order to investigate factors which could contribute towards the success or limitation of the INRE reaction (Scheme 53).

The first precursor designed, amino acid **207**, possesses an aniline moiety as the terminal nucleophile. A similar system was envisioned when designing precursor **209**, but with the change of the second internal nucleophile from a tertiary methyl amine to a less nucleophilic tertiary phenylamine. The third precursor designed, the mono-aryl precursor **211**, is near identical to precursor **162** except with the absence of an aryl group adjacent to the pyridine internal nucleophile.

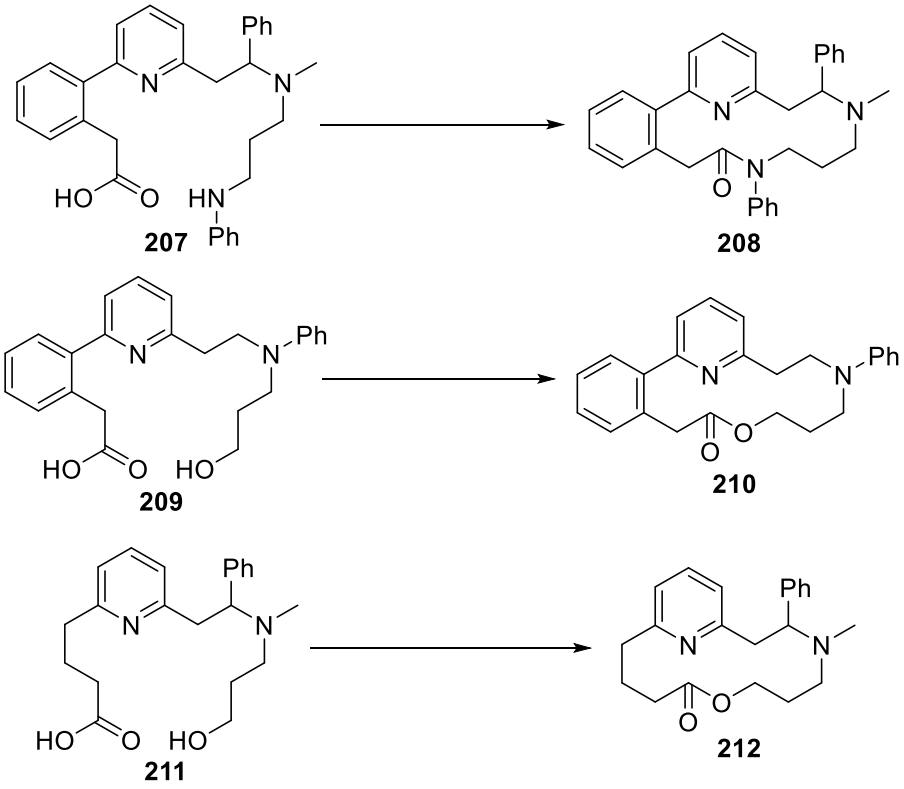

Scheme 53: Designed multi-INRE precursors and their respective INRE products.

It was hoped that a synthetic route could be developed for most, if not all, precursors listed in Scheme 53. Due to complications caused by the SARS-CoV-2 pandemic,[62] laboratory work was abruptly stopped, and many envisioned synthetic routes could not be fully

developed and no further INRE reactions could be carried out. Nonetheless, progress to date on each route is provided.

4.2 Synthesis of a Precursor with Phenylamine Terminal Nucleophile (207)

A full synthetic route was designed for precursor **207**. As the carbon framework of precursor **207** is identical to the initial multi-INRE precursor **162**, much of the synthetic route to access precursor **207** is based on the route used to access precursor **162**. The main deviation from the synthetic route to precursor **162** is the alkylation of secondary amine **174** (Scheme 54). In order to install a phenylamine as the tertiary nucleophile, an S_N2 reaction was attempted using bromo phenylamine **213**. Thus, secondary amine **174** was stirred with bromo phenylamine **213** in acetonitrile with potassium carbonate for 18 h at 85 °C to give the tertiary amine **214** in yield of 30%.

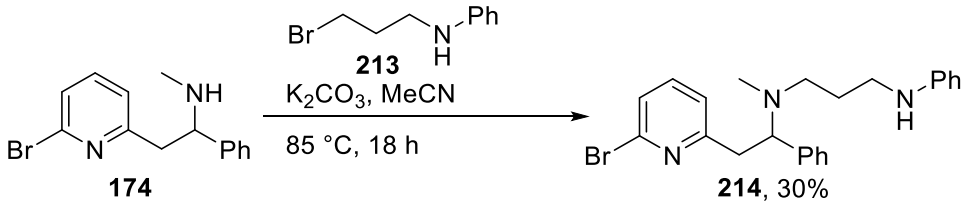

Scheme 54: Alkylation of secondary amine **174** to give phenylamine **214**.

Although the S_N2 reaction shown in Scheme 54 was low yielding, a more electrophilic replacement for bromo phenylamine **213** with a better leaving group (such as iodide) was unavailable. This is in part due to the unstable nature of reagent **213**, which contains both an electrophilic bromide and nucleophilic phenylamine, which causes reagent **213** to cyclise slowly over time. Due to the instability of phenylamine **213**, it was prepared the day of use through a separate S_N2 reaction (Scheme 55). Aniline (**215**) underwent a single addition to dibromopropane (**216**), which was in large excess (6.0 equivalents), in acetonitrile at reflux for 3 h to afford bromo phenylamine **213** in a yield of 33%. The secondary amine of product **213** would then undergo an additional S_N2 to cyclise and form heterocycle **217** when left for a prolonged time at room temperature. In view of both the low yield of product **214** and the instability of reagent **213**, this step of the synthetic route to precursor **207** would need to be revisited and improved in future work.

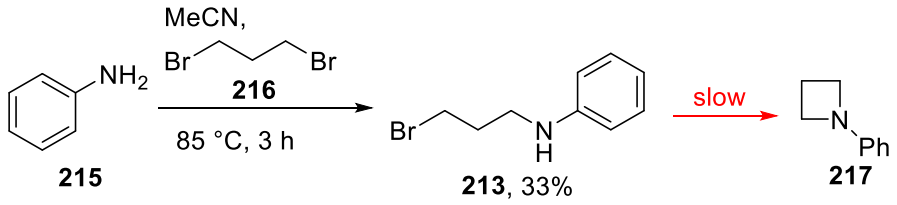

Scheme 55: Synthesis of bromo phenylamine **213** and its subsequent decomposition **213** → **217**.

The following steps of the synthetic route towards precursor **207** are near identical to the final steps towards precursor **162** (Scheme 56). Bromopyridine **214** was coupled to boronic ester pinacol **181** in a Suzuki-Miyaura cross-coupling reaction with potassium phosphate and Pd(dppf)Cl_2 to afford hydroxy ester **218** in yield of 76%, before subsequently undergoing hydrolysis with lithium hydroxide to furnish the final precursor **207** in yield of 68%. Pleasingly, both reactions provided their respective product in adequate yield, leading to no further consideration of reaction optimisation.

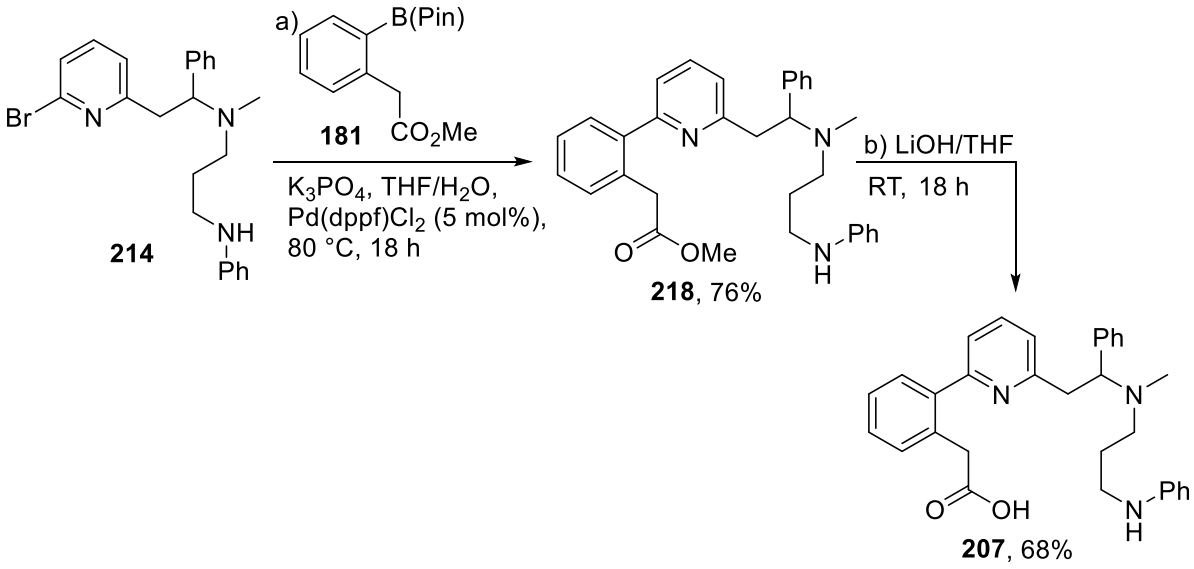

Scheme 56: Suzuki-Miyaura coupling and subsequent hydrolysis of bromopyridine **214** to award precursor **207**.

Scheme 57 shows all the reactions involved in the synthesis of the linear precursor **207** from bromomethyl pyridine **173** with an overall yield of 14%. As previously mentioned, there is room for further optimisation if time had allowed. With the synthesis of precursor **207** complete, we could now test this substrate in a novel multi-INRE precursor using a free amine as the terminal nucleophile, which in turn could be used for the synthesis of the first macrocyclic lactam containing multiple internal nucleophiles (**208**) via multi-INRE. Because of the SARS-CoV-2 pandemic, this reaction has not yet been tested.

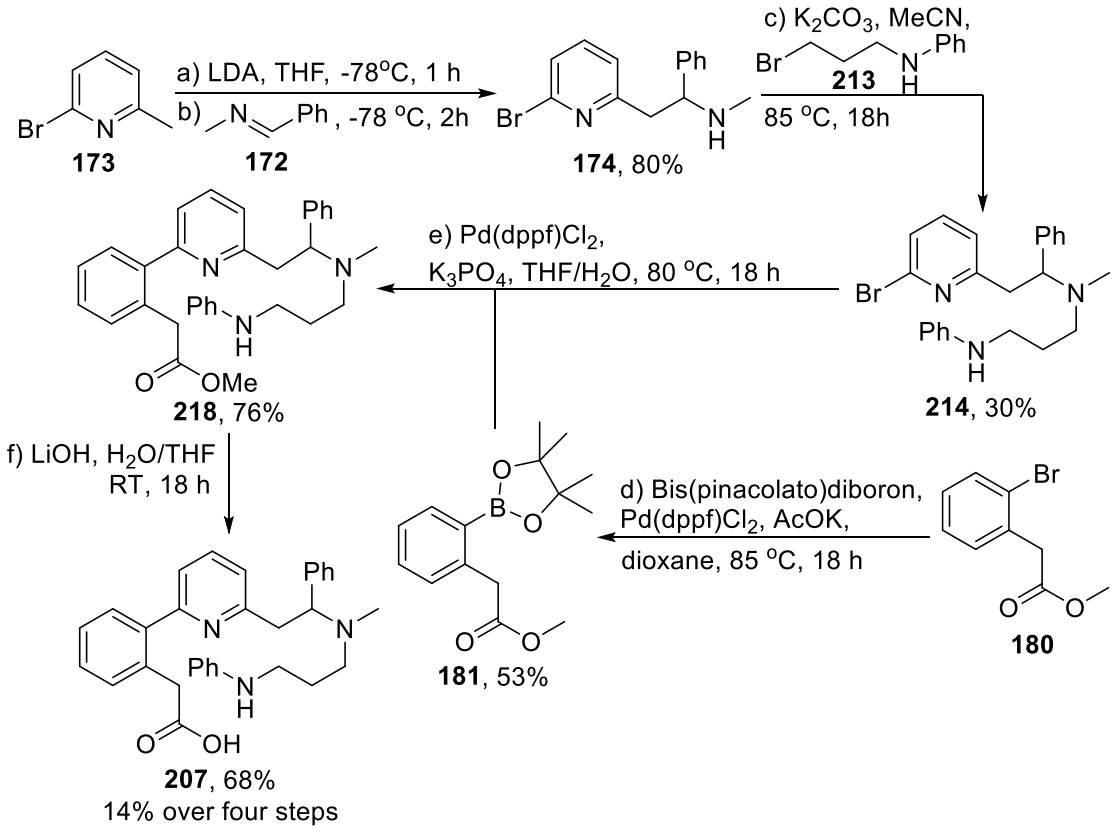

Scheme 57: Synthesis route to linear precursor **207**.

4.3 Work Towards a Precursor with Phenylamine Internal Nucleophile (210)

Considerable progress towards a linear precursor containing a phenylamine internal nucleophile (**210**) was also made. The first synthetic route to precursor **210** attempted to alkylate phenylamine **221** with an alkyl halide, similar to previous S_N2 attempts shown in Scheme 33 and Scheme 54. It was initially hoped that bromomethyl pyridine **173** could be reacted with a phenyl imine analogue similar to **172**, however, no such imine was commercially available. Instead, synthesis of phenylamine **221** was achieved via the lithiation-trapping of bromomethyl pyridine **173** and its subsequent reductive amination, using conditions previously reported in the literature (Scheme 58).[57] Bromomethyl pyridine **173** was deprotonated by LDA before subsequently attacking into *N*-methoxy-*N*-methylacetamide **219**, consequently undergoing nucleophilic substitution to give ketone **220** in a yield of 84%. Ketone **220** then underwent reductive amination with aniline using the reducing agent sodium triacetoxyborohydride (STAB) to afford phenylamine **221** in a yield of 88%.

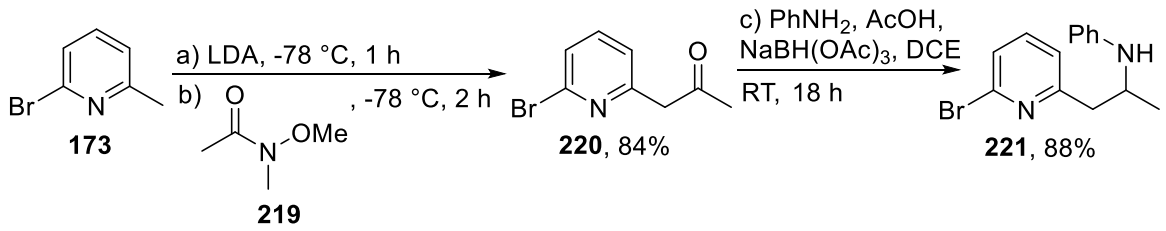

Scheme 58: Lithiation-trapping and subsequent reductive amination of bromomethyl pyridine **173** to afford phenylamine **221**.

With a large quantity of phenylamine **221** at our disposal, alkylation was attempted using a variety of alkyl halides. Scheme 59 shows all the alkylation reactions attempted in the hope of synthesising alcohol **222**. Using typical S_N2 conditions, alkylation of phenylamine was attempted with electrophilic reagents including chloropropanol **175**, bromopropanol **177**, and iodopropanol **178**. These alkylation reactions were all unsuccessful, with none of product **222** identified from either TLC or the ^{1}H NMR spectrum of the unpurified reaction mixture, and a large quantity of unreacted starting material **221** was observed in the reaction mixtures. This is likely due to the fact that the aniline group of **221** is much less nucleophilic than analogous aliphatic amines used in other systems, due to delocalisation into the bonded phenyl group.

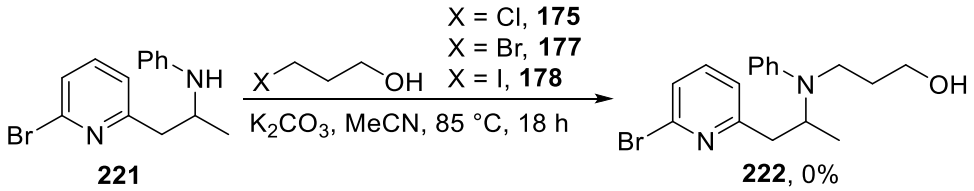

Scheme 59: Attempted alkylation of phenylamine **221** using alkyl halides **175**, **177** and **178**.

With realisation that phenylamine **221** is unable to undergo an S_N2 reaction, an alternative strategy was conceived, where ketone **220** would undergo reductive amination with a phenylamine to give tertiary amine **222** (Scheme 60). The first reductive amination attempted was with phenylamine **223**, acetic acid, and sodium triacetoxyborohydride (STAB) in 1,2-dichloroethene (DCE) overnight at room temperature. Disappointingly, this did not yield product **222**.

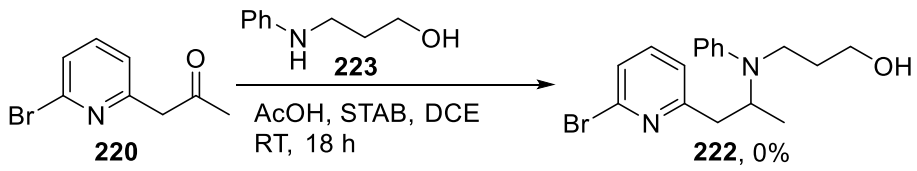

Scheme 60: Attempted reductive amination of ketone **220** with phenylamine **223**.

However, an uncharacterised side-product was identified by HRMS. Although full data was not obtained to confirm this, it was speculated that the alcohol present in phenylamine **223** was acting as a competing nucleophile, in turn attacking ketone **220** to produce a hemiaminal species (**225**) (Scheme 61). Thus, the alcohol present on phenylamine **223** could have attacked into the protonated carbonyl of ketone **220** to give the hemiketal intermediate **224a**, which would then eject water via condensation to give intermediate **224b** that could be attacked once more by the secondary phenylamine to cyclise to give hemiaminal **225**.

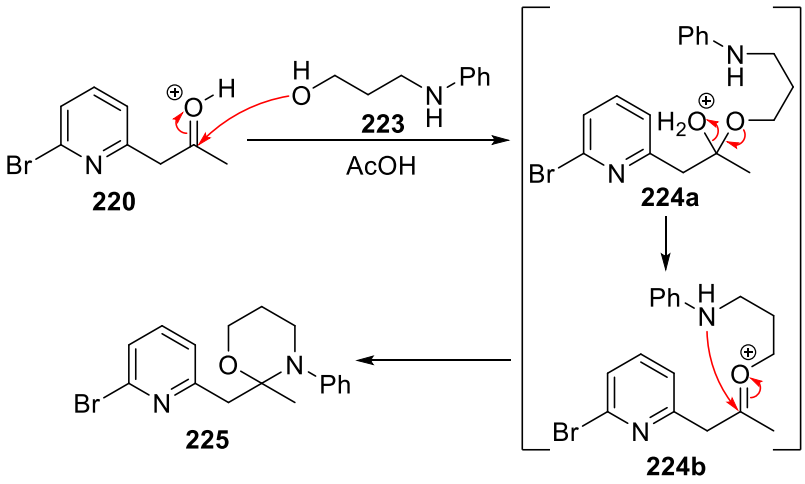

Scheme 61: Proposed mechanistic route for the formation of hemiaminal side-product **225**.

To prevent possible interference from a competing nucleophile, the alcohol of **223** was protected using TBS, to give reagent **226** (Scheme 62). However, when reductive amination of **220** was attempted using protected phenylamine **226**, the ^{1}H NMR spectrum and TLC of the unpurified reaction mixture showed no evidence of product **227** being formed.

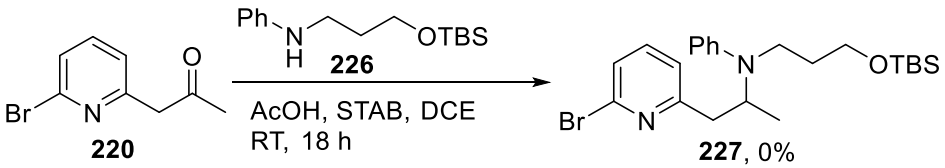

Scheme 62: Attempted reductive amination of ketone **220** with protected alcohol **226**.

A final reductive amination reaction was attempted in hope of synthesising a precursor possessing a phenylamine internal nucleophile. It was anticipated that a more electrophilic carbonyl, such as an aldehyde, would be more susceptible to attack from phenylamine **210**, and in turn would allow for reductive amination to proceed. Scheme 63 shows the *in situ* synthesis of the aldehyde **228** from bromomethyl pyridine **173**, followed by the subsequent reductive amination of aldehyde **228** with phenylamine **223**. Thus, bromomethyl pyridine

173 underwent deprotonation with LDA before undergoing nucleophilic substitution with DMF to form aldehyde **228**, which subsequently underwent reductive amination with phenylamine **223** to afford tertiary amine **229** in a yield of 24%. Pleasingly, the reaction was successful, with the novel product **229** being isolated and characterised.

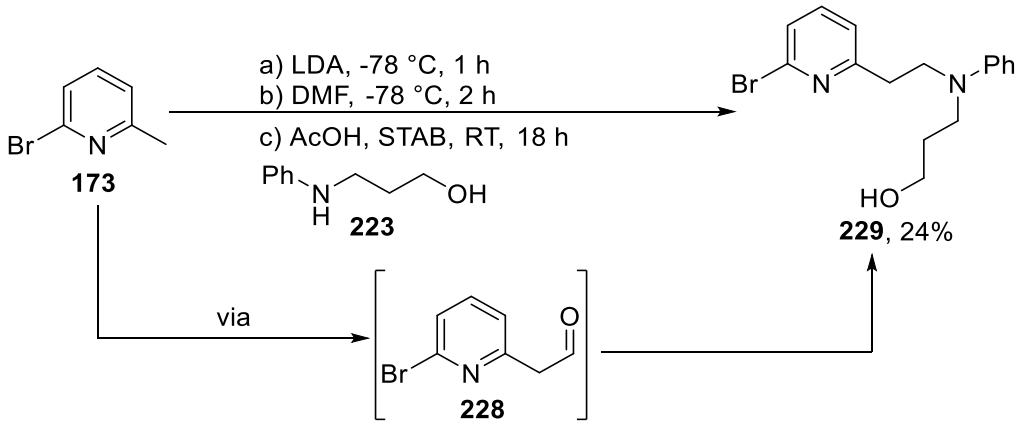

Scheme 63: Lithiation-trapping and subsequent reductive amination of bromomethyl pyridine **162**.

This is the extent of progress before lab work was halted. With bromopyridine **229** in hand, the next steps to prepare precursor **210** would be a Suzuki cross-coupling reaction with boronic ester pinacol **181** followed by a hydrolysis to furnish the final precursor. It is assumed that the conditions for the stated reactions would again be identical to the other Suzuki cross-coupling and hydrolysis conditions used previously in this report.

4.4 Work Towards a Mono-Aryl Precursor (211)

Finally, a mono-aryl precursor with a pyridine internal nucleophile (**211**) was designed, which would be used to form INRE product **212**. However, a single-INRE mono-aryl precursor with a similar carbon framework containing one internal nucleophile had not been previously synthesised by the Unsworth group. Therefore, to test the viability of a single-INRE with a mono-aryl system, a mono-aryl precursor containing one internal nucleophile was designed and its synthesis was attempted. Scheme 64 shows the desired precursor **230** and its respective single-INRE product **231**.

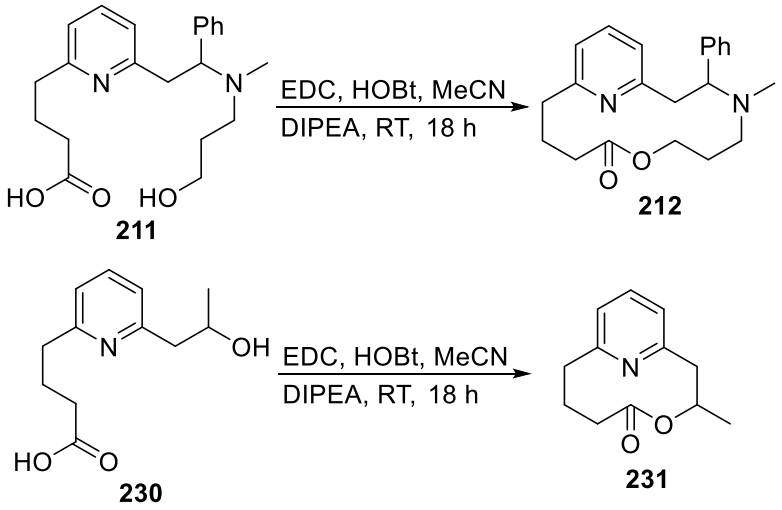

Scheme 64: Both single- and multi-INRE of precursors **211** and **230** to give lactone **212** and **231**.

The biggest challenge in the synthesis of mono-aryl precursor **230** was the C-2 alkylation of bromopyridine **220** with a linear alkyl carboxylic acid (Scheme 65). Any Heck or Wittig reactions requiring a 4-membered alkyl carboxylic acid or ester with a terminal alkene would be difficult, as the out-of-conjugation alkene would readily tautomerise in acidic or basic conditions at high temperatures to form the more thermodynamically stable conjugated alkene (Scheme 66).

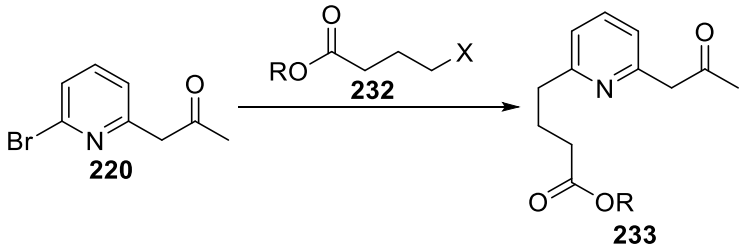

Scheme 65: Alkylation of C-2 position of bromopyridine **220** with linear ester/acid. X represents a possible synthetic handle.

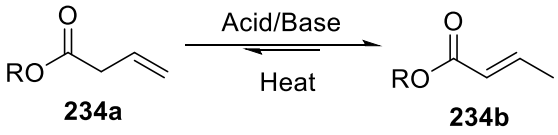

Scheme 66: Tautomerisation of out-of-conjugation alkene to thermodynamically stable conjugated alkene.

To combat this, a one-pot borylation-Suzuki-Miyaura reaction based on a literature example was attempted,[63] using vinyl ester **235** and bromopyridine **220** (Scheme 67). It was hoped that the conditions used for the initial formation of borylated ester **236** would be mild enough to avoid potential tautomerisation. Thus, 9-borabicyclo[3.3. 1]nonane (9-BBN) was added

to vinyl ester **235** in THF at 0 °C before being brought to room temperature for four hours to form the borylated ester **236** *in situ*. Bromopyridine **220** was then added before heating to 95 °C with $Pd(PPh_3)_4$ for 90 min before being cooled and directly concentrated *in vacuo*. Unfortunately, none of product **237** could be identified from the unpurified reaction mixture via TLC or ^1H NMR spectroscopy, indicating that the reaction had been unsuccessful. It is possible that 9-BBN instead reacted with the ester, leading to a side-reaction which interfered with the synthesis of alkyl borane **236** and in turn stopped the formation of product **237**. Although less likely, it is also possible that vinyl ester **235** underwent tautomerisation during the addition of 9-BBN, even with such mild reaction conditions, again interfering with the synthesis of alkyl borane **237**.

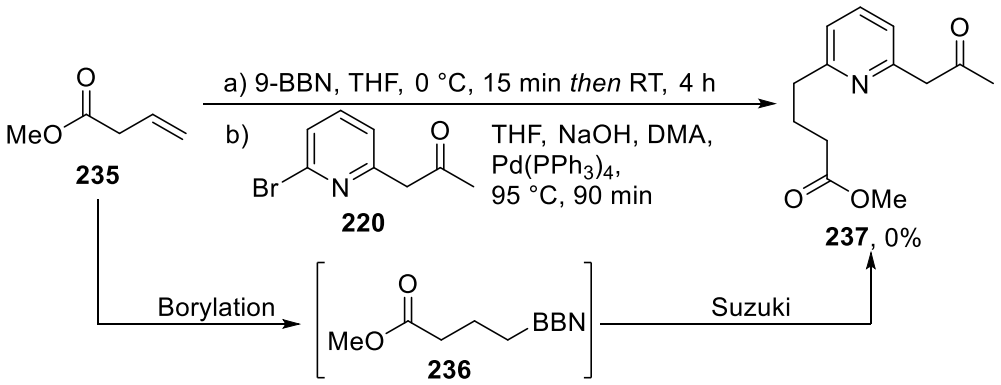

Scheme 67: Attempted one-pot borylation-Suzuki-Miyaura coupling of vinyl ester **235** with bromopyridine **220**.

With borylation of ester **235** and subsequent Suzuki-Miyaura cross-coupling unlikely, we moved onto other methods of installing an alkyl group onto bromopyridine **220**. The next attempt to synthesise **237** utilised a Negishi cross-coupling which is commonly used to install alkyl groups onto aryl rings. An organozinc bromide reagent would first need to be synthesised before undergoing cross-coupling with bromopyridine **220**. The required reagent was organozinc bromide **239**, which was synthesised from bromoester **197** via the formation of iodoester **238** (Scheme 68). Thus, bromoester **197** was heated with sodium iodide in acetonitrile for 90 mins to afford iodoester **238**. Separately, 1,2-dibromoethane was then stirred vigorously with solid zinc in DMF at 90 °C for 30 minutes, before triethylsilane chloride was added to the solution which was then stirred at room temperature for 15 minutes. Finally, iodoester **238** in THF was added to the reaction before heating to 45 °C for 2.5 hours to afford organozinc bromide **237**, which was then immediately used in the following Negishi reaction.

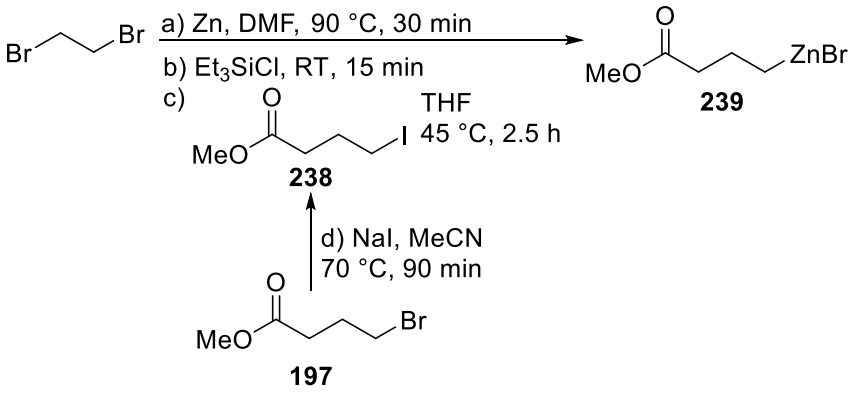

Scheme 68: Formation of organozinc bromide **239** from bromo ester **197**.

The organozinc product **239** was taken forward in solution to react with bromopyridine **220** in a Negishi cross-coupling reaction (Scheme 69). Bromopyridine **220** was stirred with organozinc bromide **239** and $Pd(PPh_3)_2Cl_2$ in THF at reflux for 4 hours to furnish keto-ester **237** in an isolated yield of 33%. Although we were pleased that some of the desired product has been formed, ^{1}H NMR spectroscopy and TLC analysis of the unpurified reaction mixture identified a large quantity of starting material still present, accounting for the modest yield of product **237**. One possible solution which could increase the amount of starting material conversion, and in turn increase the yield of product **223**, would be to leave the reaction to reflux overnight.

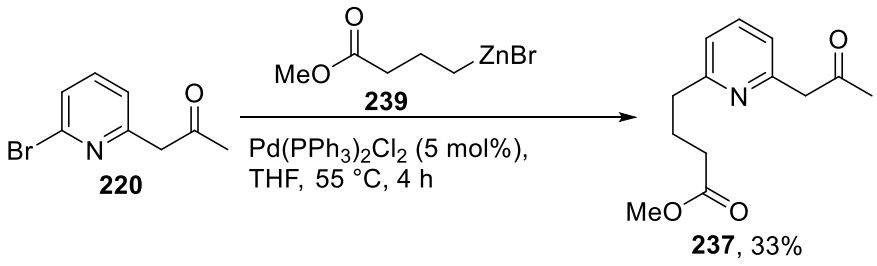

Scheme 69: Negishi cross-coupling of bromopyridine **220** with organozinc bromide **239**.

With keto-ester **237** synthesised, the rest of the synthetic route towards precursor **230** would only require two final steps, a reduction of the ketone to an alcohol followed by a hydrolysis of the methyl ester to give the acid. Similar compounds have been hydrolysed and reduced in the literature,[57] which would likely allow for an unproblematic synthesis of precursor **230** in future work.

4.5 Summary

A novel linear multi-INRE precursor containing a phenylamine terminal nucleophile (**207**) was synthesised over four steps and can now be tested in a multi-INRE reaction. Two other novel multi-INRE precursors were also designed; a linear multi-INRE precursor containing a phenylamine internal nucleophile (**210**) and a linear single-INRE mono-aryl precursor (**288**). Considerable progress has also been made towards a synthetic route to access the two aforementioned precursors.

Future Work

5.1 Short-Term Objectives

As previously stated, the SARS-CoV-2 pandemic abruptly halted all lab work prematurely.[62] As a result of the pandemic many short-term objectives were left unfinished, but we predict that they could be completed quickly and would provide much insight into the multi-INRE reaction. The most straightforward of these short-term objectives is conducting INRE tests on all synthesised precursors using the best conditions: HOBt, EDC, MeCN, DIPEA, 25 °C for 18 h (Scheme 70). If the optimised conditions are successful with the system shown in Scheme 70 it would suggest that the finalised conditions would be well suited for use in future multi-INRE reactions using novel linear precursors containing several internal nucleophiles.

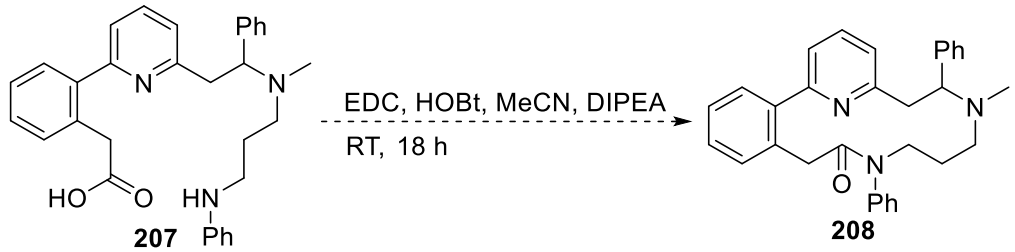

Scheme 70: Cyclisation of precursor **207** via INRE using finalised conditions.

Another short-term objective is the synthesis of the phenylamine internal nucleophile precursor **209** and the mono-aryl single-INRE precursor **230** as well as forming their respective INRE products using the finalised conditions. Scheme 71 shows the completion of the synthetic route to build precursor **209** from previously synthesised tertiary amine **229**. Thus, tertiary amine **229** would undergo a Suzuki-Miyaura cross-coupling reaction with boronic ester pinacol **181** to afford hydroxy ester **240** before undergoing hydrolysis to generate hydroxy acid **209**. Hydroxy acid **209** could then undergo cyclisation via a multi-INRE reaction using EDC and HOBt to give lactone **210**. As all reactions shown in Scheme 71 are based on previous conditions found in the literature,[57] the reactions would be hopefully be unproblematic and could be carried out in an efficient manner.

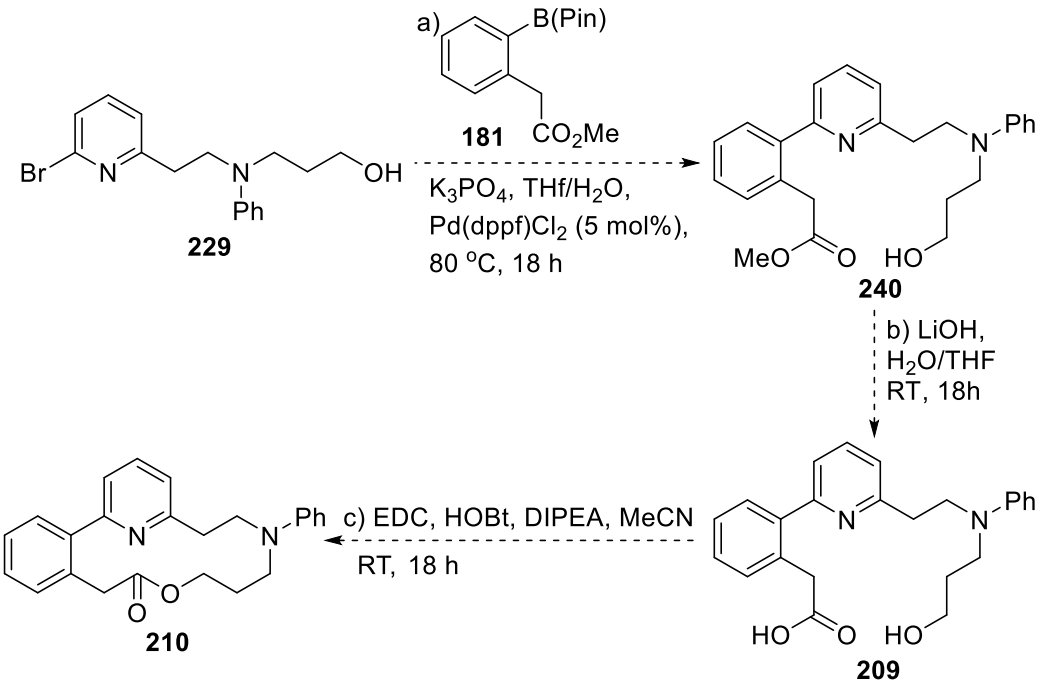

Scheme 71: Synthesis of precursor **209** from tertiary amine **229** and subsequent INRE to award lactone **210**.

Scheme 72 shows the steps necessary to complete the synthesis of precursor **230**. Reduction of keto-ester **237** using sodium borohydride should furnish hydroxy ester **241** which could then undergo hydrolysis to give hydroxy acid **230**. Hydroxy acid **230** could then undergo cyclisation via INRE to yield lactone **231**. Again, all steps use conditions reported in the literature for the synthesis of near identical analogues, therefore the synthesis of precursor **230** should be unproblematic. If formation of lactone **231** via INRE of hydroxy acid **230** is successful, work could be then focus towards preparing the mono-aryl precursor with two internal nucleophiles **211**.

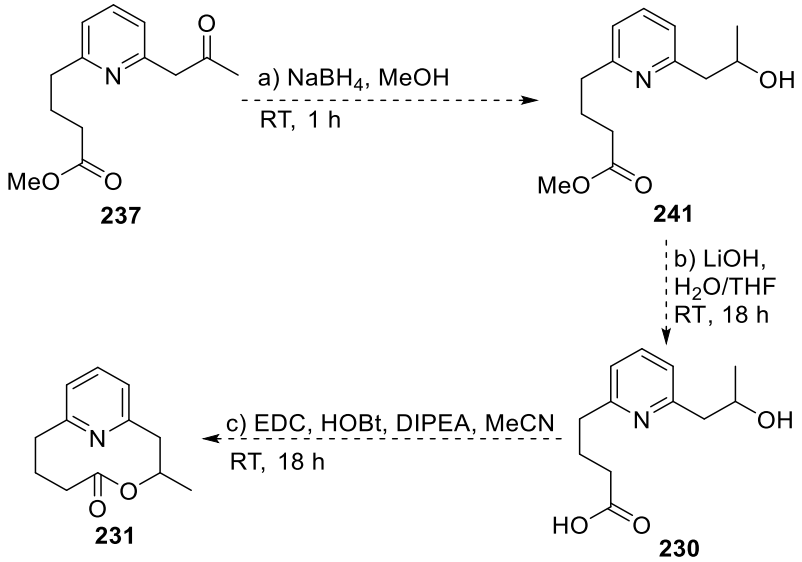

Scheme 72: Synthesis of precursor **230** from keto-ester **237** and subsequent INRE to award lactone **231**.

5.2 Long-Term Objectives

There are also many long-term objectives which could build upon the foundations achieved so far in this project. The most apparent would be further exploration of scope via the synthesis of a diverse array of linear multi-INRE precursors. The easiest would be the synthesis of precursor **211**, as again most of the steps used to build the precursor have been reported in the synthesis of previous multi-INRE precursors in this report. Scheme 73 shows the synthetic route which could potentially be used to make precursor **211** from bromopyridine **176**, and the subsequent INRE reaction. Thus, bromopyridine **176** would undergo a Negishi cross-coupling with organozinc bromide **239** to give hydroxy ester **242**, which could then be hydrolysed to give precursor **211**. Finally, hydroxy acid **211** could undergo cyclisation via a multi-INRE reaction using the finalised conditions to furnish the 14-membered lactone **212**.

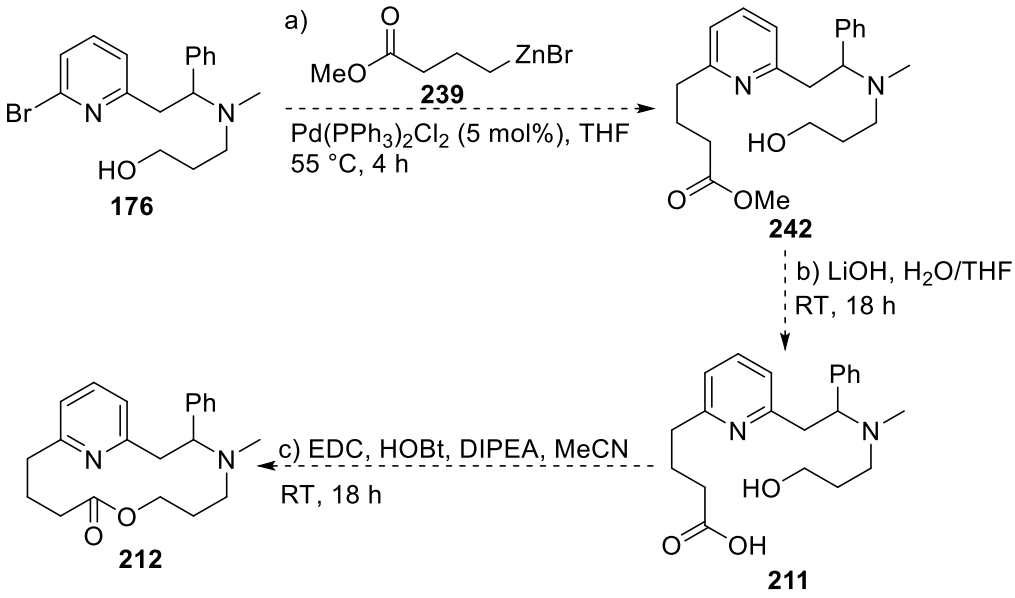

Scheme 73: Synthesis of precursor **211** from bromopyridine **176** and subsequent INRE to award lactone **212**.

To further build on the work done in this report, additional optimisation of previous synthetic routes would allow for streamlined syntheses of both multi-INRE precursors which have been previously made, and also structurally similar novel analogues, in turn making future substrate scope studies easier. One such route which could be optimised is the synthesis of saturated alkyl precursors, such as aliphatic hydroxy acid **190**. Optimisation could be achieved through the synthesis of an alternative electrophilic reagent that possesses a different leaving group, which could in turn lead to higher yielding S_N2 reactions. Scheme 74 outlines one strategy which could potentially increase the efficiency of the synthetic route

and in turn increase the yield of precursor **190**. Scheme 74 shows the tosylation of alcohol **199** with tosyl chloride to give the electrophilic alkyl tosylate **243** which could then undergo S_N2 with benzylic amine **198** to award hydroxy ester **201**. It is hoped that an S_N2 reaction between benzylic amine **198** and tosylate **243** would allow for a higher yield of hydroxy acid **201** compared to an S_N2 reaction with its bromide counterpart **200**.

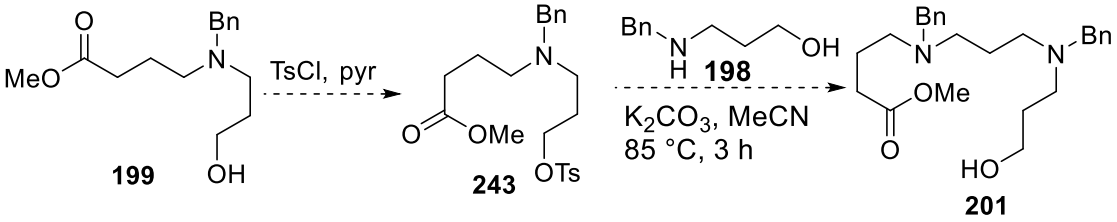

Scheme 74: Alternative route for synthesis of hydroxy ester **201**; tosylation of alcohol **199** followed by an S_N2 reaction with benzylic amine **198**.

This alternative strategy can also be employed in the synthesis of the phenylamine precursor **207**. Scheme 74 shows the synthesis of secondary phenylamine **214** from alcohol **176**. Rather than performing an S_N2 reaction between secondary amine **174** and bromo phenylamine **213**, the synthetic method shown below instead start from alcohol **176**. Scheme 75 shows the formation of tosylate **244** from alcohol **176** and the subsequent S_N2 reaction with aniline to give phenylamine **214**. This strategy would avoid the use of the unstable reagent bromo phenylamine **213**, streamlining the synthetic route and potentially increasing the yield of phenylamine **214**.

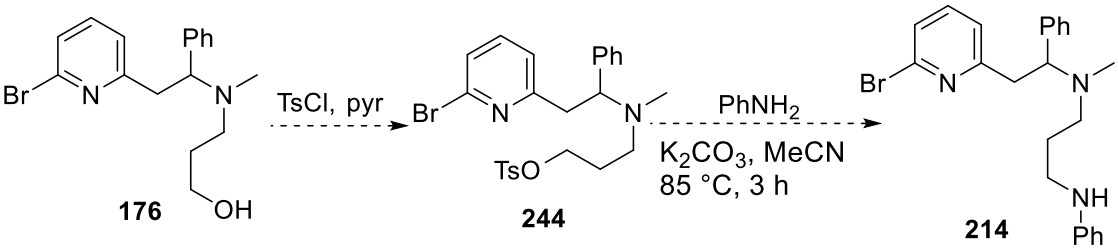

Scheme 75: Alternative route for synthesis of phenylamine **214**; tosylation of alcohol **176** followed by an S_N2 reaction with aniline.

A key step for the synthetic route of biaryl precursors is the synthesis and subsequent cross-coupling of boronic pinacol ester **181**. However, as previously stated, the purification of this compound is difficult due to the susceptibility of boronic esters to decompose on silica.[64] A potentially simple solution to this problem would be to purify the boronic ester **181** crude reaction mixture using aluminium oxide column chromatography. It is hoped that boronic pinacol ester **181** would be stable in the presence of aluminium oxide, in turn decreasing the rate of degradation and increasing the retrieval of isolated boronic pinacol ester **181**.

Finally, a number of novel linear precursors could be developed and subsequently cyclised via INRE in order to explore the scope and limitations of multi-INRE. Scheme 76 shows variety of designed precursors and their respective products. One designed precursor could contain two different heteroatoms that both function as internal nucleophiles (**225**). If the subsequent INRE reaction **245 → 246** was successful, it would prove that INRE is possible with heterocyclic linear precursors containing different heteroatoms acting as internal nucleophiles, which could lead to further exploration of other nucleophilic heteroatoms such as phosphorous. Designing precursors which have "swapped" the positions of internal nucleophiles in the linear chain would provide insight into the importance of the order of internal nucleophiles. An example is hydroxy acid **247**, which structurally is similar to precursor **162**, however, the pyridine and tertiary amine internal nucleophiles have "swapped" their positions in the linear carbon chain. If the yield of reaction **247 → 248** is significantly lower or higher than the yield of the reaction **162 → 164**, it could be concluded that the success of a multi-INRE reaction is determined not only by what internal nucleophiles are used, but also where the internal nucleophiles appear in the linear carbon chain relative to the carboxylic acid.

A precursor containing three internal nucleophiles could be designed (**249**). If INRE is possible with such a precursor (**249**) it would not only allow for the synthesis of even larger heterocyclic macrocycles from linear precursors but would suggest that INRE could hypothetically be used to build macrocycles of impressive sizes with numerous internal nucleophiles. Finally, atroposelectivity could be explored further, by designing precursors which possessed chiral centres adjacent to both nucleophiles, such as precursor **251**. If the yield of **251** is significantly higher or lower than the yield of **162→164** it would give further insight into how the multi-INRE mechanistic pathway proceeds.

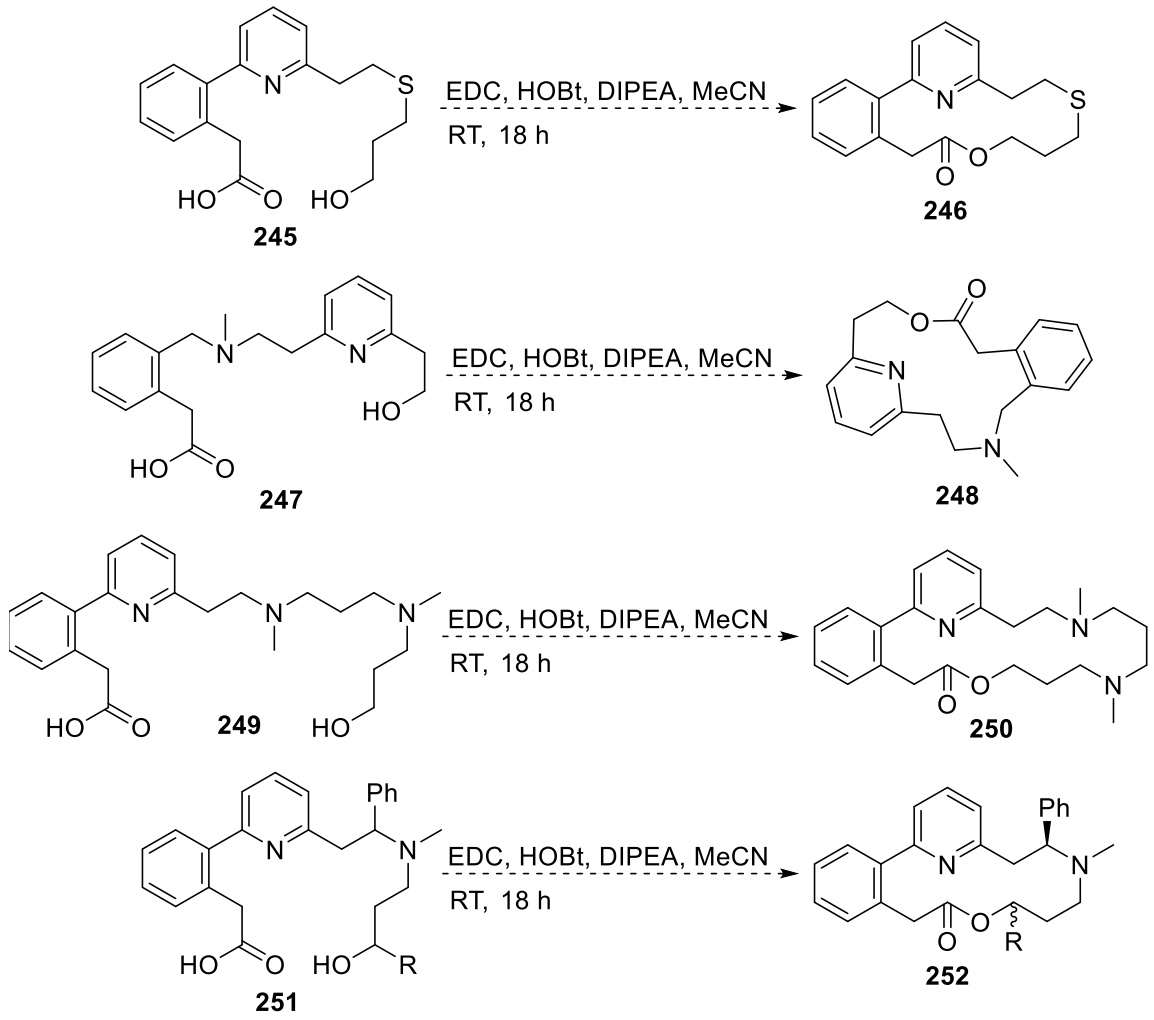

Scheme 76: Potential INRE precursors and their respective ring expanded products.

Conclusion

In conclusion, multi-INRE reactions have been developed for the synthesis of 13- and 14-membered macrocycles from linear, pre-functionalised precursors containing more than one internal nucleophile in up to 73% yield. This strategy builds on previous work using internal nucleophile induced cyclisations of single internal nucleophile precursors, allowing for efficient end-to-end cyclisation of longer linear precursors to form subsequently larger heterocyclic macrocycles.

We have shown that macrocyclic heterocycles which both do and do not possess an aryl moiety can be synthesised via INRE of linear precursors containing several internal nucleophiles (Scheme 77). As part of this process, multiple novel synthetic routes to access precursors containing several internal nucleophiles have been developed, allowing for a streamlined route to make analogues for future scope. There have also been successful attempts to build an array of other precursors with slightly altered structures, with each precursor in different stages of their development.

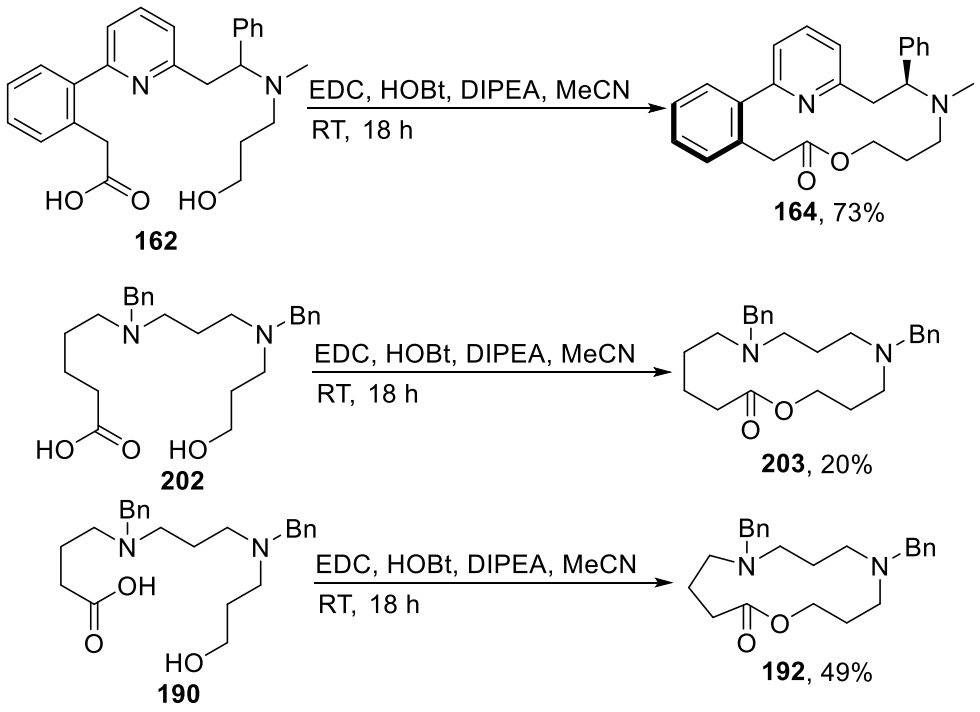

Scheme 77: All macrocycles synthesised in this report.

We have also shown that internal nucleophile induced ring expansion reactions of biaryl precursors containing two internal precursors show atroposelectivity, allowing for point-to-axial chirality transfer (Scheme 78). This form of diastereoselectivity, and the construction of heterocyclic macrocycles, is of evermore importance in drug discovery.[8] It is hoped that

the development of INRE shown in this work has allowed for INRE to become a more reliable and practical tool for the synthesis of important bioactive macrocycles via the internal nucleophile ring expansion of pre-functionalised linear precursors.

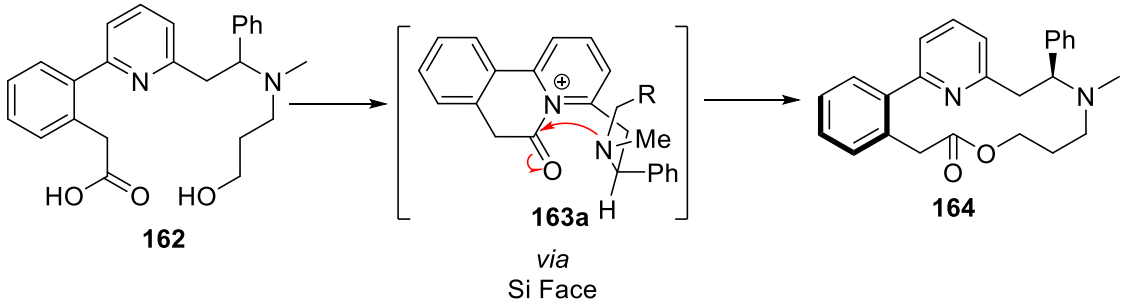

Scheme 78: Atroposelectivity of INRE of precursors containing two internal precursors.

Experimental

7.1 General Experimental

Except where stated, all reagents and solvents were purchased from commercial sources and used directly without further purification. Thin-layer chromatography was carried out using Merck silica gel 60F254 pre-coated aluminium foil sheets and visualised using UV radiation (254 nm) before being stained with basic aqueous potassium permanganate. Flash column chromatography was carried out using Fluka silica gel (SiO_2) 35–70 μm, 60 Å under light positive pressure, eluting with the specified solvent system.

All ^{1}H and ^{13}C NMR experiments were recorded on a JEOL ECS-400 operating at 400 MHz and 100 MHz respectively. Samples were taken at a temperature of 298 K dissolved in $CDCl_3$ unless specified otherwise. Chemical shifts (δ) are reported in parts per million (ppm), with residual solvent peaks δ_H 7.27 and δ_C 77.0 being used for internal reference. Coupling constants (J) are reported in Hertz (Hz) and are quoted to the nearest 0.1 Hz. Multiplicity abbreviations are as follows: s, singlet; d, doublet; t, triplet; q, quartet; m, multiplet; dd, doublet of doublets; td, triplet of doublets; ddd, doublet of doublets of doublets; where br indicates a broad signal. ^{1}H experiments are reported as: chemical shift, ppm (integration, multiplicity, coupling constant and assignment (where possible)). ^{13}C experiments are reported as: chemical shift, ppm (carbon assignment). Assignment of compounds was achieved through use of DEPT, COSY, and HMQC experiments.

High resolution mass spectra were recorded on a Bruker Micro-TOF spectrometer using electrospray ionisation (ESI). Infra-red spectra were recorded on a PerkinElmer UATR 2 spectrometer, either as a thin film dispersed with DCM or neat. Melting points were obtained using a Gallenkamp melting point apparatus.

7.2 List of Experimental Procedures and Characterisations

2-(6-Bromopyridin-2-yl)-*N*-methyl-1-phenylethan-1-amine (174)

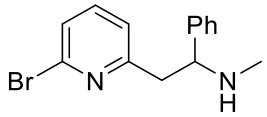

N,*N*-Diisopropylamine (4.35 mL, 35.1 mmol) was dissolved in THF (175 mL) and cooled to 0 ºC before n-BuLi (2.5 M solution in hexanes, 14.0 mL, 35.1 mmol) was added dropwise and stirred for 30 mins. The LDA solution was then cooled to −78 °C, where 2-bromo-6-methylpyridine (**173**) (1.98 mL, 17.5 mmol) was added dropwise and stirred for 1 h. *N*-Benzylidenemethylamine (4.35 mL, 35.1 mmol) was added and stirred for a further 2 h at −78 °C before slowly warming to RT. The solution was then quenched with sat. aq. NH_4Cl (150 mL) and extracted with ethyl acetate (3 × 100 mL) and washed with brine (150 mL). The combined organic extracts were dried over $MgSO_4$, filtered and removed in vacuo. Purification by flash column chromatography (SiO_2, 5% methanol in ethyl acetate) afforded the title compound as a yellow oil (3.82 g, 81%); R_f. 0.23 (5% methanol in ethyl acetate); δ_H (400 MHz, $CDCl_3$) 7.35–7.27 (7H, m, ArH), 6.86 (1H, d, *J* = 7.0 Hz, Ar**H**), 3.98 (1H, dd, *J* = 8.4, 6.1 Hz, CH_2C**H**NMe), 3.12 (1H, dd, *J* = 13.7, 6.1 Hz, CC**H**H′CHPh), 3.01 (1H, dd, *J* = 13.7, 8.4 Hz, CCH**H′**CHPh), 2.25 (3H, s, NHC**H**$_3$), 1.68–1.65 (1H, br s, N**H**).

Spectroscopic data matched those reported in the literature.[57]

Compound **174**

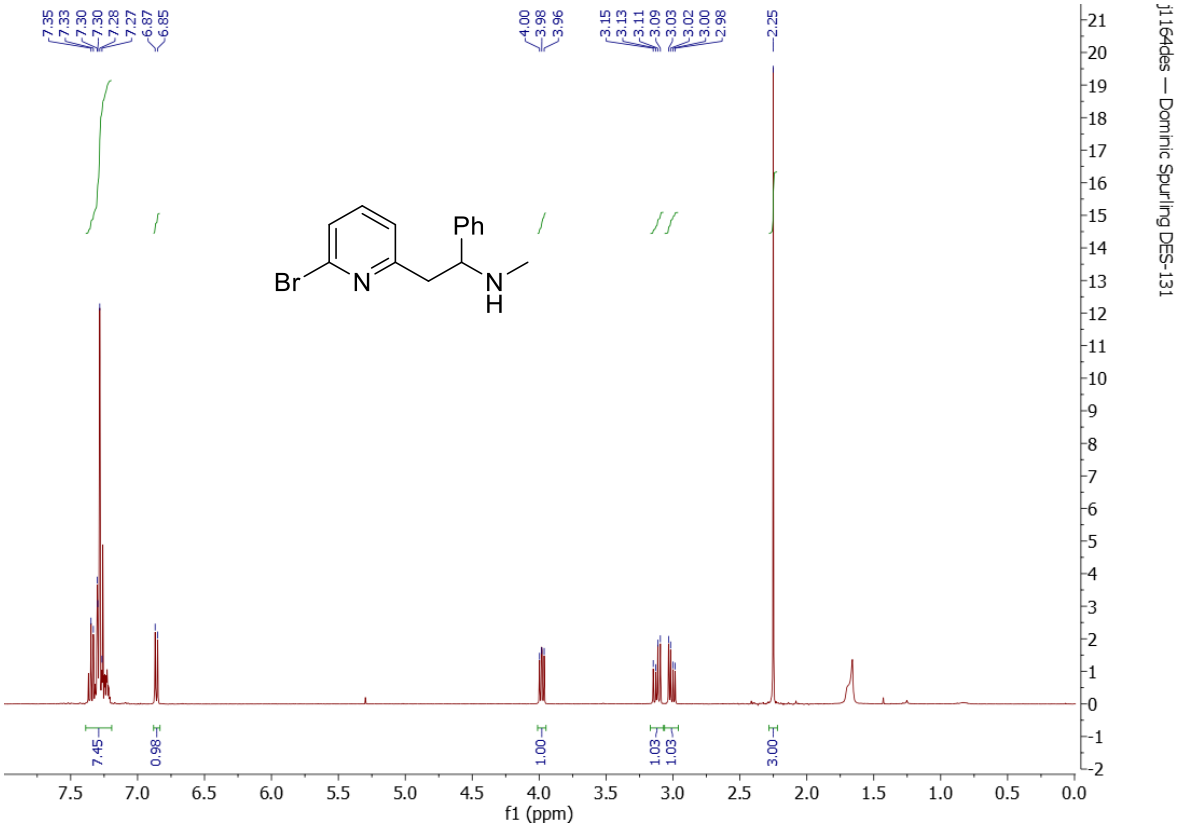

3-{[2-(6-Bromopyridin-2-yl)-1-phenylethyl](methyl)amino}propan-1-ol (176)

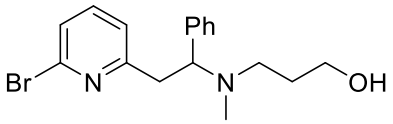

2-(6-Bromopyridin-2-yl)-*N*-methyl-1-phenylethan-1-amine (**174**) (1.00 g, 3.45 mmol), 3-iodo-1-propanol (**178**) (660 µL, 6.89 mmol) and potassium carbonate (953 mg, 6.90 mmol) were dissolved in acetonitrile (7 mL). After stirring at 85 °C for 18 h the reaction mixture was diluted with water (5 mL) and extracted with ethyl acetate (3 × 5 mL). The combined organic layers were dried with anhydrous $MgSO_4$, filtered, and then purified by flash column chromatography (SiO_2, 5% methanol in ethyl acetate) affording the *title compound* as a colourless oil (900 mg, 53%); R_f. 0.23 (5% methanol in ethyl acetate); ν_{max}/cm^{-1} (neat) 3369, 3029, 2943, 2850, 2237, 1583, 1553, 1435, 1406, 1175, 1156, 1116, 1068, 1033; δ_H (400 MHz, $CDCl_3$) 7.37–7.24 (7H, m, Ar**H**), 6.92 (1H, d, *J* = 7.0 Hz, Ar**H**), 4.19 (1H, t, *J* = 7.0 Hz, PhC**H**N), 3.71–3.68 (2H, m, C**H**$_2$OH), 3.55–3.50 (1H, dd, *J* = 13.7, 7.4 Hz, C**H**H'CHPh), 3.20–3.14 (1H, dd, *J* = 13.7 8.0 Hz, CH**H**'CHPh), 2.73–2.67 (1H, ddd, *J* = 12.1, 7.9, 4.3 Hz, NC**H**H'CH_2), 2.62–2.56 (1H, ddd, *J* = 12.1, 7.0, 4.2 Hz, NCH**H**'CH_2), 2.31 (3H, s, C**H**$_3$N), 1.74–1.63 (2H, m, C**H**$_2$); δ_C (100 MHz, $CDCl_3$) 160.8 (Ar**C**), 141.4 (Ar**C**), 138.5 (Ar**C**), 137.9 (Ar**C**H), 128.8 (Ar**C**H), 128.1 (Ar**C**H), 127.5 (Ar**C**H), 125.6 (Ar**C**H), 122.7 (Ar**C**H), 69.1 (CH_2**C**HN), 64.0 (**C**H_2OH), 54.6 (C**C**H_2CH), 40.4 (N**C**H_2), 37.5 (**C**H_3N), 27.8 (**C**H_2); HRMS (ESI): calcd. for $C_{17}H_{22}{}^{79}BrN_2O$, 349.0910. Found: $[MH]^+$, 349.0906 (1.1 ppm error)].

Compound **176**

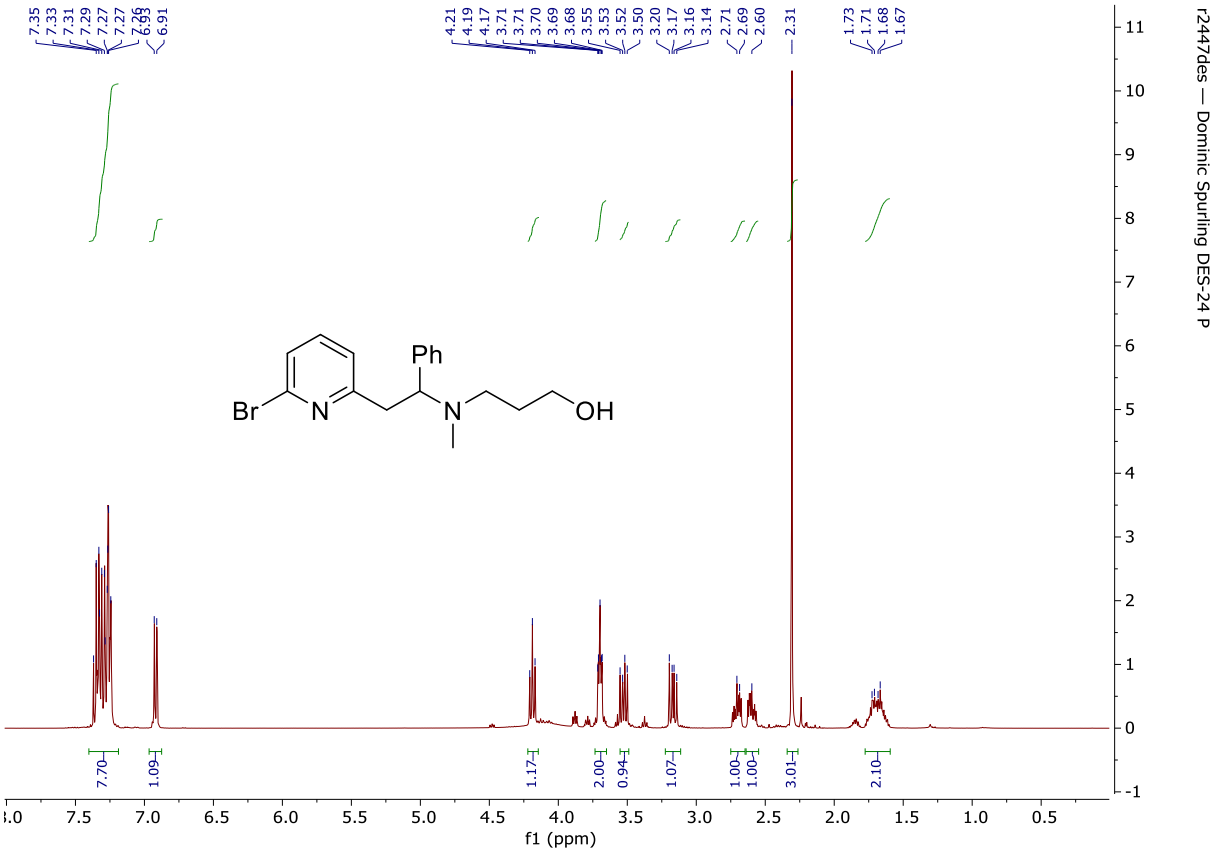

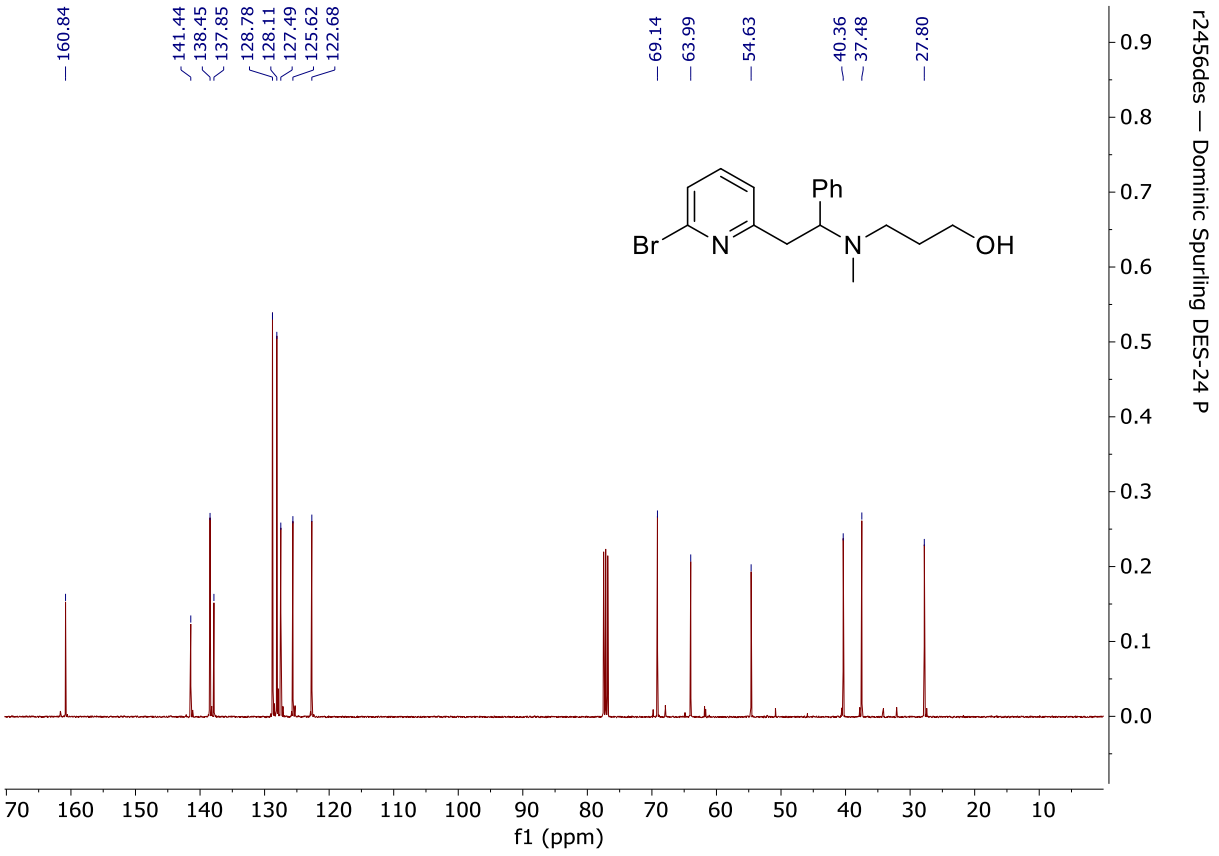

Methyl 2-(2-bromophenyl)acetate (180)

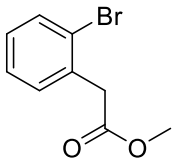

To a stirring solution of 2-(2-bromophenyl)acetic acid (**179**) (6.00 g, 28.0 mmol) in methanol (60 mL) was added concentrated sulfuric acid (1.20 mL) and the resulting solution was refluxed for 90 mins. After cooling to RT, the reaction was quenched with water (40 mL) and extracted with diethyl ether (3 × 50 mL). The organic extract was washed with sat. aq. brine (40 mL), dried over anhydrous $MgSO_4$, filtered and concentrated in vacuo to afford the title compound as a clear oil (6.33 g, 99%); δ_H (400 MHz, $CDCl_3$) 7.57 (1H, d, J = 8.2 Hz, Ar**H**), 7.30−7.26 (2H, m, Ar**H**), 7.19–7.12 (1H, m, Ar**H**), 3.81 (2H, s, C**H**$_2$), 3.72 (3H, s, C**H**$_3$).

Spectroscopic data matched those reported in the literature.[65]

Compound **180**

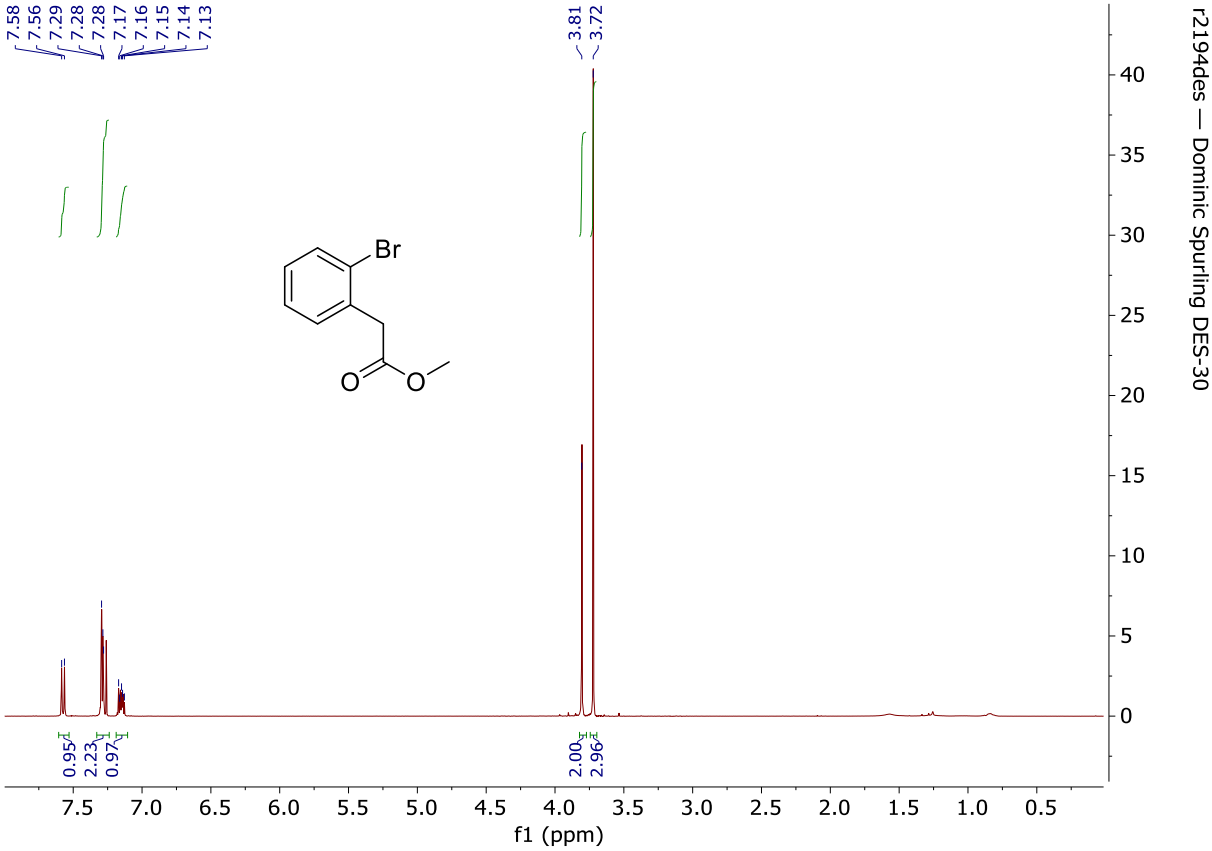

Methyl 2-(2-(4,4,5,5-tetramethyl-1,3,2-dioxaborolan-2-yl)phenyl)acetate (181)

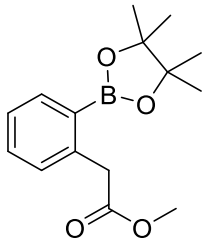

To a stirring solution of methyl 2-(2-bromophenyl)acetate (**180**) (2.05 g, 8.98 mmol) in 1,4-dioxane (36 mL), was added bis(pinacalato)diboron (2.51 g, 9.88 mmol), potassium acetate (3.35 g, 34.1 mmol) and $PdCl_2(dppf)\cdot CH_2Cl_2$ (367 mg, 450 µmol). The reaction mixture was flushed with argon and heated under reflux for 18 h. The reaction mixture was quenched with water (40 mL) and extracted with diethyl ether (3 × 30 mL). The organic extract was washed with sat. brine (30 mL), dried over anhydrous $MgSO_4$, filtered and concentrated in vacuo. Purification via silica gel chromatography (10% hexane in dichloromethane) yielded the pure product as an off-white solid (1.40 g, 56%); δ_H (400 MHz, CDCl3) 7.83 (1H, d, *J* = 7.6 Hz, Ar**H**), 7.40−7.37 (1H, m, Ar**H**), 7.29−7.25 (1H, m, Ar**H**), 7.19 (1H, d, *J* = 7.5 Hz, Ar**H**), 3.98 (2H, s, C**H**$_2$), 3.66 (3H, s, OC**H**$_3$), 1.32 (12H, s, 4 × C**H**$_3$).

Spectroscopic data matched those reported in the literature.[66]

Compound **181**

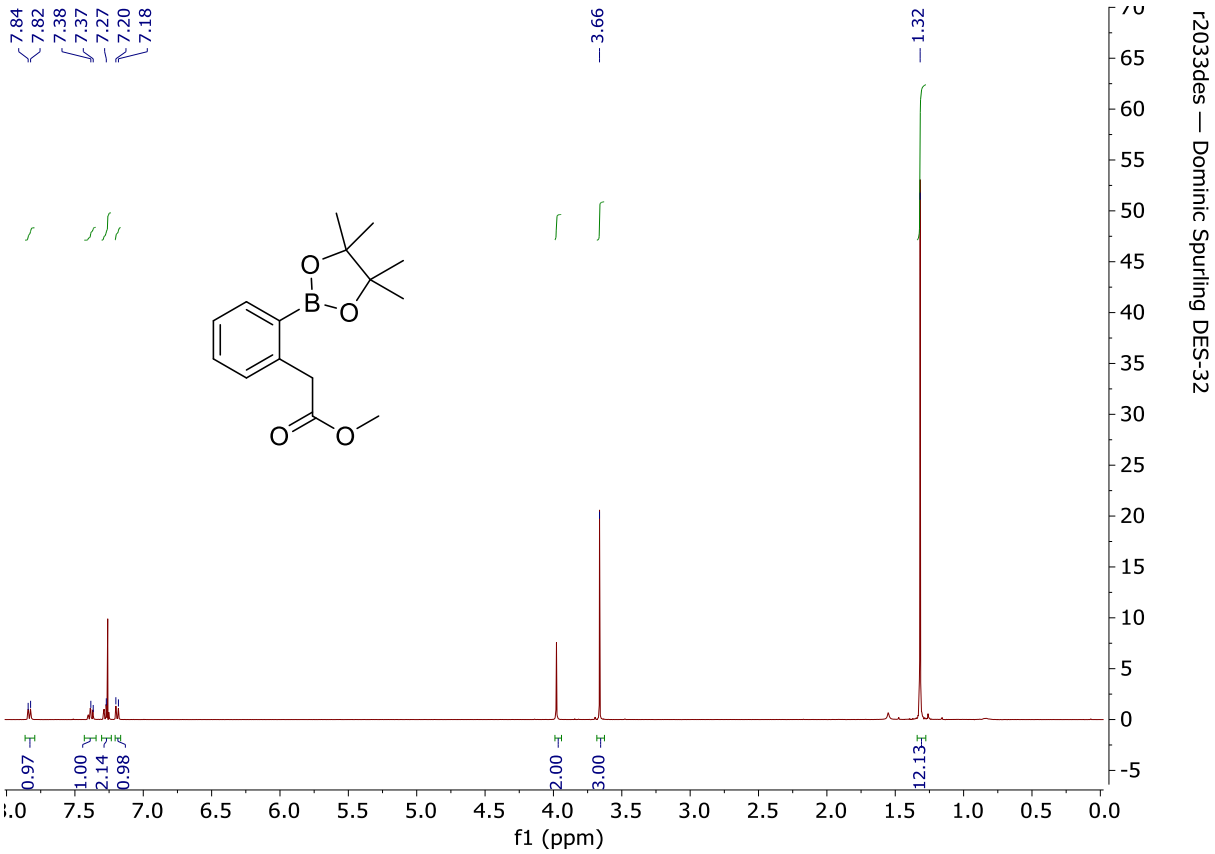

Methyl 2-[2-(6-{2-[(3-hydroxypropyl)(methyl)amino]-2-phenylethyl}pyridin-2-yl)phenyl]acetate (182)

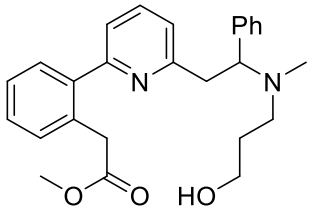

3-{[2-(6-Bromopyridin-2-yl)-1-phenylethyl](methyl)amino}propan-1-ol (**176**) (683 mg, 1.96 mmol), methyl 2-(2-(4,4,5,5-tetramethyl-1,3,2-dioxaborolan-2-yl)phenyl) acetate (**181**) (813 mg, 2.94 mmol), potassium phosphate (833 mg, 3.92 mmol) and $PdCl_2(dppf)\cdot CH_2Cl_2$ (80.0 mg, 89.0 µmol) were charged into an round bottom flask purged with nitrogen. THF (20 mL) and de-ionised water (178 µL, 9.81 mmol) were added and heated to 80 °C, at reflux, for 18 h. Upon completion the solution was cooled to room temperature, diluted with water (15 mL), extracted with ethyl acetate (3 × 20 mL) and washed with sat. brine (10 mL). The combined organic extracts were dried over $MgSO_4$, filtered, and removed *in vacuo*. Purification by flash column chromatography (SiO_2, 10% methanol in ethyl acetate) afforded the *title compound* as a brown oil (713 mg, 87%); R_f. 0.38 (10% methanol in ethyl acetate); ν_{max}/cm^{-1} (neat) 3367, 3061, 3025, 2950, 2852, 1736, 1587, 1570, 1496, 1448, 1339, 1254, 1211, 1159, 1071; δ_H (400 MHz, $CDCl_3$) 7.54 (1H, t, *J* = 7.8 Hz, Ar**H**), 7.41–7.21 (10H, m, Ar**H**), 6.91 (1H, d, *J* = 7.6 Hz, Ar**H**), 4.22 (1H, t, *J* = 8.0 Hz, NC**H**Ph), 3.85–3.74 (2H, m, C**H₂**CO_2), 3.64 (2H, t, *J* = 5.1 Hz, C**H₂**OH), 3.57–3.51 (4H, m, CO_2C**H₃** and C**H**H′CHN), 3.25–3.19 (1H, dd, *J* = 13.6, 8.0 Hz, CH**H**′CHN), 2.70–2.57 (2H, m, NC**H₂**), 2.30 (1H, s, NC**H₃**), 1.70–1.60 (2H, m, C**H₂**); δ_C (100 MHz, $CDCl_3$) 172.5 (**C**O_2), 159.0 (Ar**C**), 158.6 (Ar**C**), 140.7 (Ar**C**), 138.2 (Ar**C**), 136.7 (Ar**C**H), 132.4 (Ar**C**), 131.4 (Ar**C**H), 130.1 (Ar**C**H), 129.1 (Ar**C**H), 128.5 (Ar**C**H), 128.2 (Ar**C**H), 127.5 (Ar**C**H), 126.8 (Ar**C**H)* 122.1 (Ar**C**H), 121.7 (Ar**C**H), 69.4 (N**C**HPh), 64.3 (**C**H_2OH), 55.1 (N**C**H_2), 52.0 (CO_2**C**H_3), 40.7 (**C**H_2CHN), 39.2 (C**H₂**CO_2), 37.4 (N**C**H_3), 27.8 (**C**H_2); HRMS (ESI): calcd. for $C_{26}H_{31}N_2O_3$, 419.2329. Found: $[MH]^+$, 419.2326 (0.7 ppm error)].

*Peak obtained from HMQC, no detectable signal in the ^{13}C NMR spectrum.

Compound **182**

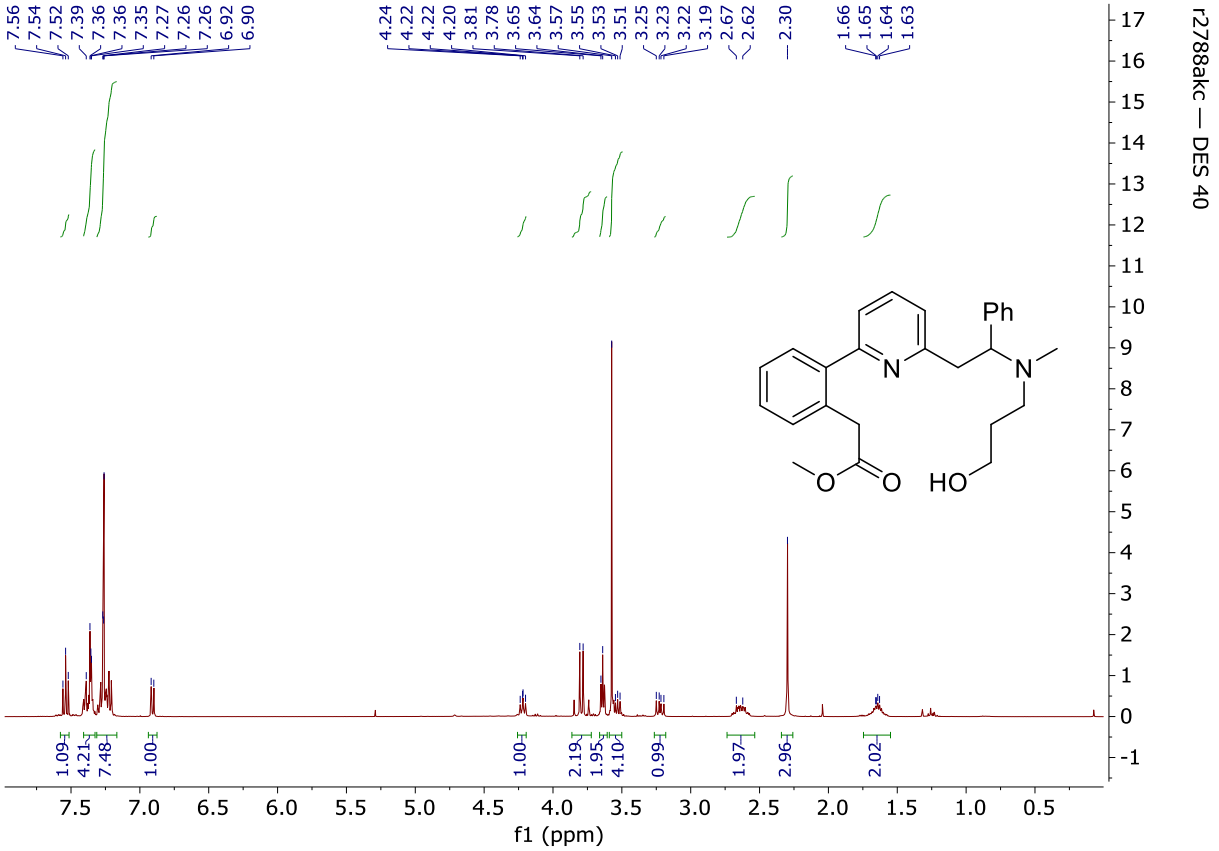

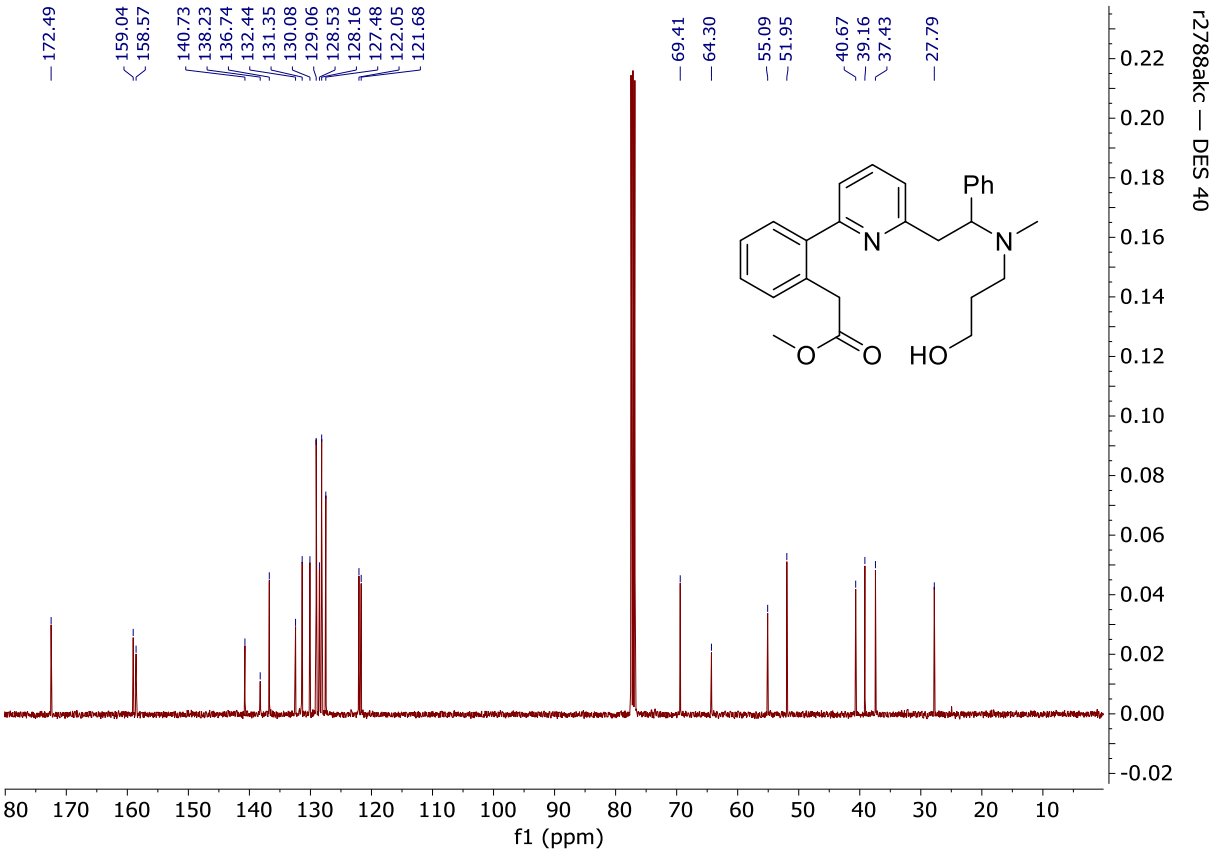

[2-(6-{2-[(3-Hydroxypropyl)(methyl)amino]-2-phenylethyl}pyridin-2-yl)phenyl]acetic acid (162)

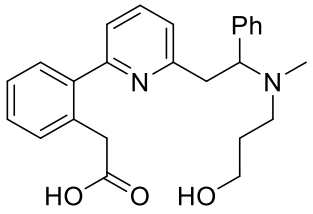

Methyl 2-[2-(6-{2-[(3-hydroxypropyl)(methyl)amino]-2-phenylethyl}pyridin-2-yl)phenyl]acetate (**182**) (713 mg, 1.70 mmol) was dissolved in aqueous lithium hydroxide solution (0.5 M, 17 mL, 8.52 mmol) and THF (17 mL). The resulting bi-phasic solution was vigorously stirred for 18 h at 25 °C. Upon completion, the solvent was removed *in vacuo*. Purification by flash column chromatography (SiO_2, 50% methanol in ethyl acetate) afforded the *title compound* as a brown powder (687 mg, 96%); m.p. 73–76 °C; R_f 0.20 (50% methanol in ethyl acetate); ν_{max}/cm^{-1} (neat) 3323, 3061, 3028, 2943, 2244, 1717, 1571, 1493, 1453, 1375, 1158, 1065; δ_H (400 MHz, $CDCl_3$) 7.36 (1H, s, Ar**H**), 7.47–7.45 (1H, d, *J* = 7.6 Hz, Ar**H**), 7.38–7.17 (9H, m, Ar**H**), 6.96 (1H, s, Ar**H**), 4.07–4.03 (1H, t, *J* = 7.0 Hz, NC**H**Ph), 3.72–3.59 (2H, br, C**H₂**CO_2), 3.55–3.48 (3H, m, C**H₂**OH and C**H**H′CHN), 3.20 (1H, br, CH**H**′CHN), 2.58 (2H, t, *J* = 7.0 Hz, NC**H₂**), 2.28 (3H, s, NC**H₃**), 1.75–1.53 (2H, m, C**H₂**); δ_C (100 MHz, $CDCl_3$) 175.4 (**C**O_2), 157.9 (Ar**C**), 157.6 (Ar**C**), 138.4 (Ar**C**), 138.2 (Ar**C**), 136.4 (Ar**C**H), 134.1 (Ar**C**), 131.3 (Ar**C**H), 130.0 (Ar**C**H), 129.1 (Ar**C**H), 129.0 (Ar**C**H), 128.3 (Ar**C**H), 127.9 (Ar**C**H), 127.1 (Ar**C**H), 123.0 (Ar**C**H), 122.6 (Ar**C**H), 69.4 (N**C**HPh), 62.7 (**C**H_2OH), 53.9 (N**C**H_2), 42.1 (**C**H_2CHN), 39.7 (C**H₂**CO_2), 37.3 (N**C**H_3), 27.6 (**C**H_2); HRMS (ESI): calcd. for $C_{25}H_{29}N_2O_3$, 405.2173. Found: $[MH]^+$, 405.2176 (−0.8 ppm error)].

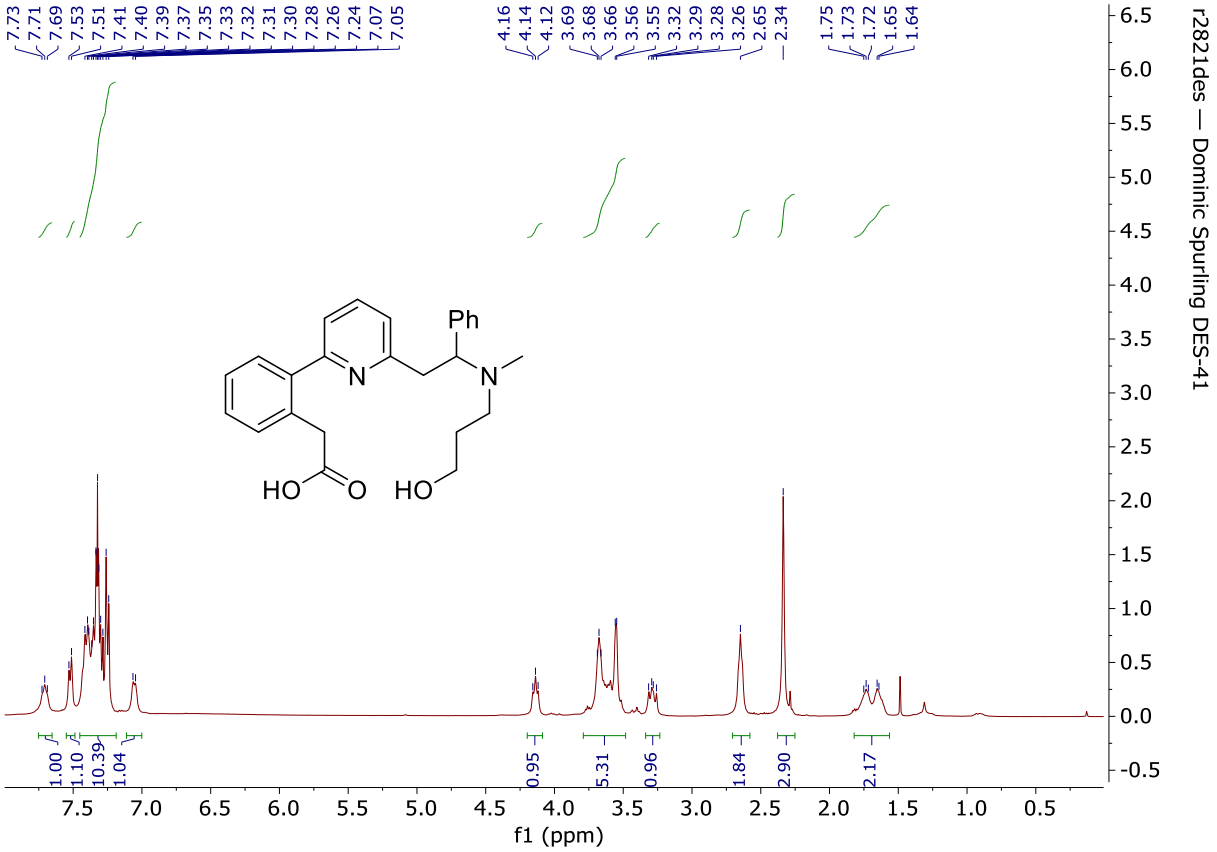
r2821des — Dominic Spurling DES-41
7.73 7.71 7.69 7.53 7.51 7.41 7.40 7.39 7.37 7.35 7.33 7.32 7.31 7.30 7.28 7.26 7.24 7.07 7.05
4.16 4.14 4.12 3.69 3.68 3.66 3.56 3.55 3.32 3.29 3.28 3.26 2.65 2.34
1.75 1.73 1.72 1.65 1.64
Ph
N
N
HO
O
HO
1.00 1.10 10.39 1.04 0.95 5.31 0.96 1.84 2.90 2.17
f1 (ppm)

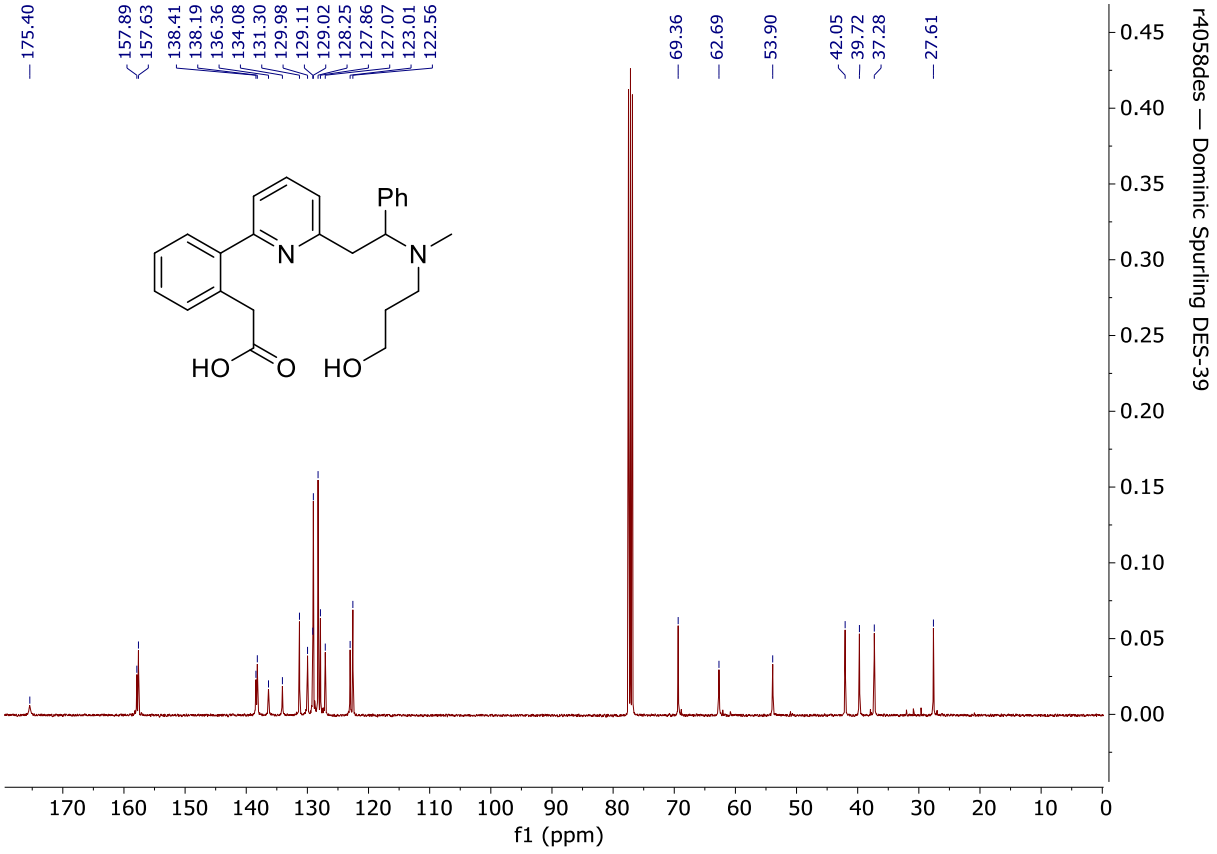
r4058des — Dominic Spurling DES-39
175.40
157.89 157.63 138.41 138.19 136.36 134.08 131.30 129.98 129.11 129.02 128.25 127.86 127.07 123.01 122.56
69.36 62.69 53.90 42.05 39.72 37.28 27.61
Ph
N
N
HO
O
HO
f1 (ppm)

14-Methyl-15-phenyl-10-oxa-14,21-diazatricyclo[15.3.1.0²,⁷]henicosa-1(21),2,4,6,17,19-hexaen-9-one (164)

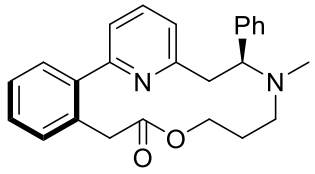

To a stirring solution of [2-(6-{2-[(3-hydroxypropyl)(methyl)amino]-2-phenylethyl}pyridin-2-yl)phenyl]acetic acid (**162**) (202 mg, 0.52 mmol) in acetonitrile (5 mL), was added diisopropylethylamine (430 µL, 2.47 mmol), followed by the addition of EDC·HCl (144 mg, 0.75 mmol) and HOBt (101 mg, 0.75 mmol). After stirring for 18 h at 25 °C, the reaction mixture was directly concentrated *in vacuo*. Only one diastereomer was observed. Purification by flash column chromatography (SiO_2, 50% ethyl acetate in hexanes) afforded the *title compound* as a red oil (142 mg, 73%); R_f 0.59 (ethyl acetate); ν_{max}/cm^{-1} (neat) 3069, 3025, 2941, 2851, 1735, 1590, 1569, 1450, 1360, 1341, 1289, 1213, 1173, 1085, 1008; δ_H (400 MHz, $CDCl_3$) 7.71 (1H, t, *J* = 7.7 Hz, Ar**H**), 7.51 (1H, dd, *J* = 6.9, 2.1 Hz, Ar**H**), 7.42–7.26 (9H, m, Ar**H**), 7.18 (1H, d, *J* = 7.7 Hz, Ar**H**), 4.48–4.40 (2H, m, NC**H**Ph and ArC**H**H'CO_2), 4.00 (1H, d, *J* = 17.5 Hz, ArCH**H'**CO_2), 3.80–3.75 (1H, m, OC**H**H'CH_2), 3.69–3.62 (2H, m, OCH**H'**CH_2 and ArC**H**H'CH), 3.10–3.05 (1H, dd, *J* = 15.2, 4.5 Hz, ArCH**H'**CH), 2.80–2.73 (1H, m, NC**H**H'CH_2), 2.28–2.20 (4H, m, NCH**H'**CH_2 and NC**H₃**), 1.66–1.60 (2H, m, CH_2C**H₂**CH_2); δ_C (100 MHz, $CDCl_3$) 172.0 (**C**O_2), 160.0 (Ar**C**), 158.9 (Ar**C**), 140.2 (Ar**C**), 138.0 (Ar**C**H), 137.0 (Ar**C**H), 133.1 (Ar**C**), 132.3 (Ar**C**H), 130.2 (Ar**C**H), 128.6 (Ar**C**H), 128.4 (Ar**C**H), 128.0 (Ar**C**H), 127.7 (Ar**C**H), 127.3 (Ar**C**H), 121.5 (Ar**C**H), 120.6 (Ar**C**H), 67.4 (N**C**HPh), 61.3 (CO_2**C**H_2CH_2), 47.5 (N**C**H_2), 40.6 (2 signals, Ar**C**H_2CH and Ar**C**H_2CO_2), 37.6 (N**C**H_3), 24.9 (CH_2**C**H_2CH_2); HRMS (ESI): calcd. for $C_{25}H_{27}N_2O_2$, 387.2067. Found: $[MH]^+$, 387.2065 (0.5 ppm error)].

Compound **164**

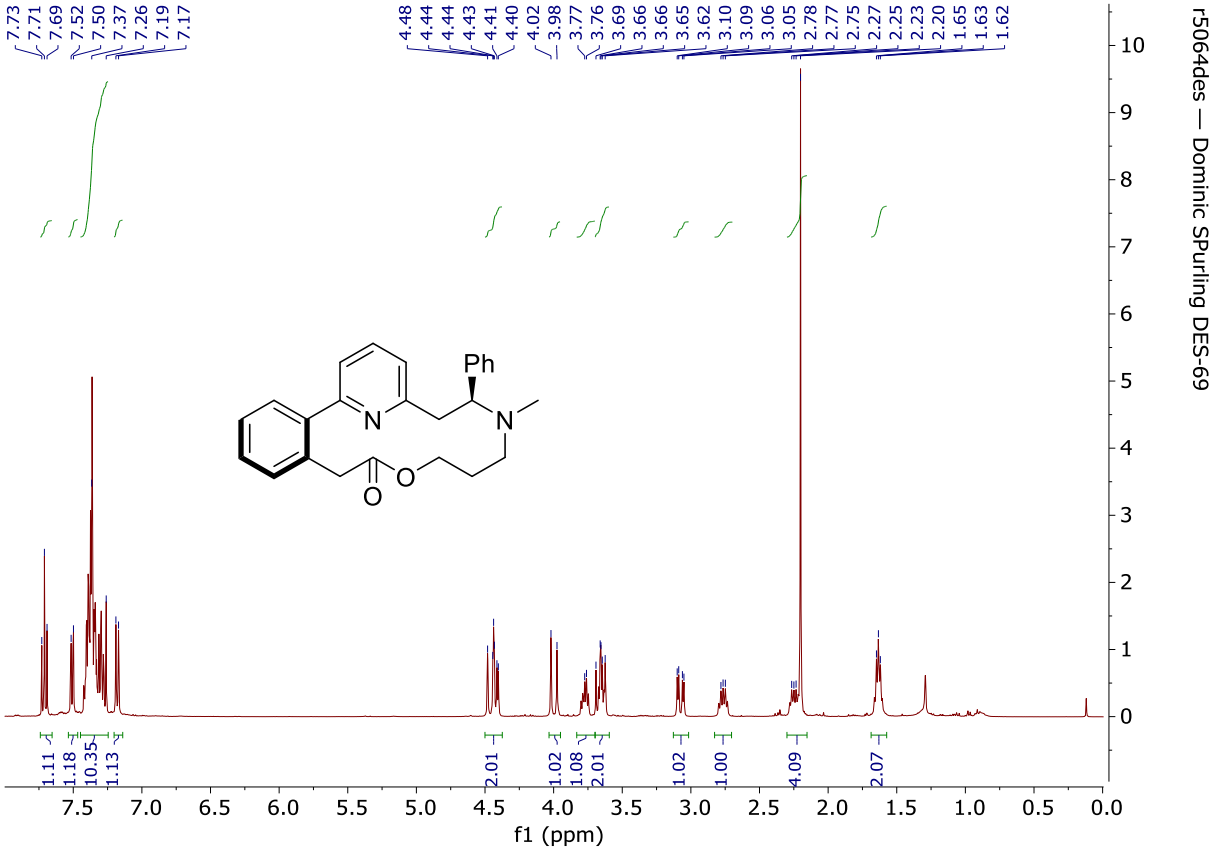

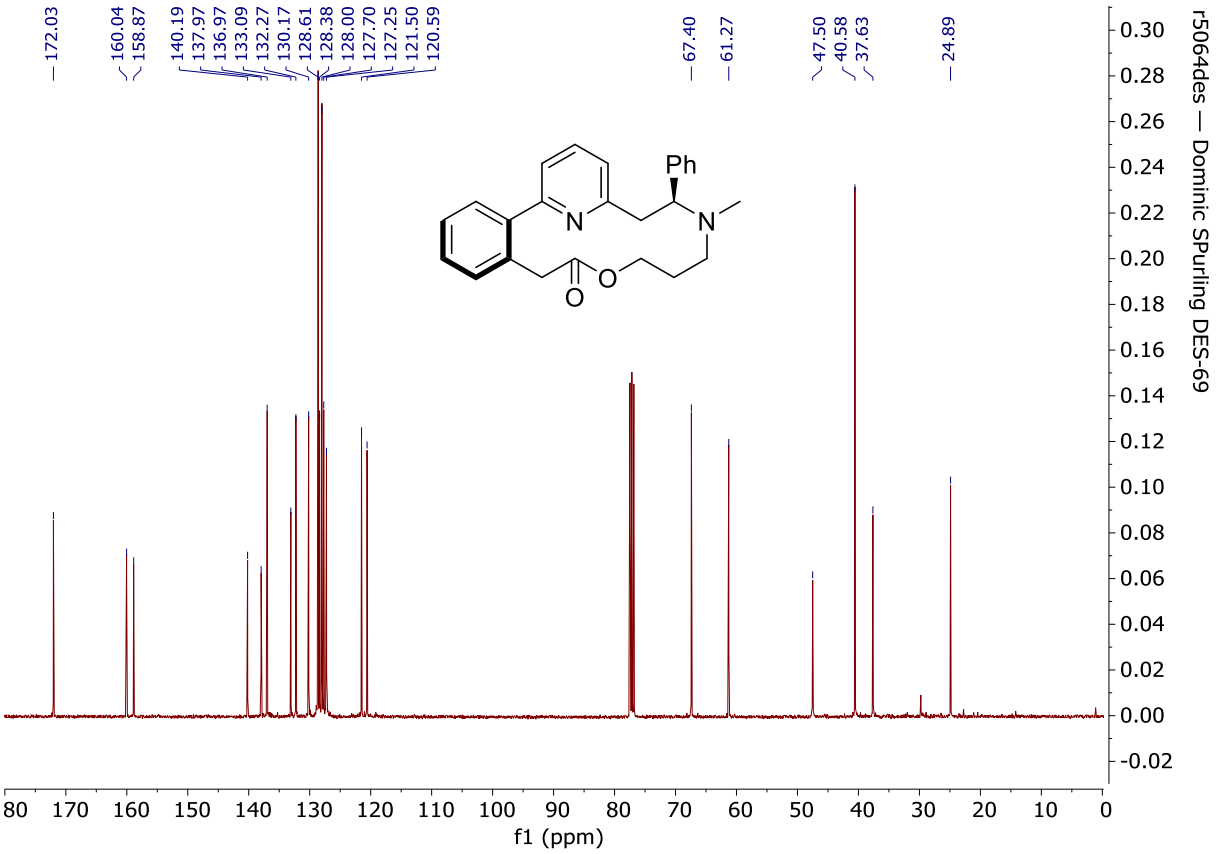

Methyl 4-[benzyl(3-hydroxypropyl)amino]butanoate (199)

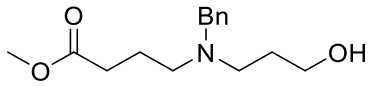

Methyl 4-bromobutyrate (**197**) (0.69 mL, 5.54 mmol) and 3-(benzylamino)propan-1-ol (**198**) (1.32 mL, 8.29 mmol) were dissolved in acetonitrile (55 mL) and potassium carbonate (1.53 g, 11.05 mmol) was added and the solution heated, at reflux, to 85 ^{o}C for 3 h. Upon completion the solution was diluted with water (50 mL) before being extracted with ethyl acetate (3 × 50 mL) and washed with sat. aq. brine (40 mL). The combined organic extracts were dried over $MgSO_4$, filtered and removed *in vacuo*. Purification by flash column chromatography (SiO_2, ethyl acetate) afforded the *title compound* as a colourless oil (572 mg, 39%); R_f 0.30 (ethyl acetate); ν_{max}/cm^{-1} (neat) 3424, 2950, 2813, 1736; δ_H (400 MHz, $CDCl_3$) 7.33–7.26 (5H, m, Ph), 3.73 (2H, t, *J* = 3.7 Hz, C**H$_2$**OH), 3.63 (1H, s, OC**H$_3$**), 3.58 (2H, s, NC**H$_2$**Ph), 2.67 (2H, t, *J* = 2.7 Hz, C**H$_2$**CO_2), 2.60 (2H, t, *J* = 2.5, NC**H$_2$**CH_2), 2.29 (2H, t, *J* = 2.3, NC**H$_2$**CH_2), 1.88–1.81 (2H, m, CH_2C**H$_2$**CH_2), 1.76–1.68 (2H, m, CH_2C**H$_2$**CH_2); δ_C (100 MHz, $CDCl_3$) 173.6 (**C**O_2Me), 138.0 (**C**), 129.2 (**C**H), 128.6 (**C**H), 127.4 (**C**H), 64.2 (**C**H_3O), 58.8 (**C**H_2OH), 54.0 (**C**H_2N), 52.9 (**C**H_2N), 51.7 (**C**H_2N), 31.8 (CH_2**C**H_2CO_2), 28.1 (CH_2**C**H_2), 22.0 (CH_2**C**H_2); HRMS (ESI): calcd for $C_{15}H_{24}NO_3$ 266.1751. Found: $[MNa]^+$, 266.1744 (2.6 ppm error).

Compound **199**

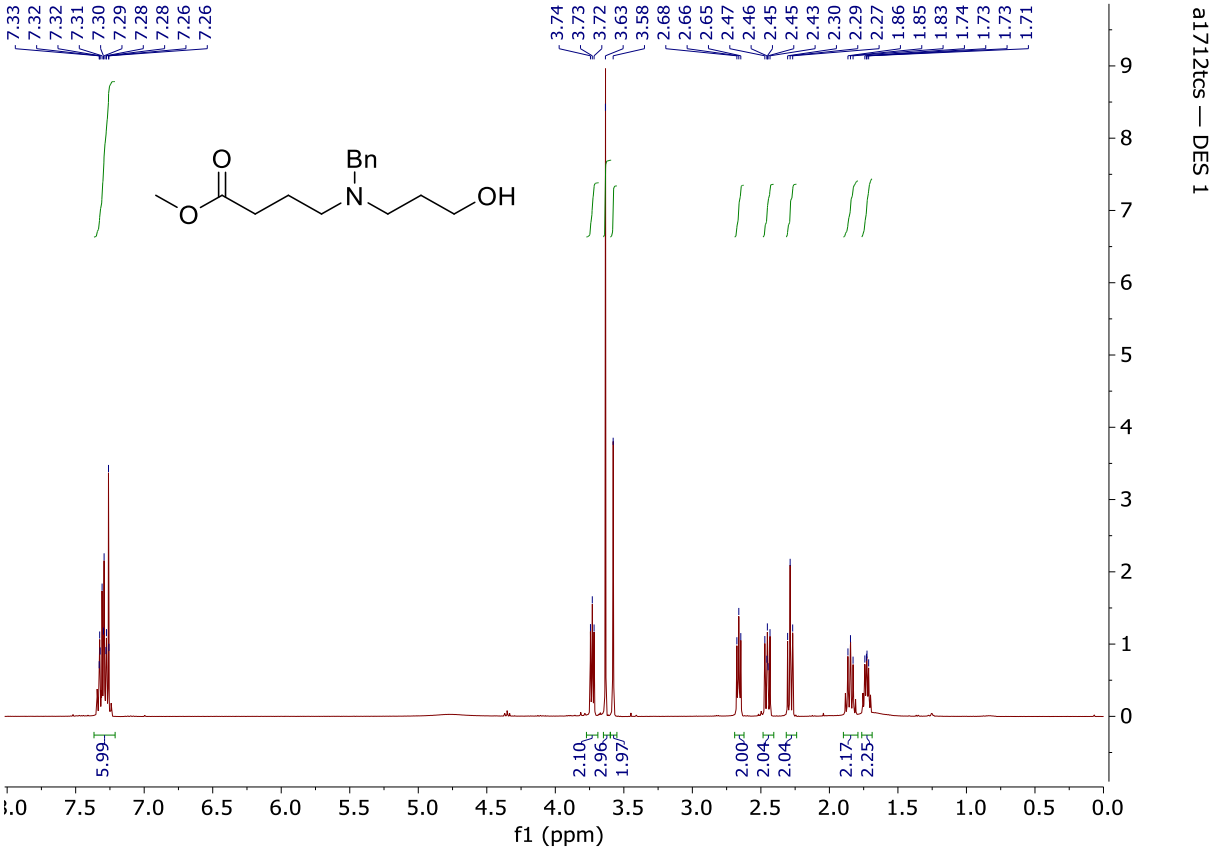

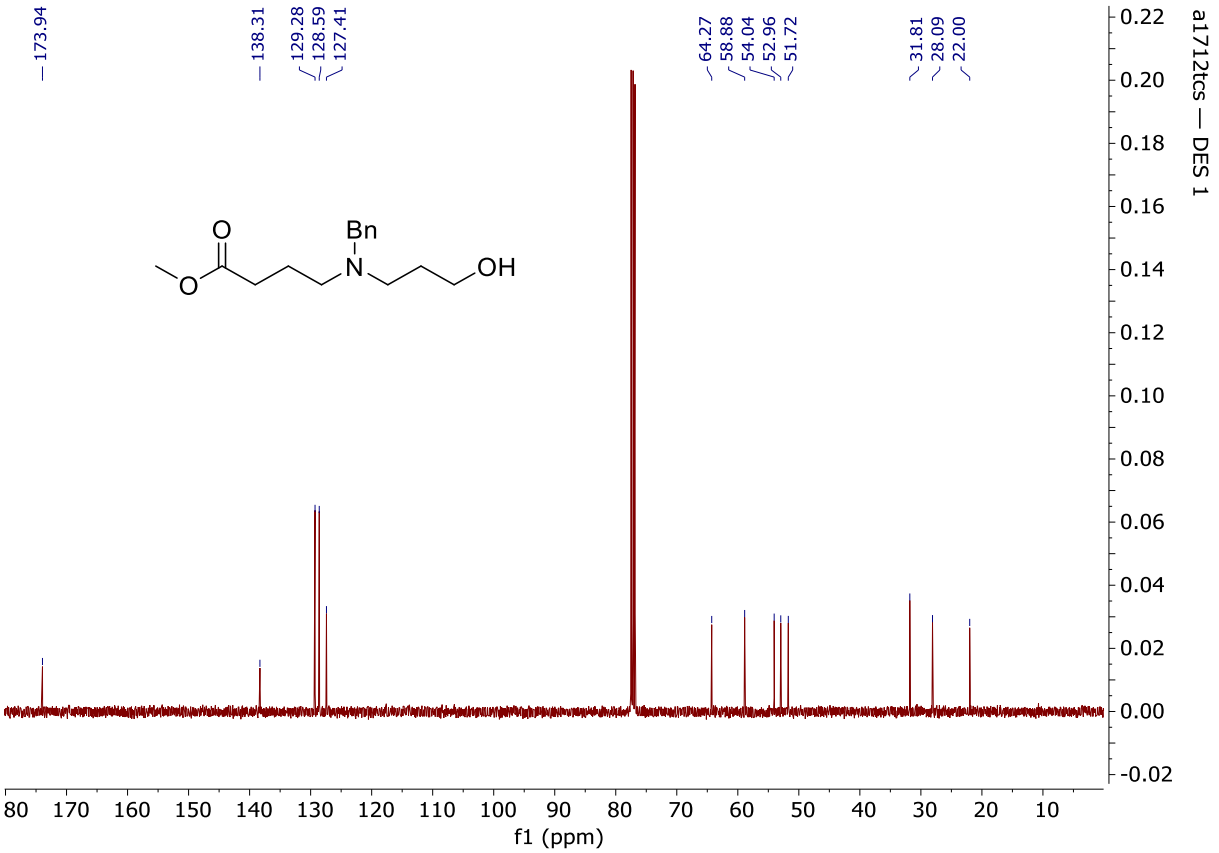

Methyl 4-[benzyl(3-bromopropyl)amino]butanoate (200)

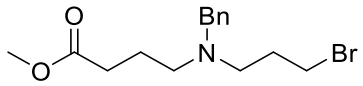

Methyl 4-[benzyl(3-hydroxypropyl)amino]butanoate (**199**) (572 mg, 2.17 mmol) and carbon tetrabromide (787 mg, 2.37 mmol) were dissolved in CH_2Cl_2 (8.6 mL) and cooled to 0 °C before triphenylphosphine (622 mg, 2.37 mmol) was added portion-wise. After stirring for 1 h at 25 °C, the reaction mixture was concentrated directly and then purified by flash column chromatography (SiO_2, 30% ethyl acetate in hexanes → 40% ethyl acetate in hexanes) affording the *title compound* as a yellow oil (582 mg, 72%); R_f 0.81 (50% ethyl acetate in hexanes); ν_{max}/cm^{-1} (neat) 2950, 2806, 1734, 1494, 1452, 1436, 1365, 1256, 1199, 1170, 1125, 1074, 1028; δ_H (400 MHz, $CDCl_3$) 7.27–7.20 (5H, m, Ph), 3.60 (3H, s, C**H₃**O), 3.52 (2H, s, C**H₂**Ph), 3.40 (2H, t, *J* = 6.8 Hz, C**H₂**Br), 2.54 (2H, t, *J* = 6.7 Hz, NC**H₂**), 2.42 (2H, t, *J* = 6.9 Hz, NC**H₂**), 2.30 (2H, t, *J* = 7.3 Hz, CO_2C**H₂**), 1.99–1.94 (2H, m, C**H₂**), 1.81–1.76 (2H, m, C**H₂**); δ_C (100 MHz, $CDCl_3$) 174.4 (**C**O), 139.5 (Ar**C**), 129.2 (Ar**C**), 128.6 (Ar**C**), 127.4 (Ar**C**), 59.0 (**C**H_2Ph), 53.2 (**C**H_2N), 52.2 (**C**H_2N), 51.9 (**C**H_3O), 32.2 (**C**H_2), 31.9 (**C**H_2), 30.8 (**C**H_2), 22.7 (**C**H_2); HRMS (ESI): calcd. for $C_{15}H_{23}{}^{79}BrNO_2$, 328.0907. Found: $[MH]^+$, 328.0899 (2.3 ppm error)].

Compound **200**

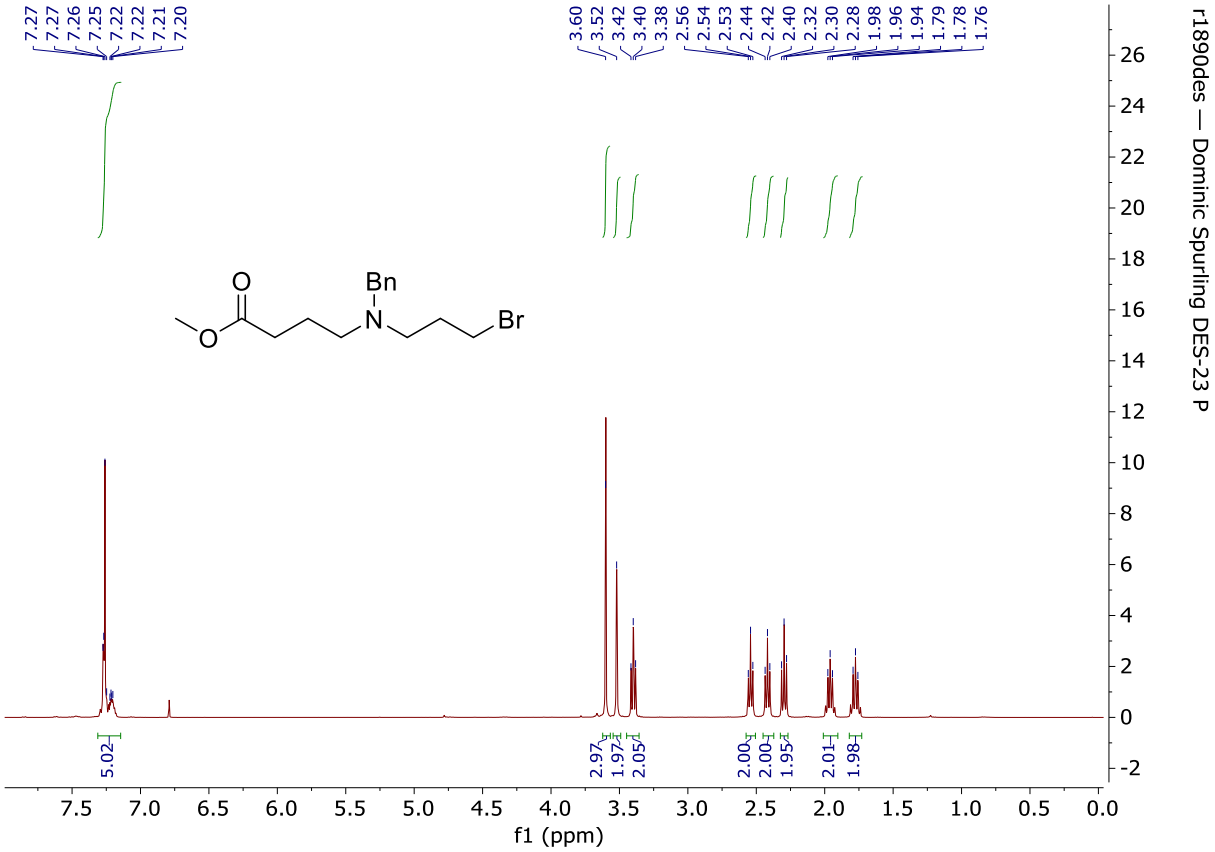

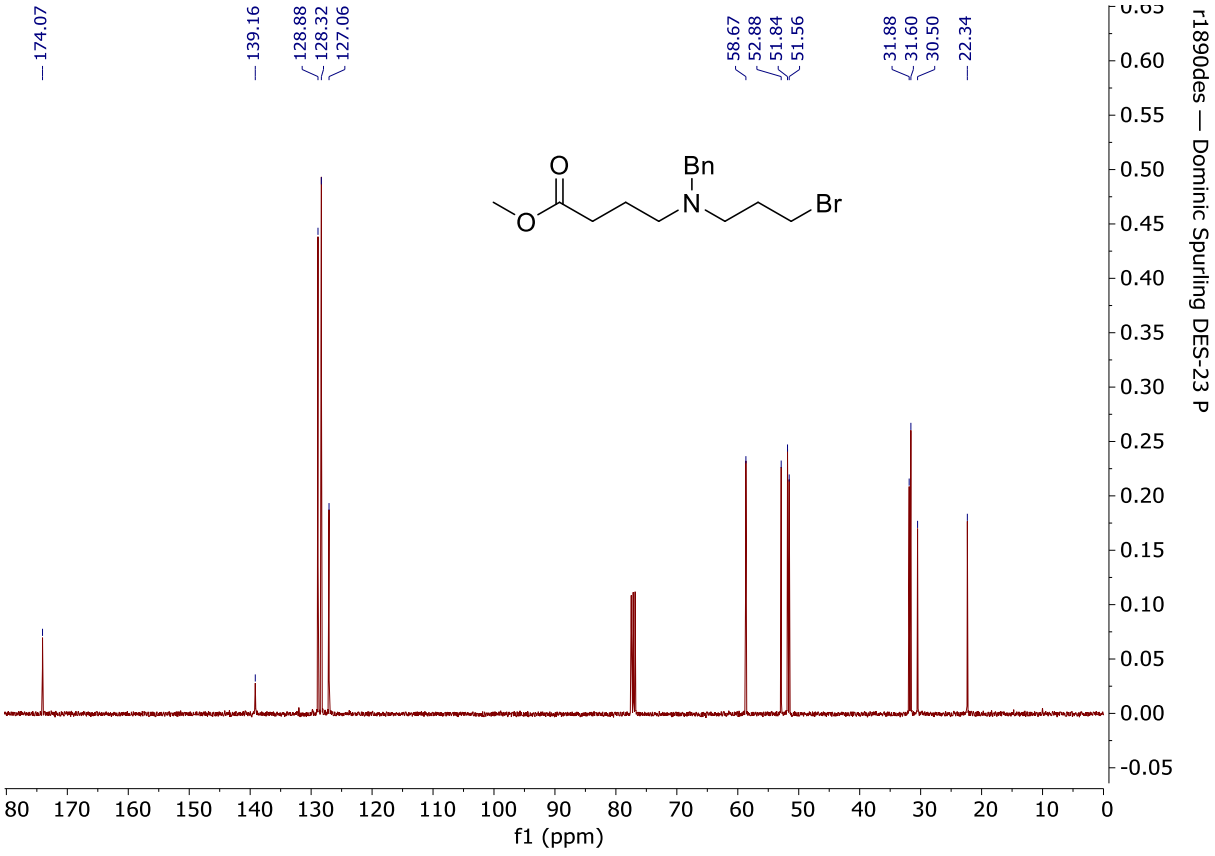

Methyl 4-[benzyl({3-[benzyl(3-hydroxypropyl)amino]propyl})amino]butanoate (201)

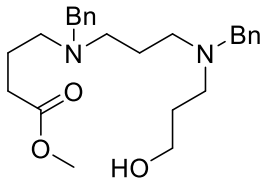

Methyl 4-[benzyl(3-bromopropyl)amino]butanoate (**200**) (1.21 g, 3.71 mmol), 3-(benzylamino)propan-1-ol (**198**) (885 µL, 5.56 mmol) and potassium carbonate (1.03 g, 7.42 mmol) were dissolved in acetonitrile (37 mL). After stirring at 85 °C for 3 h the reaction mixture was concentrated directly and then purified by flash column chromatography (SiO_2, 5% methanol in ethyl acetae) affording the *title compound* as a yellow oil (710 mg, 45%); R_f. 0.53 (10% methanol in ethyl acetate); ν_{max}/cm^{-1} (neat) 3417, 3027, 2948, 2803, 1735, 1602, 1494, 1452, 1366, 1170, 1071, 1028; δ_H (400 MHz, $CDCl_3$) 7.33–7.23 (10H, m, 2 × Ph), 3.73–3.70 (2H, m, C**H₂**OH), 3.64 (3H, s, OC**H₃**), 3.56 (2H, s, C**H₂**Ph), 3.51 (2H, s, C**H₂**Ph), 2.65–2.62 (2H, t, *J* = 5.9 Hz, NC**H₂**), 2.47–2.38 (6H, m, 3 × NC**H₂**), 2.31–2.27 (2H, t, *J* = 7.5 Hz, OCC**H₂**), 1.75–1.65 (6H, m, 3 × C**H₂**); δ_C (100 MHz, $CDCl_3$) 174.2 (**C**O), 139.6 (Ar**C**), 138.3 (Ar**C**), 129.1 (Ar**C**), 128.8 (Ar**C**), 128.4 (Ar**C**), 128.1 (Ar**C**), 127.2 (Ar**C**), 126.8 (Ar**C**), 64.0 (**C**H_2OH), 58.9 (**C**H_2Ph), 58.6 (**C**H_2Ph), 54.0 (**C**H_2N), 52.8 (**C**H_2N), 51.9 (**C**H_2N), 51.7 (**C**H_2N), 51.4 (CO**C**H_3), 31.7 (**C**H_2), 28.0 (**C**H_2), 24.3 (**C**H_2), 22.4 (**C**H_2); HRMS (ESI): calcd. for $C_{25}H_{37}N_2O_3$, 413.2799. Found: $[MH]^+$, 413.2795 (1.0 ppm error)].

Compound **201**

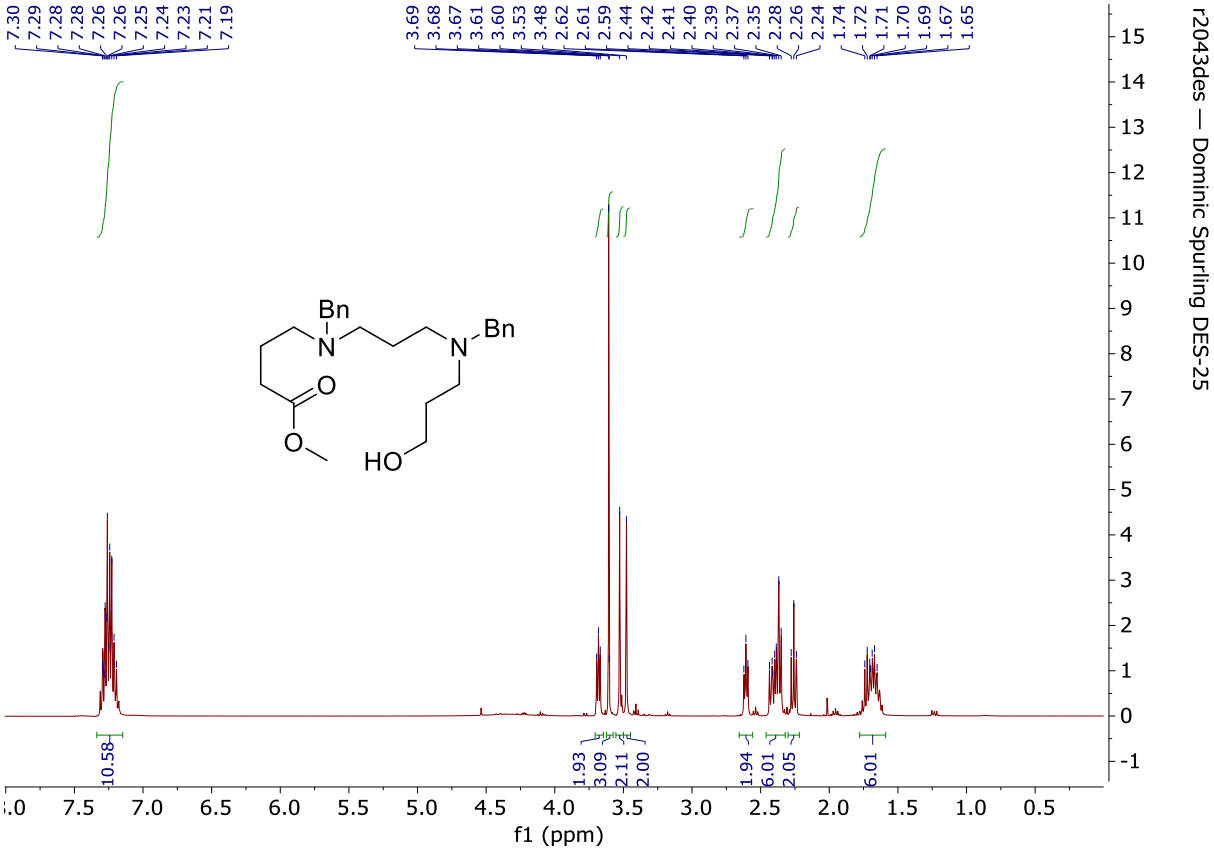

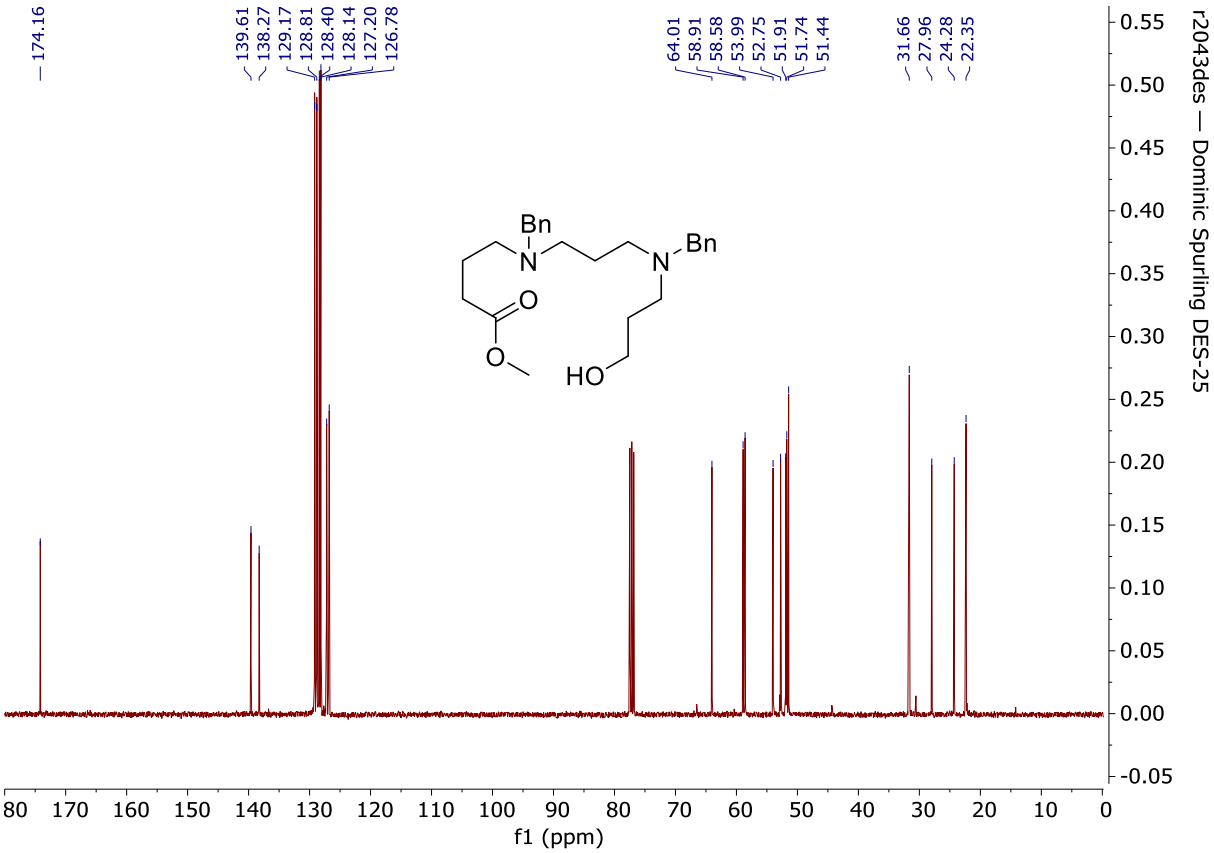

4-[Benzyl({3-[benzyl(3-hydroxypropyl)amino]propyl})amino]butanoic acid (190)

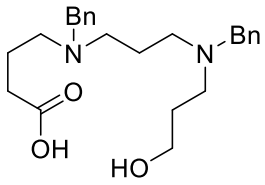

Methyl 4-[benzyl({3-[benzyl(3 hydroxypropyl)amino]propyl})amino]butanoate (**201**) (710 mg, 1.72 mmol) was dissolved in aqueous lithium hydroxide solution (0.5 M, 12 mL, 6.03 mmol) and THF (12 mL). The resulting bi-phasic solution was vigorously stirred for 18 h. Upon completion, the solvent was removed *in vacuo*. The crude material was then passed through a silica plug and eluted with 50% methanol in ethyl acetate to afford the *title compound* as a colourless oil (272 mg, 40%); R_f. 0.17 (20% methanol in ethyl acetate); ν_{max}/cm^{-1} (neat) 2943, 2811, 1575, 1494, 1453, 1407, 1072; δ_H (400 MHz, $CDCl_3$) 7.31–7.21 (10H, m, 2 × Ph), 3.69–3.64 (4H, m, C**H₂**Ph and HOC**H₂**), 3.54 (2H, s, C**H₂**Ph), 2.62–2.55 (4H, m, 2 × C**H₂**N), 2.48–2.45 (2H, m, C**H₂**N), 2.38 (2H, t, *J* = 7.1 Hz, C**H₂**N), 2.26 (2H, t, *J* = 6.5 Hz, C**H₂**CO_2H), 1.79–1.68 (6H, m, 3 × C**H₂**); δ_C (100 MHz, $CDCl_3$) 179.3 (**C**O_2H), 137.9 (Ar**C**), 136.4 (Ar**C**), 129.7 (Ar**C**H), 129.4 (Ar**C**H), 128.6 (Ar**C**H), 128.5 (Ar**C**H), 127.8 (Ar**C**H), 127.4 (Ar**C**H), 62.6 (**C**H_2OH), 58.9 (**C**H_2Ph), 58.3 (**C**H_2Ph), 53.6 (**C**H_2N), 52.8 (**C**H_2N), 51.5 (**C**H_2N), 51.2 (**C**H_2N), 35.4 (**C**H_2), 31.0 (**C**H_2), 28.3 (**C**H_2), 23.4 (**C**H_2); HRMS (ESI): calcd. for $C_{24}H_{35}N_2O_3$, 399.2624. Found: $[MH]^+$, 299.2640 (0.5 ppm error)].

Compound **190**

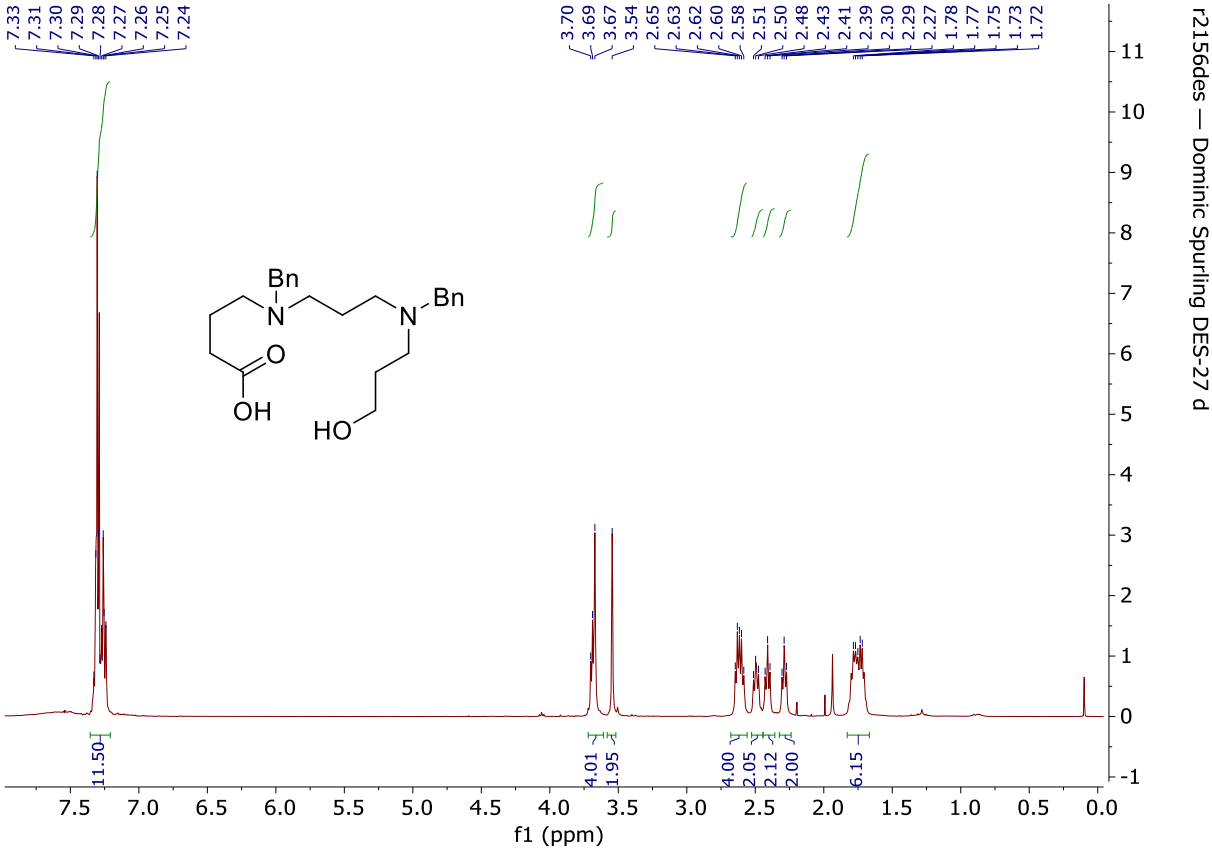

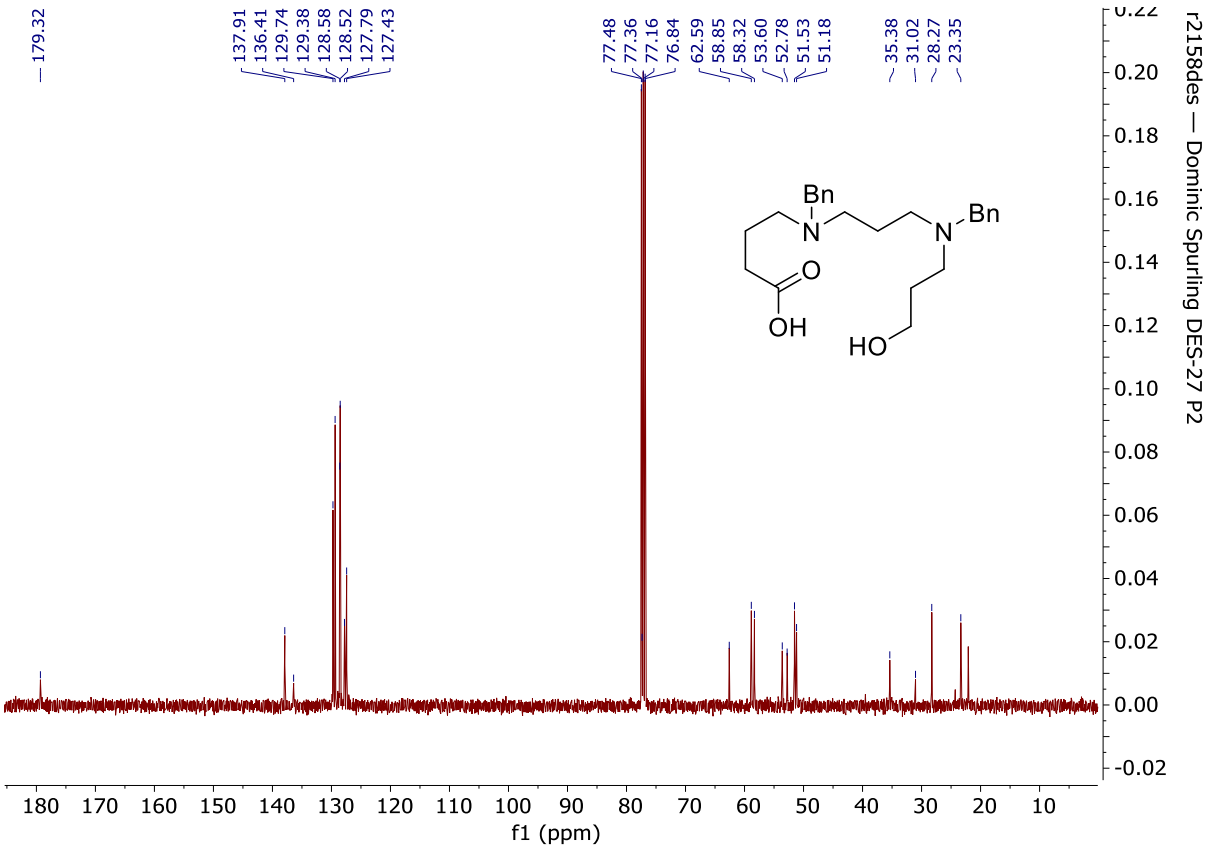

5,9-Dibenzyl-1-oxa-5,9-diazacyclotridecan-13-one (192)

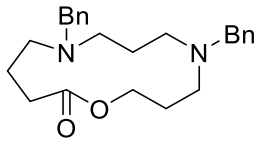

To a stirring solution of 4-[benzyl({3-[benzyl(3-hydroxypropyl)amino]propyl})amino]butanoic acid (**190**) (186 mg, 0.47 mmol) in acetonitrile (5 mL), was added diisopropylethylamine (435 μL, 2.50 mmol), followed by the addition of EDC·HCl (144 mg, 0.75 mmol) and HOBt (101 mg, 0.75 mmol). After stirring for 18 h at 25 °C, the reaction mixture was concentrated directly and then purified by flash column chromatography (SiO_2, 50% ethyl acetate in hexanes) to afford the *title compound* as a colourless oil (87 mg, 49%); $R_{f.}$ 0.40 (50% ethyl acetate in hexanes); ν_{max}/cm^{-1} (neat) 3027, 2928, 2796, 1728, 1602, 1494, 1452, 1372, 1356, 1340, 1231, 1208, 1171, 1119, 1070, 1028; δ_H (400 MHz, $CDCl_3$) 7.29–7.20 (10H, m, 2 × Ph), 4.23–4.20 (2H, m, OC**H₂**), 3.49 (2H, s, C**H₂**Ph), 3.47 (2H, s, C**H₂**Ph), 2.65–2.62 (2H, t, *J* = 6.3 Hz, NC**H₂**), 2.51–2.44 (4H, m, 2 × NC**H₂**), 2.35–2.31 (4H, m, NC**H₂** and C**H₂**CO_2), 1.19–1.68 (4H, m, 2 × C**H₂**), 1.59–1.53 (2H, m, C**H₂**); δ_C (100 MHz, $CDCl_3$) 174.3 (**C**O_2), 140.1 (Ar**C**), 139.8 (Ar**C**), 129.2 (Ar**C**H), 129.0 (Ar**C**H), 128.3 (Ar**C**H), 128.2 (Ar**C**H), 127.0 (Ar**C**H), 126.9 (Ar**C**H), 62.1 (**C**H_2O), 59.4 (**C**H_2Ph), 59.2 (**C**H_2Ph), 52.7 (**C**H_2N), 52.6 (**C**H_2N), 52.2 (**C**H_2N), 49.7 (**C**H_2N), 31.9 (**C**H_2CO_2), 26.6 (**C**H_2), 26.4 (**C**H_2), 23.3 (**C**H_2); HRMS (ESI): calcd. for $C_{24}H_{33}N_2O_2$, 381.2537. Found: $[MH]^+$, 381.2530 (1.7 ppm error)].

Compound **192**

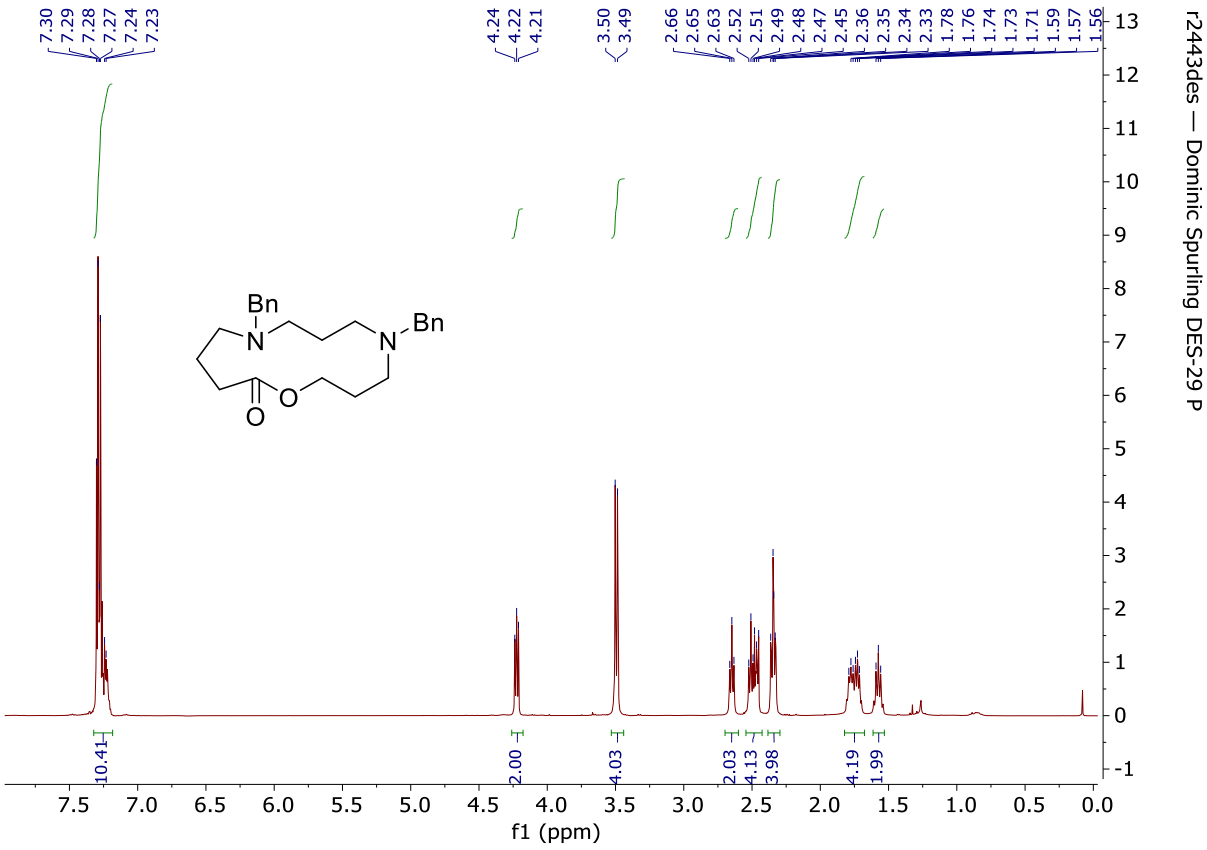

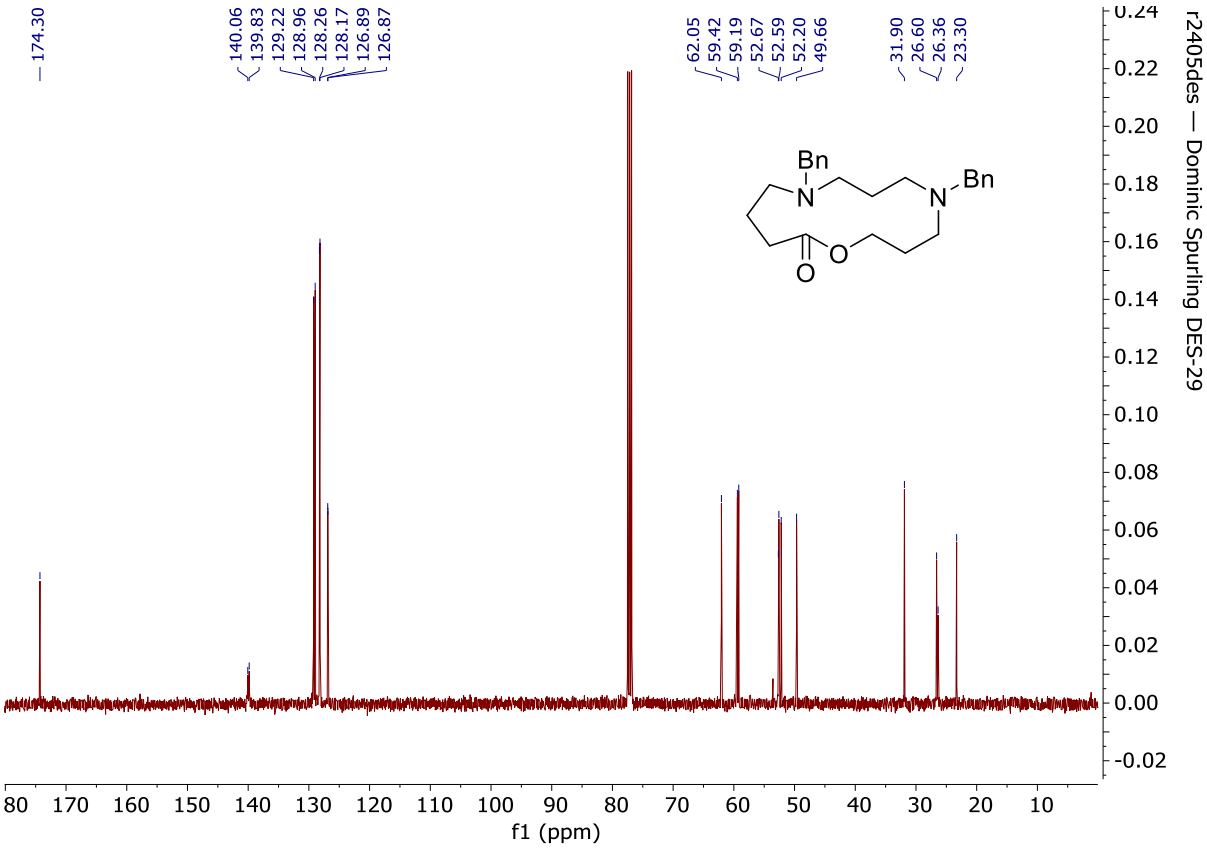

5,9-Dibenzyl-1-oxa-5,9-diazacyclotetradecan-14-one (203)

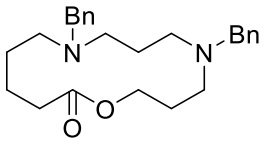

To a stirring solution of 5-(benzyl(3-(benzyl(3-hydroxypropyl)amino)propyl)amino)pentanoic acid (**202**) (261 mg, 0.633 mmol) in acetonitrile (6 mL), was added diisopropylethylamine (550 μL, 3.17 mmol), followed by the addition of EDC·HCl (182 mg, 0.95 mmol) and HOBt (128 mg, 0.95 mmol). After stirring for 18 h at 25 °C, the reaction mixture was concentrated directly and then purified by flash column chromatography (SiO_2, 50% ethyl acetate in hexanes) to afford the *title compound* as a colourless oil (52 mg, 20%); R_f 0.45 (ethyl acetate); ν_{max}/cm^{-1} (neat) 2930, 2795, 1730, 1699, 1494, 1452, 1238, 1238, 1155, 1070, 1028; δ_H (400 MHz, $CDCl_3$) 7.23–7.20 (10H, m, 2 × Ph), 4.24 (2H, t, *J* = 5.3 Hz, OC**H₂**), 3.51 (2H, s, C**H₂**Ph), 3.48 (2H, s, C**H₂**Ph), 2.63 (2H, t, *J* = 6.8 Hz, NC**H₂**), 2.47–2.34 (8H, m, 3 × NC**H₂** and C**H₂**CO_2), 1.90–1.84 (2H, m, C**H₂**), 1.73–1.60 (2H, m, C**H₂**), 1.56–1.48 (2H, m, C**H₂**); δ_C (100 MHz, $CDCl_3$) 174.1 (**C**O_2), 139.8 (2 × Ar**C**), 128.8 (Ar**C**H), 128.8 (Ar**C**H), 128.3 (Ar**C**H), 128.2 (Ar**C**H), 126.9 (Ar**C**H), 126.8 (Ar**C**H), 61.4 (**C**H_2O), 60.0 (**C**H_2Ph), 58.7 (**C**H_2Ph), 52.4 (**C**H_2N), 52.2 (**C**H_2N), 49.8 (**C**H_2N), 48.5 (**C**H_2N), 34.7 (**C**H_2CO_2), 26.66 (**C**H_2), 25.5 (**C**H_2), 24.5 (**C**H_2), 23.1 (**C**H_2); HRMS (ESI): calcd. for $C_{25}H_{35}N_2O_2$, 395.2687 Found: $[MH]^+$, 395.2693 (1.6 ppm error)].

Compound **203**

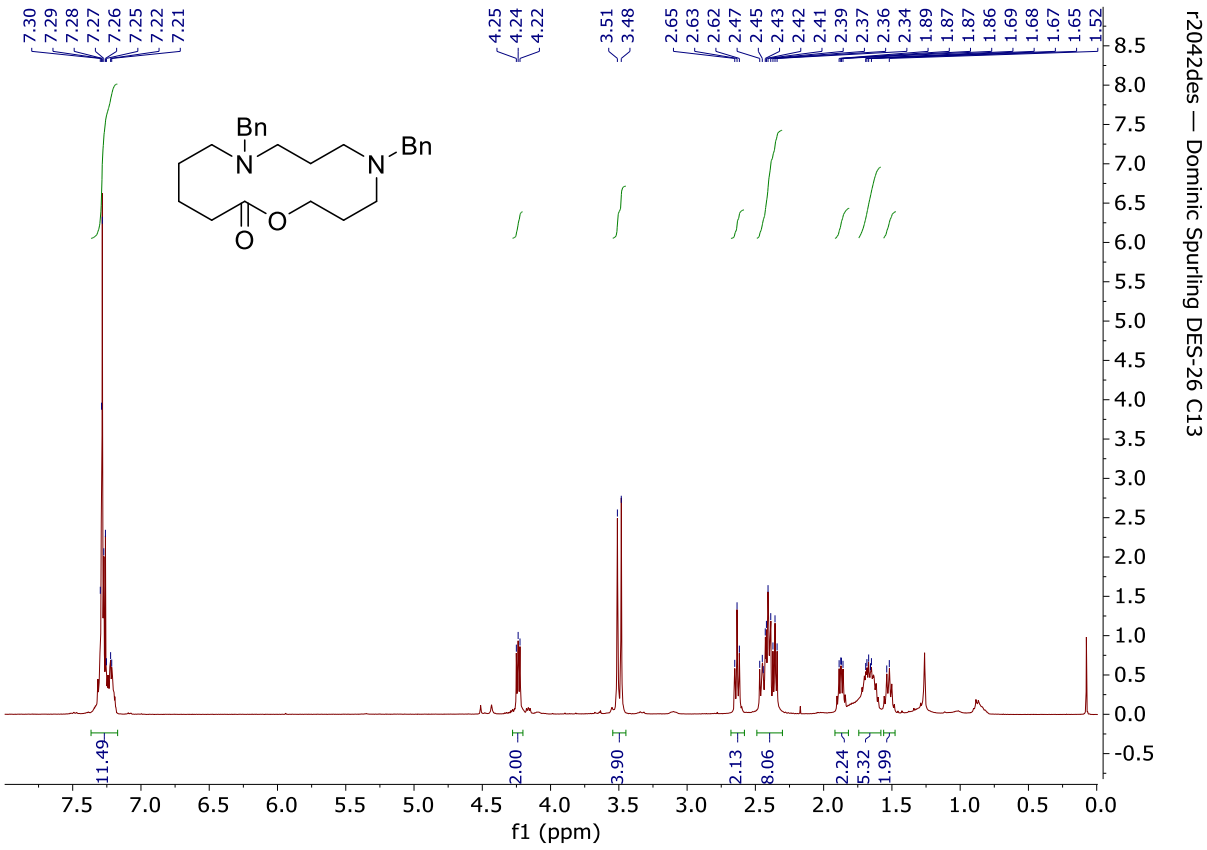

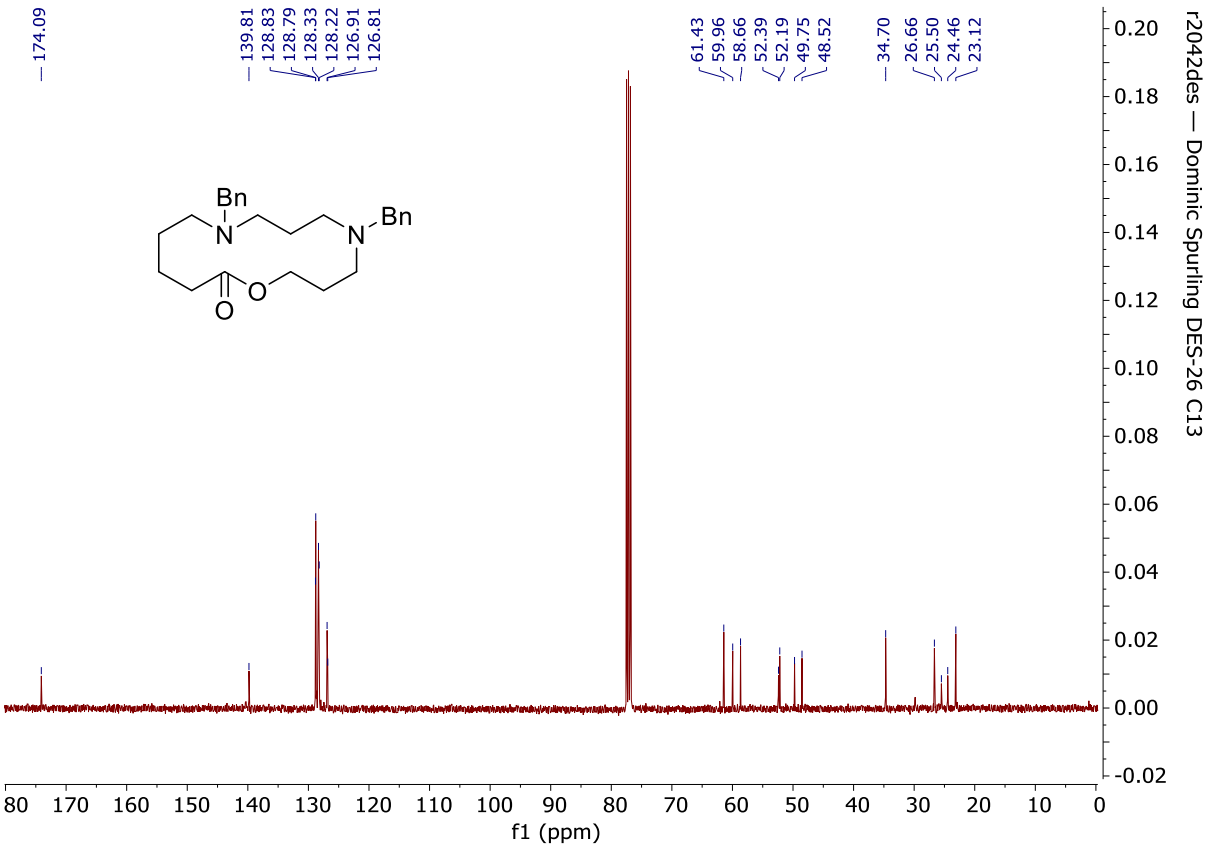

***N*-(3-bromopropyl)aniline (213)**

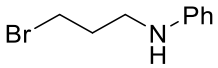

1,3-Dibromopropane (**216**) (19.6 mL, 0.19 mol) and aniline (2.94 mL, 32.2 mmol) were dissolved in acetonitrile (65 mL). After stirring at 85 °C for 3 h the reaction mixture was diluted with water (50 mL), extracted with ethyl acetate (3 × 30 mL) and washed with sat. brine (30 mL). The combined organic extracts were dried over $MgSO_4$, filtered, and then purified by flash column chromatography (SiO_2, 5% diethyl ether in hexanes) affording the *title compound* as an orange oil (2.23 g, 33%); R_f. 0.39 (10% ethyl acetate in hexanes); δ_H (400 MHz, $CDCl_3$) 7.23–7.19 (2H, m, 2 × Ph**H**), 6.80–6.71 (3H, m, 3 × Ph**H**), 3.51 (2H, t, *J* = 6.5 Hz, BrC**H₂**), 3.35 (2H, t, *J* = 6.6 Hz, C**H₂**N), 2.22–2.15 (2H, m, CH_2C**H₂**CH_2).

Spectroscopic data matched those reported in the literature.[67]

Compound **213**

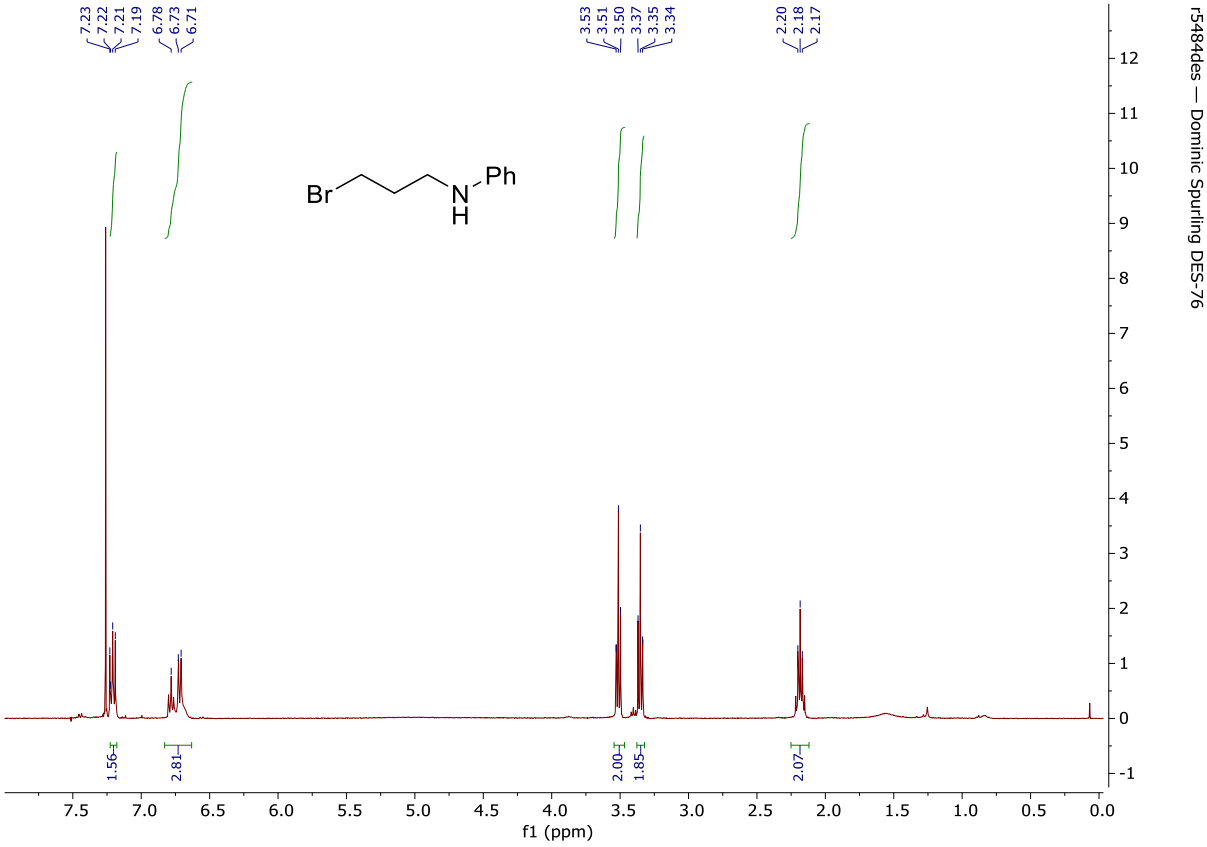

N^1-(2-(6-Bromopyridin-2-yl)-1-phenylethyl)-N^1-methyl-N^3-phenylpropane-1,3-diamine (214)

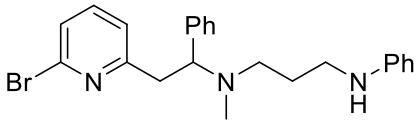

[2-(6-Bromopyridin-2-yl)-1-phenylethyl](methyl)amine (**174**) (1.53 g, 5.31 mmol), N-(3-bromopropyl)aniline (**213**) (1.69 g, 7.96 mmol) and potassium carbonate (1.46 g, 10.6 mmol) was dissolved in acetonitrile (50 mL). After stirring at 85 °C for 18 h the reaction mixture was quenched with water and extracted with ethyl acetate (3 × 30 mL). The combined organic layers were dried with anhydrous $MgSO_4$, filtered, and concentrated *in vacuo*. Purification *via* flash column chromatography (SiO_2, 50% diethyl ether in hexane) afforded the title compound as a yellow oil (667 mg, 30%); R_f 0.61 (ethyl acetate); ν_{max}/cm^{-1} (neat) 3030, 2941, 2856, 2796, 1602, 1583, 1563, 1505, 1434, 1405, 1319, 1259, 1178, 1115; δ_H (400 MHz, $CDCl_3$) 7.34–7.17 (9H, m, Ar**H**), 6.93 (1H, d, *J* = 7.4 Hz, Ar**H**), 6.71 (1H, t, *J* = 7.3 Hz, Ar**H**), 6.54 (2H, d, *J* = 7.8 Hz, Ar**H**), 4.18 (1H, t, *J* = 7.0 Hz, NC**H**Ph), 3.54–3.48 (1H, dd, *J* = 13.7, 7.0 Hz, ArC**H**H'CH), 3.16–3.10 (1H, dd, *J* = 13.7, 7.0 Hz, CCH**H**'CH), 3.08–3.03 (2H, m, C**H₂**NHPh), 2.60–2.53 (1H, dt, *J* = 12.8, 6.2 Hz, CH_3NC**H**H'CH_2), 2.47–2.41 (1H, dt, *J* = 12.8, 6.2 Hz, CH_3NCH**H'**CH_2), 2.26 (3H, s, C**H₃**N), 1.78–1.67 (2H, m, CH_2C**H₂**CH_2); δ_C (100 MHz, $CDCl_3$) 161.6 (Ar**C**), 148.6 (Ar**C**), 141.3 (Ar**C**), 138.8 (Ar**C**), 138.3 (Ar**C**), 129.7 (Ar**C**), 128.8 (Ar**C**), 128.0 (Ar**C**), 127.3 (Ar**C**), 125.4 (Ar**C**), 122.7 (Ar**C**), 116.8 (Ar**C**), 112.8 (Ar**C**), 68.3 (Ph**C**HN), 52.2 (CH_3N**C**H_2), 42.1 (CH_2**C**H_2NHPh), 40.3 (C**C**H_2CHN), 37.7 (**C**H_3N), 26.2 (CH_2**C**H_2CH_2); HRMS (ESI): calcd. for $C_{23}H_{27}{}^{79}BrN_3$, 424.1383. Found: $[MH]^+$, 424.1388 (−1.1 ppm error)].

Compound **214**

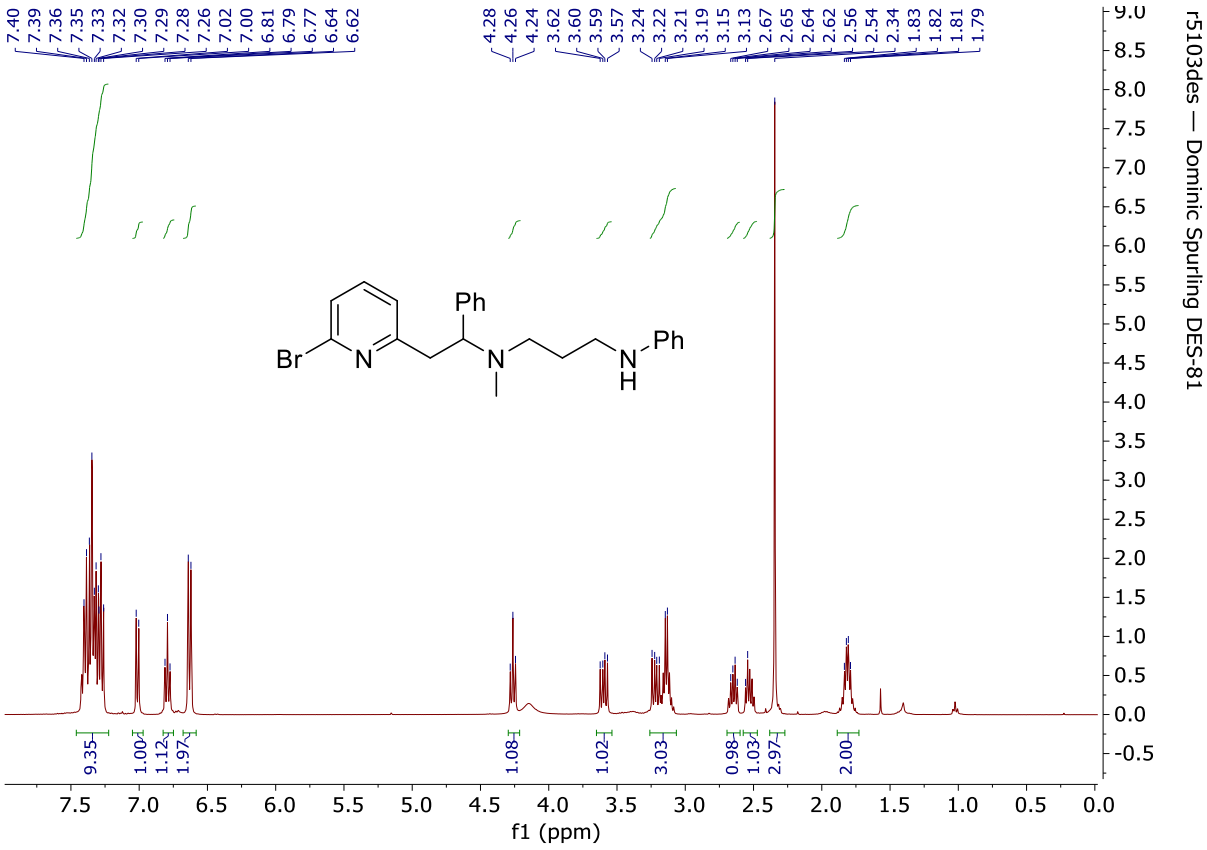

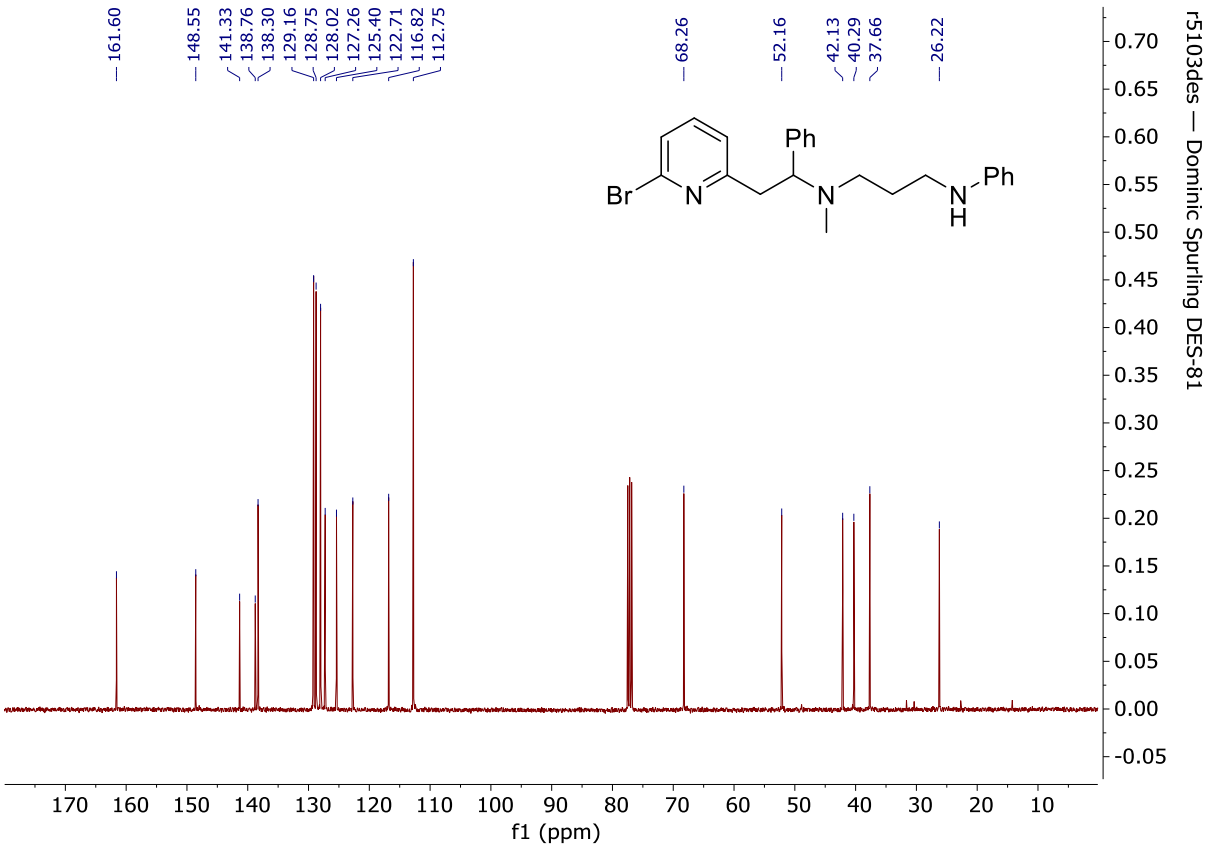

Methyl 2-(2-(6-(2-(methyl(3-(phenylamino)propyl)amino)-2-phenylethyl)pyridin-2-yl)phenyl)acetate (218)

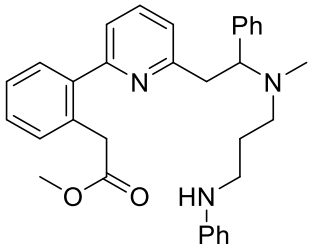

N^1-(2-(6-bromopyridin-2-yl)-1-phenylethyl)-N^1-methyl-N^3-phenylpropane-1,3-diamine (**214**) (667 mg, 1.85 mmol), methyl 2-(2-(4,4,5,5-tetramethyl-1,3,2-dioxaborolan-2-yl)phenyl) acetate (**181**) (765 mg, 2.77 mmol), potassium phosphate (784 mg, 3.69 mmol) and $PdCl_2(dppf).CH_2Cl_2$ (75.0 mg, 0.092 mmol) were charged into an RBF purged with nitrogen. THF (18 mL) and de-ionised water (140 µL, 4.37 mmol) were added and heated to 80 °C, at reflux, for 18 h. Upon completion the solution was cooled to room temperature, diluted with water (20 mL), extracted with ethyl acetate (3 × 30 mL) and washed with brine (15 mL). The combined organic extracts were dried over $MgSO_4$, filtered, and removed *in vacuo*. Purification by flash column chromatography (SiO_2, 5% methanol in diethyl ether) afforded the *title compound* as a yellow oil (715 mg, 76%); R_f 0.70 (10% methanol in ethyl acetate); ν_{max}/cm^{-1} (neat) 3403, 3025, 2948, 2848, 2803, 1733, 1602, 1569, 1506, 1447, 1320, 1254, 1211, 1157, 1083, 1044, 1004; δ_H (400 MHz, $CDCl_3$) 7.49 (1H, t, *J* = 7.7 Hz, Ar**H**), 7.40–7.18 (10H, m, Ar**H**), 6.92 (1H, d, *J* = 7.7 Hz, Ar**H**), 6.64–6.66 (1H, m, Ar**H**), 6.46 (2H, d, *J* = 7.9, Ar**H**), 4.19 (1H, dd, *J* = 8.3, 6.7 Hz, NC**H**Ph), 3.80 (2H, d, *J* = 9.9 Hz, C**H**$_2$$CO_2$Me), 3.55–3.50 (4H, m, CO_2C**H**$_3$ and CC**H**H'CHPh), 3.23–3.18 (1H, dd, *J* = 13.4, 8.3 Hz, CCH**H'**CHPh), 3.06–2.99 (2H, m, CH_2C**H**$_2$CNHPh), 2.58–2.51 (1H, dt, *J* = 13.4, 6.7 Hz, MeNC**H**H'CH_2), 2.48–2.41 (1H, dt, *J* = 12.9, 6.7 Hz, MeNCH**H'**CH_2), 2.27 (3H, s, C**H**$_3$N), 1.75–1.64 (2H, m, CH_2C**H**$_2$$CH_2$); δ_C (100 MHz, $CDCl_3$) 172.4 (**C**O_2Me), 159.1 (Ar**C**), 158.8 (Ar**C**), 148.6 (Ar**C**), 140.6 (Ar**C**), 139.3 (Ar**C**), 136.5 (Ar**C**H), 132.4 (Ar**C**), 131.4 (Ar**C**H), 130.0 (Ar**C**H), 129.1 (Ar**C**H), 128.9 (Ar**C**H), 128.4 (Ar**C**H), 128.0 (Ar**C**H), 127.4 (Ar**C**H), 127.1 (Ar**C**H), 122.0 (Ar**C**H), 121.3 (Ar**C**H), 116.8 (Ar**C**H), 112.7 (Ar**C**H), 68.5 (N**C**HPh), 52.4 (MeN**C**H_2CH_2), 51.8 (CO_2**C**H_3), 42.2 (CH_2**C**H_2NHPh), 40.5 (C**C**H_2CHPh), 39.1 (C**C**H_2CO_2), 37.7 (**C**H_3N), 26.3 (CH_2**C**H_2CH_2); HRMS (ESI): calcd. For $C_{32}H_{36}N_3O_2$, 494.2802. Found: $[MH]^+$, 494.2809 (−1.4 ppm error)].

Compound **218**

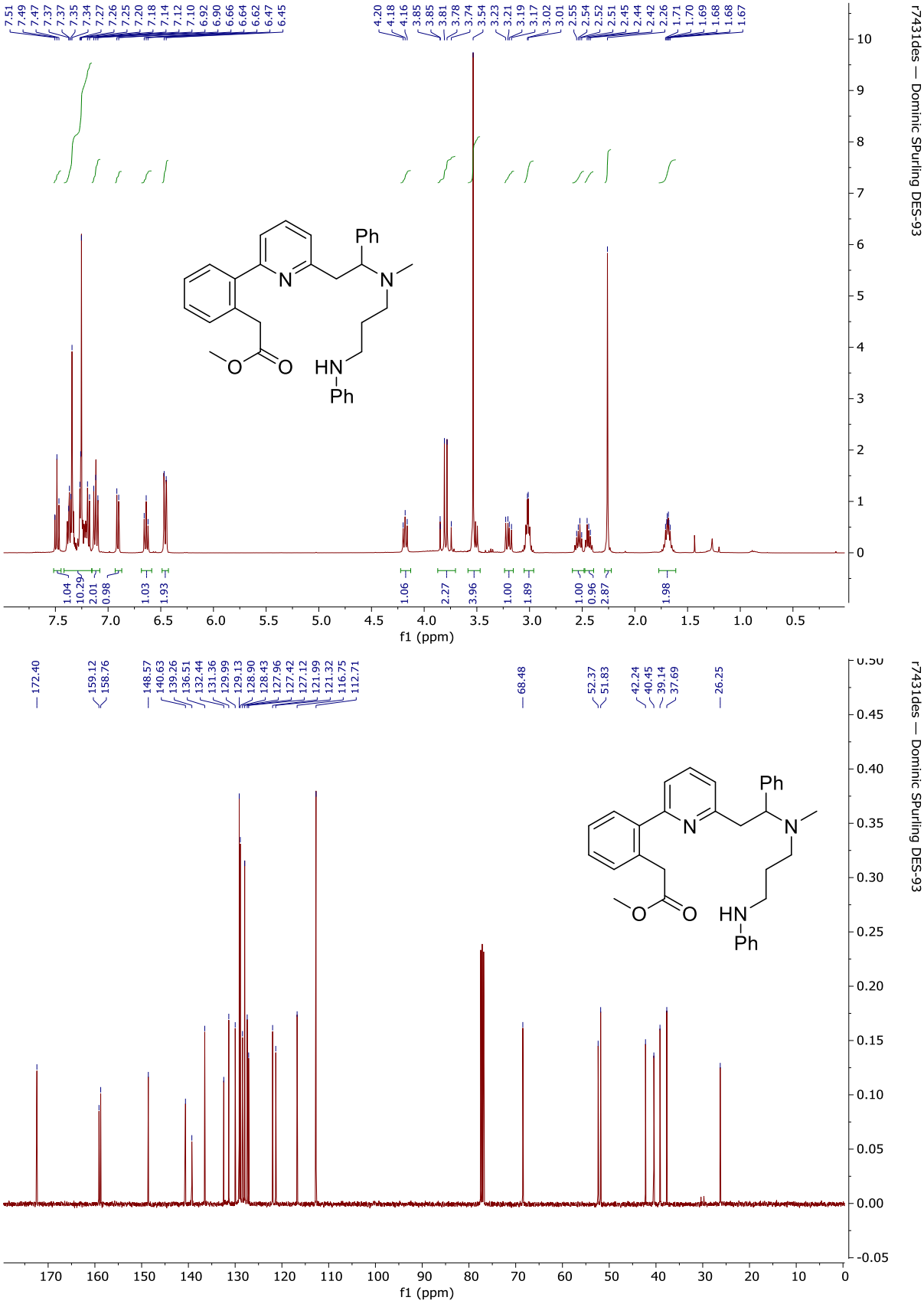

2-(2-(6-(2-(Methyl(3-(phenylamino)propyl)amino)-2-phenylethyl)pyridin-2-yl)phenyl)acetic acid (207)

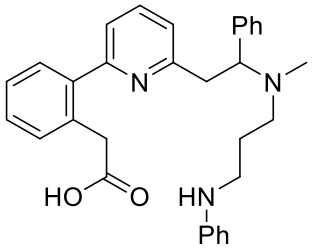

Methyl 2-(2-(6-(2-(methyl(3-(phenylamino)propyl)amino)-2-phenylethyl)pyridin-2-yl)phenyl)acetate (**218**) (587 mg, 1.19 mmol) was dissolved in aqueous lithium hydroxide solution (0.5 M, 12 mL, 5.95 mmol) and THF (12 mL). The resulting bi-phasic solution was vigorously stirred at room temperature for 18 h. Upon completion, the solvent was removed *in vacuo*. Purification by flash column chromatography (SiO_2, 30% methanol in diethyl ether) afforded the *title compound* as a white powder (378 mg, 68%); mp. 56–59 °C; R_f 0.26 (10% methanol in ethyl acetate); ν_{max}/cm^{-1} (neat) 3371, 3026, 2945, 2851, 2798, 1721, 1601, 1505, 1452, 1320, 1260, 1145, 1098; δ_H (400 MHz, $CDCl_3$) 7.85 (1H, t, *J* = 7.9 Hz, Ar**H**), 7.65 (1H, d, *J* = 7.5 Hz, Ar**H**), 7.57–7.24 (13H, m, Ar**H**), 6.78 (1H, t, *J* = 7.4 Hz, Ar**H**), 6.62 (2H, d, *J* = 7.8 Hz, Ar**H**), 4.13 (1H, t, *J* = 7.8 Hz, NC**H**Ph), 3.82–3.67 (1H, dd, *J* = 13.6, 7.8 Hz, CC**H**H'CHPh), 3.69 (1H, d, *J* = 12.7 Hz, CC**H**H'CO_2), 3.56 (1H, d, *J* = 12.7 Hz, CCH**H'**CO_2), 3.43–3.38 (1H, dd, *J* = 13.6, 7.8 Hz, CCH**H'**CHPh), 3.20–3.10 (2H, m, $CH_2C\mathbf{H_2}NHPh$), 2.73–2.66 (1H, dt, *J* = 13.0, 6.5 Hz, MeNC**H**H'), 2.63–2.56 (1H, dt, *J* = 13.0, 6.5 Hz, MeNCH**H'**), 2.42 (3H, s, $C\mathbf{H_3}N$), 1.93–1.77 (2H, m, $CH_2C\mathbf{H_2}CH_2$); δ_C (100 MHz, $CDCl_3$) 173.0 (**C**O_2H), 158.2 (Ar**C**), 157.0 (Ar**C**), 148.6 (Ar**C**), 139.1 (Ar**C**H), 137.5 (Ar**C**), 133.1 (Ar**C**), 131.6 (Ar**C**H), 130.7 (Ar**C**H), 129.9 (Ar**C**H), 129.2 (Ar**C**H), 128.8 (Ar**C**H), 128.4 (Ar**C**H), 127.9 (Ar**C**H), 127.8 (Ar**C**H), 123.7 (Ar**C**H), 122.8 (Ar**C**H), 117.0 (Ar**C**H), 112.8 (Ar**C**H), 69.6 (N**C**HPh), 52.6 (MeN**C**H_2CH_2), 42.2 ($CH_2\mathbf{C}H_2NHPh$), 42.2 (C**C**H_2CHPh), 39.7 (C**C**H_2CO_2), 38.0 (**C**H_3N), 26.2 ($CH_2\mathbf{C}H_2CH_2$); HRMS (ESI): calcd. For $C_{31}H_{33}N_3NaO_2$, 502.2465. Found: $[MNa]^+$, 502.2475 (−2.1 ppm error)].

Compound **207**

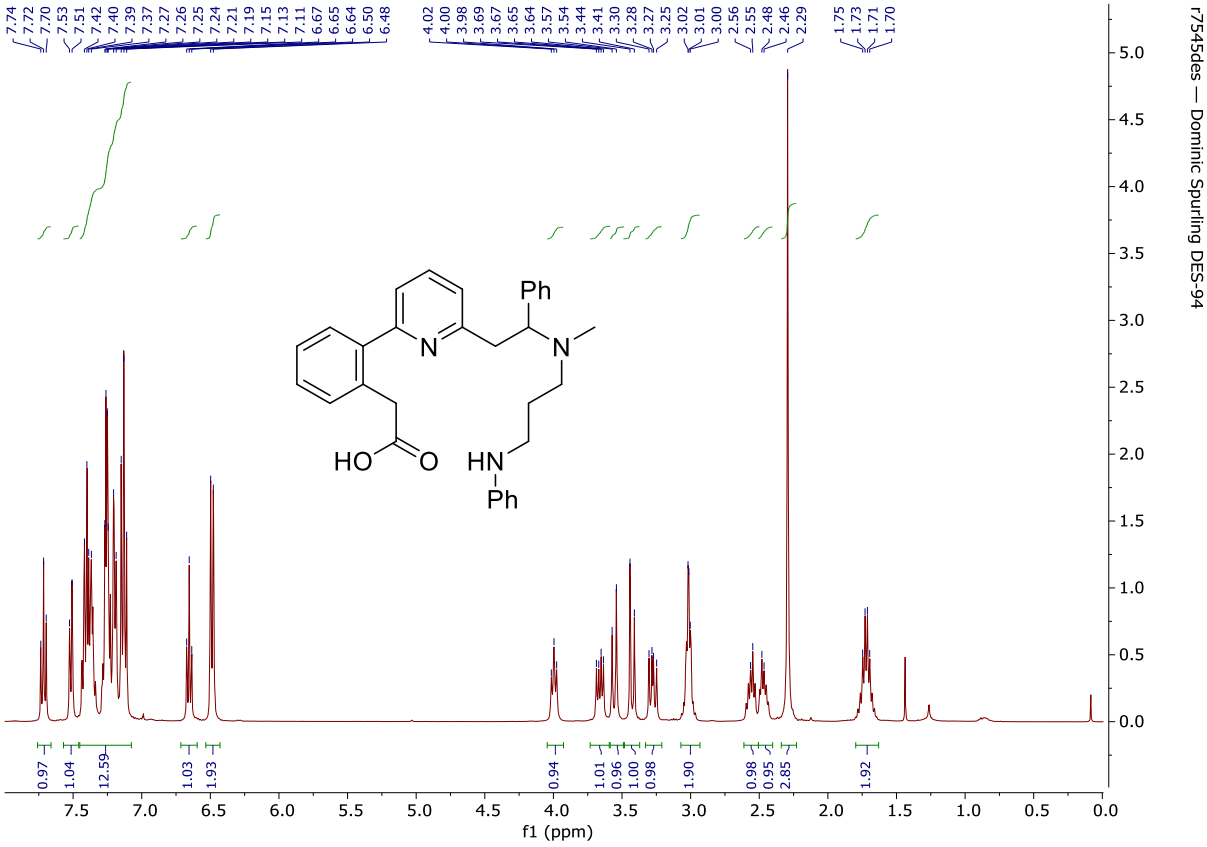

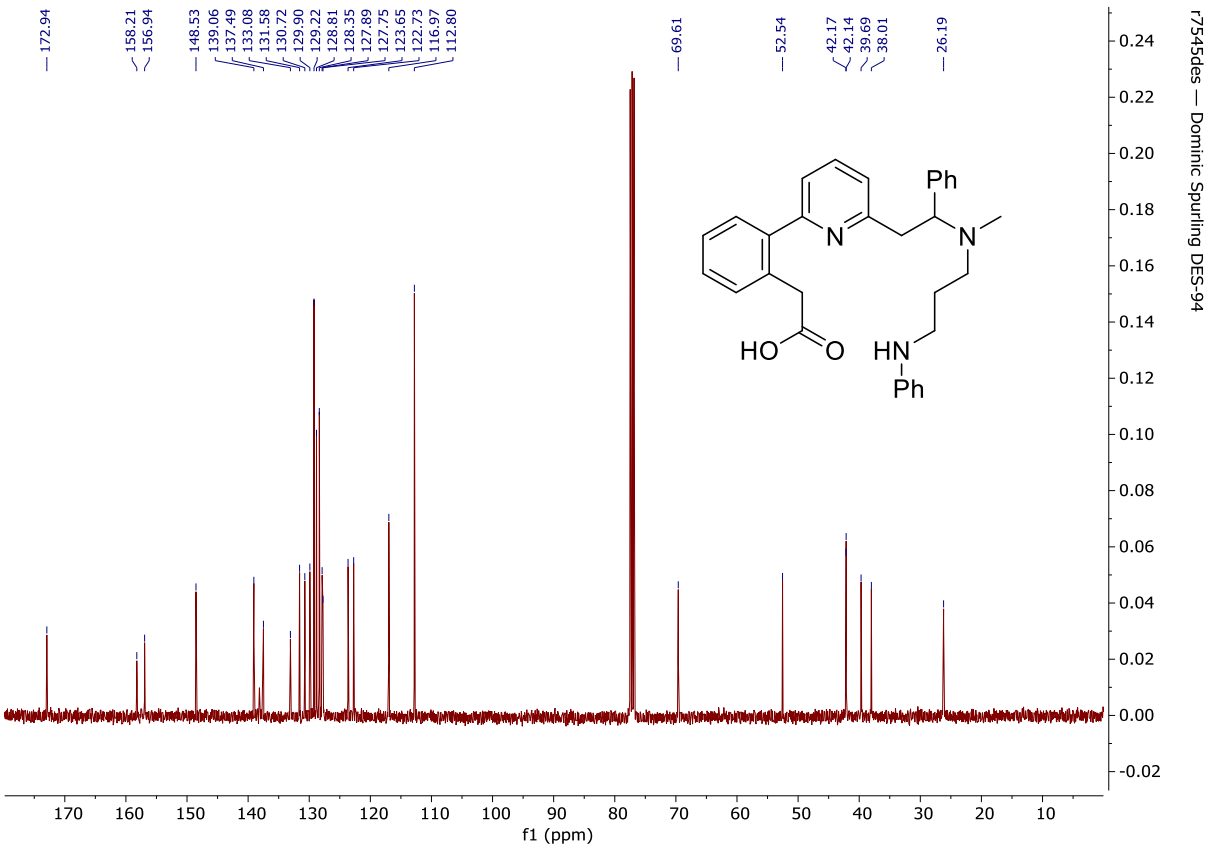

1-(6-Bromopyridin-2-yl)propan-2-one (220)

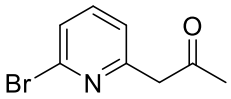

N,*N*-Diisopropylamine (4.95 mL, 35.1 mmol) was dissolved in THF (90 mL) and cooled to 0 ºC before n-BuLi (2.5 M solution in hexanes, 14.0 mL, 35.1 mmol) was added dropwise and stirred for 30 mins. The LDA solution was then cooled to −78 °C, where 2-bromo-6-methylpyridine (**173**) (1.98 mL, 17.5 mmol) was added dropwise and stirred for 1 h. *N*-Methoxy-*N*-methylacetamide (3.74 mL, 35.1 mmol) was added and stirred for a further 2 h at −78 °C before slowly warming to RT. The solution was then quenched with H_2O (70 mL) and extracted with ethyl acetate (3 × 50 mL) and washed with sat. brine (50 mL). The combined organic extracts were dried over $MgSO_4$, filtered and removed in vacuo. Purification by flash column chromatography (SiO_2, 20% ethyl acetate in hexanes) afforded the title compound as a yellow oil (3.15 g, 84%); R_f. 0.37 (30% ethyl acetate in hexanes); δ_H (400 MHz, $CDCl_3$) 7.52 (1H, t, *J* = 7.7 Hz, Ar**H**), 7.39 (1H, d, *J* = 7.7 Hz, Ar**H**), 7.17 (1H, d, *J* = 7.7 Hz, Ar**H**), 3.19 (2H, s, CC**H**$_2$CO), 2.25 (3H, s, COC**H**$_3$).

Spectroscopic data matched those reported in the literature.[57]

Compound **220**

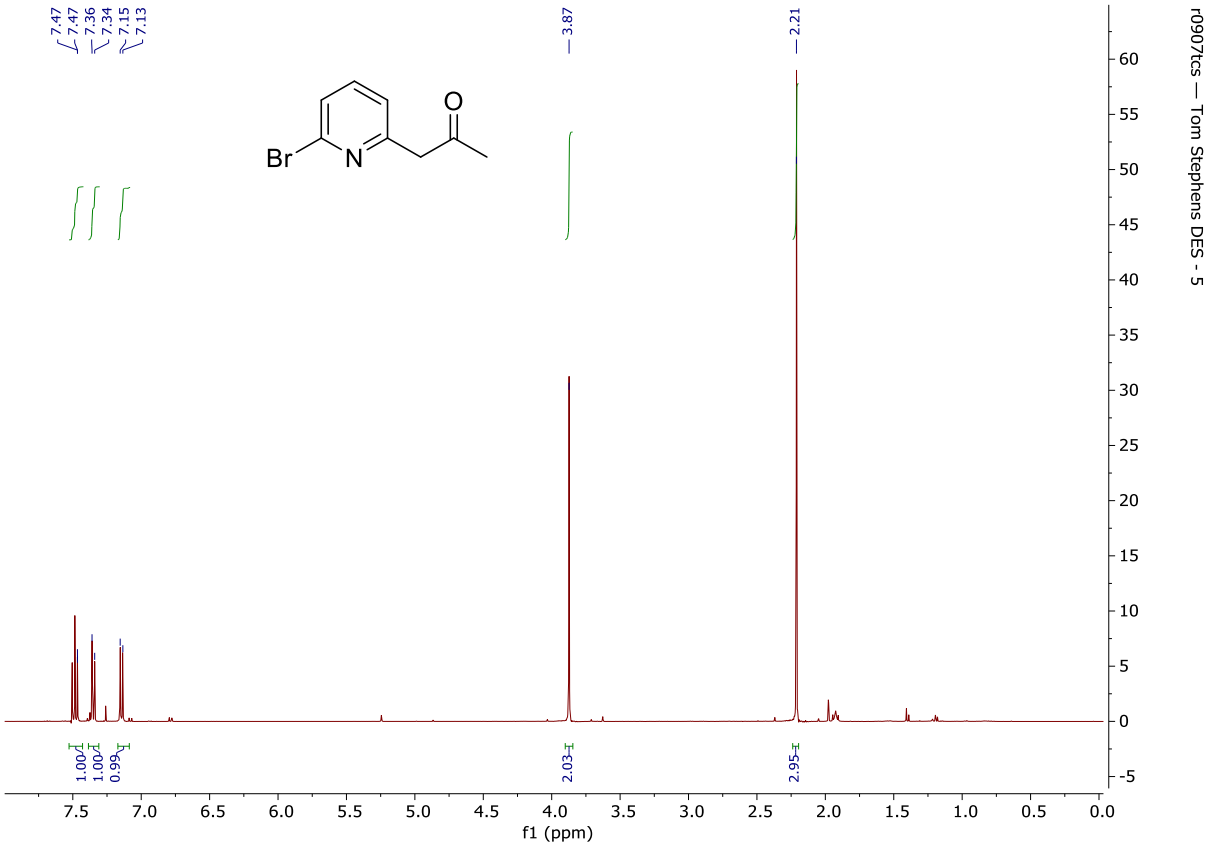

N-(1-(6-Bromopyridin-2-yl)propan-2-yl)aniline (221)

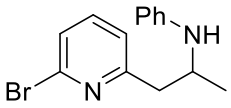

To a solution of 1-(6-bromopyridin-2-yl)propan-2-one (**220**) (3.15 g, 14.8 mmol) in dichloroethane (73 mL) at room temperature, aniline (1.62 mL, 17.7 mmol), acetic acid (1.02 mL, 17.7 mmol) and sodium triacetoxyborohydride (4.70 g, 22.2 mmol) were added sequentially. The reaction mixture was stirred at room temperature overnight. The solution was then quenched with 70 mL of 1 M NaOH and extracted with ethyl acetate (3× 50 mL) and washed with sat. brine (50 mL). The combined organic layers were dried over anhydrous $MgSO_4$, filtered and concentrated in vacuo. Purification via flash column chromatography (SiO_2, 20% ethyl acetate in hexanes) afforded the title compound as a yellow oil (3.76 g, 88%); R_f. 0.41 (20% ethyl acetate in hexanes); δ_H (400 MHz, $CDCl_3$) 7.43 (1H, t, *J* = 7.7 Hz, Ar**H**), 7.32 (1H, d, *J* = 7.7 Hz, Ar**H**), 7.18–7.10 (3H, m, Ar**H**), 6.69 (1H, t, *J* = 7.32 Hz, Ar**H**), 6.62 (2H, d, *J* = 7.3 Hz, Ar**H**), 3.97–3.89 (1H, m, $CH_2C\mathbf{H}N$), 3.01 (1H, dd, *J* = 13.7, 6.7 Hz, C**H**H'CHN), 2.90 (1H, dd, *J* = 13.7, 6.7 Hz, CH**H'**CHN), 1.22 (3H, d, *J* = 6.2 Hz, C**H**$_3$).

Spectroscopic data matched those reported in the literature. [57]

Compound **221**

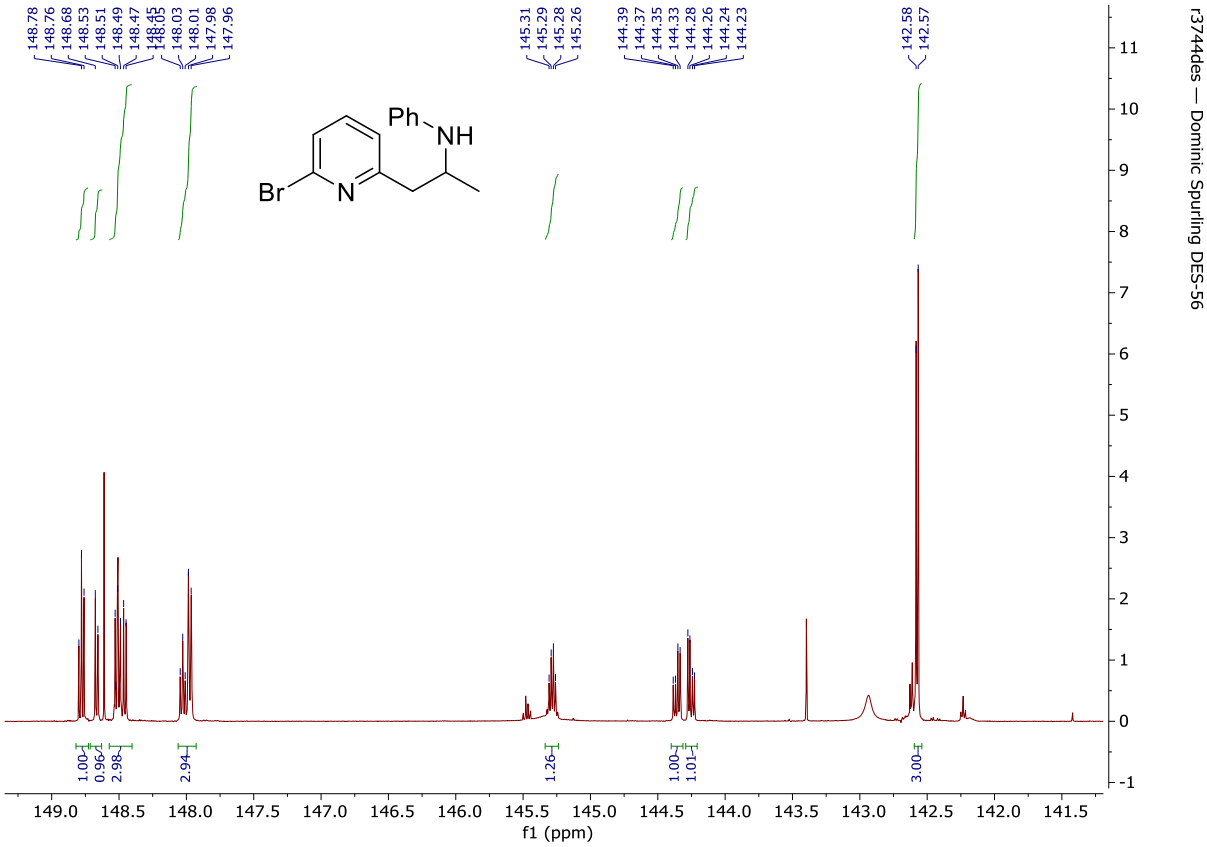

N-(3-((*tert*-Butyldimethylsilyl)oxy)propyl)aniline (226)

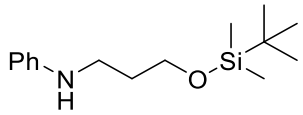

To a solution of 3-(phenylamino)propan-1-ol (**223**) (1.81 mL, 13.2 mmol) in dichloromethane (130 mL) at room temperature, *tert*-butylchlorodimethylsilane (3.99 g, 26.5 mmol), imidazole (1.35 g, 19.9 mmol) and 4-dimethylaminopyridine (162 mg, 1.33 mmol) were added. The reaction mixture was stirred at room temperature for 2 hours. The solution was then worked up with 100 mL of water and extracted with ethyl acetate (3× 50 mL) and washed with sat. brine (50 mL). The combined organic layers were dried over anhydrous $MgSO_4$, filtered and concentrated in vacuo. Purification via flash column chromatography (SiO_2, 5% ethyl acetate in hexanes) afforded the title compound as a yellow oil (2.06 g, 59%) R_f. 0.45 (5% ethyl acetate in hexanes); δ_H (400 MHz, $CDCl_3$) 7.18 (2H, t, *J* = 7.8 Hz, Ph), 6.72–6.70 (1H, m, Ph), 6.63 (2H, d, *J* = 7.8 Hz, Ph), 3.77 (2H, t, *J* = 5.8 Hz, PhNC**H₂**), 3.24 (2H, t, *J* = 6.4, C**H₂**OTBS), 1.88–1.82 (2H, m, CH_2C**H₂**CH_2), 0.92 (9H, s, 3 × SiCC**H₃**), 0.07 (6H, s, 2 × SiC**H₃**).

Spectroscopic data matched those reported in the literature.[68]

Compound **226**

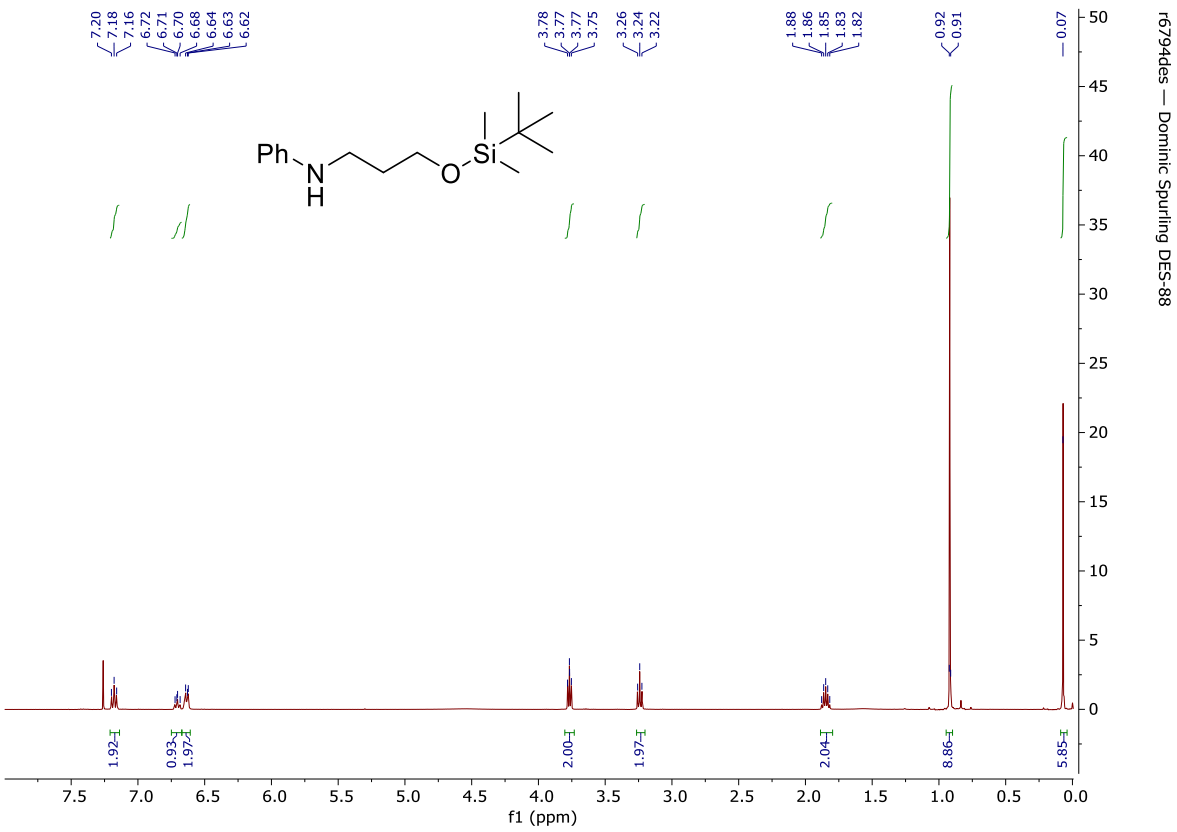

3-((2-(6-Bromopyridin-2-yl)ethyl)(phenyl)amino)propan-1-ol (229)

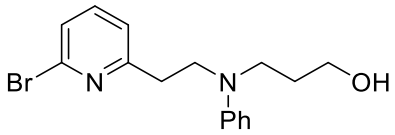

To a stirring solution of diisopropylamine (825 µL, 5.85 mmol) in dry THF (30 mL), was added n-butyllithium (2.5 M solution in hexane, 2.34 mL, 5.85 mmol) dropwise at 0 °C. The resulting solution was stirred at 0 °C for 30 mins, after which the solution was cooled to −78 °C. 2-Bromo-6-methylpyridine (**173**) (330 µg, 2.92 mmol) was then added dropwise and the solution was stirred for an additional 1 h. Dimethylformamide (340 µL, 4.39 mmol) was then added and the solution was stirred for a further 2 h at −78 °C. Sodium triacetoxyborohydride (930 mg, 4.39 mmol) dissolved in 1,2-dichloroethane (5.0 mL), was added, followed by acetic acid (536 µL) and 3-(phenylamino)propan-1-ol (491 µL, 3.51 mmol) and the reaction mixture was stirred overnight at r.t. The reaction mixture was quenched with 1 M NaOH (30 mL) and extracted with ethyl acetate (3 × 20 mL). The combined organic layers were dried ($MgSO_4$), filtered and concentrated *in vacuo*. Purification by flash column chromatography (SiO_2, 50% toluene in diethyl ether) afforded the *title compound* as a yellow oil (230 mg, 24%); R_f 0.33 (50% toluene in diethyl ether); ν_{max}/cm^{-1} (neat) 3366, 2936, 2872, 1598, 1553, 1505, 1436, 1405, 1359, 1124, 1040; δ_H (400 MHz, $CDCl_3$) 7.44 (1H, t, *J* = 7.7 Hz, Ar**H**), 7.33 (1H, d, *J* = 7.7 Ar**H**), 7.26–7.22 (2H, m, Ph**H**), 7.08 (1H, d, *J* = 7.7, Ar**H**), 6.77 (2H, d, *J* = 8.3, Ph**H**), 6.71 (1H, t, *J* = 7.3, Ph**H**), 3.72–3.68 (4H, m, $ArCH_2C\mathbf{H_2}N$ and $NC\mathbf{H_2}CH_2CH_2$), 3.37 (2H, t, *J* = 6.9 Hz, $C\mathbf{H_2}OH$), 3.02 (2H, t, *J* = 7.3 Hz, $ArC\mathbf{H_2}$), 1.83–1.76 (2H, tt, *J* = 6.9, 6.5 Hz, $CH_2C\mathbf{H_2}CH_2$); δ_C (100 MHz, $CDCl_3$) 161.2 (Ar**C**), 147.9 (Ar**C**), 141.9 (Ar**C**), 138.9 (Ar**C**H), 129.5 (Ar**C**H), 125.9 (Ar**C**H), 122.6 (Ar**C**H), 116.8 (Ar**C**H), 113.1 (Ar**C**H), 60.8 ($N\mathbf{C}H_2CH_2CH_2$), 51.5 ($ArCH_2\mathbf{C}H_2N$), 48.2 ($\mathbf{C}H_2OH$), 35.5 (Ar-$\mathbf{C}H_2$), 30.2 ($CH_2\mathbf{C}H_2CH_2$); HRMS (ESI): calcd. For $C_{16}H_{20}{}^{79}BrN_2O$, 335.0754. Found: $[MH]^+$, 335.0743 (3.2 ppm error).

Compound **229**

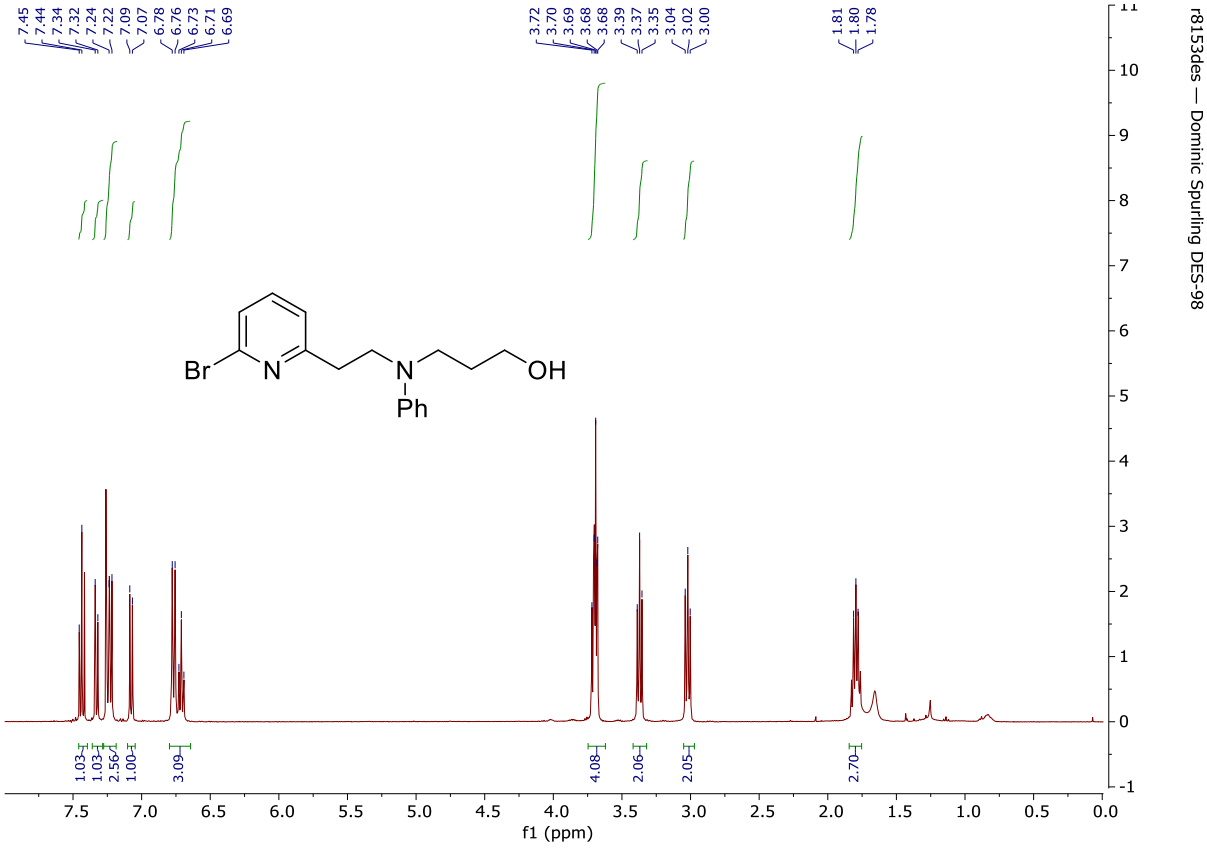

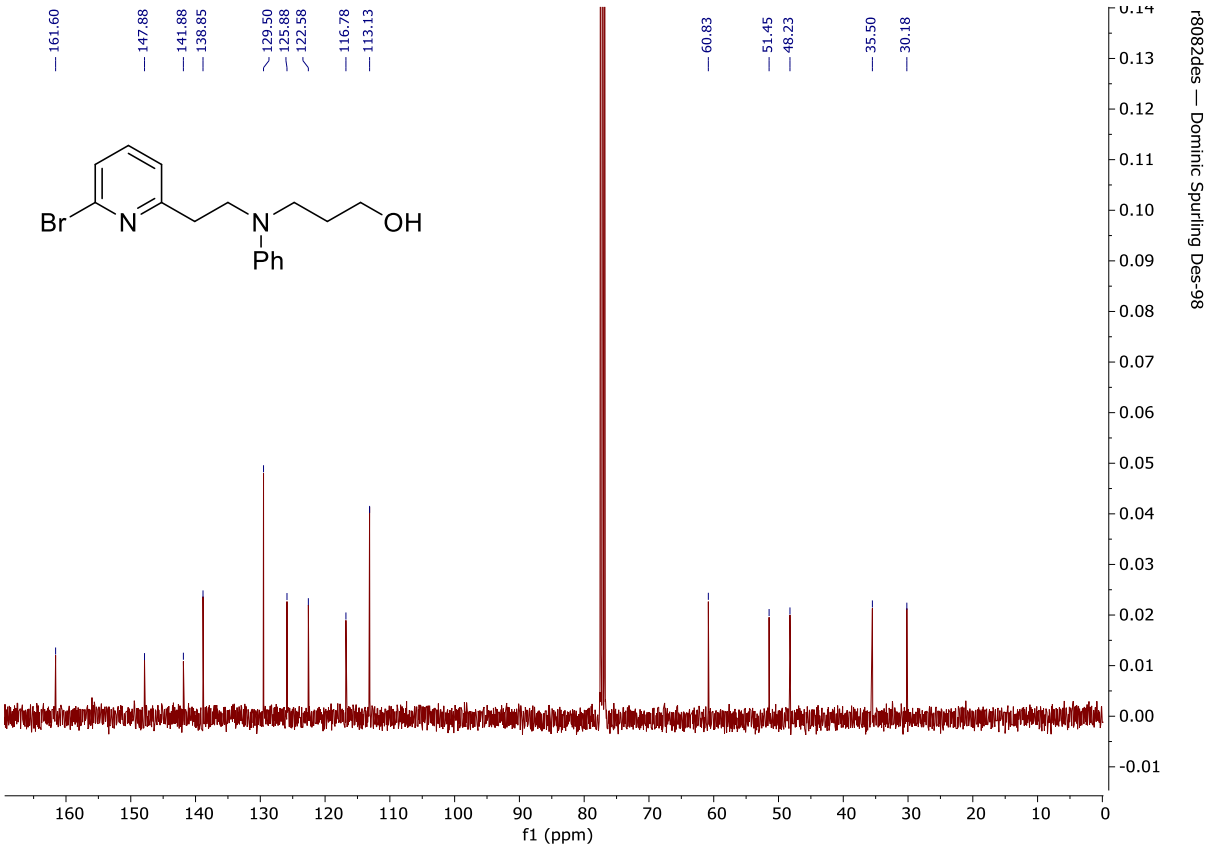

Methyl 4-iodobutanoate (238)

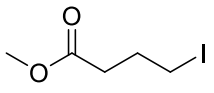

Methyl 4-bromobutanoate (**197**) (630 µL, 5.00 mmol) and sodium iodide (2.98 g, 20.0 mmol) was dissolved in acetonitrile (12 mL). After stirring at 70 °C for 90 min the reaction mixture was quenched with sat. aq. sodium thiosulfate (20 mL), extracted with ethyl acetate (3 × 20 mL) and washed with sat. brine (10 mL). The combined organic extracts were dried over $MgSO_4$, filtered and concentrated in vacuo to afford the *title compound* as a yellow oil (1.14 g, 100%); R_f. 0.8 (50% ethyl acetate in hexanes); δ_H (400 MHz, $CDCl_3$) 3.69 (3H, s, C**H**$_3$$CO_2$), 3.24 (2H, t, *J* = 6.0 Hz, IC**H**$_2$), 2.46 (2H, t, *J* = 7.0 Hz, CO_2C**H**$_2$), 2.16–2.11 (2H, tt, *J* = 7.0, 6.0 Hz, CH_2C**H**$_2$$CH_2$).

Spectroscopic data matched those reported in the literature.[69]

Compound **238**

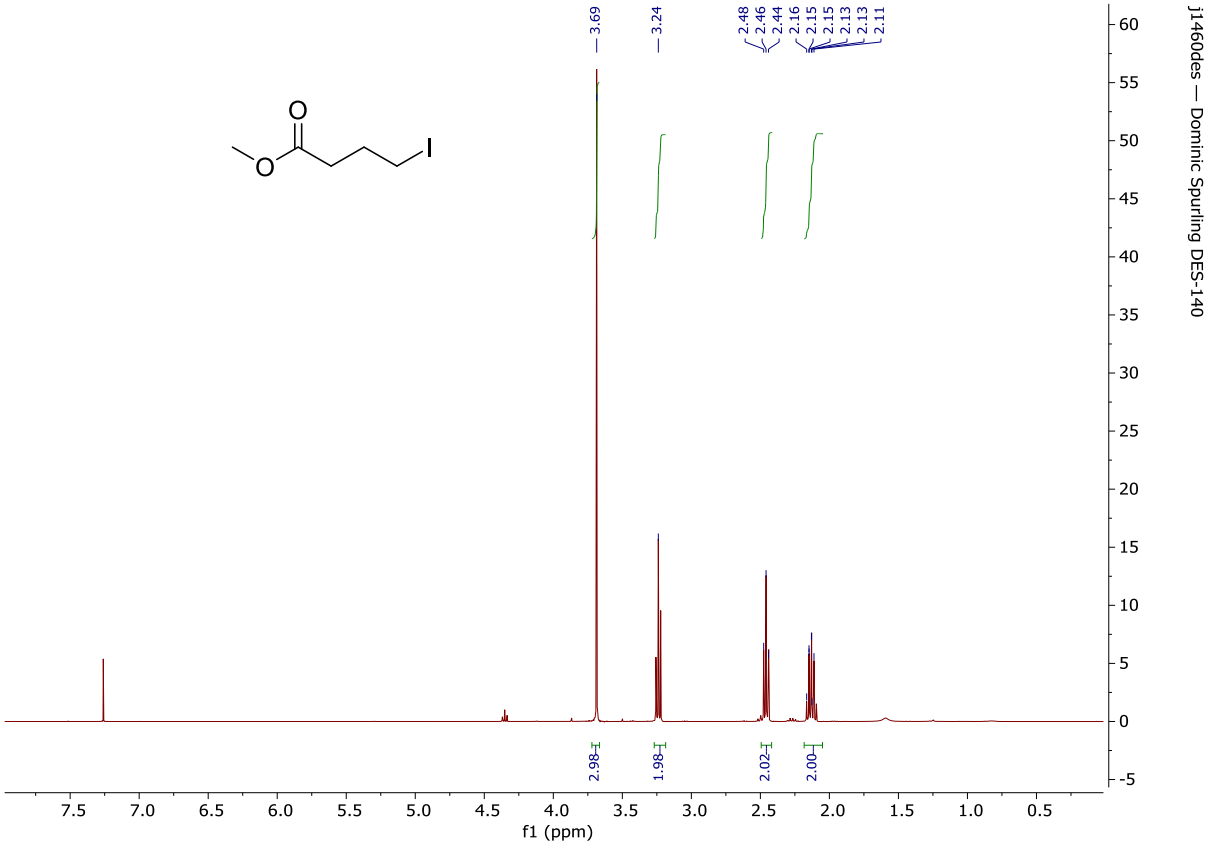

(4-Methoxy-4-oxobutyl)zinc(II) bromide (239)

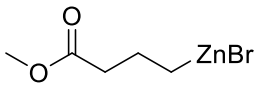

To a round bottom flask purged with nitrogen 1,2-dibromoethane (43 µL, 0.50 mmol) was dissolved in dry DMF (8 mL) before zinc powder (654 mg, 10.0 mmol) was added and the solution was heated at 90 ºC and stirred for 30 mins. The solution was then cooled to r.t., where chlorotriethylsilane (23.0 µL, 0.13 mmol) was added and stirred for 15 min. Methyl 4-iodobutanoate (**238**) (1.14 g, 5.00 mmol) dissolved in THF (4 mL) was then added and stirred for a further 2.5 h at 40 °C before cooling to room temperature. The resulting grey precipitate in the solution was then left to settle for 18 h before the supernatant liquid was transferred and stored in a separate round bottom flask purged with nitrogen.

Methyl 4-(6-(2-oxopropyl)pyridin-2-yl)butanoate (237)

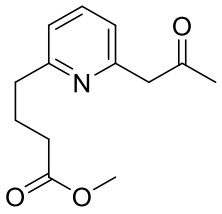

1-(6-bromopyridin-2-yl)propan-2-one (**220**) (355 mg, 1.67 mmol) and $Pd(PPh_3)_2Cl_2$ (60.0 mg, 83.0 μmol) were charged into a round bottom flask purged with nitrogen. (4-ethoxy-4-oxobutyl)zinc(II) bromide (**239**) dissolved in solution was added and heated to 55 °C for 4 h. Upon completion the solution was cooled to room temperature, concentrated *in vacuo*, quenched with sat. aq. $NaHCO_3$ (10 mL), extracted with dichloromethane (3 × 10 mL) and washed with brine (15 mL). The combined organic extracts were dried over $MgSO_4$, filtered, and removed *in vacuo*. Purification by flash column chromatography (SiO_2, 30% diethyl ether in hexanes → diethyl ether) afforded the *title compound* as a yellow oil (129 mg, 33%); R_f 0.51 (ethyl acetate); ν_{max}/cm^{-1} (neat) 2953, 2735, 1651, 1592, 1576, 1456, 1358, 1209, 1160; δ_H (400 MHz, $CDCl_3$) 7.55 (1H, t, *J* = 7.6 Hz, Ar**H**), 7.05–7.01 (2H, m, 2 × Ar**H**), 3.87 (2H, s, ArC**H**$_2$CO), 3.65 (3H, s, CO_2C**H**$_3$), 2.79 (2H, t, *J* = 7.7 Hz, CH_2C**H**$_2$Ar), 2.36 (2H, t, *J* = 7.6 Hz, C**H**$_2CO_2$), 2.21 (3H, s, COC**H**$_3$), 2.08–2.01 (2H, m, CH_2C**H**$_2CH_2$); δ_C (100 MHz, $CDCl_3$) 205.9 (CH_2**C**OCH_3), 174.0 (**C**O_2), 161.2 (Ar**C**), 154.3 (Ar**C**), 137.1 (Ar**C**H), 121.6 (Ar**C**H), 121.2 (Ar**C**H), 53.4 (C**C**H_2CO), 51.7 (O**C**H_3), 37.5 (CH_2**C**H_2CN), 33.5 (**C**H_2CO_2), 30.1 (CO**C**H_3), 25.0 (CH_2**C**H_2CH_2); HRMS (ESI): calcd. For $C_{13}H_{18}NO_3$, 236.1281. Found: $[MH]^+$, 236.1281 (0.3 ppm error).

Compound **237**

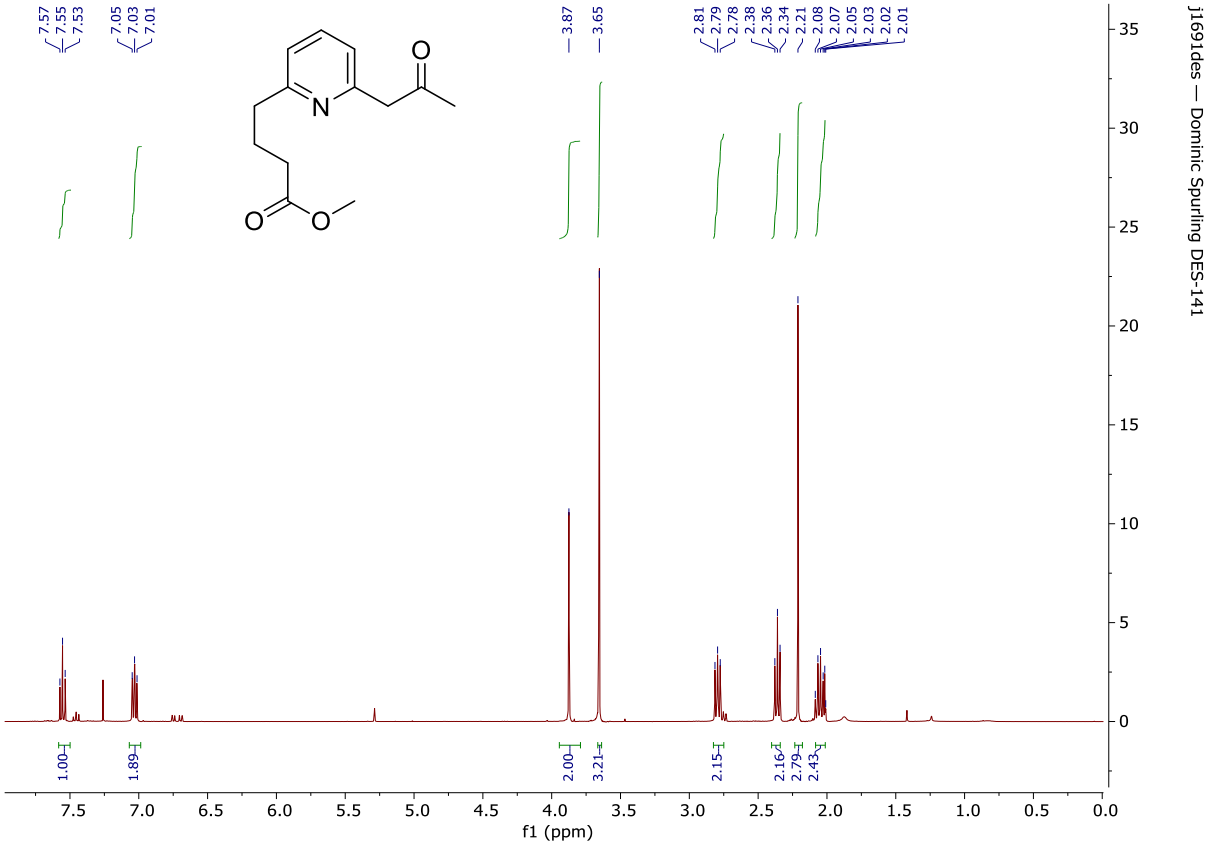

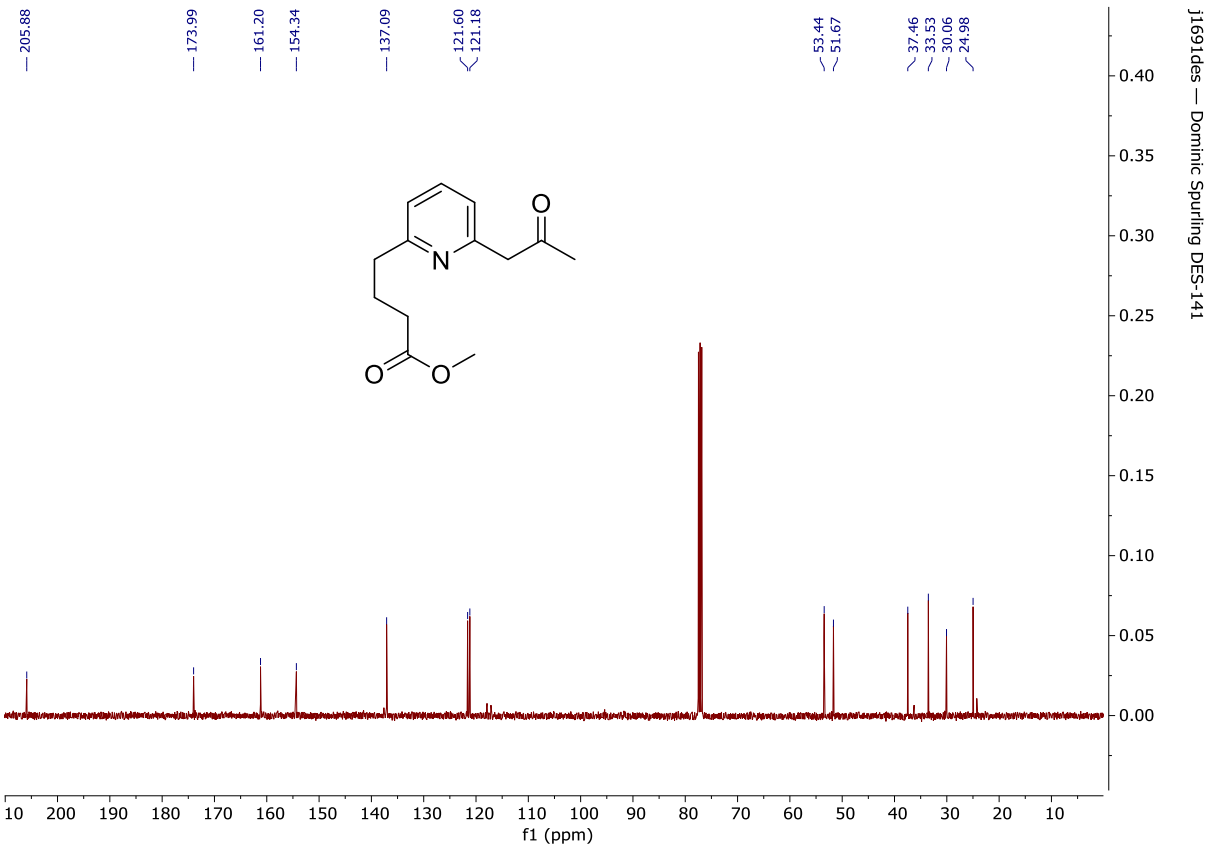

Abbreviations

Ac	Acetyl
AIBN	Azobisisobutyronitrile
a.q.	Aqueous
Ar	Aromatic
Bn	Benzyl
bp	Boiling Point
br	Broad
^{n}Bu	*n*-Butyl
^{t}Bu	*tert*-Butyl
CAN	Ceric ammonium nitrate
calcd.	Calculated
CDI	Carbonyl diimidazole
cm^{-1}	Wavenumber
cod	1,5-Cyclooctadiene
COSY	Correlated Spectroscopy
Cy	Cyclohexyl
d	Doublet
DBU	1,8-Diazabicyclo[5.4.0]undec-7-ene
DCE	1,2-Dichloroethane
dd	Doublet of doublets
ddd	Doublet of doublets of doublets
DCM	Dichloromethane
DEAD	Diethyl azodicarboxylate
DEPT	Distortionless enhancement by polarization transfer
DFT	Density functional theory
DIPA	Diisopropylamine
DIPEA	N, N-Diisopropylethylamine
DMA	Dimethylacetamide
DMAP	4-Dimethylaminopyridine

DMF	Dimethylformamide
DMSO	Dimethyl sulfoxide
dppf	1,1'-Bis(diphenylphosphino)ferrocene
EDC	N-(3-Dimethylaminopropyl)-N′-ethylcarbodiimide
Equiv.	Equivalents
ESI	Electrospray Ionisation
Et	Ethyl
Fmoc	Fluorenylmethoxycarbonyl
g	Gram(s)
h	Hour(s)
HATU	Hexafluorophosphate Azabenzotriazole Tetramethyl Uronium
HMQC	Heteronuclear multiple-quantum coherence
HOBt	Hydroxybenzotriazole7
HRMS	High resolution mass spectroscopy
Hz	Hertz
hν	Energy
INRE	Internal nucleophile ring expansion
IR	Infra-red
J	Coupling constant in Hz
K	Kelvin
KAPA	Potassium 3-aminopropylamide
L	Ligand
LDA	Lithium diisopropylamide
LHMDS	Lithium bis(trimethylsilyl)amide

M	Molar
$[M]^+$	Molecular Ion
m	multiplet
m-CPBA	*Meta*-chloroperbenzoic acid
Me	Methyl
mg	milligram(s)
MHz	Megahertz
min	Minute(s)
mL	Millilitre(s)
mmol	Millimole(s)
mol	Mole(s)
mp	Melting point
Ms	Mesyl
m/z	Mass to charge ratio
NMR	Nuclear magnetic resonance
Ph	Phenyl
Pin	Pinacol
ppm	Parts per million
Pyr	Pyridine
P13K	Phosphoinositide 3-kinase inhibitor
q	Quartet
RCM	Ring closing metathesis
Red-Al	Sodium bis(2-methoxyethoxy)aluminium hydride
REMP	Ring expansion metathesis polymerisation
R_f	Retention Factor
RT	Room temperature
sat.	Saturated
STAB	Sodium triacetoxyborohydride
SuRE	Successive ring expansion

t	Triplet
TBS	*tert*-Butylsilane
td	Triplet of doublets
Tf	Triflyl
TFA	Trifluoroacetic acid
THF	Tetrahydrofuran
TLC	Thin layer chromatography
TMS	Trimethylsilane
Ts	Tosyl
T3P	Propylphosphonic anhydride
UV	Ultra-violet
W	Week(s)
XRD	X-ray diffraction
9-BBN	9-Borabicyclo[3.3.1]nonane
µL	Microlitre(s)
µmol	Micromole(s)
δ	Chemical Shift

References

1 A. Hussain, S. K. Yousuf and D. Mukherjee, *RSC Adv.*, 2014, **4**, 43241–43257.

2 A. Parenty, X. Moreau and J.-M. Campagne, *Chem. Rev.*, 2006, **106**, 911–939.

3 A. T. Frank, N. S. Farina, N. Sawwan, O. R. Wauchope, M. Qi, E. M. Brzostowska, W. Chan, F. W. Grasso, P. Haberfield and A. Greer, *Mol. Divers.*, 2007, **11**, 115–118.

4 K. C. Majumdar and S. K. Chattopadhyay, *Heterocycles in Natural Product Synthesis*, John Wiley & Sons, 2011.

5 J. I. Levin, *Macrocycles in Drug Discovery*, Royal Society of Chemistry, 2015.

6 C. Drahl, *Chem. Eng. News*, 2009, **87**, 54–57.

7 M. R. Lambu, S. Kumar, S. K. Yousuf, D. K. Sharma, A. Hussain, A. Kumar, F. Malik and D. Mukherjee, *J. Med. Chem.*, 2013, **56**, 6122–6135.

8 E. M. Driggers, S. P. Hale, J. Lee and N. K. Terrett, *Nat. Rev. Drug Discov.*, 2008, **7**, 608–624.

9 E. Marsault and M. L. Peterson, *J. Med. Chem.*, 2011, **54**, 1961–2004.

10 T. Ema, D. Tanida and T. Sakai, *Org. Lett.*, 2006, **8**, 3773–3775.

11 M. A. Winnik, *Acc. Chem. Res.*, 1985, **18**, 73–79.

12 L. F. Lindoy, *The Chemistry of Macrocyclic Ligand Complexes*, Cambridge University Press, 1990.

13 A. K. Yudin, *Chem. Sci.*, 2015, **6**, 30–49.

14 J. Fastrez, *J. Phys. Chem.*, 1989, **93**, 2635–2642.

15 M. Malesevic, U. Strijowski, D. Bächle and N. Sewald, *J. Biotechnol.*, 2004, **112**, 73–77.

16 K. Haas, W. Ponikwar, H. Nöth and W. Beck, *Angew. Chem. Int. Ed.*, 1998, **37**, 1086–1089.

17 H. Fu, H. Chang, J. Shen, L. Yu, B. Qin, K. Zhang and H. Zeng, *Chem. Commun.*, 2014, **50**, 3582–3584.

18 V. Martí-Centelles, M. D. Pandey, M. I. Burguete and S. V. Luis, *Chem. Rev.*, 2015, **115**, 8736–8834.

19 J. R. Donald and W. P. Unsworth, *Chem. Eur. J.*, 2017, **23**, 8780–8799.

20 M. Hesse, *Ring enlargement in organic chemistry*, VCH, Weinheim, 1991.

21 T. C. Stephens and W. P. Unsworth, *Synlett*, 2020, **31**, 133–146.

22 U. Kramer, A. Guggisberg, M. Hesse and H. Schmid, *Angew. Chem. Int. Ed. Engl.*, 1977, **16**, 861–862.

23 U. Kramer, A. Guggisberg, M. Hesse and H. Schmid, *Angew. Chem. Int. Ed. Engl.*, 1978, **17**, 200–202.

24 L. Crombie, R. C. F. Jones, A. Rasid Mat-Zin and S. Osborne, *J. Chem. Soc. Chem. Commun.*, 1983, **0**, 960–961.

25 H. H. Wasserman, R. P. Robinson and H. Matsuyama, *Tetrahedron Lett.*, 1980, **21**, 3493–3496.

26 B. M. Trost and J. Cossy, *J. Am. Chem. Soc.*, 1982, **104**, 6881–6882.

27 E. J. Corey, D. J. Brunelle and K. C. Nicolaou, *J. Am. Chem. Soc.*, 1977, **99**, 7359–7360.

28 J. P. Tam, Y.-A. Lu and Q. Yu, *J. Am. Chem. Soc.*, 1999, **121**, 4316–4324.

29 L. Yet, *Tetrahedron*, 1999, **55**, 9349–9403.

30 P. Dowd and S. C. Choi, *J. Am. Chem. Soc.*, 1987, **109**, 3493–3494.

31 W. Zhang and P. Dowd, *Tetrahedron Lett.*, 1996, **37**, 957–960.

32 G. Pattenden and D. J. Schulz, *Tetrahedron Lett.*, 1993, **34**, 6787–6790.

33 K. Prantz and J. Mulzer, *Chem. Rev.*, 2010, **110**, 3741–3766.

34 C. Fehr, J. Galindo, O. Etter and W. Thommen, *Angew. Chem.*, 2002, **114**, 4705–4708.

35 M. Ikeda, M. Takahashi, T. Uchino, K. Ohno, Y. Tamura and M. Kido, *J. Org. Chem.*, 1983, **48**, 4241–4247.

36 G. H. Posner, M. A. Hatcher and W. A. Maio, *Org. Lett.*, 2005, **7**, 4301–4303.

37 A. P. Marchand and R. E. Lehr, *Pericyclic Reactions: Organic Chemistry: A Series of Monographs, Vol. 35.2*, Academic Press, 2013.

38 E. Vedejs and J. P. Hagen, *J. Am. Chem. Soc.*, 1975, 3.

39 R. Schmid and H. Schmid, *Helv. Chim. Acta*, 1977, **60**, 1361–1366.

40 E. Vedejs, M. J. Mullins, J. M. Renga and S. P. Singer, *Tetrahedron Lett.*, 1978, **19**, 519–522.

41 M. H. Weston, K. Nakajima and T. G. Back, *J. Org. Chem.*, 2008, **73**, 4630–4637.

42 Y.-S. Lee, J.-W. Jung, S.-H. Kim, J.-K. Jung, S.-M. Paek, N.-J. Kim, D.-J. Chang, J. Lee and Y.-G. Suh, *Org. Lett.*, 2010, **12**, 2040–2043.

43 E. Fouque, G. Rousseau and J. Seyden-Penne, *J. Org. Chem.*, 1990, **55**, 4807–4817.

44 R. H. Grubbs, *Tetrahedron*, 2004, **60**, 7117–7140.

45 C. W. Lee and R. H. Grubbs, *J. Org. Chem.*, 2001, **66**, 7155–7158.

46 A. J. Boydston, Y. Xia, J. A. Kornfield, I. A. Gorodetskaya and R. H. Grubbs, *J. Am. Chem. Soc.*, 2008, **130**, 12775–12782.

47 C. W. Lee, T.-L. Choi and R. H. Grubbs, *J. Am. Chem. Soc.*, 2002, **124**, 3224–3225.

48 S. S. Nadif, T. Kubo, S. A. Gonsales, S. VenkatRamani, I. Ghiviriga, B. S. Sumerlin and A. S. Veige, *J. Am. Chem. Soc.*, 2016, **138**, 6408–6411.
49 M. H. Shaw and J. F. Bower, *Chem. Commun.*, 2016, **52**, 10817–10829.
50 C. Li, H. Zhang, J. Feng, Y. Zhang and J. Wang, *Org. Lett.*, 2010, **12**, 3082–3085.
51 O. Boyd, G.-W. Wang, O. O. Sokolova, A. D. J. Calow, S. M. Bertrand and J. F. Bower, *Angew. Chem. Int. Ed.*, 2019, **58**, 18844–18848.
52 M. Murakami, T. Tsuruta and Y. Ito, *Angew. Chem. Int. Ed.*, 2000, **39**, 2484–2486.
53 C. Kitsiou, J. J. Hindes, P. I'Anson, P. Jackson, T. C. Wilson, E. K. Daly, H. R. Felstead, P. Hearnshaw and W. P. Unsworth, *Angew. Chem. Int. Ed.*, 2015, **54**, 15794–15798.
54 L. G. Baud, M. A. Manning, H. L. Arkless, T. C. Stephens and W. P. Unsworth, *Chem. – Eur. J.*, 2017, **23**, 2225–2230.
55 T. C. Stephens, M. Lodi, A. M. Steer, Y. Lin, M. T. Gill and W. P. Unsworth, *Chem. – Eur. J.*, 2017, **23**, 13314–13318.
56 T. C. Stephens, A. Lawer, T. French and W. P. Unsworth, *Chem. – Eur. J.*, 2018, **24**, 13947–13953.
57 A. Lawer, J. A. Rossi-Ashton, T. C. Stephens, B. J. Challis, R. G. Epton, J. M. Lynam and W. P. Unsworth, *Angew. Chem.*, 2019, **131**, 14080–14085.
58 S. R. LaPlante, L. D. Fader, K. R. Fandrick, D. R. Fandrick, O. Hucke, R. Kemper, S. P. F. Miller and P. J. Edwards, *J. Med. Chem.*, 2011, **54**, 7005–7022.
59 E. Vitaku, D. T. Smith and J. T. Njardarson, *J. Med. Chem.*, 2014, **57**, 10257–10274.
60 J. Clegg, Masters Dissertation, University of York, 2020.
61 T. Stephens, PhD, University of York, 2019.
62 Coronavirus, https://www.who.int/emergencies/diseases/novel-coronavirus-2019, (accessed 27 April 2020).
63 H. Kroth, N. Sreenivasachary, A. Hamel, P. Benderitter, Y. Varisco, V. Giriens, P. Paganetti, W. Froestl, A. Pfeifer and A. Muhs, *Bioorg. Med. Chem. Lett.*, 2016, **26**, 3330–3335.
64 D. Duran, N. Wu, B. Mao and J. Xu, *J. Liq. Chromatogr. Relat. Technol.*, 2006, **29**, 661–672.
65 J. Kim, Y. Ohk, S. H. Park, Y. Jung and S. Chang, *Chem. Asian J.*, 2011, **6**, 2040–2047.
66 H. Tsukamoto and Y. Kondo, *Org. Lett.*, 2007, **9**, 4227–4230.

67 T. Yokoi, H. Tanimoto, T. Ueda, T. Morimoto and K. Kakiuchi, *J. Org. Chem.*, 2018, **83**, 12103–12121.

68 D. Basavaiah, G. C. Reddy and K. C. Bharadwaj, *Eur. J. Org. Chem.*, 2014, **2014**, 1157–1162.

69 G. J. Lovinger and J. P. Morken, *J. Am. Chem. Soc.*, 2017, **139**, 17293–17296.